Deciphering Chlorohydrocarbon Transformation Mechanisms by Advancing $\delta^{13}C/\delta^{37}Cl$ Compound-Specific Isotope Analysis

Dissertation

der Mathematisch-Naturwissenschaftlichen Fakultät

der Eberhard Karls Universität Tübingen

zur Erlangung des Grades eines

Doktors der Naturwissenschaften

(Dr. rer. nat.)

vorgelegt von

M.Sc. Christina Marie Lihl

aus München

Tübingen

2019

Gedruckt mit Genehmigung der Mathematisch-Naturwissenschaftlichen Fakultät der Eberhard Karls Universität Tübingen.

Tag der mündlichen Qualifikation: 10.03.2020

Dekan: Prof. Dr. Wolfgang Rosenstiel

1. Berichterstatter: Prof. Dr. Martin Elsner

2. Berichterstatter: Prof. Dr. Stefan Haderlein

DANKE

Table of Contents

Summary

Chlorinated organic compounds are ubiquitous in daily life. Chlorohydrocarbons are used as solvents in industry (e.g. chlorinated ethenes) and as herbicides in agriculture (e.g. atrazine). However, when present in ground- and surface water, they pose a threat to drinking water resources. Therefore, investigating and understanding their environmental fate is important to guarantee correct pesticide management and to develop successful (bio)remediation strategies at contaminated sites. When traditional concentration-based assessments fall short because mass balances cannot be closed, a promising approach for tracing the sources of contamination and studying the transformation pathways of such contaminants is compound-specific stable isotope analysis (CSIA). Analyzing changes in natural occurring isotope ratios (e.g. $^{13}C/^{12}C$, $^{15}N/^{14}N$, $^{37}Cl/^{35}Cl$) during (bio)chemical transformations allows the detection and the assessment of degradation processes. Furthermore, isotopic information from more than one element enables the differentiation and even the identification of different (bio)chemical reaction mechanisms.

The first part of this thesis focuses on advancing CSIA of chlorine. In the last years instrumental and methodical optimizations continually improved chlorine isotope analysis facilitating also the analysis of more complex organic compounds. For accurate chlorine isotope analysis, however, in-house referencing and substance-specific working standards are critically needed. Ideally two standards of each substance are required that display different isotope values to enable a two-point calibration. However, almost all international chlorine isotope reference materials have similar isotope values except one which is, therefore, very valuable and should not be used for routine analysis. Here, a synthesis route was identified resulting in a chloride salt which shows a pronounced negative chlorine isotope value. This chloride salt can be used as a second anchor for two-point calibration of in-house working standards in the future. Furthermore, it was demonstrated that substance-specific working standards of more complex organic chlorohydrocarbons (like the herbicides acetochlor and S-metolachlor) can be generated easily by using chemical reactions with pronounced chlorine isotope effects from organic chemistry. With these synthesis routes every laboratory has the opportunity to generate its own in-house standards leading to more accurate results in chlorine isotope analysis.

The second part of the thesis tackles the question why bioremediation of the chlorinated ethenes tetrachloroethene (PCE) and trichloroethene (TCE) often stops at toxic *cis*-1,2-dichloroethene (*cis*-DCE) or vinyl chloride (VC). By studying dual element isotope plots of carbon and chlorine a model study recently identified two different chemical mechanisms which are at work during reductive dechlorination of PCE (addition-elimination) and *cis*-DCE (addition-protonation). For TCE dechlorination both mechanisms could be observed. In this thesis it was investigated whether the same mechanisms can also be observed during microbial reductive dechlorination with pure and mixed cultures. Dual element isotope trends of carbon and chlorine indeed indicated that bacteria dechlorinating *cis*-DCE or PCE followed the same mechanisms which were identified in the model study. Microbial TCE dechlorination followed the addition-protonation pathway if the cultures were already adapted to higher chlorinated substrates. If the bacteria were maintained on less chlorinated substrates before TCE dechlorination, they followed the addition-elimination pathway. Therefore, it was concluded that reductive dehalogenases (RDases, the enzymes catalyzing reductive dechlorination) are likely specialized in different chemical mechanisms. The fact that some RDases are specifically tailored to the dechlorination of PCE and TCE, but are not able to degrade *cis*-DCE or VC may offer an explanation for the question why bioremediation often stalls at *cis*-DCE or VC. Based on these results, a new classification system based on dual element isotope trends (C, Cl) and detected RDases could help to identify natural processes at contaminated field sites.

The third part of this thesis studies chlorine, carbon and nitrogen isotope fractionation during microbial atrazine hydrolysis with the pure culture *Arthrobacter aurescens* TC1 and oxidative dealkylation with *Rhodococcus* sp. NI86/21. Carbon and nitrogen isotope effects confirmed that the bacteria followed the pathways which were proposed in previous studies. Dual element isotope plots of the measured elements (C/N, Cl/C, Cl/N) allowed a reliable distinction of the two pathways. In contrast to nitrogen and carbon isotope effects, chlorine isotope effects are not diluted by non-reacting atoms which could turn chlorine isotope fractionation into a sensitive indicator for transformation processes. During microbial hydrolysis of atrazine unexpected small chlorine isotope effects were observed indicating that the cleavage of the C-Cl bond is not the rate-limiting step in this reaction. On the other hand, oxidative dealkylation resulted in unexpected large chlorine isotope effects suggesting the involvement of enzymatic interactions. Regarding these unexpected results this study demonstrated that a complete understanding of chemical mechanisms is very important

before applying this new approach to the field. Additionally, triple element isotope analysis, not only of atrazine, but also of other chlorohydrocarbons, will improve the source identification of contaminants and also the differentiation of degradation pathways.

IV

Zusammenfassung

Chlorierte organische Verbindungen sind im täglichen Leben allgegenwärtig. Chlorkohlenwasserstoffe werden in der Industrie als Lösungsmittel (z.B. chlorierte Ethene) und in der Landwirtschaft als Herbizide (z.B. Atrazin) verwendet. Kommen sie aber im Grund- und Oberflächenwasser vor, stellen sie eine Gefahr für die Trinkwasserressourcen dar. Aus diesem Grund ist es wichtig ihr Verhalten in der Umwelt zu untersuchen und zu verstehen, um einen korrekten Umgang mit Pestiziden zu gewährleisten und erfolgreiche (biologische) Sanierungsstrategien an kontaminierten Standorten zu entwickeln. Wenn sich traditionelle konzentrationsbasierte Beurteilungen als unzureichend erweisen, da Massenbilanzen nicht geschlossen werden können, ist ein vielversprechender Ansatz um Kontaminationsquellen zurückzuverfolgen und Transformationsprozesse zu erforschen, die substanz-spezifische stabile Isotopenanalyse (CSIA). Die Untersuchung von Veränderungen bei natürlich vorkommenden Isotopenverhältnissen (z.B. $^{13}C/^{12}C$, $^{15}N/^{14}N$, $^{37}Cl/^{35}Cl$) während (bio)chemischen Vorgängen erlaubt den Nachweis und die Bewertung von Abbauprozessen. Des Weiteren ermöglicht die gleichzeitige Analyse von mehreren Elementen die Unterscheidung und die Identifizierung von unterschiedlichen (bio)chemischen Reaktionsmechanismen.

Der erste Teil dieser Doktorarbeit konzentriert sich darauf, die Chlor-Isotopenanalytik weiter voran zu bringen. In den letzten Jahren verbesserten instrumentelle und methodische Optimierungen die Chlor-Isotopenanalyse und erleichterten dadurch auch die Untersuchung von komplexeren organischen Verbindungen. Für exakte Chlor-Isotopenanalysen sind allerdings hausinterne Referenz- und substanz-spezifische Messstandards dringend erforderlich. Idealerweise werden zwei Standards für jede Substanze benötigt, die unterschiedliche Isotopenwerte aufweisen und somit eine Zweipunkt-Kalibrierung ermöglichen. Allerdings weisen fast alle internationalen Referenzmaterialien für Chlor ähnliche Isotopenwerte auf, außer einem, der daher sehr wertvoll ist und nicht für Routineanalysen verwendet werden sollte. Im Rahmen dieser Arbeit wurde ein Syntheseweg für ein Chlorid-Salz identifiziert, das einen ausgeprägten negativen Chlorisotopenwert besitzt. Dieses Chlorid-Salz kann zukünftig als zweiter Anker bei der Zweipunkt-Kalibrierung von hausinternen Messstandards verwendet werden. Auch wurde gezeigt, dass substanz-spezifische Messstandards für komplexere organische Chlorkohlenwasserstoffe

(wie die Herbizide Acetochlor und S-Metolachlor) mit Hilfe von chemischen Reaktionen aus der organischen Chemie, die einen ausgeprägten Chlorisotopeneffekt aufweisen, einfach hergestellt werden können. Diese Synthesewege bieten jedem Labor die Möglichkeit eigene hausinterne Standards herzustellen, was die Exaktheit von Chlorisotopenmessungen verbessert.

Teil Zwei dieser Doktorarbeit beschäftigt sich mit der Frage, warum die biologische Sanierung im Fall von Tetrachlorethen (PCE) und Trichlorethen (TCE) oft bei den toxischen Zwischenprodukten *cis*-1,2-Dichlorethen (*cis*-DCE) oder Vinylchlorid (VC) stoppt. Durch die Untersuchung von Doppel-Element Isotopen Plots der Elemente Kohlenstoff und Chlor gelang es kürzlich zwei unterschiedliche Reaktionsmechanismen für die reduktive Dechlorierung von PCE (Additions-Eliminierung) und *cis*-DCE (Additions-Protonierung) in einer Modellstudie zu identifizieren. Im Fall von TCE konnten beide Mechanismen nachgewiesen werden. Im Rahmen dieser Arbeit wurde untersucht, ob dieselben Mechanismen auch für die bakterielle reduktive Dechlorierung bei Rein- und Mischkulturen verantwortlich sind. Die Trends der Doppel-Element Isotopen Plots für Kohlenstoff und Chlor deuteten in der Tat darauf hin, dass die bakterielle Dechlorierung von *cis*-DCE oder PCE auf denselben Abbauwegen erfolgte, die auch in der Modellstudie identifiziert wurden. Die bakterielle TCE Dechlorierung verlief nach dem Additions-Protonierungs-Mechanismus, wenn die Bakterienkulturen schon an höhere chlorierte Substanzen angepasst waren. Waren die Kulturen vor dem TCE Abbau an weniger chlorierte Substanzen angepasst, verlief der Abbauprozess nach dem Additions-Eliminierungs-Mechanismus. Daraus wurde gefolgert, dass reduktive Dehalogenasen (RDasen, Enzyme, die die reduktive Dechlorierung katalysieren) wahrscheinlich auf verschiedene Reaktionsmechanismen spezialisiert sind. Die Tatsache, dass einige RDasen speziell für die Dechlorierung von PCE und TCE zuständig sind, aber nicht in der Lage sind *cis*-DCE oder VC abzubauen, könnte eine Erklärung für die Frage liefern, warum die biologische Sanierung häufig bei *cis*-DCE oder VC zum Stoppen kommt. Basierend auf diesen Ergebnissen könnte ein neues Klassifizierungssystem, das auf Doppel-Element Isotopen Trends (C, Cl) und detektierten RDasen aufgebaut ist, helfen, natürliche Prozesse an kontaminierten Standorten zu identifizieren.

Der dritte Teil dieser Doktorarbeit untersucht die Isotopenfraktionierung von Chlor, Kohlenstoff und Stickstoff während dem bakteriellen Abbau von Atrazin mittels Hydrolyse mit *Arthrobacter aurescens* TC1 und mittels oxidativer Dealkylierung mit *Rhodococcus* sp.

NI86/21. Kohlenstoff- und Stickstoffisotopeneffekte bestätigten, dass die bakteriellen Abbauwege denen folgten, die schon in früheren Studien beschrieben worden sind. Doppel-Element Isotopen Plots der analysierten Elemente (C/N, Cl/C, Cl/N) erlaubten eine zuverlässige Unterscheidung der beiden Abbauwege. Im Gegensatz zu den Isotopeneffekten bei Kohlenstoff und Stickstoff, erfolgt bei den Chlorisotopeneffekten keine Verdünnung durch nicht-reagierende Atome, was die Chlorisotopenfraktionierung zu einem sensitiven Indikator für Transformierungsprozesse machen könnte. Während der mikrobiellen Hydrolyse von Atrazin wurden unerwartet kleine Chlorisotopeneffekte beobachtet, die darauf hindeuten, dass die Spaltung der Chlor-Kohlenstoffbindung nicht der geschwindigkeitsbestimmende Schritt in dieser Reaktion ist. Anderseits führte die oxidative Dealkylierung zu unerwartet großen Chlorisotopeneffekten, was auf eine Involvierung von enzymatischen Interaktionen schließen lässt. Die unerwarteten Resultate in diese Studie haben gezeigt, dass ein komplettes Verständnis der chemischen Reaktionswege sehr wichtig ist, bevor dieser neue Ansatz im Feld erprobt werden kann. Zusätzlich dazu können Triple-Element Isotopenanalysen, nicht nur von Atrazin, sondern auch von anderen chlorierten Kohlenwasserstoffen, dazu beitragen, die Identifizierung von Kontaminationsquellen sowie die Unterscheidung von Abbauwegen zu verbessern.

VIII

Declaration according to § 5 Abs. 2 No. 8 of the PhD regulations of the Faculty of Science

- Share in publications done in team work -

List of Publications:

1. Lihl, C.; Renpenning, J.; Kümmel, S.; Gelman, F.; Schürner, H.K.V.; Daubmeier, M.; Heckel, B.; Melsbach, A.; Bernstein, A.; Shouakar-Stash, O.; Gehre, M.; Elsner, M.: Toward Improved Accuracy in Chlorine Isotope Analysis: Synthesis Routes for In-House Standards and Characterization via Complementary Mass Spectrometry Methods. *Analytical Chemistry* **2019**, 91, (19), 12290-12297.

2. Lihl, C.; Douglas, L.M.; Franke, S.; Pérez-de-Mora, A.; Meyer, A.H.; Daubmeier, M.; Edwards, E.A.; Nijenhuis, I.; Sherwood Lollar, B.; Elsner, M.: Mechanistic Dichotomy in Bacterial Trichloroethene Dechlorination Revealed by Carbon and Chlorine Isotope Effects. *Environmental Science & Technology* **2019**, 53, (8), 4245-4254.

3. Lihl, C.; Heckel, B.; Grzybkowska, A.; Dybala-Defratyka, A.; Ponsin, V.; Torrentó, C.; Hunkeler, D.; Elsner, M.: Compound-Specific Chlorine Isotope Fractionation in Biodegradation of Atrazine. *Environmental Science: Processes & Impacts* **2020**, 22 (3), 792-801.

Nr.	Accepted for publication yes/no	Number of all authors	Position of the candidate in list of authors	Scientific ideas of candidate (%)	Data generation by the candidate (%)	Analysis and interpretation by the candidate (%)	Paper writing done by the candidate (%)
1	Yes	12	1	30	70	70	75
2	Yes	10	1	30	40	60	55
3	Yes	8	1	30	90	85	80

X

1

General Introduction

1.1 Contamination of Groundwater Resources

Contamination of groundwater by chemical pollutants is a prominent problem of our times which threatens the quality of drinking water resources worldwide[1, 2]. Although many of these contaminants are only present at very low concentrations (microgram to nanogram per liter level), they can show negative long-term effects on humans and other living organisms[2]. Most commonly detected contaminants are chlorohydrocarbons. Prominent examples of such chlorohydrocarbons are chlorinated ethenes, like tetrachloroethene (PCE) and trichloroethene (TCE), originating from industry[3], or chlorinated micropollutants, like the agricultural herbicide atrazine[4].

1.1.1 Chlorinated Ethenes

In industry the chlorinated ethenes PCE and TCE are extensively used as dry-cleaning solvents and metal degreasing agents. Due to improper handling or leakage numerous sites were contaminated throughout the United States and Europe. Since PCE and TCE have toxic effects on living organisms, (bio)remediation of these sites is of major importance[3]. Under anoxic conditions certain bacteria are able to stepwise dechlorinate PCE and TCE via a process called reductive dehalogenation. This process is catalyzed by reductive dehalogenase

enzymes (RDases). Unfortunately, only a few bacteria are capable of a complete dehalogenation from PCE or TCE down to the non-toxic ethene. Therefore, degradation often stalls at the point of the highly toxic *cis*-1,2-dichloroethene (*cis*-DCE) or vinyl chloride (VC) which is one of the long-standing barriers to successful bioremediation[5].

1.1.2 Atrazine

In the U.S. atrazine is a widely used herbicide applied in agriculture for broadleaf and weed control[6, 7]. In Germany and in the E.U. it was also intensively used until it was banned in Germany in 1991[8] and in the E.U. in 2004[9]. However, in Germany atrazine and its metabolites can still be detected in the groundwater[10]. Furthermore, its wide-ranging presence and accumulation in the environment can have negative effects on living organisms[11]. Therefore, the environmental fate of this herbicide and its monitoring are of major concern.

1.2 Monitoring Strategy – Compound-Specific Stable Isotope Analysis (CSIA)

Monitoring of these chlorohydrocarbons as well as detecting and identifying their degradation pathways at contaminated sites is of significant importance since this is the fundamental basis for the development of appropriate remediation techniques and strategies. With conventional methods it is highly challenging to assess groundwater contaminants in natural environments. These methods typically aim to identify degradation by analyzing mass balances or measuring parent compound and metabolite concentration over time. However, to close mass balances becomes difficult, if additional natural attenuating processes like sorption or dilution are at work. Such processes do not affect the metabolite to parent compound ratio, which is calculated from the respective concentrations. However, since metabolites can be further degraded, also this method often fails to prove degradation or to provide information about the degradation mechanisms[12, 13]. Therefore, a powerful approach to get insight into the fate of the contaminants is needed in order to develop and optimize bioremediation strategies.

One approach, that can fulfill this demand, is compound-specific stable isotope analysis (CSIA) which has become a promising tool to study groundwater contamination. With this

approach, the isotopic signature of environmental contaminants can be determined by measuring isotope ratios of certain elements at their natural abundance. Subsequently this isotopic signature can help trace the source of contamination since analytes from different sources mostly show different isotopic compositions[12, 14]. On the other hand, it is possible not only to detect but also to quantify degradation processes of contaminants in the environment[12, 15, 16], to differentiate degradation pathways[12, 13] and even to identify chemical reaction mechanisms[17], which will be further discussed in the following sections.

1.2.1 *Principals of CSIA*

Isotope values or isotopic signatures are isotope ratios (heavy vs. light isotopes) of certain elements which are determined at their low natural abundance and expressed in the δ-notation, e.g. for carbon:

$$\delta^{13}C = [(^{13}C/^{12}C)_{Sample} - (^{13}C/^{12}C)_{Reference}] / (^{13}C/^{12}C)_{Reference} \tag{1-1}$$

The relation to an international reference material, as expressed in Equation 1-1, enables the comparison of isotope ratios determined in different laboratories worldwide. Positive δ-values indicate an enrichment and negative δ-values indicate a depletion of the heavy relative to the light isotope in the sample compared to the reference material. During transformation processes isotope fractionation takes place, leading to a change in the isotope ratio of the reacting compound. This is based on the fact that heavy and light isotopes behave differently during chemical reactions. Chemical bonds with heavy isotopes are slightly more stable than bonds with light isotopes. Therefore, molecules containing chemical bonds with light isotopes typically react faster than molecules with heavy isotopes (normal kinetic isotope effect). This kinetic isotope effect can be expressed by:

$$KIE = {}^{l}k / {}^{h}k \tag{1-2}$$

Here ^{l}k and ^{h}k are the reaction rates of light and heavy isotopes.

Due to this basic principal the remaining substrate of a transformation reaction becomes gradually enriched with molecules containing heavy isotopes over time. Such a trend can be described by the Rayleigh equation, e.g. for carbon:

$$\ln [(\delta^{13}C + 1) / (\delta^{13}C_0 + 1)] = \varepsilon_c \cdot \ln f \tag{1-3}$$

For this equation, isotopes values have to be determined at a given time ($\delta^{13}C$) and at the starting point of the reaction ($\delta^{13}C_0$). The enrichment factor ε reflects the extent of isotope fractionation. The magnitude of this degradation-induced isotope fractionation can be used to detect contaminant degradation in the field[18-20].

1.2.2 Instrumentation of CSIA

Isotope ratios of single compounds in environmental samples can be determined by coupling gas chromatography (GC) to isotope ratio mass spectrometry (IRMS). In case of carbon and nitrogen isotope analysis, the target compounds are separated via gas chromatography and subsequently converted online into an analyte gas (CO_2, N_2) (see Figure 1-1A and 1-1B). Afterwards, the analyte gas is transferred in a helium carrier stream into the IRMS where the isotope ratios are measured[21].

Advances in analytical instrumentation have enabled also the online analysis of chlorine isotope ratios in organic chlorinated compounds. Here the target compounds are directly transferred from the GC to the IRMS (see Figure 1-1C)[22].

For all three elements, target compounds are measured against respective monitoring gases which are introduced into the IRMS during measurement (see Figure 1-1A – 1-1C). According to Equation 1-1 the resultant isotope ratios are converted to δ-values which are relative to an international scale[21, 23].
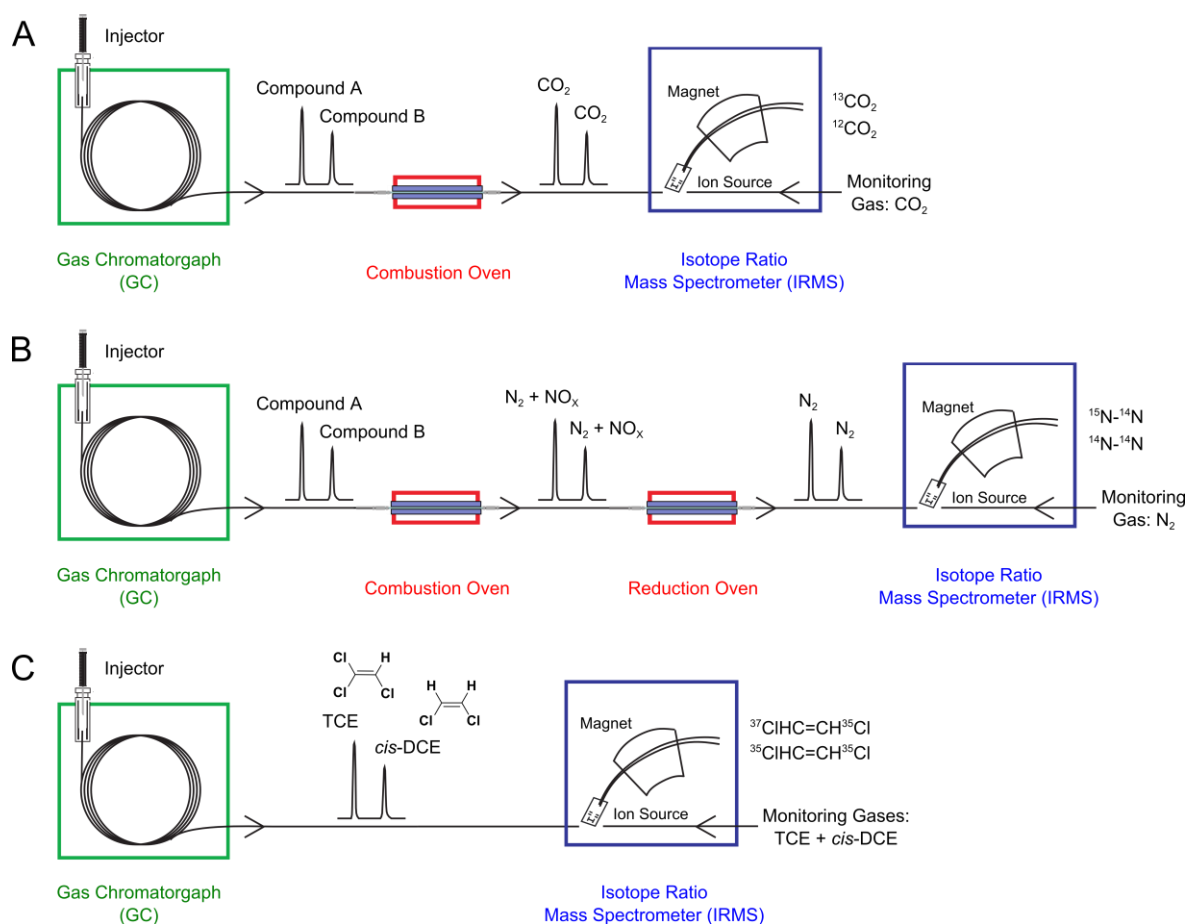
Figure 1-1. Instrumentation of compound-specific isotope analysis for (A) carbon, (B) nitrogen and (C) chlorine via GC-IRMS (adapted from Elsner et al.[20]).

1.2.3   Prospects and Challenges of CSIA

The possibility to analyze more than one element, further strengthens the possibilities of CSIA. By combining isotope changes of two elements, dual element isotope plots can be formed, e.g. for carbon and nitrogen:

$$\Lambda_{C/N} = \Delta\delta^{15}N \, / \, \Delta\delta^{13}C \approx \varepsilon_N \, / \, \varepsilon_C \tag{1-4}$$

Dual element isotope plots and the corresponding regression slopes Λ are effective indicators for the differentiation of chemical reaction mechanisms. A remarkable advantage of such regression slopes is that they are insensitive towards masking[19, 24]. Microbial transformation processes often include preceding steps like uptake of the substrate into the cell or binding of the substrate to the enzyme. Such processes can mask the isotope fractionation and

consequently the observed ε-values may be inconclusive because they do not reflect the full isotope effect of the underlying chemical mechanism[25, 26]. To circumvent this problem, isotope ratio changes of two elements can be measured. If the preceding steps do not cause isotope fractionation, isotope effects of both elements decrease to the same extent meaning that the regression slope Λ remains constant[19, 24].

Furthermore, the analysis of additional elements can lead to an even better mechanistic understanding of the underlying reaction chemistry. At field sites isotopic information from multiple elements could be a more sensitive indication of ongoing natural transformation processes and it could improve the ability to identify different sources of contamination[27, 28].

Especially the application of chlorine CSIA has increased a lot in the last years[12, 22, 29, 30] and recently it became even possible to analyze more complex structured chlorohydrocarbons like herbicides[31, 32]. This ongoing progress could advance chlorine CSIA to the method of choice for studying environmental chlorohydrocarbon contamination in the future. However, as chlorine CSIA is based on the analysis of unconverted target compounds, the availability of certain referencing standards and substance-specific working standards is of highest importance to guarantee accurate and comparable results. Additionally, it is even recommended to use two standards during analysis enabling a two-point calibration. Equation 1-1 leads to accurate results as long as samples and reference material show similar values. However, if samples and reference material lie farther apart, it becomes important to rely on a second characterized standard, which shows an isotopic shift compared to the first standard, to guarantee accurate results[20, 23, 33]. In case of referencing standards, laboratories are instructed to generate their own in-house standards. These in-house standards should be characterized against the international referencing materials which are highly valuable[34]. On the other hand, the above-mentioned increasing range of measurable compounds demands also substance-specific working standards, which have to be calibrated against the referencing standards. These working standards have to be substance-specific since target compounds are not converted to an analyte gas. The measurement process of CISA can contain steps which alter the chlorine isotope ratios of the target compounds. Therefore, substance-specific working standards, which undergo the same processes as the samples, are needed to guarantee the trueness of analysis[20, 35].

1.3 Objectives

As compound-specific stable isotope analysis is a powerful tool for studying the fate of chlorohydrocarbons, this thesis aimed to further advance chlorine isotope analysis (Chapter 2) and to investigate underlying transformation processes of chlorinated ethene (Chapter 3) and atrazine (Chapter 4) degradation.

Almost all international referencing standards for chlorine analysis have a similar value of approx. 0 ‰. Only the recently synthesized international standard USGS38 shows a pronounced negative value of $\delta^{37}Cl$ = -87.90 ± 0.24 ‰. With its isotopic shift, it enabled for the first time the two-point calibration of working standards[36, 37]. Consequently, this international standard is of a very high value and an easy synthesis route to generate an in-house referencing standard with a pronounced isotopic shift for routine characterization of chlorine isotope working standards is urgently needed. Such a standard has to be characterized against the international standard USGS38 and a second international standard to pinpoint its $\delta^{37}Cl$-value on the international scale. Therefore, one objective within Chapter 2 was the identification of a facile synthesis route for a chloride salt showing a shift in its isotope value compared to other international standards. This chloride salt had to be characterized, so that it can be used as a second anchor for two-point calibration of in-house working standards in the future. Furthermore, the instrumental advances in chlorine isotope analysis led to an increasing range of measurable substances, especially in case of more complex chlorinated organic compounds, like herbicides[38]. For such compounds, a strategy for the development of substance-specific in-house working standards has to be established. Thus, the second objective within Chapter 2 was to demonstrate that substance-specific working standards for more complex organic chlorinated micropollutants can be produced by certain chemical reactions due to their isotope fractionation effects. Here the herbicides S-metolachlor and acetochlor were chosen.

The work presented in Chapters 3 and 4 focused on exploring insights from chlorine CSIA to investigate the environmental fate of chlorinated ethenes and atrazine as most prominent chlorohydrocarbons in the environment.

In Chapter 3 reductive dechlorination pathways of chlorinated ethenes were studied with special respect to the question why bioremediation of chlorinated ethene at contaminated sites often stalls at the point of toxic *cis*-DCE or VC. Recently a vitamin B_{12} model study

revealed that two different mechanisms are responsible for dechlorination of chlorinated ethenes based on evidence from carbon and chlorine isotope analysis[17]. Whether these mechanisms are also at work during microbial dechlorination is still not known. Therefore, in this chapter carbon and chlorine isotope effects during microbial reductive dehalogenation of chlorinated ethenes were analyzed. Subsequently, the observed dual element isotope trends of carbon and chlorine were compared to the trends observed for the two mechanisms identified in the vitamin B_{12} model study. In addition, the influence of the involved predominant RDases was investigated.

In Chapter 4 chlorine isotope fractionation during atrazine microbial degradation was studied. Chlorine isotope fractionation could be a particularly more sensitive indicator of natural transformation processes of atrazine since chlorine isotope effects are fully represented in the molecular average while carbon and nitrogen isotope effects are diluted by non-reacting atoms. Carbon and nitrogen isotope effects of atrazine during microbial hydrolysis with *A. aurescens* TC1 and oxidative dealkylation with *Rhodococcus* sp. NI86/21 were analyzed in the past and chemical mechanisms could be proposed corresponding to the observed carbon and nitrogen isotope effects[39-41]. Information from chlorine isotope fractionation, in addition, could also optimize pathway distinction and source identification. Therefore, the objectives of this chapter were to degrade atrazine via microbial hydrolysis with *A. aurescens* TC1 and oxidative dealkylation with *Rhodococcus* sp. NI86/21 and subsequently analyze carbon and nitrogen and, for the first time, chlorine isotope effects. Especially the observed chlorine isotope fractionation was analyzed intensively to get insight whether it can be used as a sensitive indicator for natural transformation processes and whether it can confirm previously proposed chemical mechanisms for the two microbial degradation pathways.

2

Toward Improved Accuracy in Chlorine Isotope Analysis: Synthesis Routes for In-House Standards and Characterization via Complementary Mass Spectrometry Methods

2.1 Abstract

Increasing applications of compound-specific chlorine isotope analysis (CSIA) emphasize the need for chlorine isotope standards that bracket a wider range of isotope values in order to ensure accurate results. With one exception (USGS38),

however, all international chlorine isotope reference materials (chloride and perchlorate salts) fall within the narrow range of one per mille. Furthermore, compound-specific working standards are required for chlorine CSIA but are not available for most organic substances. We took advantage of isotope effects in chemical dehalogenation reactions to generate (i) silver chloride (CT16) depleted in $^{37}Cl/^{35}Cl$ and (ii) compound-specific standards of the herbicides acetochlor and S-metolachlor (Aceto2, Metola2) enriched in $^{37}Cl/^{35}Cl$. Calibration against the international reference standards USGS38 (-87.90 ‰) and ISL-354 ($+0.05$ ‰) by complementary methods (gas chromatography – isotope ratio mass spectrometry, GC-IRMS, versus gas chromatography – multicollector inductively coupled plasma mass spectrometry, GC-MC-ICPMS) gave a consensus value of $\delta^{37}Cl_{CT16} = -26.82 \pm 0.18$ ‰. Preliminary GC-MC-ICPMS characterization of commercial Aceto1 and Metola1 versus Aceto2 and Metola2 resulted in tentative values of $\delta^{37}Cl_{Aceto1} = 0.29 \pm 0.29$ ‰, $\delta^{37}Cl_{Aceto2} = 18.54 \pm 0.20$ ‰, $\delta^{37}Cl_{Metola1} = -4.28 \pm 0.17$ ‰ and $\delta^{37}Cl_{Metola2} = 5.12 \pm 0.27$ ‰. The possibility to generate chlorine isotope in-house standards with pronounced shifts in isotope values offers a much-needed basis for accurate chlorine CSIA.

10

2.2 Introduction

Isotopes, atomic nuclei that are identical in their chemical properties but show differences in their atomic mass, may be present in varying proportions. Stable isotope ratios are typically expressed in the δ-notation relative to a common international reference material (see Equation 2-1). This has the advantage that values, when measured in different laboratories against the same reference material, are comparable on an absolute scale[13, 33].

$$\delta^h E = [(^h E/^l E)_{Sample} - (^h E/^l E)_{Reference}] / (^h E/^l E)_{Reference} \qquad (2\text{-}1)$$

$\delta^h E$ refers to the isotope value of an element E and $(^h E/^l E)$ to the absolute ratio of the respective heavy (h) and light (l) isotopes. Positive delta values imply an enrichment, and negative delta values indicate a depletion of heavy relative to light isotopes when compared to the international reference standard[42, 43]. Isotope ratios are used in a wide field of applications. In archeology, stable isotope ratios inform about prehistoric lifestyle and diet[44]; in food sciences they serve to test the quality and the origin of foods[45]. In forensic science, isotope analysis can help trace the production site of drugs[46] and in competitive sports it can reveal doping violations[47]. Isotope analysis is equally important in the field of environmental sciences where environmental contaminants threaten the quality of groundwater resources. By analyzing isotope ratios of single compounds, compound-specific isotope analysis (CSIA) is able to allocate a contaminant to a certain source[12]. In addition, CSIA can help to detect and quantify isotope fractionation to trace degradation processes of environmental contaminants. Since bonds of molecules with heavy versus light isotopes are transformed at different rates, isotope ratios change during degradation. Hence, isotope analysis has the potential to identify degradation of contaminants even if no metabolites can be detected. As isotope effects are reaction-specific, isotope ratio analysis of the parent compound may in addition deliver information about chemical transformation pathways, even without metabolite analysis[13, 43, 48-50].

Chlorine isotope analysis ($^{37}Cl/^{35}Cl$) has increased in importance with its role in deciphering central geochemical and biological processes. Since chloride is one of the most abundant anions in geological fluids, its isotopes were measured early on to obtain information about geological processes and about the origin of chlorine found in brines and basalts[51, 52]. Furthermore, chlorine isotope analysis of perchlorate has been used to identify the source of

environmental contamination[53]. "Offline" methods such as the Holt method[54] were for a long time the only way to accomplish such chlorine stable isotope analysis. They rely on a chemical conversion of a compound in sealed glass or metal tubes and complex vacuum lines followed by isotope ratio mass spectrometry (IRMS). Hence, to enable isotope analysis of single compounds, target substances have to be purified beforehand. Afterward, they must be converted into a suitable analyte containing only one chlorine atom such as methyl chloride in the case of the Holt method[54] or CsCl for thermal ionization mass spectrometry[55]. This approach, however, is rather time, labor, and cost intensive, requires a large sample amount[54, 56] and is therefore prohibitive for compound-specific isotope analysis (CSIA) of organic compounds in trace concentrations. In turn, such chlorine CSIA has recently been made possible by advancing and optimizing instrumentation for online chlorine isotope analysis. Chromatographic separation of a sample is combined with subsequent isotope ratio analysis by a dedicated IRMS[57]. First instrumental solutions for chlorine CSIA were realized by transferring the separated chlorinated compounds in a helium carrier gas stream directly to an IRMS with dedicated cup configuration[12] or into a quadrupole mass spectrometer (qMS)[23, 29, 30]. In a most recent development, chlorine isotope analysis via GC-MC-ICPMS (gas chromatography – multicollector inductively coupled plasma mass spectrometer) has even been realized by converting organic compounds into Cl^+ ions in an inductively coupled plasma and, therefore, offering for the first time an opportunity of universal online chlorine CSIA at very low analyte concentrations (2-3 nmol of Cl)[31, 32].

Chlorine CSIA has played a key role in elucidating chlorinated ethene transformation mechanisms in lab studies[17, 58-62] and is at the verge of becoming a method of choice to study the environmental fate of chlorinated hydrocarbons at contaminated sites. Even chlorinated compounds with more complex structures like herbicides are getting within reach. At this point, however, an issue is becoming increasingly important that is crucial for chlorine CSIA on unconverted target compounds and is particularly warranted for comparison of analyses by different instrumental approaches: the need for chlorine isotope reference materials and compound-specific in-house isotope working standards.

As expressed by Equation 2-1 isotope reference standards, ideally two standards which bracket the isotope values of the samples, are crucial for true isotope measurements[23, 33, 63, 64]. International reference materials are highly valuable, rather expensive, and sometimes even available only in limited amounts. Therefore, laboratories are advised to prepare their own

in-house reference standards. These standards should be calibrated against the international reference standards[34]. In the case of chlorine, two international reference materials are available, ISL-354 (NaCl, $\delta^{37}Cl = +0.05 \pm 0.03 ‰$) and NIST SRM 975a (NaCl, $\delta^{37}Cl = +0.01 ‰$)[36, 37, 65]. Additionally, Böhlke et al.[37] were able to synthesize and characterize the oxygen and chlorine isotope reference materials USGS37 (KClO$_4$, $\delta^{37}Cl = +0.90 \pm 0.04 ‰$), USGS38 (KClO$_4$, $\delta^{37}Cl = -87.90 \pm 0.24 ‰$) and USGS39 (KClO$_4$, $\delta^{37}Cl = +0.05 ‰$) on the international scale for ClO$_4^-$ isotopic analysis. Unfortunately, most of these standards show very similar chlorine isotope values. Only one perchlorate standard, USGS38, shows a large isotopic shift, which has solved the long-standing problem that working standards for daily chlorine isotope analysis could be characterized against only one international reference standard. The availability of the standard USGS38 with its pronounced negative $\delta^{37}Cl$-value enables for the first time a two-point calibration of other chlorine standards. Since such international reference materials are very valuable, the next logical step is the preparation of in-house standards with a pronounced isotopic shift that can be routinely used for calibration on the delta scale. For example, this approach is well-entrenched for hydrogen and oxygen isotope analysis of water, where laboratories typically possess their own in-house standards that have been calibrated against the international water standards SLAP (standard light antarctic precipitation) and VSMOW (Vienna standard mean ocean water)[34].

A second challenge lies in the upcoming opportunity of chlorine CSIA which, requires sets of compound-specific working standards that bracket a suitable range of isotope values. For chlorine CSIA these working standards have to be substance-specific since there is no combustion to an analyte gas. In accordance with the IT-Principal (principal of identical treatment of referencing material and sample), the process of measurement can include isotope fractionating steps. Therefore, for each substance, the trueness of analysis has to be validated by using chemically identical standards with a known isotope value, which are subject to the same reaction conditions as the sample[20, 30, 35]. Hence, our second objective was to create such compound-specific working standards.

Even though it is well established that isotopologues can be separated by physical properties like diffusivity or vapor pressure, the corresponding processes require an extensive number of repetitions. To this end, dedicated instrumentation is needed that is beyond the scope of typical isotope laboratories. Alternatively, because most chemical reactions are accompanied

by larger isotopic fractionation than physical processes, chemical reactions can be used as a tool to synthesize standards with a more negative or a more positive isotope value than the starting material. To harvest the isotope fractionation of such a chemical reaction, three strategies may be pursued (see Scheme 2-1). Strategy 1: a substrate may be converted to a large degree, the reaction may be stopped and the remaining substrate may be purified from the reaction mixture. Strategy 2: a product may be continuously recovered in the presence of a large pool of substrate. Strategy 3: if two products are formed simultaneously, a reaction may be brought to completion, and the products may be separated to take advantage of the differences in isotope effects to the parallel products.
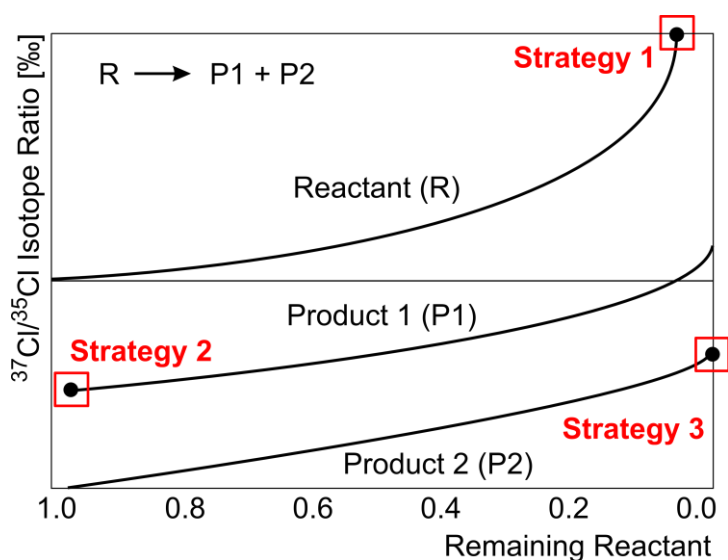
Scheme 2-1. Possible strategies to generate a standard with a shifted chlorine isotope ratio compared to the starting material.

The first objective of this study was to identify a synthesis route to easily generate and to characterize a chloride salt as chlorine isotope in-house standard. To this end, strategy 3 of Scheme 2-1 was pursued to synthesize a chloride in-house standard with a negative isotope value. Subsequently, this standard was characterized against the international chlorine reference standards USGS38 and ISL-354.

The second objective of this study was to show that chemical reactions and their corresponding isotope fractionation can be used according to strategy 1 to generate in-house working standards for chlorine CSIA of specific organic compounds. Since isotope

fractionation of micropollutants such as pesticides is receiving increasing attention[38], the herbicides S-metolachlor and acetochlor were chosen. These compounds are among the most commonly used herbicides for the protection of plants against weeds in U.S. agriculture[7]. In the environment they can have toxic effects on living organisms[66]. Thus, studying the environmental fate and the transformation pathways of these herbicides by chlorine CSIA is of particular interest.

2.3 Experimental Section

2.3.1 Synthesis of the Chlorine Isotope In-House Standard CT16

Following the protocol of Somsak et al.[67], 2,2,2-trichloroethyl acetate (14 mL) was used as a starting material. As depicted in Scheme 2-2A, the trichloroethyl group was removed by zinc in 90 % aqueous acetic acid (140 mL) via a reductive elimination process under reflux conditions at 0 °C. After 24 h, a silver nitrate solution (350 mL, 17 g/L) was added to precipitate the formed chloride as silver chloride. After filtering, the pure silver chloride (2.61 g) was dried at 40 °C overnight in the dark. Silver chloride decomposes upon exposure to light but remains perfectly stable when stored in a desiccator in the dark (brown glass bottles wrapped with aluminum foil). Even through its use may, therefore, be limited as a reference material, it represents an ideal in-house standard, because it may be directly converted to methyl chloride, which is the common measurement gas in chlorine isotope analysis.

Scheme 2-2. (A) Synthesis route to the silver chloride reference standard CT16 via reductive elimination of Cl⁻ and subsequent precipitation with $AgNO_3$. (B) Expected fractionation and the corresponding strategy to recover chloride with pronounced changes in chlorine isotope values.

2.3.2 Synthesis of the Chlorine Isotope Working Standards Aceto2 for Acetochlor and Metola2 for S-Metolachlor

Acetochlor and S-metolachlor were purchased in their pure forms (Chemos). As such they could be used as primary working standards Aceto1 and Metola1, representing one anchor point of the two-point calibration. To generate working standards with an isotopic shift for a second anchor point, 18 g of the purchased acetochlor and S-metolachlor, respectively, and NaN_3 (21.6 g/20.7 g) were dissolved in acetone (500 mL) according to the protocol of Weigl & Wünsch[68]. Like that illustrated in Scheme 2-3A, the solution was heated up to 70 °C under reflux. During the reaction, chloride was substituted by an azide group. The progress of the reaction was monitored via HPLC analysis. The reactions were stopped when 32.2 % of the initial acetochlor (approx. after 40 h) and 29.4 % of initial S-metolachlor (approx. after 94 h) were left. By flushing the solution with N_2, the solvent was evaporated at room temperature. The residue was twice dissolved in diethyl ether (200 mL), and the ether phase was washed

three times with H_2O (300 mL) and dried over Na_2SO_4. After filtering and evaporating with a rotary evaporator, the unconverted respective chloroacetanilide was purified and recovered from the rest of the reaction mixture via silica column chromatography. The eluent was n-hexane/ethyl acetate (6/1) for acetochlor, ($R_f = 0.36$) and n-hexane/ethyl acetate (4/1) for S-metolachlor ($R_f = 0.447$), respectively. In a last step the eluent was removed by rotary evaporation. 1.43 g of acetochlor (reddish oil) and 2.53 g S-metolachlor (yellowish oil) were obtained.

Scheme 2-3. (A) Synthesis of chlorine isotope working standards of acetochlor Aceto2 and S-metolachlor Metola2. (B) Expected fractionation and resultant strategy to recover unreacted acetochlor/S-metolachlor with pronounced changes in chlorine isotope values.

2.3.3 Monitoring of the Reaction Progress of Acetochlor and S-Metolachlor via HPLC

For HPLC analysis, 1 mL of reaction solution was sampled and the solvent was evaporated by flushing the sample with N_2. The residue was dissolved in 1 mL acetonitrile and analyzed on a Shimadzu UHPLC-20A system. To this end, samples were diluted (1:200) with Milli-Q/acetonitrile (80/20). A C18 column [Purospher STAR, RP-18 end-capped (5 µm), LiChroCART 125-2, Merck] was used together with acetonitrile and a KH_2PO_4 buffer (0.1 mM) as eluents. A volume of 5 µL was injected, and the oven temperature was set to 40 °C. Separation was accomplished by gradient elution at a flow rate of 0.3 mL/min starting with 40 % acetonitrile and 60 % buffer. For separation of acetochlor and acetoazide, a linear gradient to 70 % acetonitrile within 33 min was used, whereas S-metolachlor and S-metolaazide were separated in a linear gradient to 60 % acetonitrile within 22 min. The respective final conditions were maintained isocratic for 4 and 3 min, respectively, before a subsequent gradient led back to the initial conditions of 40 % acetonitrile within 1 and 0.5 min, respectively. Subsequent equilibration was for 5 min (acetochlor) and 7.5 min (S-metolachlor). Compound detection took place by UV absorbance at a wavelength of 216 nm for acetochlor and at 214 nm for S-metolachlor. Quantification was performed by the software "Lab Solutions".

2.3.4 Conversion of the International Reference Standard ISL-354 (NaCl) to Silver Chloride

The conversion of ISL-354 (NaCl (56 mg) dissolved in 50 mL Milli-Q) was accomplished by precipitation with 30 mL of silver nitrate solution (20.3 mg/mL). The precipitated silver chloride was washed twice with methanol and once with acetone. Afterward, it was dried at room temperature in the dark.

2.3.5 Conversion of the International Reference Standard USGS38 (KClO₄) to Silver Chloride

Following the protocol of Böhlke et al.[37] $KClO_4$ (2.5 mg) was filled into quartz glass ampules which were then evacuated and sealed with an oxygen torch. After heating the ampules to 720 °C for 20 min in a preheated oven, they were cracked and the Cl^- that was formed from decomposed ClO_4^- was dissolved in 2 mL warm Milli-Q water. Silver chloride

was precipitated by adding 0.1 mL of silver nitrate solution (83.3 mg/mL). The silver chloride was then washed twice with methanol and once with acetone and dried at room temperature in the dark.

2.3.6 Conversion of Silver Chloride to Methyl Chloride

A method for the conversion of silver chloride to methyl chloride was modified from Holt et al.[54]. Silver chloride (300 µg) was weighted into 10 mL headspace vials and flushed for 20 s with N_2 gas. Methyl iodide (150 µL) which was filled into 1.5 mL quartz glass inserts was added. Afterward, the vials were closed and tightly crimped with PTFE coated septa (Carl Roth) and put into the oven at 80 °C for 48 h.

2.3.7 Chlorine Isotope Analysis via GC-IRMS (Munich)

The method for chlorine isotope analysis was adapted from Shouakar-Stash et al.[22]. Measurements were performed on a gas chromatograph (Thermo Scientific, Trace GC Ultra) coupled to an isotope ratio mass spectrometer (Thermo Scientific, Finnegan MAT 253 IRMS) equipped with a direct transfer line so that the methyl chloride samples were directly transferred from the GC to the IRMS in a He carrier stream. There, the compounds were ionized and fragmented for isotope ratio analysis at the masses m/z of 50/52. To achieve optimal separation, a Vocol column (Supelco, 30 m × 0.25 mm, 1.5 µm film thickness) was used. Samples from the headspace (250 µL) were injected into the GC at a split ratio of 1:50. The GC oven temperature program started at 40 °C (1 min), increased to 100 °C at 30 °C/min, and was held for 2 min. Methyl chloride reference gas pulses were injected via a dual inlet system at the beginning and at the end of each measurement as described in Bernstein et al.[23]. Two-point calibrations were performed with the international reference standards ISL-354 ($\delta^{37}Cl = +0.05$ ‰)[36] and USGS38 ($\delta^{37}Cl = -87.90$ ‰)[37] to convert measurements to $\delta^{37}Cl$ values relative to standard mean ocean chloride (SMOC).

2.3.8 Chlorine Isotope Analysis via GC-MC-ICPMS (Leipzig)

Measurements were performed according to the protocols described in Horst et al.[31] and Renpenning et al.[32]. Samples were separated using a gas chromatograph (Thermo Scientific, Trace 1310) equipped with a Zebron ZB-1 column (Phenomenex Inc., 60 m × 0.32 mm,

1 µm film thickness). A heated transfer line coupled the GC to a multicollector inductively coupled plasma mass spectrometer (MC-ICPMS, Thermo Fisher Scientific, Neptune). For analysis of methyl chloride, 80 µL of gaseous sample were manually injected into a split/splitless injector at a temperature of 280 °C. For achieving chromatographic separation of methyl chloride and methyl iodide, the GC started at 30 °C (8 min) followed by a gradient of 10 °C/min to 100 °C. The transfer line was kept at 160 °C. A constant column flow of 2 mL/min with a split ratio of 1:10 was applied. For the analysis of acetochlor and S-metolachlor the pure substances were diluted in acetone to a final concentration of 2 ppm. Three microliters of liquid sample were manually injected into the same injector kept at a temperature of 250 °C. The GC started at a temperature of 100 °C, and after 3 min it increased to 240 °C at 20 °C/min, followed by an increase to 300 °C at 5 °C/min where the temperature was held for 5 min. The transfer line had a temperature of 280 °C. A constant column flow of 2 mL/min with a split ratio of 1:10 was applied. In-house referencing standards "TCE-2" (-2.54 ± 0.13 ‰) and "MeCl" (4.49 ± 0.10 ‰) were calibrated against methyl chloride from ISL-354 and USGS38 and subsequently used for preliminary characterization of acetochlor and S-metolachlor. In addition, further compounds (acetochlor, S-metolachlor, and atrazine) were purchased and calibrated in the same way. For results see Table 6A-S1 (Appendix).

2.4 Results and Discussion

2.4.1 Synthesis Route to a Chlorine Isotope In-House Standard on the International Scale

Reductive dehalogenation of 2,2,2-trichloroethyl acetate by zinc powder produced 1,1-dichloroethene (not analyzed) and chloride, which could be precipitated and isolated as AgCl. The pure silver chloride in-house reference standard was given the name "CT16". For chlorine isotope analysis, it was subsequently converted to methyl chloride in order to facilitate isotopic characterization by GC-MC-ICPMS and GC-IRMS against international reference standards treated in the same way.

Figure 2-1 shows that the synthesized CT16 in-house chlorine isotope reference standard was adequately bracketed by the international reference standards ISL-354 and USGS38. A first characterization of CT16 via GC-IRMS in September 2017 resulted in a value of

$\delta^{37}Cl_{CT16}$ = -26.82 ± 0.17 ‰ (see Figure 2-1A). These measurements were repeated in February 2018, yielding a value of $\delta^{37}Cl_{CT16}$ = -26.88 ± 0.28 ‰ that was identical to the first one within the analytical uncertainty (see Figure 2-1B). In a third approach CT16 was characterized via GC-MC-ICPMS giving even more precise values ($\delta^{37}Cl_{CT16}$ = -26.75 ± 0.08 ‰) which were in accordance with the GC-IRMS results (see Figure 2-1C). Consequently, the mean value over all measurements, $\delta^{37}Cl_{CT16}$ = -26.82 ± 0.18 ‰ (n = 16), is considered as a "true" consensus value for this in-house standard. As intended, this value shows a relatively large shift when compared to most international chlorine isotope reference standards which center on an isotope value of 0 ‰[36, 37, 65].

This strong negative value can be explained by the isotope effect of the reaction. During the reductive elimination depicted in Scheme 2-2A, chlorine isotope fractionation is expected to take place according to Scheme 2-2B. Bonds containing heavy isotopes are slightly more stable than bonds containing light isotopes so that bonds with light isotopes break faster[13, 58]. Consequently, ^{35}Cl is preferentially cleaved off from 2,2,2-trichloroethyl acetate meaning that the produced chloride in solution is expected to contain less ^{37}Cl per ^{35}Cl. This leads to isotope values that are strongly negative compared to the formed 1,1-dichloroethene, compared to the original substrate, and also compared to most available reference materials to date.

Identifying this synthesis route provides every laboratory the opportunity to create materials with negative chlorine isotope values. This represents a significant advance for future characterization of chlorine isotope standards: in-house working standards can be calibrated against two different reference standards, against one reference standard with an isotope value close to 0 ‰ and against a negative reference standard like CT16. By covering a wider range of isotope values, also results for the characterization of secondary in-house chlorine working standards will become more accurate which will consequently propagate into the precision and trueness of daily chlorine isotope measurements of samples. With regard to interlaboratory comparability, characterization against two reference standards leads to very accurate result relative to the international SMOC scale which will improve the quality and the international comparability of the obtained chlorine isotope values[23, 33, 63].
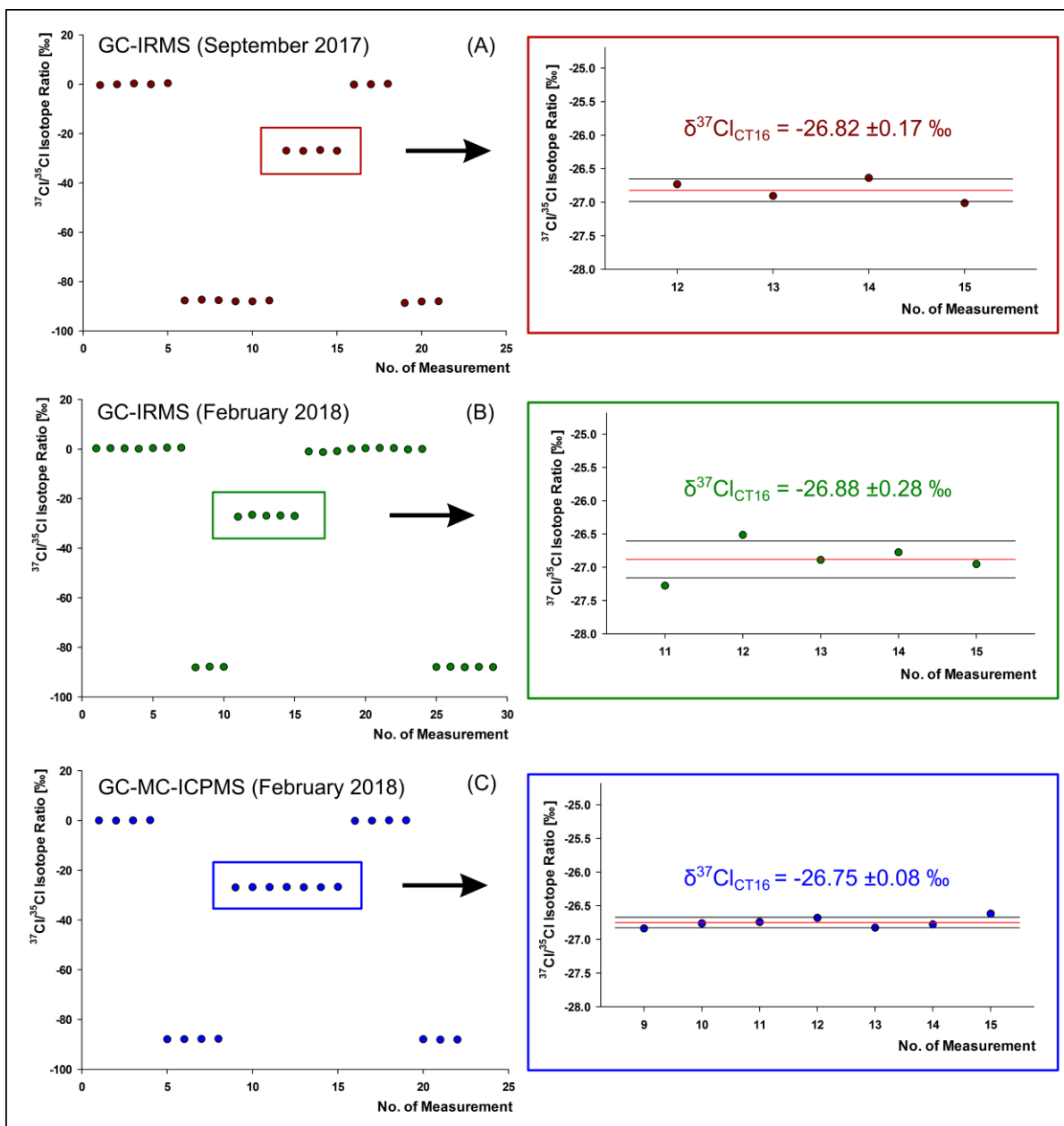
Figure 2-1. Characterization of the synthesized silver chloride reference standard CT16 against the international reference standards ISL-354 ($\delta^{37}Cl = +0.05$ ‰) and USGS38 ($\delta^{37}Cl = -87.90$ ‰). (A, B) CT16 measured via GC-IRMS in Munich at two different time points in (A) September 2017 and (B) February 2018, and (C) CT16 measured via GC-MC-ICPMS in Leipzig in February 2018. (The mean is given as value and as red line, while standard deviations are given as values and as black lines).

2.4.2 Candidate Compounds for Compound-Specific Chlorine Isotope Working Standards

Reactions of acetochlor and S-metolachlor with sodium azide were stopped when ~70 % of the substrates were converted to sodium chloride and acetoazide and metolaazide, respectively. The remaining substrates were named "Aceto2" and "Metola2". Together with the original substances, which were named "Aceto1" and "Metola1", the isolated Aceto2 and Metola2 were measured via GC-MC-ICPMS.

Figure 2-2 shows that the synthesized working standards Aceto2 and Metola2 exhibit significantly more positive chlorine isotope values than the initial substances Aceto1 and Metola1. For acetochlor, the initial substance Aceto1 was characterized to have an isotope value of $\delta^{37}Cl_{Aceto1} = 0.29 \pm 0.29$ ‰ tentatively determined by GC-MC-ICPMS. The synthesized working standard Aceto2 shows an isotope value of $\delta^{37}Cl_{Aceto2} = 18.54 \pm 0.20$ ‰ corresponding to an isotopic shift of ~18 ‰ (see Figure 2-2A). Measurements of S-metolachlor resulted in an isotopic shift of ~9 ‰. By the same GC-MC-ICPMS analysis Metola1, the initial substance, was attributed a chlorine isotope value of $\delta^{37}Cl_{Metola1} = -4.28 \pm 0.17$ ‰ and the synthesized working standard, Metola2, a value of $\delta^{37}Cl_{Metola2} = 5.12 \pm 0.27$ ‰ (see Figure 2-2B).
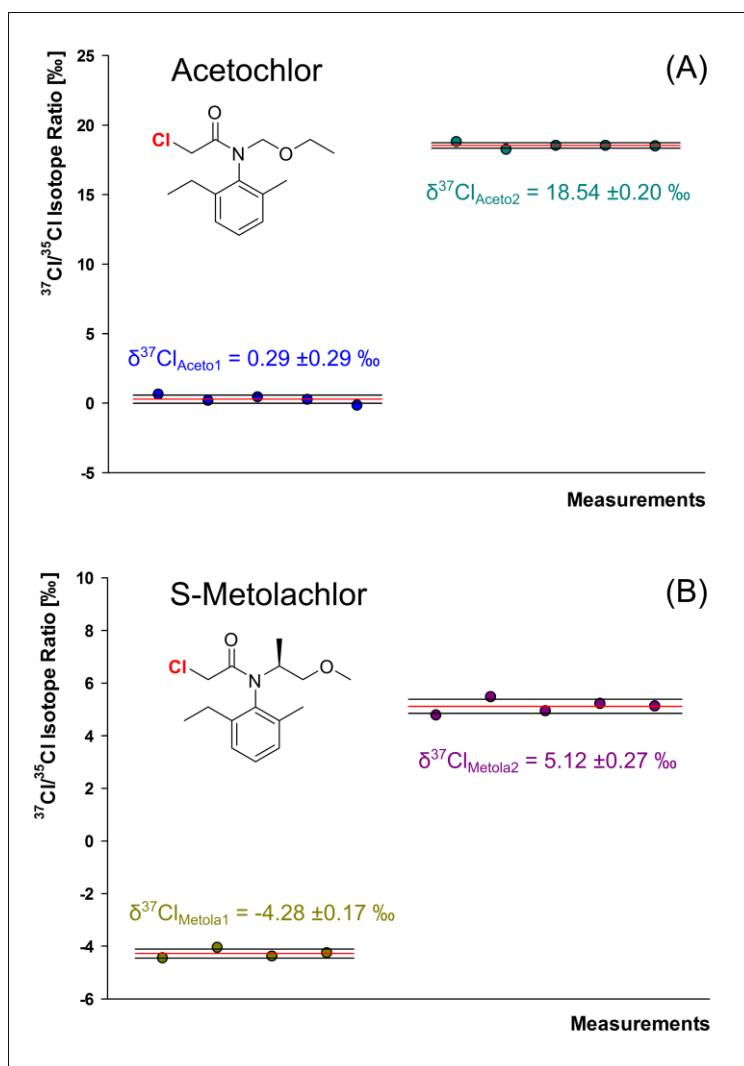
Figure 2-2. Characterization of (A) the acetochlor working standards Aceto1 and Aceto2 and (B) the S-metolachlor working standards Metola1 and Metola2. (The mean is given as value and as red line, while standard deviations are given as values and as black lines).

The change in chlorine isotope values for each of the two substances happened due to the isotope effect of the underlying second order nucleophilic chemical substitution reaction (S_N2, Scheme 2-3A). As illustrated in Scheme 2-3B, owing to the leaving group isotope effect associated with chloride substitution, the remaining substrate got enriched in heavy relative to light chlorine isotopes leading to a more positive chlorine isotope value compared to the value of the original substrate before the start of the reaction.

These results illustrate that organic chemistry can be used to generate substance-specific working standards with pronounced shifts in chlorine isotope values. Thus, working standards for other chlorinated complex organic compounds may also be generated in the

future so that stable chlorine isotope analysis of these compounds will help to further illuminate sources and transformation (pathways).

2.5 Conclusion

Specific synthesis routes were identified to generate five standards, the in-house anchor CT16 and the working standards Aceto1 / Aceto2 and Metola1 / Metola2, for stable chlorine isotope analysis. In particular, the synthesis route to silver chloride (CT16) provides an opportunity to generate much-needed in-house standards for chlorine isotope analysis. The possibility to use two standards which differ in their chlorine isotope value will optimize future characterization results of secondary chlorine working standards. More accurate in-house working standards will in turn optimize the precision and trueness of daily chlorine isotope measurements. In addition, the synthesis of the working standards for acetochlor (Aceto1 and Aceto2) and S-metolachlor (Metola1 and Metola2) showed that organic synthesis can generate substance-specific isotope working standards also of more complex chlorinated organic compounds. These working standards become even more important as GC-qMS methods for stable chlorine isotope analysis of acetochlor and S-metolachlor were recently developed by Ponsin et al.[69]. However, two of the working standards show a chlorine isotope value larger than 0 ‰ ($\delta^{37}Cl_{Aceto2}$ = 18.54 ± 0.20 ‰ and $\delta^{37}Cl_{Metola2}$ = 5.12 ± 0.27 ‰). Therefore, future work has to strive for synthesis routes to generate AgCl in-house standards with a more positive chlorine isotope value that would optimize the characterization process of secondary in-house working standards even further. The ongoing development of new calibration standards together with the advancement of stable chlorine isotope analysis now offers a suite of accurate methods for chlorine isotope analysis (offline DI-IRMS, online GC-MS and GC-IRMS, offline and online MC-ICPMS). By using these synergistic effects, the development of stable isotope analysis of chlorine can be further accelerated which will open up new perspectives to study environmental contaminants and to characterize commercial products in the future.

3

Mechanistic Dichotomy in Bacterial Trichloroethene Dechlorination Revealed by Carbon and Chlorine Isotope Effects

Lihl, C.; Douglas, L.M.; Franke, S.; Pérez-de-Mora, A.; Meyer, A.H.; Daubmeier, M.; Edwards, E.A.; Nijenhuis, I.; Sherwood Lollar, B.; Elsner, M.; *Environmental Science & Technology* **2019**, 53, (8), 4245-4254.

3.1 Abstract

Tetrachloroethene (PCE) and trichloroethene (TCE) are significant groundwater contaminants. Microbial reductive dehalogenation at contaminated sites can produce nontoxic ethene but often stops at toxic *cis*-1,2-dichloroethene (*cis*-DCE) or vinyl chloride (VC). The magnitude of

carbon relative to chlorine isotope effects (as expressed by $\Lambda_{C/Cl}$, the slope of $\delta^{13}C$ versus $\delta^{37}Cl$ regressions) was recently recognized to reveal different reduction mechanisms with vitamin B_{12} as a model reactant for reductive dehalogenase activity. Large $\Lambda_{C/Cl}$ values for *cis*-DCE reflected cob(I)alamin addition followed by protonation, whereas smaller $\Lambda_{C/Cl}$ values for PCE evidenced cob(I)alamin addition followed by Cl^- elimination. This study addressed dehalogenation in actual microorganisms and observed identical large $\Lambda_{C/Cl}$ values for *cis*-DCE ($\Lambda_{C/Cl} = 10.0$ to 17.8) that contrasted with identical smaller $\Lambda_{C/Cl}$ for TCE and PCE ($\Lambda_{C/Cl} = 2.3$ to 3.8). For TCE, the trend of small $\Lambda_{C/Cl}$ could even be reversed when mixed cultures were precultivated on VC or DCEs and subsequently confronted with TCE ($\Lambda_{C/Cl} = 9.0$ to 18.2). This observation provides explicit evidence that substrate adaptation must have selected for reductive dehalogenases with different mechanistic motifs. The patterns of $\Lambda_{C/Cl}$ are consistent with practically all studies published to date, while the difference in reaction mechanisms offers a potential answer to the long-standing question of why bioremediation frequently stalls at *cis*-DCE.

3.2 Introduction

Chlorinated ethenes such as tetrachloroethene (PCE) and trichloroethene (TCE), are among the most frequent groundwater pollutants at contaminated sites worldwide[3]. Under anoxic conditions they may be reductively dechlorinated by microorganisms in a process known as organohalide-respiration. Chloroethenes act as electron acceptors so that their C-Cl bonds are reduced to C-H bonds (sequential hydrogenolysis) leading to nontoxic ethene as final product (see Figure 3-1)[5]. While this reaction stoichiometry is straightforward, the exact nature of the underlying biochemical reaction mechanism has been elusive.
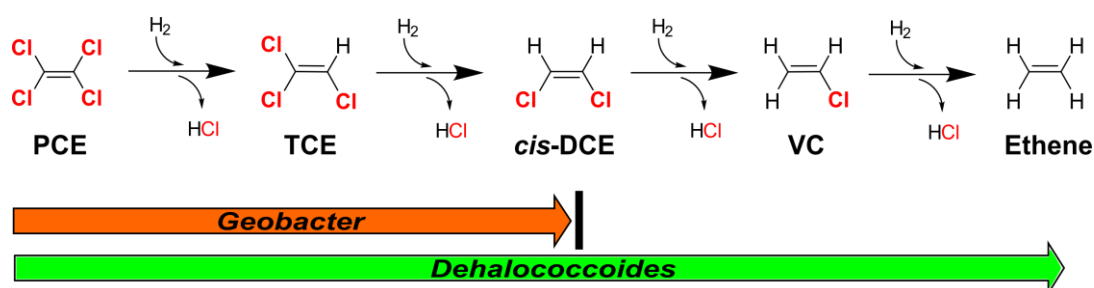
Figure 3-1. Reductive dechlorination of PCE to ethene with different end-points for two bacterial cultures.

Transformation frequently stalls at the stage of *cis*-1,2-dichloroethene (*cis*-DCE) or vinyl chloride (VC) constituting one of the long-standing barriers to successful bioremediation of these ubiquitous priority pollutants. Only specialized degrader strains, bacteria belonging to the class *Dehalococcoidia* (e.g., certain *Dehalococcoides mccartyi* and *Dehalogenimonas* strains), were found to be capable of complete dechlorination to harmless ethene[70-77]. In contrast, other microorganisms, such as *Geobacter lovleyi*, cannot dechlorinate beyond *cis*-DCE[71] (see Figure 3-1). Pinpointing the underlying mechanistic reasons, however, has remained an elusive goal. Even though the catalytic site of all known reductive dehalogenases (RDases) contains cobalamin as an essential Co(I)-containing corrinoid cofactor, these enzymes occur in a great structural variety[5, 71, 78-80]. Very few dehalogenase protein structures have been solved yet[78, 79], and no reductive dehalogenase has been uniquely characterized for its underlying biochemical transformation mechanism (i.e., bond cleavage and formation). Consequently, critical research gaps in the chemistry of reductive dechlorination exist. Is the mechanism the same for all substrates? Does the mechanism

correlate with a given substrate? Or do mechanisms vary with the observed variety of reductive dehalogenases and organisms?

With reduced vitamin B_{12} as a chemical model system, we recently achieved a breakthrough in understanding reaction mechanisms *in vitro*[17]. Our evidence suggests that cob(I)alamin acts as a supernucleophile and adds to the double bond in chlorinated ethenes so that a carbanion complex is formed. If the free electron pair of this complex faces two vicinal Cl substituents (as in the reaction of PCE) one of them will be in the *anti*-position, leading to fast elimination of Cl⁻ and producing a cobalamin chlorovinyl complex as short-lived intermediate (Scheme 3-1). In contrast, if there is only one vicinal Cl substituent (as in the reaction of *cis*-DCE) the molecular conformation is unfavorable for subsequent elimination so the carbanion is protonated instead. This results in a slower reaction pathway involving an intermediate chloroalkyl complex (Scheme 3-1). If there can be either one or two vicinal Cl substituents (as in the reaction of TCE) the addition-protonation pathway is favored at low pH, whereas the addition-elimination pathway is favored at high pH (Scheme 1). In contrast, the number and position of geminal Cl substituents does not seem to have an effect on the reaction mechanism.
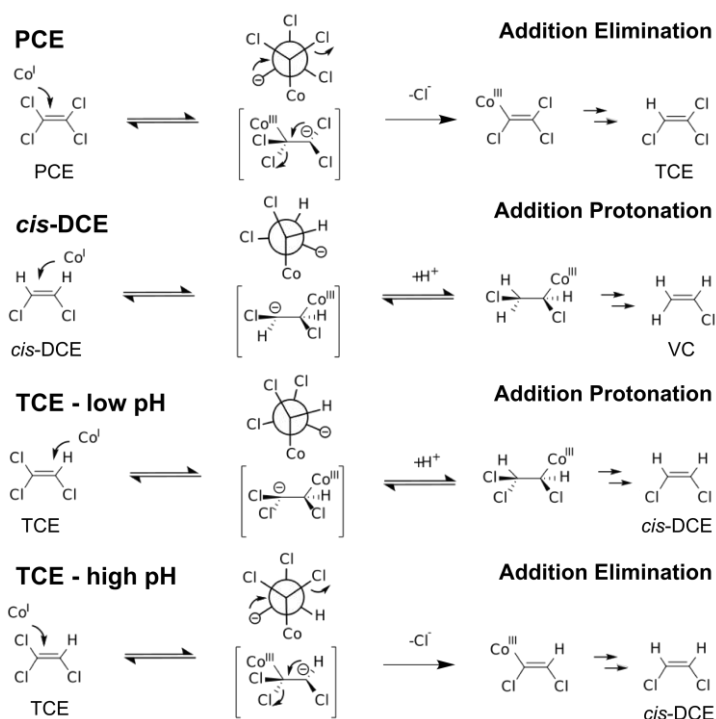
Scheme 3-1. Reaction mechanisms for the reductive dehalogenation of chlorinated ethenes via addition protonation or addition elimination (adapted from Heckel et al.[17]).

30

Both TCE dechlorination pathways eventually produce *cis*-DCE as the respective hydrogenolysis product (Scheme 3-1) so that the different mechanisms are difficult to distinguish from product analysis alone. Additional experimental evidence is, therefore, warranted to determine whether the mechanistic dichotomy identified with vitamin B_{12} is also at work in reductive dehalogenases or in dehalogenating organisms.

Compound-specific stable isotope effect analysis offer precisely such a complementary line of evidence. Gas-chromatography (GC) coupled to isotope ratio mass spectrometry (IRMS) measures carbon $(^{13}C/^{12}C)$[81, 82] and chlorine $(^{37}Cl/^{35}Cl)$ isotope ratios at natural isotopic abundance[22, 23, 57]. Measured isotope ratios are expressed in the δ-notation; for example, for carbon:

$$\delta^{13}C = [(^{13}C/^{12}C)_{Sample} - (^{13}C/^{12}C)_{Reference}] / (^{13}C/^{12}C)_{Reference} \qquad (3\text{-}1)$$

where $(^{13}C/^{12}C)_{Reference}$ is the isotope ratio of an international reference material to ensure comparability between laboratories[42, 43]. An analogous equation applies to chlorine. When correlating these isotope values of two elements relative to each other the regression slope

$$\Lambda_{C/Cl} = (\delta^{13}C - \delta^{13}C_0) / (\delta^{37}Cl - \delta^{37}Cl_0) \approx \varepsilon_C/\varepsilon_{Cl} \qquad (3\text{-}2)$$

reflects the magnitude of the underlying compound-specific isotope effects during a reaction[13]. Here δ-values express the isotope ratios of carbon and chlorine at a given time and at the beginning of the reaction ($\delta^{13}C_0$ and $\delta^{37}Cl_0$), respectively. Carbon and chlorine enrichment factors (ε_C and ε_{Cl}, respectively) reflect compound-specific isotope effects[13] that express by how much molecules with heavy isotopes react slower than molecules with light isotopes[43, 83]. A value of $\varepsilon = -10\,‰$, for example, corresponds to a compound-specific isotope effect of $^{12}k/^{13}k = 1.01$ (for the experimental evaluation of ε see Equation 3-3 below). Our vitamin B_{12} study demonstrated that the slope $\Lambda_{C/Cl}$ can provide a sensitive indicator of the underlying reaction mechanisms in reductive chlorinated ethene dehalogenation with vitamin B_{12}[17]. Values of $\Lambda_{C/Cl}$ were much larger in the addition-protonation mechanism, reflecting the fact that no C-Cl bond was cleaved in the initial step so that chlorine isotope effects were small. In contrast, values of $\Lambda_{C/Cl}$ were smaller in the addition-elimination mechanism, reflecting the larger chlorine isotope effect associated with C-Cl bond cleavage.

The objective of this study was to analyze carbon and chlorine isotope effects during reductive dehalogenation of chloroethenes with different bacterial cultures. The resulting $\Lambda_{C/Cl}$ values were compared with the $\Lambda_{C/Cl}$ values of two mechanistic trends recently

observed in a vitamin B_{12} model system. To this end, we investigated in particular whether the isotope fractionation trends in microbial dechlorination of *cis*-DCE and PCE correlate with trends of the addition-protonation and the addition-elimination mechanism observed with vitamin B_{12}, respectively. For TCE dechlorination both mechanisms were observed in the vitamin B_{12} study depending on pH. To test whether evidence of both mechanisms may be observed for TCE in living bacteria as well, microbial dechlorination of TCE was studied in seven different experiments, either varying in precultivation substrate or in the type of predominant RDases inside the bacteria. Finally, the isotopic data of the dechlorination experiments of this study were compared with the literature data of available C/Cl isotope studies to test whether the picture of a mechanistic dichotomy is consistent with published evidence to date.

3.3 Materials and Methods

3.3.1 *cis*-DCE and TCE Dechlorinating Cultures

Dehalogenation experiments with *cis*-DCE were carried out using *Dehalococcoides mccartyi* strain 195[73] and the highly enriched *Dehalococcoides mccartyi* strain BTF08 culture[75, 84]. Dehalogenation experiments with TCE were conducted with a single pure culture (*Geobacter lovleyi* strain KB-1) and six mixed cultures (KB-1/1,2-DCA, KB-1/VC, KB-1/cDCE, WBC-2/tDCE, KB-1 RF and Donna II) (see Table 3-1 for further details). *G. lovleyi* strain KB-1, KB-1/1,2-DCA, KB-1/VC, KB-1/cDCE and KB-1 RF were derived from KB-1, a commercially available enrichment culture, which is specialized in the dehalogenation of chlorinated ethenes. It contains *G. lovleyi* strain KB-1 and a minimum of three strains of *Dehalococcoides* as well as non-dechlorinating bacteria such as acetogens and methanogens[85-89]. Prior to the experiment the cultures were enriched on different maintenance substrates for many years (see Table 3-1).

Table 3-1. Summary of precultivation conditions, RDases and compound-specific isotope enrichment factors of carbon and chlorine.

Substrate for Dehalogenation and Isotope Analysis	Culture	Dechlorinators	Precultivation Substrate (electron donor)	Most abundant functional *rdhA* Genes*		Slope $\Lambda_{C/Cl}$**	ε_{Cl} [‰]**	ε_{C} [‰]**	Duration
				before	**after**				
cis-DCE	*D. mccartyi* 195	*D. mccartyi* 195 (pure culture)	*cis*-DCE (hydrogen)	*tceA* [90]	*tceA* [90]	10.0 ±0.4	-2.3 ±0.4	-23.2 ±4.1	no lag period, *cis*-DCE dehalogenation completed after one month
cis-DCE	*D. mccartyi* BTF08	*D. mccartyi* BTF08 (enrichment culture)	*cis*-DCE (hydrogen)	*tceA* [74]	*tceA* [74]	17.8 ±1.0	-1.7 ±0.4	-31.1 ±6.3	no lag period, *cis*-DCE dehalogenation completed after one month
TCE	*G. lovleyi* KB-1	*G. lovleyi* KB-1 (pure culture)	PCE (acetate)	*Geo-pceA* [91]	*Geo-pceA* [91]	3.1 ±0.1	-3.3 ±0.3	-10.3 ±0.8	no lag period, TCE dehalogenation completed within one day
TCE	KB-1 RF	multiple *D. mccartyi* strains (enrichment culture; no *Geobacter*)	TCE (methanol)	*vcrA* [91]	*vcrA* [91]	2.7 ±0.2	-3.3 ±0.3	-9.6 ±0.5	no lag period, TCE dehalogenation completed within one day
TCE	Donna II	*D. mccartyi* 195 (mixed culture; only one strain of *D. mccartyi*)	TCE (butyrate)	*tceA* [92]	*tceA* [92]	2.3 ±0.1	-5.7 ±0.4	-13.5 ±0.6	no lag period, TCE dehalogenation completed within one day
TCE	KB-1/1,2-DCA	multiple *D. mccartyi* strains (enrichment cultures)	1,2-DCA (methanol)	*tceA* [93]	*tceA, vcrA*	4.5 ±0.8	-1.2 ±0.3	-5.4 ±1.5	long lag period (30-40 days), TCE dehalogenation completed after 70-100 days
TCE	KB-1/VC	multiple *D. mccartyi* strains (enrichment cultures)	VC (methanol)	*vcrA* [91]	*vcrA*	18.2 ±4.3	-0.5 ±0.6	-10.6 ±9.3	long lag period (30-40 days), TCE dehalogenation completed after 70-100 days
TCE	KB-1/cDCE	multiple *D. mccartyi* strains (enrichment cultures)	*cis*-DCE (methanol)	*bvcA vcrA* [91]	*vcrA (tceA)*	11.8 ±2.4	-0.7 ±0.2	-8.3 ±3.4	long lag period (30-40 days), TCE dehalogenation completed after 70-100 days
TCE	WBC-2/tDCE	*Dehalogenimonas* sp., *D. mccartyi* (enrichment culture)	*trans*-DCE (lactate/ethanol)	*tdrA (Dhgm), vcrA (Dhc)* [76]	*vcrA (tceA, tdrA)*	9.0 ±1.1	-0.7 ±0.3	-7.0 ±1.9	long lag period (30-40 days), TCE dehalogenation completed after 70-100 days

* The abundance of specific *rdhA* genes known to be present in the cultures was used as a way to track which of multiple strains grew in the mixed culture; *rdhA* genes in brackets were only detected in minor abundance; the KB-1 enrichments were selected because each harbored a different dominant expressed RDase initially.
** ±95 % confidence intervals

3.3.2 Biotic Dechlorination of cis-DCE under Anoxic Conditions with D. mccartyi Strain 195 and Strain BTF08

D. mccartyi strain 195 was cultivated as described in Cichocka et al.[94] and Maymo-Gatell et al.[73] with addition of butyrate pellets. *D. mccartyi* strain BTF08 was cultivated following the protocol of Cichocka et al.[75] and Schmidt et al.[95]. For each strain a set of 23 serum bottles (50 mL) was filled with 25 mL anoxic medium and flushed with N_2 and CO_2 (70/30 %). After closing the bottles by crimping with Teflon-lined grey butyl rubber stoppers they were sterilized for 40 min at 120 °C. Next, they were spiked with *cis*-DCE (500 µM) as electron acceptor and equilibrated overnight. On the next day, the bottles were inoculated with a culture grown on *cis*-DCE (2.5 % v/v for strain 195, 5 % v/v for strain BTF08). For each set, three non-inoculated bottles with substrate served as the negative control. The bottles were complemented with hydrogen as electron donor (0.5 bar overpressure). All cultures were incubated in the dark without shaking at 20 °C (BTF08) or 30 °C (195). Progress of substrate dehalogenation was monitored by concentration measurements with gas chromatography paired with flame ionization detection (GC-FID). At different levels of dechlorination bottles were sacrificed for analysis by stopping the dechlorination reaction with 1 mL acidic sodium sulfate solution (280 g/L, pH ≈1) following the protocol of Cichocka et al.[94]. Samples were stored at 4 °C in the dark for later carbon and chlorine isotope analysis via gas chromatography – isotope ratio mass spectrometry (GC-IRMS).

3.3.3 Biotic Dehalogenation of TCE under Anoxic Conditions with G. lovleyi Strain KB-1, KB-1/1,2-DCA, KB-1/VC, KB-1/cDCE and WBC-2/tDCE

A total of 200 mL defined mineral medium[96] and 55 µL resazurin (0.4 %) were filled in glass bottles (250 mL). Subsequently they were capped with Mininert valves (Supelco) and purged for 40 min with a N_2/CO_2 gas mixture (80/20 %). Each bottle of *G. lovleyi* strain KB-1 was complemented with 50 µL of acetate (1 M) and 9 µL of TCE, whereas each bottle of KB-1/VC, KB-1/cDCE, and KB-1/1,2-DCA was complemented with 20 µL of methanol and 9 µL of TCE and each bottle of WBC-2/tDCE was complemented with 22 µL of lactate solution (75 g/L), 44 µL of ethanol and 9 µL of TCE. All substances and solutions for complementation were taken from anoxic stocks. Afterwards all bottles were continuously agitated on an orbital shaker at 60 rpm at room temperature for 24 h for equilibration. Biotic

dehalogenation started by inoculating each bottle with 20 mL of active culture. To eliminate the carryover of volatile organic compounds the active cultures had been purged for 1 h with a N_2/CO_2 gas mixture (80/20 %). The bottles were prepared in triplicates for each culture. Furthermore, for each culture, non-inoculated bottles with substrate served as negative control and were monitored alongside the experimental bottles. A total of 5 min after inoculation, the first samples were taken. The next samples were taken in intervals throughout the dehalogenation process. At each sampling point, 7 mL of liquid were removed from all the bottles. The sample of 7 mL was then divided into 1 mL aliquots that were distributed into seven glass vials (1.5 mL each) and closed with PTFE-lined screw-top caps. All samples were fixed with 50 µL NaOH (1 M) to stop biological activity. One of the seven vials was used for instant concentration analysis that was performed on a GC-FID. The other six vials were frozen upside down for later isotope analysis of carbon and chlorine performed via GC-IRMS[97, 98]. Preparation of the cultures (except the purging with N_2/CO_2) and taking of the samples was conducted in a glovebox containing an anoxic atmosphere (80 % N_2, 20 % H_2).

3.3.4 Biotic Dehalogenation of TCE under Anoxic Conditions with KB-1 RF and Donna II

The whole experiment was conducted in a glovebox containing an anoxic atmosphere (80 % N_2, 10 % H_2, 10 % CO_2). Glass bottles (260 mL) were filled with 200 mL (KB-1 RF) or 210 mL (Donna II) of defined mineral medium[96] and inoculated with 20 mL (KB-1 RF) or 10 mL (Donna II) active culture. Beforehand, the cultures were purged with a N_2/CO_2 gas mixture for 30 min to eliminate carryover of volatile organic compounds. Triplicate experimental bottles were capped with Mininert valves (Supelco) and complemented by adding 20 µL of methanol (KB-1 RF), 8.75 µL of butyrate (Donna II) and 9 µL of TCE. Furthermore, for each culture non-inoculated bottles with substrate and killed control bottles (sterilized before TCE addition) served as negative control and were monitored alongside the experimental bottles. All replicates were continuously shaken at 350 rpm at room temperature (24 °C). At each time point, headspace samples were removed first for concentration measurements via GC-FID and then for carbon isotope analysis via GC-IRMS. Subsequently 4 mL liquid samples were removed and split into 1 mL aliquots. Liquid samples were acidified to a pH of < 2 with 50 µL of 1 M H_2SO_4 and closed with PTFE-lined

screw-top caps and then frozen upside down in 1.5 mL glass vials for later chlorine isotope measurements via GC-IRMS[97, 98]. Sample volumes removed were compensated with identical volumes of glovebox atmosphere to maintain a constant pressure within the bottle. Septa inside the stopper of the Mininert vials were replaced after every second piercing to minimize leakage.

3.3.5 Concentration Measurements and Carbon and Chlorine Isotope Analysis

Concentration measurements via GC-FID and compound-specific isotope analysis of carbon and chlorine via GC-IRMS were performed according to defined protocols (see Appendix).

3.3.6 Evaluation of Carbon and Chlorine Isotope Fractionation

Carbon and chlorine enrichment factors (ε_C and ε_{Cl}) of *cis*-DCE and TCE dechlorination were calculated according to the Rayleigh equation (Equation 3-3) using Sigma-Plot. The Rayleigh equation describes the gradual enrichment of the residual substrate fraction f with molecules containing heavy isotopes[13, 43]; for example, for carbon:

$$\ln [(\delta^{13}C+1) / (\delta^{13}C_0+1)] = \varepsilon_C \cdot \ln f \qquad\qquad (3\text{-}3)$$

The isotope ratios of carbon refer to certain time points, with one of them at the beginning of an experiment ($\delta^{13}C_0$). By plotting values of $\delta^{13}C$ versus $\delta^{37}Cl$ (see Equation 3-2), dual element isotope plots were obtained. These processes are also illustrated in Figure 3-2. 95 % confidence intervals (CI) show the uncertainties of the calculated slopes $\Lambda_{C/Cl}$ ($\Delta\delta^{13}C/\Delta\delta^{37}Cl$). In chemical reactions, isotope effects occur predominantly at the reacting position. Therefore, in many cases, a position-specific apparent kinetic isotope effect (AKIE) may be estimated under the assumption that there are no isotope effects at the other positions according to

$$\text{AKIE}_{\text{position-specific}} = 1 / (n \cdot \varepsilon_{\text{reacting position}} + 1) \qquad\qquad (3\text{-}4)$$

where n is the number of atoms in intramolecular competition[13]. However, for chlorinated ethene reduction our mechanistic picture (Scheme 3-1) suggests that the situation is more complex because isotope effects occur in different steps of the reaction sequence, and they may occur at different positions of the molecule[17, 58]. In addition, from IRMS measurements alone, intramolecular isotope effects are difficult to resolve. Thus, in this study, we decided

not to estimate position-specific isotope effects but instead to report compound-specific isotope effects in the form of ε-values.

3.3.7 qPCR Analysis of KB-1/1,2-DCA, KB-1/VC, KB-1/cDCE and WBC-2/tDCE

Quantitative polymerase chain reaction (qPCR) analyses were conducted after the completion of the TCE experiment. An 8.5 mL sample of each culture was collected and, subsequently, 1.5 mL of 50 % glycerol were added. The samples were stored at -80 °C after freezing in liquid nitrogen. For qPCR analysis, 8 mL of each thawed sample were filtered through a sterile 0.22 µM Sterivex filter (Millipore) using an Air Cadet vacuum/pressure pump 400-1902 (Barnant Company). After filtration, the Sterivex filters were immediately frozen at -80 °C. The filters were removed from the filter casing, sliced into small pieces with a sterile surgical blade, and then transferred to a bead-beating tube. For DNA extraction the PowerSoil DNA isolation kit (Mo Bio Laboratories Inc.) was used. The DNA was extracted by following the manufacturer's protocol for maximum yields except that DNA was eluted in 50 µL of sterile UltraPure distilled water (Invitrogen) rather than in the eluent provided with the kit. Using a spectrophotometer (NanoDrop ND-1000; NanoDrop Technologies) the DNA concentration and quality were assessed. Afterwards, the DNA samples were 10 times diluted with sterile UltraPure distilled water. All subsequent steps were performed in a PCR cabinet (ESCO Technologies). qPCR reactions were run in triplicates in which each run was calibrated by constructing a standard curve using known plasmid DNA concentrations containing the gene insert of interest. The standard curve was run with eight concentrations ranging from 10 to 108 gene copies per microliter. qPCR reaction solutions (20 µL) were prepared in sterile UltraPure distilled water containing 10 µL of EvaGreen Supermix, 0.5 µL of each primer (forward and reverse, each from 10 µM stock solutions) and 2 µL of diluted template (DNA extract or standard plasmids). The qPCR reactions were conducted using a CFX96 real-time PCR detection system with a C1000 Thermo Cycler using SsoFast EvaGreen supermix (Bio-Rad Laboratories). The thermocycling program started with the initial denaturation at 95 °C for 2 min, followed by 40 cycles of denaturation at 98 °C for 5 s, annealing for 10 s (see Table 6B-S1 in the Appendix for annealing temperatures), and a plate read. A final melting curve analysis was conducted at the end of the program. The following genes were targeted by qPCR using the defined primer sets (see Table 6B-S1 in the Appendix): the phylogenetic 16S rRNA genes of

Dehalococcoides and *Dehalogenimonas*; the functional genes *vcrA*, *tceA*, *bvcA* and *tdrA*; as well as the 16S rRNA genes of total bacteria and total archaea.

3.4 Results and Discussion

3.4.1 *Starkly Contrasting Carbon and Chlorine Isotope Effects in Microbial Dechlorination of cis-DCE and PCE*

To take advantage of compound-specific isotope effects and evaluate whether the mechanistic dichotomy observed *in vitro* can also be identified in pure strains of living organisms, we began with a comparison between PCE and *cis*-DCE. Carbon and chlorine isotope values of *cis*-DCE were measured in dehalogenation experiments with the strictly anaerobic organism *D. mccartyi* strain 195[73] and the highly enriched *D. mccartyi* strain BTF08 culture[75, 84]. Results were compared with our previous data on reductive dechlorination of PCE by *Desulfitobacterium* sp. strain Viet1[58]. Figure 3-2 shows the changes in carbon and chlorine isotope ratios with decreasing fraction of respective substrate and the corresponding enrichment factors. Combining the isotope ratios of panel A (carbon) and B (chlorine) leads to a dual element isotope plot as illustrated in panel C.
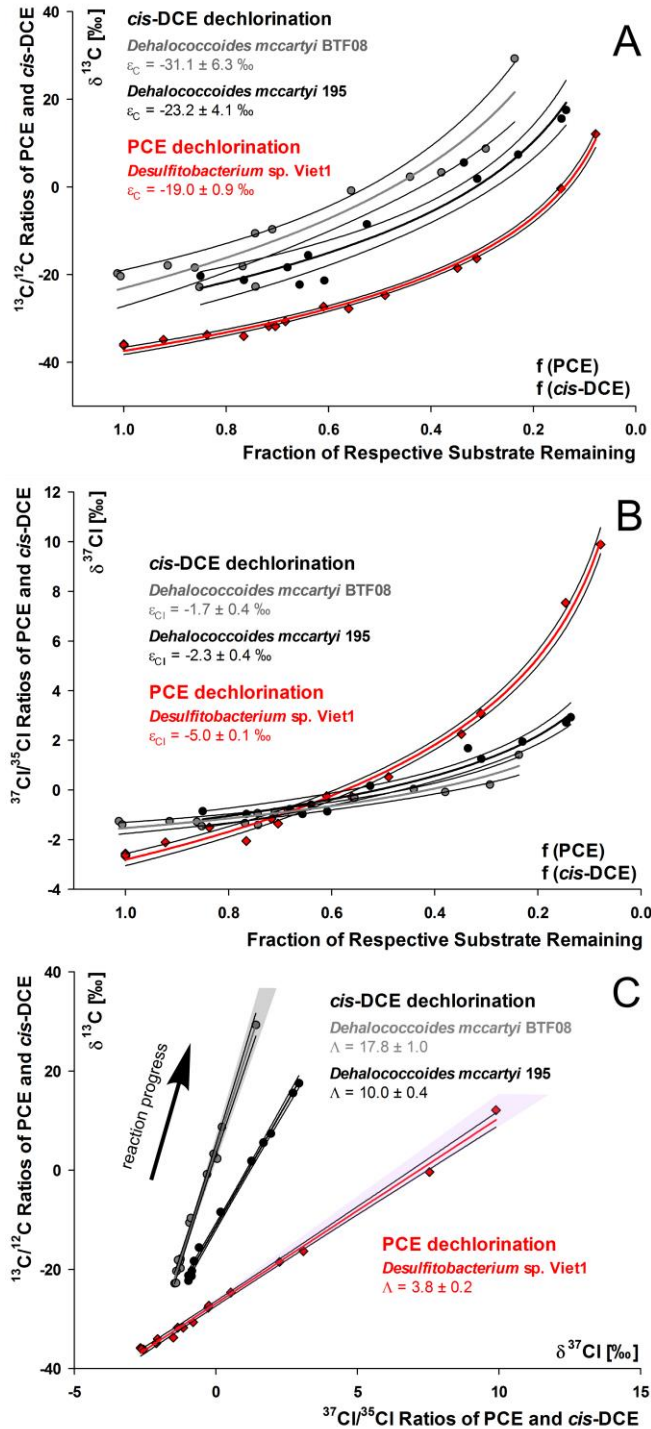
Figure 3-2. Carbon and chlorine isotope effects in reductive dehalogenation of *cis*-DCE by *D. mccartyi* BTF08 (grey) and *D. mccartyi* 195 (black) and PCE by *Desulfitobacterium* sp. Viet1 (red) (data from Cretnik et al.[58]), resulting in a dual element isotope plot. (The 95 % confidence intervals are given as values and as black lines next to the regression slopes). (A) Carbon isotope fractionation and corresponding carbon enrichment factors ε_C. (B) Chlorine isotope fractionation and corresponding chlorine enrichment factors ε_{Cl}. (Both ε-values were evaluated according to Equation 3-3). (C) Resulting dual element isotope plots ($\delta^{13}C$ versus $\delta^{37}Cl$) indicate the occurrence of different underlying transformation mechanisms corresponding to mechanisms observed with *cis*-DCE (shaded in grey) and PCE (shaded in pink) by model reactions with vitamin B_{12}[17].

39

The dual element isotope trends with bacteria reproduced the trends obtained with vitamin B_{12} and were reflected on the level of compound-specific carbon and chlorine isotope effects, illustrated by ε_C and ε_{Cl}. The dechlorination of *cis*-DCE was associated with large carbon and small chlorine isotope effects (*D. mccartyi* 195: $\varepsilon_C = -23.2 \pm 4.1$ ‰, $\varepsilon_{Cl} = -2.3 \pm 0.4$ ‰; *D. mccartyi* BTF08: $\varepsilon_C = -31.1 \pm 6.3$ ‰, $\varepsilon_{Cl} = -1.7 \pm 0.4$ ‰) resulting in large dual element isotope slopes $\Lambda_{195} = 10.0 \pm 0.4$ and $\Lambda_{BTF08} = 17.8 \pm 1.0$. In contrast, dechlorination of PCE was associated with pronounced isotope effects in both elements ($\varepsilon_C = -19.0 \pm 0.9$ ‰, $\varepsilon_{Cl} = -5.0 \pm 0.1$ ‰) giving rise to a smaller dual element isotope slope $\Lambda_{Desulfitobacterium} = 3.8 \pm 0.2$. This large chlorine isotope effect is even more striking when one considers that it is averaged over four chlorine atoms in PCE (of which only one is cleaved off), while in *cis*-DCE the average is taken over only two chlorine atoms. Hence, kinetic isotope effects of PCE and *cis*-DCE at the reacting position (after correcting for the dilution by non-reacting chlorine atoms) would show even greater differences[19]. The same would be true for dual element isotope slopes $\Lambda_{C/Cl}$. Our results therefore provide key lines of evidence suggesting that *cis*-DCE and PCE must be dechlorinated via different mechanisms, and that they exemplify the pattern observed for addition-protonation versus addition-elimination pathways (Scheme 3-1 and Figure 3-2)[17].

3.4.2 Dual Element Isotope Trends in TCE Dechlorination by Pure Cultures: Indication of an Addition-Elimination Mechanism

In an *in vitro* study using vitamin B_{12} as model system, TCE was recently observed to be dechlorinated via two different reaction mechanisms depending on pH (see Figure 3-3A and Scheme 3-1). To probe which mechanism would be observed for TCE *in vivo* with bacterial pure cultures, a *Geobacter* subculture (*Geobacter lovleyi* KB-1) of the mixed consortium KB-1 that had been cultivated to purity was investigated and compared with previously observed trends for *Geobacter lovleyi* SZ and *Desulfitobacterium hafniense* Y51[98] (Figure 3-3B). The dual element isotope slopes of the pure cultures correspond to the dual element isotope slopes of the vitamin B_{12} study at high pH values, indicating that *in vivo* TCE is dechlorinated via the addition-elimination pathway.
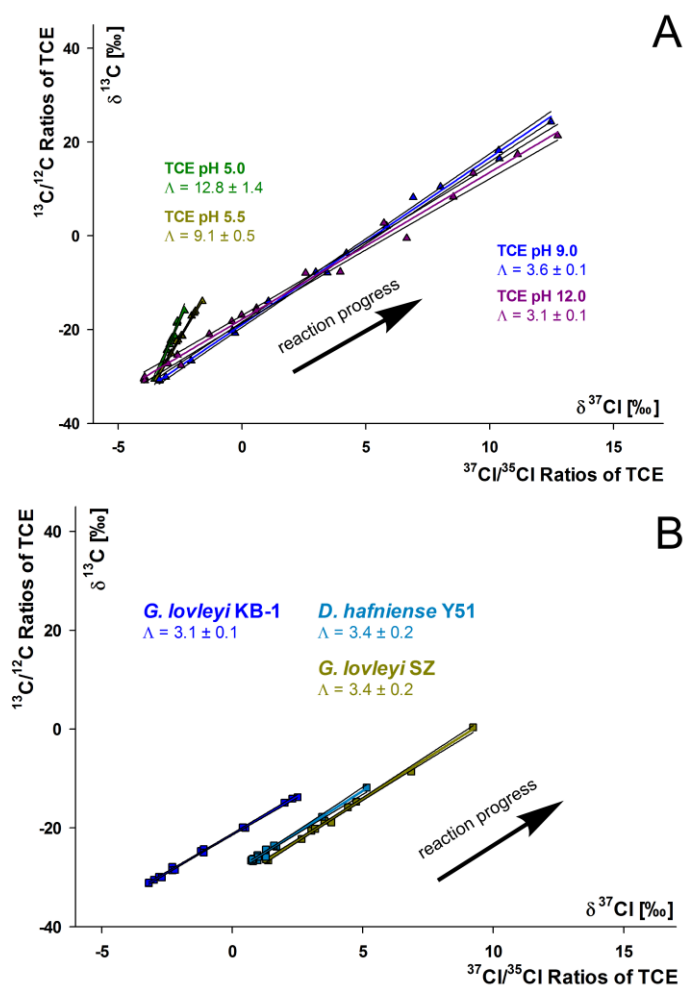
Figure 3-3. Carbon and chlorine isotope effects in TCE reductive dehalogenation (A) by vitamin B_{12} at different pH values and (B) with pure cultures resulted in similar dual element isotope plots. (The 95 % confidence intervals are given as values and as black lines next to the regression slopes). (A) TCE reductive dehalogenation at low (green/yellow) and high (purple/blue) pH values (adapted from Heckel et al.[17]). (B) TCE reductive dechlorination with the pure culture *G. lovleyi* KB-1 (dark blue, this work) and the pure cultures *G. lovleyi* SZ (yellow) and *D. hafniense* Y51 (blue) (adapted from Cretnik et al.[98]).

3.4.3 Precultivation of Bacteria on Less Chlorinated Ethenes and TCE Dual Element Isotope Trends: Indication of an Addition-Protonation Mechanism

To investigate whether a different reaction mechanism can nonetheless be observed for TCE when using precultivation conditions to select for organisms with a different substrate preference, we conducted another set of experiments. Mixed cultures, Donna II and KB-1 RF, were precultivated on PCE or TCE for years (see Table 3-1), meaning that they were already adapted to TCE (substrate or daughter product of PCE dechlorination).

41

However, we maintained another set of cultures on less chlorinated precultivation substrates: three subcultures of the dechlorinating consortium KB-1 RF that were maintained on *cis*-DCE (KB-1/cDCE), VC (KB-1/VC) and 1,2-DCA (KB-1/1,2-DCA) for at least two years and a fourth mixed culture that was enriched on *trans*-DCE (WBC-2/tDCE) for many years. As expected, cultures precultivated on TCE and PCE started to dechlorinate TCE immediately and the dechlorination was completed within one day (see Table 3-1). In contrast, the set of cultures enriched and precultivated on less chlorinated ethenes showed a lag period of 30-40 days before they started to dechlorinate TCE and dechlorination took 70-100 days for completion.
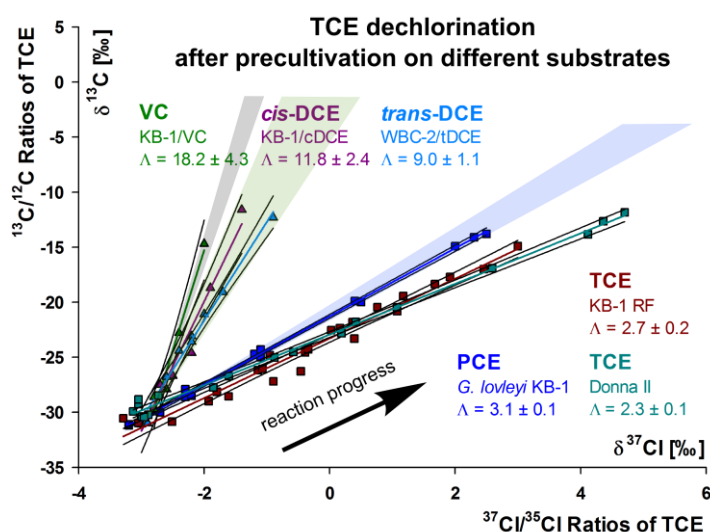
Figure 3-4. Dual element isotope trends indicate a mechanistic divide between TCE dechlorination by cultures precultivated on PCE (*G. lovleyi* KB-1, blue) and TCE (KB-1 RF, brown and Donna II, cyan) vs. cultures precultivated on VC (KB-1/VC, light green), *cis*-DCE (KB-1/cDCE, purple), and *trans*-DCE (WBC-2/tDCE, light blue). Shaded areas show the corresponding trends observed with *cis*-DCE (grey, pH 6.5) and TCE (green, low pH/blue, high pH) in the vitamin B_{12} model[17]. (95 % confidence intervals are given as values and as black lines next to the regression slopes).

Figure 3-4 shows that precultivation affected the carbon and chlorine isotope effects. A clear divide appears between two dual element isotope trends depending on precultivation conditions. Cultures precultivated on less chlorinated ethenes such as VC (KB-1/VC), *cis*-DCE (KB-1/cDCE) and *trans*-DCE (WBC-2/tDCE) showed large carbon isotope effects in combination with small chlorine isotope effects corresponding to $\Lambda_{C/Cl}$ values between 9.0

and 18.2 ($\Lambda_{KB-1/VC} = 18.2 \pm 4.3$, $\Lambda_{KB-1/cDCE} = 11.8 \pm 2.4$ and $\Lambda_{WBC-2/tDCE} = 9.0 \pm 1.1$). In contrast the cultures *G. lovleyi* strain KB-1, KB-1 RF, and Donna II, precultivated on TCE or PCE, showed significantly smaller $\Lambda_{C/Cl}$ values of 2.3 to 3.1 ($\Lambda_{Donna\ II} = 2.3 \pm 0.1$, $\Lambda_{KB-1\ RF} = 2.7 \pm 0.2$, $\Lambda_{G.\ lovleyi\ KB-1} = 3.1 \pm 0.1$) indicative of larger chlorine isotope effects. These results are similar to the dual element isotope slopes $\Lambda_{C/Cl}$ observed for an addition-elimination mechanism with vitamin B_{12}. In contrast, cultures precultivated on less chlorinated substrates [*cis*-DCE (KB-1/cDCE), VC (KB-1/VC), and *trans*-DCE (WBC-2/tDCE)] resulted in $\Lambda_{C/Cl}$ values of TCE dechlorination that correspond to an addition-protonation pathway with vitamin B_{12}.

Our observations suggest that in the bacterial cells a similar mechanistic dichotomy of cob(I)alamin addition-elimination versus cob(I)alamin addition-protonation took place as in the model reaction with vitamin B_{12} at different pH (Scheme 3-1). In experiments with bacterial cells, however, both the medium and the inside of the cells were buffered so that catalysis of the different pathways must be effectuated by functional groups inside the enzymes' catalytic sites rather than by a different pH in bulk solution. We therefore hypothesize that the enzyme architecture of RDases is tailored to different specific reaction mechanisms, possibly due to the presence/absence of amino acids with specific protonation functionalities.

3.4.4 *Mechanism-Specific Dual Element Isotope Trends of TCE: Lack of Correlation with RDase Predominance*

Given that we observed evidence of different reaction mechanisms in bacterial reductive dehalogenation of TCE, we further explored whether this mechanistic dichotomy could be correlated with the predominance of specific reductive dehalogenases. Therefore, three different bacterial cultures, which had been adapted to TCE and for which the predominance of different RDases can be inferred (see Table 3-1), were compared. *G. lovleyi* strain KB-1 has been shown to harbor only one RDase, *Geo*-PceA[91]. For the mixed culture KB-1 RF, the RDase VcrA is considered to be responsible for dechlorination[91]. In the mixed culture Donna II, *D. mccartyi* strain 195 is the organism responsible for dechlorination, and the RDase TceA was identified as the most prominent dechlorinating enzyme[92].

The key outcome of this approach was that the dual element isotope plot of these three cultures shows similar regression slopes ($\Lambda_{Donna\ II} = 2.3 \pm 0.1$, $\Lambda_{KB-1\ RF} = 2.7 \pm 0.2$,

$\Lambda_{G. lovleyi \text{KB-1}} = 3.1 \pm 0.1$, see Table 3-1 and Figure 6B-S2) for all three experiments, indicating that TCE was dechlorinated via a similar chemical mechanism, irrespective of the type of RDase (*Geo*-PceA versus VcrA versus TceA). The three slopes agree with those at high pH in the vitamin B_{12} study[17], suggesting that in all three cases, a sequence of addition-elimination was the predominant reaction pathway.

Subsequently, quantitative polymerase chain reaction (qPCR) analysis was applied to detect changes in the reductive dehalogenase gene (*rdhA*) composition when cultures that had been precultivated on less chlorinated ethenes were adapting to TCE reductive dechlorination (see Table 3-1). qPCR analysis indicated a significant shift in the culture KB-1/cDCE after changing the electron acceptor from *cis*-DCE to TCE. Typically, KB-1/cDCE is dominated by the RDase BvcA when precultivated on *cis*-DCE[91]. After the TCE dechlorination experiment, however, the *rdhA* gene *bvcA* was no longer detected in the qPCR analysis. Instead, the *rdhA* gene *vcrA* was most abundant, indicating that TCE dechlorination was likely performed by a *vcrA*-containing strain of *Dehalococcoides*. For the WBC-2/tDCE culture, only minor changes in the RDase composition were observed. Here the *vcrA* and *tdrA* genes were predominant before[76] and after the experiment. WBC-2/tDCE contains *Dehalogenimonas* sp., which expresses TdrA for the dechlorination of *trans*-DCE to VC[76]. Additionally, after the TCE dechlorination experiment, a small number of *tceA* genes were detected by qPCR. In case of KB-1/VC, no changes in the *rdhA* gene composition were discernible. Before[91] and after the TCE dechlorination experiment with KB-1/VC, *vcrA* was the most abundant RDase gene analyzed. The information obtained from the qPCR data therefore suggests that the maintenance on one specific precultivation substrate has a significant influence on the microbial community and the prevalence of RDase genes[93]. Nevertheless, isotope effects of all cultures still gave evidence of the same addition-protonation mechanism (see Table 3-1 and Figure 6B-S2) suggesting that the reaction mechanism was conserved in precultivated cultures even though shifts in the dominantly expressed RDase were observed.

Finally, a comparison of Figure 3-4 and the qPCR data on predominant RDases (see Table 3-1 and Figure 6B-S2) suggests that there can be different mechanisms at work ($\Lambda_{\text{KB-1 RF}} = 2.7 \pm 0.2$ versus $\Lambda_{\text{KB-1/VC}} = 18.2 \pm 4.3$) even though the same nominal RDase gene (*vcrA*) was predominant. One possibility is that the VrcA dehalogenase complex in organisms adapted to less chlorinated substrates is different from those enriched on TCE.

Kublik et al.[99] showed that in *Dehalococcoides*, the reductive dehalogenase is part of a complex containing a variety of proteins. Potentially, these other electron transport proteins may affect the enzyme and its isotope fractionation. In addition, the role of corrinoid prosthetic groups, which can affect dechlorination[80, 100], has to be further investigated because it was unclear what types of corrinoids were produced in the mixed cultures. Another possibility is that the RDase catalyzing the dechlorination in the non-TCE-adapted cultures is not VcrA, even though the strains contained that gene. Quantitative polymerase chain reaction can only reveal that the *vcrA* gene became more abundant after switching the electron acceptor, but qPCR cannot provide direct information about whether the RDase was actually expressed. For example, Heavner et al.[101] described that in all *Dehalococcoides* spp., particularly in KB-1, a specific RDase (DET 1545 homologue) shows elevated expression upon stress.

The observation that the predominance of nominal RDases did not correlate with isotope effect trends therefore highlights the need for a complementary approach to classify degradation in natural and engineered systems: a classification based not only on the metagenomic detection of RDase genes but also on dual element (C, Cl) isotope fractionation as indicator of underlying (bio)chemical transformation mechanisms. For the transformation of TCE with different pure corrinoid cofactors, dual element isotope slopes between 3.7 and 4.5 were recently observed[61], which we may now interpret as indicative of an addition-elimination mechanism.

3.4.5 Previously Observed Stable Isotope Fractionation: Consistency with the Mechanistic Dichotomy Observed in This Study

Figure 3-5 shows our data in the context of previously reported dual element isotope trends $\Lambda_{C/Cl}$ in reductive dehalogenation by bacteria[58-60, 62, 98, 102-104], in enzyme extracts[61] and by pure cofactors[61, 98] or model systems[17, 98]. To account for the potential effect of masking, these values of $\Lambda_{C/Cl}$ are plotted against the corresponding carbon isotope enrichment factors ε_C. Pronounced negative ε_C-values indicate that intrinsic isotope effects are strongly expressed meaning that the influence of masking is small. Vice versa, only slightly negative ε_C-values (corresponding to data points Figure 3-5, region shaded in green) indicate that intrinsic isotope effects were strongly masked meaning that observable $\Lambda_{C/Cl}$ values did not necessarily reflect the intrinsic biochemical reaction. Data points located in this putative

masking-dominated domain are derived from microbial degradation of PCE ($\Lambda_{C/Cl}$ values of 0.7 to 2.8 and slightly negative ε_C-values of -0.7 ‰ to -5.6 ‰)[59-61], as well as from the TCE dechlorinating culture KB-1/1,2-DCA (ε_C = -5.4 ± 1.5 ‰ and $\Lambda_{KB-1/1,2-DCA}$ = 4.5 ± 0.8) of this study. These smaller dual element isotope slopes potentially do not reflect the chemical bond conversion but rather a preceding step (e.g., mass transfer into the cell, substrate-enzyme binding, etc.)[61] and are, therefore, not discussed further here.

Pronounced negative ε_C, together with moderate $\Lambda_{C/Cl}$ values (Figure 3-5, region shaded in yellow) are indicative of the addition-elimination mechanism[17] brought forward in this study. Indeed, the microbial data in this domain[58, 59, 98, 102-104] originate almost exclusively from the dechlorination of PCE and TCE, including this study's data with cultures adapted to TCE ($\Lambda_{Donna\ II}$ = 2.3 ± 0.1, $\Lambda_{KB-1\ RF}$ = 2.7 ± 0.2 and $\Lambda_{G.\ lovleyi\ KB-1}$ = 3.1 ± 0.1). Similar trends were observed in transformation of TCE with enzymatic extracts[61] and purified cofactors[61, 98] in which all values fell in a rather narrow experimental range ($\Lambda_{C/Cl}$ = 3.7 - 5.3), indicating that the predominance of an addition-elimination mechanism can be traced down to the enzyme level[17]. An exception is a former *cis*-DCE degradation study ($\Lambda_{C/Cl}$ = 4.5). The nature of this degradation with field sediment rather than bacterial cultures was, however, little constrained, so general conclusions are difficult[104].

In contrast, data points corresponding to pronounced negative ε_C, together with large $\Lambda_{C/Cl}$ values (Figure 3-5, region shaded in grey) are indicative of the addition-protonation mechanism[17]. Indeed, all data are derived from either *cis*-DCE dechlorination (this and previous[62, 104] studies), or from TCE reductive dechlorination at low pH in the vitamin B_{12} model system[17] or by cultures precultivated on less chlorinated ethenes (this study). Taken together, the regions of Figure 3-5 confirm that also all dual element isotope trends reported so far are consistent with the mechanistic dichotomy observed in this study.
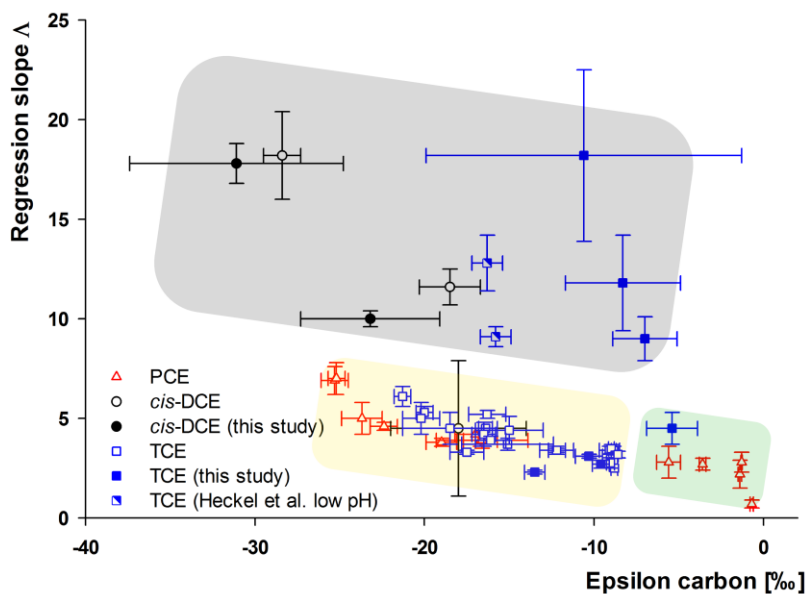
Figure 3-5. Carbon isotope fractionation factors ε_C and dual element isotope regression slopes $\Lambda_{C/Cl}$ in reductive chlorinated ethene dehalogenation by bacteria[58-60, 62, 98, 102-104], in enzyme extracts[61], by pure cofactors[61, 98] or model systems[17, 98] observed in this study (filled symbols) and reported from previous studies (empty and half-filled symbols). Reductive dechlorination of PCE is depicted by red triangles, of TCE by blue squares and of *cis*-DCE by black circles. (Error bars show 95 % confidence intervals of respective values). Shaded areas illustrate regions which indicate that intrinsic isotope effects are masked (green) or that they follow an addition-elimination mechanism (yellow) or an addition-protonation mechanism (grey).

3.5   Environmental Significance

Available dual element isotope data reveal a surprising dichotomy in reductive dechlorination chemistry of microbial communities. These results suggest that for dehalogenation of chlorinated ethenes catalyzed by RDases two different reductive dechlorination mechanisms exist, which are mimicked by the addition-elimination versus addition-protonation pathways identified in a recent vitamin B$_{12}$ study[17]. The evidence that reductive dehalogenases may be optimized to catalyze fundamentally different mechanisms, despite an identical net reaction (hydrogenolysis), offers an explanation why some RDases can be specialized in the dechlorination of PCE and TCE but cannot dechlorinate *cis*-DCE or VC. These results, therefore, hold promise to potentially resolve a fundamental challenge to our understanding of reductive dechlorination that has been a long-standing barrier to successful bioremediation in the field: why dechlorination of chlorinated ethenes often stops at *cis*-DCE or VC. A new RDase classification system based on catalyzed mechanisms may,

therefore, represent a transformative advance to the field in the future. Finally, this study highlights the potential of dual element compound-specific stable isotope analysis as an enabling technology with which to overcome these long-standing dilemmas of organic (bio)chemistry: to bridge the gap between *in vitro* and *in vivo*, to probe for reaction mechanisms in organisms, and to directly observe a change of the involved RDases by detecting underlying dechlorination mechanisms at contaminated sites.

4

Compound-Specific Chlorine Isotope Fractionation in Biodegradation of Atrazine

4.1 Abstract

Atrazine is a frequently detected groundwater contaminant. It can be microbially degraded by oxidative dealkylation or by hydrolytic dechlorination. Compound-specific isotope analysis is a powerful tool to assess its transformation. In previous work, carbon and nitrogen isotope effects were found to reflect these different transformation pathways. However, chlorine isotope fractionation could be a particularly sensitive indicator of natural transformation since chlorine isotope effects are fully represented in the molecular average while carbon and nitrogen isotope effects are diluted by non-reacting atoms. Therefore, this study explored chlorine isotope effects during atrazine hydrolysis with *Arthrobacter aurescens* TC1 and oxidative dealkylation with *Rhodococcus* sp. NI86/21. Dual element isotope slopes of chlorine vs. carbon isotope fractionation ($\Lambda^{Arthro}_{Cl/C} = 1.7 \pm 0.9$ vs. $\Lambda^{Rhodo}_{Cl/C} = 0.6 \pm 0.1$) and chlorine vs. nitrogen isotope fractionation ($\Lambda^{Arthro}_{Cl/N} = -1.2 \pm 0.7$ vs. $\Lambda^{Rhodo}_{Cl/N} = 0.4 \pm 0.2$) provided reliable indicators of different pathways. Observed chlorine isotope effects in oxidative dealkylation ($\varepsilon_{Cl} = -4.3 \pm 1.8$ ‰) were surprisingly large, whereas in hydrolysis ($\varepsilon_{Cl} = -1.4 \pm 0.6$ ‰) they were small, indicating that C-Cl bond cleavage was not the rate-determining step. This demonstrates the importance of constraining expected isotope effects of new elements before using the approach in the field. Overall, the triple element isotope information brought forward here enables a more reliable identification of atrazine sources and degradation pathways.

4.2 Introduction

The herbicide atrazine has been used in agriculture to inhibit growth of broadleaf and grassy weeds[6]. In the U.S. atrazine was the second most commonly used herbicide in 2012 and is still in use today[7]. In the European Union atrazine was banned in 2004[9], but together with its metabolites it is still frequently detected at high concentrations in groundwater[10, 105]. The massive and widespread use has led to a wide-ranging presence of atrazine in the environment, which can have harmful effects on living organisms and humans[11]. Therefore, the environmental fate of atrazine is of significant concern and much attention has been directed at detecting and enhancing its natural biodegradation. However, assessing microbial degradation of atrazine in the environment is challenging with conventional methods like concentration analysis. Sorption and remobilization of the parent compound and its metabolites, as well as further transformation of the metabolites inevitably lead to fluctuations in concentrations[39, 40, 106, 107], which make it difficult to assess the net extent of atrazine degradation in the field.

In recent years, compound-specific isotope analysis (CSIA) has been proposed as an alternative approach to detect and quantify the degradation of atrazine[108-110].

In contrast to, and complementary to traditional methods, CSIA informs about transformation without the need to detect metabolites. The reason is that during (bio)chemical transformations molecules with heavy isotopes are typically enriched in the remaining substrate since their bonds are more stable and, therefore, usually react slower than molecules containing light isotopes (normal kinetic isotope effect). The ratios of heavy to light isotopes (e.g. $^{13}C/^{12}C$ for carbon) in the remaining substrate, therefore, change during transformation. Observing such changes can be used as direct (and concentration-independent) indicator of degradation[12, 13].

Isotope values are reported in the δ-notation relative to an international reference material, e.g. for carbon[12, 13]:

$$\delta^{13}C = [(^{13}C/^{12}C)_{Sample} - (^{13}C/^{12}C)_{Reference}] / (^{13}C/^{12}C)_{Reference} \qquad (4\text{-}1)$$

The magnitude of the degradation-induced isotope fractionation depends on different factors, which can make isotope ratios of specific elements particularly attractive to observe degradation-induced isotope fractionation. To this end, first, an element needs to be directly

involved in the (bio)chemical reaction. For example, a carbon isotope effect would be quite generally expected in organic molecules, whereas a chlorine isotope effect would be primarily expected if a C-Cl bond is cleaved. Second, isotope fractionation depends on the underlying kinetic isotope effect (see above), but also on the extent to which this effect is represented in the molecular average isotope fractionation described by the enrichment factor ε (see below). Atrazine, for example, contains only one chlorine atom but eight carbon and five nitrogen atoms. Hence, chlorine isotope effects at the reacting position are fully represented in the molecular average, whereas position-specific carbon and nitrogen isotope effects are diluted by non-reacting atoms[12, 13].

Most of the publications studying the chemical mechanisms of abiotic and microbial atrazine degradation have focused on the analysis of carbon ($^{13}C/^{12}C$) and nitrogen ($^{15}N/^{14}N$) isotope fractionation. Thereby, ε-values in the range of -5.4 ‰ to -1.8 ‰ for carbon and -1.9 ‰ to 3.3 ‰ for nitrogen were observed[39-41, 111]. Chlorine isotope effects for microbial atrazine degradation were so far not reported due to analytical challenges[48]: Until recently[32, 69], suitable methods were not available for chlorine isotope analysis of atrazine. However, from the magnitude of chlorine isotope effects observed for dechlorination of trichloroethenes (-5.7 ‰ to -3.3 ‰, where intrinsic isotope effects are diluted by a factor of three[112]), very large chlorine enrichment factors ε_{Cl} (-8 ‰ to -10 ‰ or even larger) could potentially occur for a C-Cl bond cleavage in atrazine. For example, enzymatic hydrolysis of the structural homologue ametryn (atrazine structure with a -SCH_3 instead of a -Cl group) yielded a sulfur isotope enrichment factor ε_S of -14.7 $\pm$ 1.0 ‰[111]. If the cleavage of carbon-chlorine bonds is involved in the rate-determining step of a (bio)transformation, chlorine isotope effects could, therefore, enable a particularly sensitive detection of natural transformation processes by compound-specific (i.e., molecular average) isotope analysis.

The measurement of chlorine isotope fractionation is attractive for yet another reason – multiple element isotope analysis bears potential for a better distinction of sources and transformation pathways. From isotope analysis of one element alone, it is difficult to distinguish sources of a particular compound, or competing transformation pathways that may lead to metabolites of different toxicity[13]. For example, two different microbial transformation pathways can lead to the degradation of atrazine in the environment. Hydrolysis forms the nontoxic dehalogenated product 2-hydroxyatrazine (HAT) whereas oxidative dealkylation degrades atrazine to the still herbicidal products desethyl- (DEA) or

desisopropyl-atrazine (DIA)[113, 114]. Prominent examples for microorganisms catalyzing these pathways are *Arthrobacter aurescens* TC1 and *Rhodococcus* sp. NI86/21 (see Figure 4-1). *A. aurescens* TC1 was directly isolated from an atrazine-contaminated soil[115]. By expressing the enzyme TrzN, it is capable of performing hydrolysis of atrazine[115, 116]. *Rhodococcus* sp. NI86/21 uses a cytochrome P450 system for catalyzing oxidative dealkylation of atrazine[117].
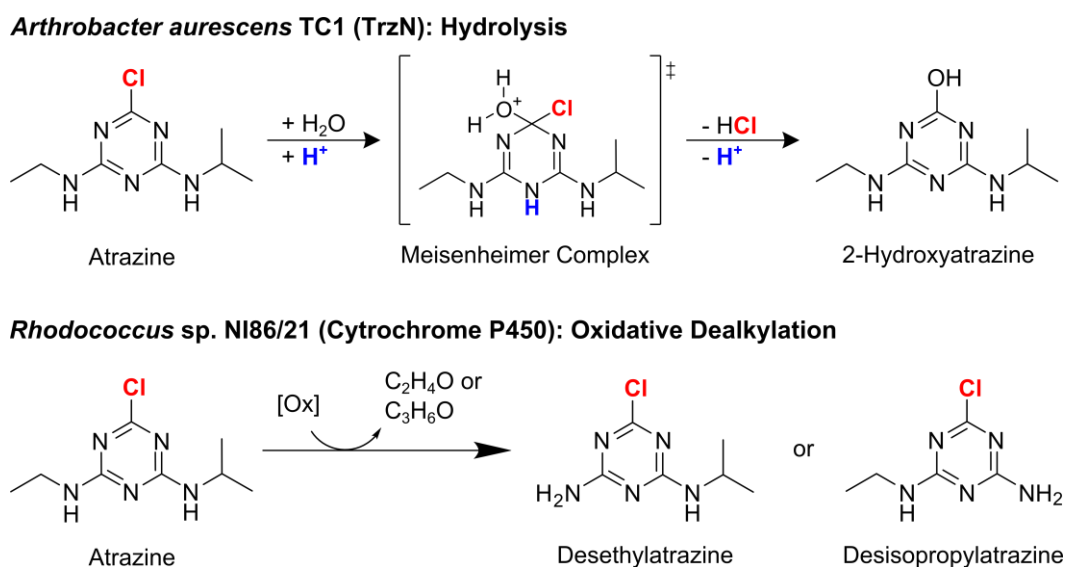
Figure 4-1. Microbial degradation of atrazine by *Arthrobacter aurescens* TC1 and *Rhodococcus* sp. NI86/21 (adapted from Meyer et al.[39] and Meyer & Elsner[40]).

For these two pathways, carbon isotope fractionation was very similar, but significant differences were observed in nitrogen isotope effects[39-41, 111]. Plotting the changes of isotope ratios of these two elements relative to each other results in the regression slope Λ for carbon and nitrogen[19, 24]

$$\Lambda_{C/N} = \Delta\delta^{15}N / \Delta\delta^{13}C \approx \varepsilon_N / \varepsilon_C \qquad (4\text{-}2)$$

Hence, dual element (C, N) isotope trends for oxidative dealkylation of atrazine with *Rhodococcus* sp. NI86/21 ($\Lambda^{Rhodo}_{C/N} = 0.4 \pm 0.1$)[41] were significantly different compared to hydrolysis with *A. aurescens* TC1 ($\Lambda^{Arthro}_{C/N} = -0.6 \pm 0.1$)[39] offering an opportunity to distinguish atrazine degradation pathways in the field. However, in environmental assessments it is advantageous to have isotopic information of as many elements as possible in order to distinguish degradation pathways and sources at the same time[27, 118, 119]. Therefore, information from a third element, chlorine, would be highly valuable. Also on the

mechanistic end, information gained from a change in the chlorine isotope value could lead to a more reliable differentiation of transformation pathways and contribute to a better mechanistic understanding of the underlying chemical reaction[27]. Along these lines, triple element (3D) isotope analysis was already accomplished for chlorinated alkanes[27, 28] and alkenes[17, 103].

Until now, however, compound-specific chlorine isotope analysis has not been accessible so that chlorine isotope ratio changes for hydrolysis of atrazine have only been analyzed in abiotic systems or via computational calculations[120, 121]. For oxidative dealkylation, chlorine isotope effects have, so far, not been studied. Recently a GC-qMS method for chlorine isotope analysis of atrazine has been brought forward[69] which offers the opportunity to enable deeper mechanistic insights into its transformation processes. Therefore, our objective was to analyze carbon, nitrogen and chlorine isotope effects associated with the biodegradation of atrazine via hydrolysis with *A. aurescens* TC1 and via oxidative dealkylation with *Rhodococcus* sp. NI86/21. In addition, we computationally predicted the chlorine isotope effect associated with hydrolysis and oxidative dealkylation for comparison. Further, we evaluated whether the additional information from chlorine isotope fractionation is a particularly sensitive indicator for transformation processes and whether it can confirm previously proposed mechanisms of different pathways. With this study, we bring forward information about degradation-induced chlorine isotope fractionation of atrazine as a basis to apply triple element (3D) isotope analysis in environmental assessments.

4.3   Material and Methods

4.3.1   Bacterial Strains and Cultivation

A. aurescens strain TC1 was grown in mineral salt medium supplemented with approx. 20 mg/L of atrazine according to the protocol of Meyer et al.[39] Likewise, *Rhodococcus* sp. strain NI86/21 was cultivated in autoclaved nutrient broth (8 g/L, Difco[TM]) with approx. 20 mg/L of atrazine according to the protocol of Meyer et al.[41]. In the late-exponential growth phase the strains were harvested via centrifugation (4000 rpm, 15 min). For the start of the degradation experiments, cell pellets of each strain were transferred to 400 mL fresh media and atrazine was added to achieve a starting concentration of 20 mg/L. All experiments were performed in triplicate at 21 °C on a shaker at 150 rpm. Control

experiments, which were performed without the bacterial strains, did not show any degradation of atrazine.

4.3.2 Concentration Measurements via HPLC

The process of atrazine degradation was monitored by concentration measurements. For analysis, 1 mL samples were taken and filtered through a 0.22 µm filter. Atrazine and its degradation products were directly analyzed using a Shimadzu UHPLC-20A system, which was equipped with an ODS column 30 (Ultracarb 5 µM, 150 × 4.6 mm, Phenomenex). After sample injection (10 µL) an adequate gradient program (see Appendix) was used for compound separation. The oven temperature was set to 45 °C and the compounds were detected by their UV absorbance at 222 nm. Quantitation was performed by the software "Lab Solutions" based on internal calibration curves.

4.3.3 Preparation of Samples for Isotope Analysis

According to the protocol of Meyer et al.[39] between 10 and 260 mL of sample were taken for isotope analysis of atrazine at every sampling event. After centrifugation (15 min, 4000 rpm) the supernatant was collected in a new vial. Subsequently, samples were extracted by adding dichloromethane (5-130 mL) and shaking the vial for at least 20 min. The sample extracts were dried at room temperature under the fume hood. Afterwards, the dried extracts were dissolved in ethyl acetate to a final atrazine concentration of approx. 200 mg/L.

4.3.4 Isotope Analysis of Carbon and Nitrogen

The protocol for isotope analysis of carbon and nitrogen was adapted from the studies of Meyer et al.[39, 41]. A TRACE GC Ultra gas chromatograph hyphenated with a GC-III combustion interface and coupled to a Finnigan MAT 253 isotope ratio mass spectrometer (GC-C-IRMS, all Thermo Fisher Scientific) was used. Each sample was analyzed in triplicate. Sample injection (2-3 µL) was performed by a Combi-PAL autosampler (CTC Analysis). The injector had a constant temperature of 220 °C, was equipped with an "A" type packed liner for large volume injections (GL Sciences) and was operated for 1 min in splitless and then in split mode (split ratio 1:10) with a flow rate of 1.4 mL/min. For peak separation, the GC oven was equipped with a DB-5 MS column (30 m × 0.25 mm, 1 µm film

thickness, Agilent). The temperature program of the oven started at 65 °C (held for 1 min), ramped at 20 °C/min to 180 °C (held for 10 min) and ramped again at 15 °C/min to 230 °C (held for 8 min). In the combustion interface, a GC Isolink II reactor (Thermo Fisher Scientific) was installed, which was operated at a temperature of 1000 °C. After combustion of the analytes to CO_2 and subsequent reduction of any nitrogen oxides, the compounds were analyzed as CO_2 for carbon and N_2 for nitrogen isotope measurements. Three pulses of CO_2 or N_2, respectively, were introduced at the beginning and at the end of each run as monitoring gas. Beforehand, these monitoring gases were calibrated against RM8563 (CO_2) and NSVEC (N_2), which were supplied by the International Atomic Energy Agency (IAEA). The analytical uncertainty 2σ was $\pm 0.5\,‰$ for carbon isotope values and $\pm 1.0\,‰$ for nitrogen isotope values.

4.3.5   *Isotope Analysis of Chlorine*

For chlorine isotope analysis of atrazine, a 7890A gas chromatograph coupled to a 5975C quadrupole mass spectrometer (GC-qMS, both Agilent) was used. Sample injection (2 µL) was performed by a Pal Combi-xt autosampler (CTC Analysis). For the injector and the GC oven, the same parameters as for carbon and nitrogen isotope analysis were used with the exception that a different liner type, a "FocusLiner" (SGE), was used. The ion source had a constant temperature of 230 °C and the quadrupole of 150 °C. Prior to sample analysis, the method of Ponsin et al.[69] was tested and optimized for our instrument (see details in the Appendix). Chlorine isotope ratios were evaluated by monitoring the mass-to-charge ratio m/z of 202/200. Standards and samples were measured ten times each and uncertainties were reported as standard deviation. Results were only evaluated if the peak areas of samples were inside a defined linearity range (peak area of $1.2 \times 10^8 - 3.0 \times 10^8$ for m/z 200). Inside the linearity range, the determined precision of the method is associated with a maximal deviation of $\pm 1.1\,‰$. For analysis, the samples were diluted with ethyl acetate to a final concentration of approx. 75 mg/L and measured with a dwell time of 100 ms. Correction of the chlorine isotope values relative to Standard Mean Ocean Chloride (SMOC) was performed by an external two-point calibration with characterized standards of atrazine (Atr #4 $\delta^{37}Cl = -0.89\,‰$ and Atr #11 $\delta^{37}Cl = +3.59\,‰$)[122]. To this end, the standards were measured at the beginning, in between and at the end of each sequence.

4.3.6 Evaluation of Stable Isotope Fractionation

Determination of isotope enrichment factors ε was achieved by the Rayleigh equation, which describes the gradual enrichment of the residual substrate fraction f with molecules containing heavy isotopes, as expressed by isotope values according to Equation 4-1[13, 43]. For example, for chlorine:

$$\ln \left[(\delta^{37}Cl + 1) / (\delta^{37}Cl_0 + 1) \right] = \varepsilon_{Cl} \cdot \ln f \qquad (4\text{-}3)$$

Here $\delta^{37}Cl_0$ refers to the chlorine isotope value at the starting point (t = 0) of an experiment. Regression slopes Λ of dual element isotope plots were obtained by plotting isotope ratios of two different elements against each other, e.g. carbon vs. nitrogen (see Equation 4-2). The uncertainties of the calculated ε-values and Λ-values are reported as 95 % confidence intervals (CI). Furthermore, (apparent) kinetic isotope values, (A)KIE$_{Cl}$, that express the ratio of reaction rates ^{35}k and ^{37}k of heavy and light isotopologues, respectively,

$$KIE_{Cl} = {^{35}k} / {^{37}k} \qquad (4\text{-}4)$$

were calculated according to Elsner et al.[13] by converting ε$_{Cl}$-values into (A)KIE$_{Cl}$ and taking into account that atrazine contains only one chlorine atom (n = 1):

$$(A)KIE_{Cl} = 1 / (n \cdot \varepsilon_{Cl} + 1) \qquad (4\text{-}5)$$

4.3.7 Prediction of Chlorine Kinetic Isotope Effect on Oxidative Dealkylation of Atrazine

In the computational part of the study, we considered hydrogen atom transfer and hydride transfer taking place at the α-position of the ethyl side chain of the atrazine molecule in the oxidative dealkylation reaction promoted by permanganate and the hydronium ion, respectively. Furthermore, we considered hydrolysis under acidic/enzymatic, neutral and alkaline conditions. All molecular structures and analytical vibrational frequencies for involved reactant complexes and transition states were taken from a previous study[41]. Chlorine kinetic isotope effects on dealkylation were calculated using the complete Bigeleisen equation[123] implemented in the ISOEFF program[124] at 300 K. Additional isotope effects predictions for hydrolysis under acidic as well as neutral conditions were performed following the previous computational protocol[121]. The tunneling contributions to the overall kinetic isotope effect were omitted.

4.4 Results and Discussion

4.4.1 Observation of Normal Chlorine Isotope Effects in Biotic Hydrolysis and Oxidative Dealkylation

Atrazine degradation by *A. aurescens* TC1 resulted in the metabolite 2-hydroxyatrazine, whereas the metabolites DEA and DIA were observed for *Rhodococcus* sp. NI86/21 (see Figure 6C-S4 and 6C-S5 in the Appendix). Detection of these expected degradation products (Figure 4-1) demonstrates that hydrolysis and oxidative dealkylation were the underlying biochemical reactions during atrazine degradation, respectively. In both biodegradation experiments – biotic hydrolysis with *A. aurescens* TC1 and oxidative dealkylation with *Rhodococcus* sp. NI86/21 – normal chlorine isotope fractionation was observed (see Figure 4-2A). In the three replicates of hydrolytic degradation by *A. aurescens* TC1 90 %, 90 % and 60 % transformation of atrazine was reached after approx. 26 h, respectively (see Appendix, Figure 6C-S4). Evaluation of δ^{37}Cl values during biotic hydrolysis according to Equation 4-3 resulted in a small normal isotope effect of $\varepsilon_{Cl} = -1.4 \pm 0.6$ ‰. In oxidative dealkylation with *Rhodococcus* sp. NI86/21 approx. 90 % degradation was reached after approx. 186 h in all three replicates (see Appendix, Figure 6C-S5). Evaluation of changes in chlorine isotope ratios resulted in a surprisingly large normal isotope effect of $\varepsilon_{Cl} = -4.3 \pm 1.8$ ‰ considering that the C-Cl bond is not broken during the reaction (see Figure 4-1). In a next step, carbon and nitrogen isotope effects were therefore analyzed to confirm whether the same reactions mechanisms are at work as observed in previous studies[39, 41].
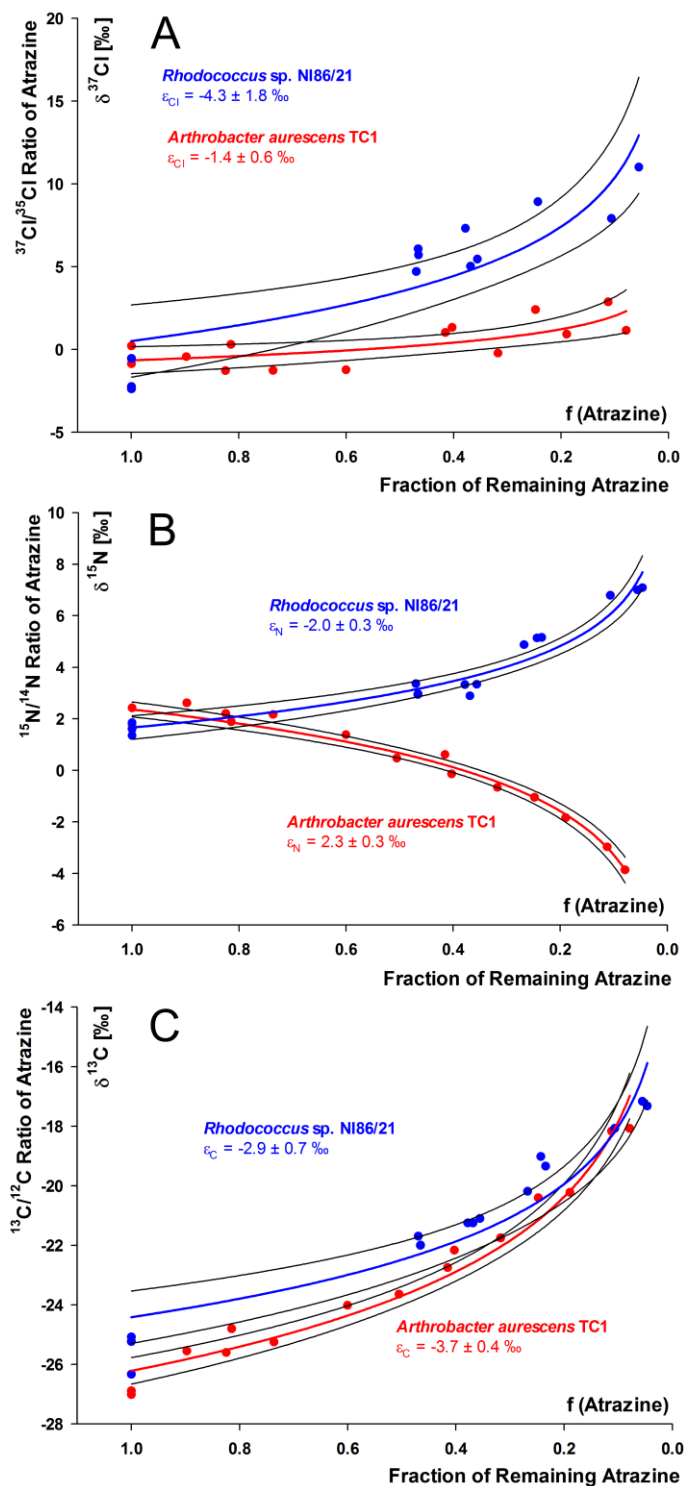
Figure 4-2. Isotope fractionation of (A) chlorine, (B) nitrogen and (C) carbon during microbial degradation of atrazine by *A. aurescens* TC1 (red) and *Rhodococcus* sp. NI86/21 (blue) and corresponding enrichment factors ε evaluated according to Equation 4-3. (The 95 % confidence intervals are given as values and as black lines).

4.4.2 *Observed Carbon and Nitrogen Isotope Fractionation is Consistent with Previous Studies*

Carbon and nitrogen isotope fractionation for atrazine degradation by *A. aurescens* TC1 and *Rhodococcus* sp. NI86/21 was consistent with previous studies: Both experiments showed significant changes in isotope ratios (see Figure 4-2B and 4-2C). For hydrolysis with *A. aurescens* TC1, an inverse nitrogen isotope effect (ε_N = 2.3 $\pm$ 0.3 ‰) and a normal carbon isotope effect (ε_C = -3.7 $\pm$ 0.4 ‰) were observed, which were slightly smaller compared to the results of a former publication of Meyer et al. (ε_N = 3.3 $\pm$ 0.4 ‰, ε_C = -5.4 $\pm$ 0.6 ‰)[39], but gave the same dual element isotope plot ($\Lambda^{Arthro}_{C/N}$ = -0.6 $\pm$ 0.1) confirming that the same mechanism was at work (see Figure 4-3A).

Oxidative dealkylation of atrazine with *Rhodococcus* sp. NI86/21 resulted in a normal nitrogen isotope effect of ε_N = -2.0 $\pm$ 0.3 ‰ and a normal carbon isotope effect of ε_C = -2.9 $\pm$ 0.7 ‰. These ε-values are similar to those published by Meyer & Elsner[40] (ε_N = -1.5 $\pm$ 0.3 ‰, ε_C = -4.0 $\pm$ 0.2 ‰) and Meyer et al.[41] (ε_N = -1.4 $\pm$ 0.3 ‰, ε_C = -3.8 $\pm$ 0.2 ‰). The slightly more pronounced nitrogen isotope fractionation in this study can probably be attributed to the fact that oxidation was primarily observed at the C-H bond adjacent to the nitrogen atom (α-position of the ethyl or isopropyl group, see closed mass balance in Figure 6C-S5 in the Appendix)[41]. In the study of Meyer et al.[41] 48 % of the oxidation was observed at the β-position of the ethyl or isopropyl group resulting in a smaller nitrogen isotope fractionation effect. The obtained regression slope of $\Lambda^{Rhodo}_{C/N}$ = 0.7 $\pm$ 0.1 in this study is slightly larger than the previously reported regression slopes ($\Lambda^{Rhodo}_{C/N}$ = 0.4 $\pm$ 0.1)[40, 41] which may again be explained by the small difference in average nitrogen isotope effects. Also here, however, the similar dual element isotope trend confirms that in this study atrazine was transformed by the same mechanism as in Meyer et al.[41] leading to the observed oxidative dealkylation products by *Rhodococcus* sp. NI86/21.
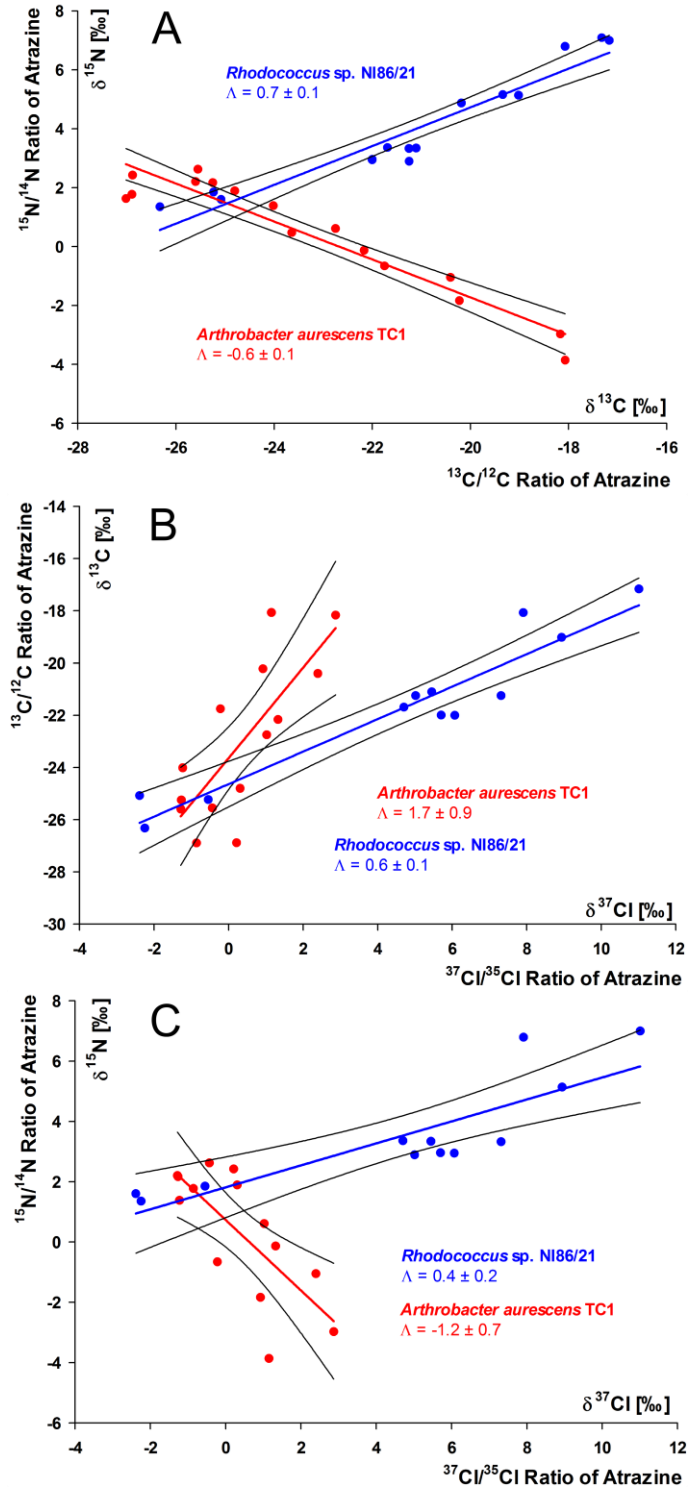
Figure 4-3. Isotope effects in microbial degradation of atrazine by *A. aurescens* TC1 (red) and *Rhodococcus* sp. NI86/21 (blue) resulting in dual element isotope plots. (The 95 % confidence intervals are given as values and as black lines next to the regression slopes). (A) Regression slopes of nitrogen and carbon isotope values ($\Lambda_{C/N}$). (B) Regression slopes of chlorine and carbon isotope values ($\Lambda_{Cl/C}$). (C) Regression slopes of chlorine and nitrogen isotope values ($\Lambda_{Cl/N}$).

4.4.3 Multi-Element Isotope Approach

Results of chlorine isotope analysis were combined with data for carbon and nitrogen isotope measurements in dual element isotope plots (see Figure 4-3B and 4-3C). For hydrolysis with *A. aurescens* TC1 regression slopes of $\Lambda^{Arthro}_{Cl/C} = 1.7 \pm 0.9$ and $\Lambda^{Arthro}_{Cl/N} = -1.2 \pm 0.7$ were obtained. Oxidative dealkylation by *Rhodococcus* sp. NI86/21 resulted in regression slopes of $\Lambda^{Rhodo}_{Cl/C} = 0.6 \pm 0.1$ and $\Lambda^{Rhodo}_{Cl/N} = 0.4 \pm 0.2$. Since the dual element isotope plots of chlorine and carbon and of chlorine and nitrogen provide significantly different regression slopes for the respective elements, they can provide an additional line of evidence to differentiate the two degradation mechanisms of atrazine from each other.

4.4.4 Surprising Mechanistic Evidence from Chlorine Isotope Effects

For degradation with *A. aurescens* TC1, rather small chlorine isotope fractionation was observed ($\varepsilon_{Cl} = -1.4 \pm 0.6$ ‰) despite the fact that the chlorine is cleaved off during hydrolysis (see Figure 4-1). For oxidative dealkylation with *Rhodococcus* sp. NI86/21, the chlorine is not cleaved off (see Figure 4-1), therefore, no or just a small chlorine isotope effect was expected. However, here more pronounced chlorine isotope fractionation was observed ($\varepsilon_{Cl} = -4.3 \pm 1.8$ ‰).

The corresponding apparent kinetic isotope effects ($AKIE_{Cl}$, see Table 4-1) were compared to the $AKIE_{Cl}$ values of other studies focusing on the same degradation mechanisms. In addition, the $AKIE_{Cl}$ values were compared to the theoretical maximum Streitwieser Limit associated with the cleavage of a C-Cl bond ($KIE_{Cl} = 1.02$)[125-127] and to the predictions of computational calculations (Table 4-2).

Table 4-1. $AKIE_{Cl}$ values associated with atrazine degradation.

Mechanism	$AKIE_{Cl}$	Study
Experimental Data		
Abiotic alkaline hydrolysis (21 °C)	1.0069 ± 0.0005	Dybala-Defratyka et al.[120]
Abiotic alkaline hydrolysis (50 °C),	1.0009 ± 0.0006	Grzybkowska et al.[121]
Microbial hydrolysis (*A. aurescens* TC1)	$1.0014 \pm 0.0006*$	This study
Microbial dealkylation (*Rhodococcus* sp. NI86/21)	$1.0043 \pm 0.0018*$	This study
Computational Data		
Abiotic acidic/enzymatic hydrolysis (transition state 1)	range of 1.0002 to 1.0011	Grzybkowska et al.[121]
Abiotic acidic/enzymatic hydrolysis (transition state 2)	1.0099	This study
Abiotic neutral hydrolysis	1.0045	This study
Abiotic alkaline hydrolysis	range of 1.0003 to 1.0014	Grzybkowska et al.[121]
Enzymatic hydrolysis	range of 0.9996 to 1.0003	Szatkowski et al.[128]
Abiotic dealkylation (hydrogen atom transfer by MnO_4^-)	0.9999	This study
Abiotic dealkylation (hydride transfer by H_3O^+)	0.9997	This study

* Calculated according to Equation 4-5

For microbial hydrolysis of atrazine an experimental $AKIE^{Arthro}_{Cl}$ value of 1.0014 ± 0.0006 was calculated (see Table 4-1). Dybala-Defratyka et al.[120] reported a more pronounced $AKIE^{alk.hydrol.}_{Cl}$ value of 1.0069 ± 0.0005 (see Table 4-1). However, that study[120] was conducted in an abiotic alkaline solution at 21 °C so that another hydrolysis pathway was involved. Newer data reported a much smaller value of $AKIE^{alk.hydrol.}_{Cl} = 1.0009 \pm 0.0006$[121] for the same alkaline hydrolysis at 50 °C. Later on it was confirmed that abiotic alkaline hydrolysis performed earlier at 21 °C resembles rather neutral than alkaline conditions[121]. Table 4-2 illustrates the different computed mechanisms that lie at the heart of the computational predictions. It shows the different mechanistic routes between the alkaline (substitution of Cl without protonation of the atrazine ring) and the acidic/enzymatic pathway characterized in Meyer et al.[39] (substitution of Cl with protonation of the atrazine ring) including different possible transition states. Chlorine KIEs are, among other factors[129], determined by the percent extension of the C-Cl bond in the transition state. As this is directly related to the structure of the transition state, it can be linked to the C-Cl bond orders (Table 4-2), which decrease in the studied hydrolysis reactions when the C-Cl bond is more ruptured as compared to its length in the reactants, resulting in increased chlorine KIEs. Previously performed computations[121] and computations of this study mimicking alkaline, acidic, and neutral conditions indicated that the largest $AKIE_{Cl}$ should be expected under

neutral conditions (except for transition state 2 of acidic/enzymatic hydrolysis). Under neutral conditions the C-Cl bond is elongated leading to a transition state geometry which differs substantially from hydrolysis reactions promoted either by alkaline or acidic conditions (see Table 4-2). However, hydrolysis at neutral pH is too slow to be of relevance. Computational calculations taking into account the transition state structures at a molecular level predicted $AKIE_{Cl}$ values ranging from 0.9996 to 1.0014 for alkaline, acidic and enzymatic hydrolysis (see Table 4-1 and 4-2)[121, 128]. Hence, on the mechanistic level, the computational studies predict that the formation of a Meisenheimer complex rather than the subsequent C-Cl bond cleavage is the rate-determining step during the nucleophilic aromatic substitution reaction catalyzed by TrzN[121, 128]. In both abiotic pathways the C-Cl bond at the transition state of the rate determining step is almost intact giving rise to very small $AKIE_{Cl}$ (the computed bond orders for both alkaline and acidic hydrolysis are the same and equal to 1.03, see also Table 4-2). In this study, we therefore observed a similarly small $AKIE^{Arthro}_{Cl}$ value for enzymatic hydrolysis in *A. aurescens* TC1 which resembles acid-catalyzed hydrolysis rather than alkaline hydrolysis[39]. Hence, the picture emerges that different hydrolytic pathways give rise to experimental $AKIE_{Cl}$ values much lower than the Streitwieser Limit of 1.02[125-127] indicating that the chlorine isotope effect is masked in all cases and that the C-Cl bond cleavage is not the rate-determining step. Interestingly, this is in contrast to ametryn hydrolysis where strong sulphur isotope effects were observed in enzymatic hydrolysis by TrzN[111]. Further experimental work, including degradation experiments with other strains, hydrolysis and crude enzyme experiments, will be required to further substantiate the picture on chlorine isotope effects observed in this study. For the moment, since chlorine isotope effects were found to be masked, we must conclude, however, that information from chlorine isotope analysis alone would not be enough to differentiate the different reaction mechanisms. This illustrates the importance of analyzing more than one element for mechanistic differentiation.

Table 4-2. Mechanisms and transition states of acidic/enzymatic, neutral and alkaline hydrolysis and corresponding calculated and measured isotope effects.

Mechanism	Calculated Transition State[a]	Calculated Isotope Effect (position-specific and compound average AKIE values)	Measured Isotope Effect
Acidic/Enzymatic Hydrolyis (Transition State 1)	**C-Cl Bond Order: 1.03**	Cl 1.0002; 1.037; 1.0003; 0.9995; 1.0000; 1.0014; 0.9973; 0.9974; 1.0019; 0.9996; 0.9902; 0.9997; 1.0005; 1.0007 Compound average: $AKIE_{Cl} = 1.0002^a$; $AKIE_N = 0.9983^a$; $AKIE_C = 1.0042^a$	**Compound average:** $AKIE_{Cl} = 1.0014 \pm 0.0006^b$; $AKIE_N = 0.9886 \pm 0.0015^b$; $AKIE_C = 1.0271 \pm 0.0034^b$
Acidic/Enzymatic Hydrolyis (Transition State 2)	**C-Cl Bond Order: 0.55**	Cl 1.0099; 1.0113; 1.0015; 0.9999; 1.0016; 1.0005; 1.0005; 1.0007; 1.0006; 0.9999; 0.9995; 0.9992; 0.9993; 1.0000 Compound average: $AKIE_{Cl} = 1.0099$; $AKIE_N = 1.0002$; $AKIE_C = 1.0017$	-
Neutral Hydrolyis	**C-Cl Bond Order: 0.87**	Cl 1.0045; 1.0362; 1.0041; 0.9992; 1.0041; 0.9996; 0.9984; 0.9993; 0.9998; 0.9990; 1.0013; 1.0009; 1.0011; 1.0014 Compound average: $AKIE_{Cl} = 1.0045$; $AKIE_N = 1.0024$; $AKIE_C = 1.0041$	-
Alkaline Hydrolyis	**C-Cl Bond Order: 1.03**	Cl 1.0003; 1.0314; 1.0010; 1.0006; 1.0009; 1.0001; 1.0007; 1.0007; 0.9998; 1.0007; 1.0011; 1.0007; 1.0027; 1.0026 Compound average: $AKIE_{Cl} = 1.0003^a$; $AKIE_N = 1.0017^a$; $AKIE_C = 1.0043^a$	**Compound average:** $AKIE_{Cl} = 1.0009 \pm 0.0006^a$; $AKIE_N = 1.001 \pm 0.000^c$; $AKIE_C = 1.031 \pm 0.003^c$

[a] Taken from Grzybkowska et al.[121]; [b] Calculated according to Equation 4-5 with n = 5 for N and n = 8 for C; [c] Taken from Meyer et al.[39]

For oxidative dealkylation, so far, no chlorine isotope effects were reported. Regarding the reaction mechanism, Meyer et al.[41] concluded that oxidative dealkylation of atrazine with *Rhodococcus* sp. NI86/21 is initiated by hydrogen atom transfer based on the observed product distribution and the carbon and nitrogen isotope effects. Hydrogen atom transfer leads directly to a homolytic cleavage of the C-H bond adjacent to the nitrogen atom (α-position of the ethyl or isopropyl group) producing a relative unstable 1,1-aminoalcohol which is then further transformed to DEA or DIA[41]. In parallel, two additional products could be detected which were formed by oxidation of the C-H bond in the β-position of the ethyl or isopropyl group. For this mechanistic pathway, chlorine isotope effects would be expected to be rather small since the chlorine is not involved in the reaction steps. The closed mass balance of the concentration analysis (see Figure 6C-S5 in the Appendix) of this study and the results of product distribution of Meyer et al.[41] also indicate that there is no C-Cl bond cleavage taking place since corresponding hydrolysis products were not detected. Furthermore, our computations for hydrogen atom transfer at a catalytic center mimicking cytochrome P450 predicted no chlorine isotope effect ($\text{AKIE}^{\text{hydro.atom trans.}}_{\text{Cl}} = 0.9999$, see Table 4-1). Hydride transfer promoted by the hydronium ion also resulted in no chlorine isotope effect ($\text{AKIE}^{\text{hydride trans.}}_{\text{Cl}} = 0.9997$, see Table 4-1). At previously located transition state structures for these two reactions[41] the carbon-chlorine bond remains intact and no stretching of this bond is involved in the reaction coordinate (hydrogen transfer) mode. The observed more pronounced $\text{AKIE}^{Rhodo}_{\text{Cl}}$ value of 1.0043 ± 0.0018 in this study (see Table 4-1) could, therefore, be indicative of isotope effects caused by enzymatic interactions. Meyer et al.[41] proposed that for oxidative dealkylation no selectivity itself is observed, however, the preferred oxidation of the α-position over the β-position could be explained by steric factors of the catalyzing enzyme which could have an influence on the transformation pathway. Thus, the sensitive chlorine isotope effect, which is observed even though the C-Cl bond is not cleaved during degradation, can be interpreted as an indicator that non-covalent interactions between the cytochrome P450 complex and the chlorine cause significant chlorine isotope fractionation[130].

4.5 Conclusion

Since atrazine is frequently detected in groundwater systems, major efforts should be put into understanding its environmental fate. We provide an approach to 3D-isotope (C, N, Cl)

analysis of atrazine and explored isotope fractionation in different transformation pathways. Together, this provides the basis to more confidently assess sources and degradation of atrazine in the environment. Specifically, we demonstrated that pronounced changes in chlorine isotope values are not an indicator of microbial hydrolysis (as one might have expected without knowledge of our experimental data), but – surprisingly – rather of oxidative dealkylation. Therefore, although trends are different than expected, they can nonetheless be used for a more confident identification of different sources and transformation pathways in field samples. Regarding the sensitivity of chlorine isotope effects, our study demonstrates the importance of performing controlled laboratory experiments before applying the approach in the field. Specifically, in other cases chlorine isotope fractionation can be much more pronounced than observed for atrazine in this study. Large chlorine isotope effects were observed in proof-of-principle experiments by Ponsin et al.[69] studying hydrolytic dechlorination of S-metolachlor, an herbicide containing also only one chlorine atom. Here preliminary data suggest a large chlorine isotope effect of $\varepsilon_{Cl} = -9.7 \pm 2.9$ ‰ for abiotic alkaline hydrolysis. Therefore, in the case of other substances, chlorine isotope effects can be even more sensitive indicators of degradation provided that the C-Cl bond cleavage occurs in the rate-determining step of a reaction. Further, gaining deeper insights into these chemical processes is the basis for understanding the biotic catalysis of organic micropollutant degradation. This, in turn, is essential for identifying and developing optimized strategies for micropollutant removal in order to make successful bioremediation possible.
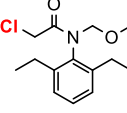
5

General Conclusion
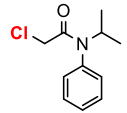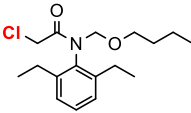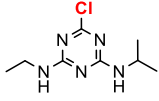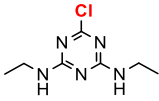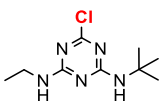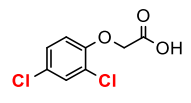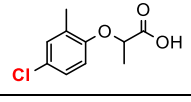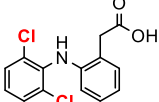
In the last years compound-specific stable isotope analysis (CSIA) has evolved further and further. Especially in terms of chlorine isotope analysis, new methods were developed and instrumentational improvements made the analysis of new compounds possible[31, 32, 64, 69]. Today it is an important and widely used tool for the detection and evaluation of contaminant transformation in the environment. Since it even enables the differentiation and identification of underlying chemical mechanisms of contaminant degradation, this thesis aimed to improve and use this powerful approach to study the transformation mechanisms of selected prominent chlorohydrocarbons.

Due to the urgent need of in-house referencing standards and substance-specific working standards for chlorine isotope analysis, Chapter 2 focused on identifying synthesis routes to generate such standards in a straightforward way. Chemical dehalogenation reactions, which are accompanied by chlorine isotope fractionation effects, were used to produce the in-house silver chloride referencing standard CT16 and substance-specific working standards of the herbicides acetochlor and S-metolachlor (Aceto2 / Metola2). CT16 resulted from a reductive elimination reaction of 2,2,2-trichloroethyl acetate which produced a chloride depleted in ^{37}Cl. Aceto2 and Metola2 were produced by a second order nucleophilic chemical substitution reaction leading to remaining substrate fractions enriched in ^{37}Cl. The purchased acetochlor (Aceto1) and S-metolachlor (Metola1) were used as starting material. The generated standards were subsequently characterized against the international reference

standards USGS38 (-87.90 ‰) and ISL-354 (+0.05 ‰) by gas chromatography – isotope ratio mass spectrometry (GC-IRMS) and gas chromatography – multicollector inductively coupled plasma mass spectrometry (GC-MC-ICPMS). For CT16 both methods resulted in a consensus value of $\delta^{37}Cl_{CT16} = -26.82 \pm 0.18$ ‰. Preliminary two-point calibration by GC-MC-ICPMS of the acetochlor and S-metolachlor standards gave values of $\delta^{37}Cl_{Aceto1} = 0.29 \pm 0.29$ ‰, $\delta^{37}Cl_{Aceto2} = 18.54 \pm 0.20$ ‰, $\delta^{37}Cl_{Metola1} = -4.28 \pm 0.17$ ‰ and $\delta^{37}Cl_{Metola2} = 5.12 \pm 0.27$ ‰. The successful synthesis and characterization of these chlorine standards will improve chlorine isotope analysis in the future. Until today chlorine working standards were typically characterized against only one anchor point. With the synthesis route of CT16 every laboratory can easily generate its own second anchor point so that two-point calibration will be used on a regular basis for tomorrow's chlorine isotope standard characterization. The opportunity to synthesis a pronounced negative in-house referencing standard and to use two referencing standards which differ in their isotope value for characterization is an important step which will improve the accuracy of future calibration results of chlorine working standards. Consequently, the accuracy of daily chlorine isotope analysis will also improve due to calibration with these optimized working standards. Furthermore, the generated working standards for acetochlor and S-metolachlor together with the recently published GC-qMS (gas chromatography – quadrupole mass spectrometry) method for chlorine isotope analysis of these herbicides[69] make it now possible to analyze not only carbon and nitrogen isotope fractionation but also chlorine isotope fractionation. This multi-element approach will certainly improve the outcome of lysimeter studies investigating the environmental fate of these herbicides. However, the pronounced positive $\delta^{37}Cl$-values of the standards Aceto2 and Metola2 are already outside of the range covered by the international chlorine reference standards. Therefore, a synthesis route for the generation of an in-house chlorine reference standard with a more positive chlorine value is also needed which would optimize the accuracy of characterization results for chlorine working standards even further. The successful generation of the acetochlor and S-metolachlor working standards also demonstrated that organic synthesis can be used as effective tool to produce essential substance-specific working standards of more complex organic chlorohydrocarbons. Future work has to target the generation of substance-specific working standards of other chlorinated micropollutants. Table 5-1 provides a list of examples for such compounds and corresponding possible strategies for dechlorination reactions which could result in a pronounced chlorine isotope shift.

Table 5-1. List of chlorinated micropollutants and corresponding possible strategies for the generation of substance-specific working standards.

Substance Class	Compound	Structure	Strategy	Reference
Chloroacetanilide herbicides	Alachlor		S_N2 reaction	Lihl et al.[122]
	Propachlor			
	Butachlor			
s-Triazine herbicides	Atrazine		Alkaline hydrolysis	Dybala-Defratyka et al.[120]
	Simazine			
	Terbuthylazine			
Phenoxy acid herbicides	2,4-D		Photodegradation	Burrows et al.[131]
	Mecoprop			
Pharmaceuticals	Diclofenac		Bio-Pd/Au catalyzed dechlorination / UV photolysis	Corte et al.[132] / Keen et al.[133]

The herbicides alachlor, propachlor and butachlor belong to the same substance class as the herbicides S-metolachlor and acetochlor (chloroacetanilide herbicides). Due to their similar structure, the strategy of a S_N2 reaction, as explained in Chapter 2, should be suited to generate also substance-specific working standards of these herbicides. However, for the listed s-triazine and phenoxy acid herbicides and the pharmaceutical product diclofenac substance-specific working standards cannot be generated via this strategy. The chlorine atoms of these compounds are directly connected to the respective aromatic rings (see structures in Table 5-1) making a S_N2 reaction impossible[134]. Therefore, the generation of substance-specific working standards has to follow other strategies. A possible approach for

the listed s-triazine herbicides could be alkaline hydrolysis. Dybala-Defratyka et al.[120] observed a relatively pronounced chlorine isotope effect for alkaline hydrolysis of atrazine which could, therefore, serve as possible strategy to generate substance-specific working standards. This strategy could also work for the similar structured simazine and terbuthylazine. The phenoxy acid herbicides 2,4-D and mecoprop can be dechlorinated via photodegradation[131] and the chlorinated pharmaceutical product diclofenac can be degraded via bio-Pd/Au catalyzed dechlorination[132] or UV photolysis[133]. The chemical structures of 2,4-D and diclofenac contain two chlorine atoms, respectively, which will lead to a dilution of the chlorine isotope effect by the non-reacting chlorine atom. Consequently, smaller chlorine isotope effects have to be expected for these compounds[13]. However, whether these strategies are suited for the generation of chlorine working standards of theses substances has to be tested in the future. The generation of such substance-specific working standards is an important step for stable chlorine isotope analysis. Together with future development of analytical methods, this will enable the accurate analysis of chlorinated contaminants in the environment.

Chapter 3 addressed the question why microbial reductive dehalogenation of the chlorinated ethenes PCE and TCE, which is catalyzed by reductive dehalogenases (RDases), often stops at toxic cis-DCE or VC. Compound-specific isotope analysis of carbon and chlorine was used to investigate this question by comparing dual element regression slopes $\Lambda_{C/Cl}$. The $\Lambda_{C/Cl}$ values were larger during microbial dechlorination of less chlorinated cis-DCE ($\Lambda_{C/Cl} = 10.0$ to 17.8) compared to PCE and TCE ($\Lambda_{C/Cl} = 2.3$ to 3.8). Even in TCE transformation $\Lambda_{C/Cl}$ was larger when mixed cultures had previously been adapted to VC or DCEs ($\Lambda_{C/Cl} = 9.0$ to 18.2). These values were compared to a model study using vitamin B_{12} as a model reactant for reductive dehalogenase activity which identified two chemical mechanisms responsible for reductive dehalogenation[17]. The trend for less chlorinated ethenes (smaller $\Lambda_{C/Cl}$ values) parallels that of cob(I)alamin addition followed by protonation and the opposite trend (larger $\Lambda_{C/Cl}$ values) matches cob(I)alamin addition followed by Cl⁻ elimination. Additionally, the observed dual element isotope trends did not correlate with the predominant RDases of the studied microbial cultures. These results indicate that reductive dehalogenases show different mechanistic motifs which are tailored to certain substrates. This could potentially explain why some RDases are optimized in the dechlorination of PCE and TCE, but are not able to dechlorinate cis-DCE or VC. Furthermore, future field studies could benefit from an advanced classification system for

microbial dechlorination. Classifying dehalogenation not only based on detected RDase genes but also on observed dual element (C, Cl) isotope trends could facilitate the identification of underlying (bio)chemical reaction mechanisms at contaminated sites. The power of this approach could be even strengthened by additional information about other degradation pathways of chlorinated ethenes like cometabolic oxidation. Under aerobic conditions a variety of microorganisms containing different oxygenases is able to oxidize chlorinated ethenes to CO_2[3]. Gafni et al.[135, 136] already studied carbon and chlorine isotope fractionation during cometabolic oxidation of TCE with different microbial cultures. For toluene and ammonia oxidizers they observed normal carbon but small inverse chlorine isotope effects resulting in very steep and negative regression slopes $\Lambda_{C/Cl}$ ($\Lambda_{C/Cl}$ = -10.9 to -38.0) which can be differentiated from the dual element isotope trends of reductive dehalogenation. However, during cometabolic TCE oxidation by methane oxidizers substrate-binding seems to be the rate-limiting step resulting in very small normal carbon and normal chlorine isotope effects. The resultant small $\Lambda_{C/Cl}$ values ($\Lambda_{C/Cl}$ = 1.1 to 1.7) could be difficult to distinguish from dual element isotope trends of reductive dehalogenation[136]. These contrasting dual element isotope trends during cometabolic TCE oxidation emphasize the importance of investigating and understanding the cometabolic oxidation mechanisms also of other microbial groups, e.g. propane and aromatic compound oxidizers, and also of other substrates, like PCE and *cis*-DCE. With this information dual element (C, Cl) isotope analysis could help to differentiate aerobic and anaerobic degradation pathways of chlorinated ethenes at contaminated sites. Another possible pathway of chlorinated ethene degradation is abiotic transformation occurring on metal surfaces such as zero-valent iron. Zero-valent iron permeable reactive barriers are introduced into contaminated plumes for *in situ* remediation. While passing through such barriers chlorinated ethenes are reductively dechlorinated[137, 138]. However, the chemical mechanisms behind reductive dechlorination on metal surfaces and to what extent the properties of the metal have an effect on the chemical mechanism are hardly understood[137]. Chlorine isotope analysis could now offer a possibility to get deeper mechanistic insights. Audì-Mirò et al.[139] already used dual element isotope analysis of carbon and chlorine to distinguish the effectiveness of abiotic and biotic dechlorination. In addition, chlorine and carbon isotope fractionation obtained from laboratory studies investigating reductive dechlorination on metal surfaces could also lead to a better mechanistic understanding of the underlying processes. Having a detailed knowledge about the chemical mechanisms behind chlorinated

ethene degradation pathways, the involved enzymes or metals and the corresponding dual element (C, Cl) isotope slopes gained by experimental studies will help to identify and assess ongoing transformation processes at field sites and facilitate (bio)remediation in the future.

In Chapter 4 carbon and nitrogen and, for the first time, chlorine isotope effects of the s-triazine herbicide atrazine were studied during microbial hydrolysis with *Arthrobacter aurescens* TC1 and oxidative dealkylation with *Rhodococcus* sp. NI86/21. Both experiments degraded atrazine via the so far proposed mechanisms[39-41] which was confirmed by carbon and nitrogen isotope effects. Dual element regression slopes Λ of the analyzed elements (C/N, Cl/C, Cl/N) allowed a reliable differentiation of the two mechanisms. For hydrolysis the unexpected small chlorine isotope effect (ε_{Cl} = -1.4 ± 0.6 ‰) verified that the formation of a Meisenheimer complex is the rate-determining step instead of the cleavage of the C-Cl bond. On the other hand, the small chlorine isotope effect implies that chlorine isotope fractionation cannot be used as a sensitive indicator for ongoing microbial hydrolysis. In contrast, for oxidative dealkylation an unexpected pronounced chlorine isotope effect (ε_{Cl} = -4.3 ± 1.8 ‰) was observed. Here, a C-Cl bond cleavage can be excluded as possible explanation. However, this fractionation effect could be caused by enzymatic interactions. Thus, future studies have to further investigate the role of the cytochrome P450 enzyme complex to completely understand the processes behind this pathway. Despite our expectations the multi-element approach holds promise to enable a more confident source identification of atrazine contamination and to improve the differentiation of atrazine degradation pathways. Regarding the sensitivity of chlorine isotope fractionation this study demonstrated that laboratory research is urgently needed before using this approach in the field. Another study focused on the dechlorination of the herbicide S-metolachlor which also contains only one chlorine atom[69]. They observed very pronounced ε-values for chlorine isotope fractionation showing that chlorine isotope fractionation can serve as a sensitive indicator if the C-Cl bond cleavage is involved in the rate-determining step. Therefore, future laboratory work has to investigate and identify the transformation mechanisms of other chlorinated pesticides or pharmaceuticals which are frequently detected in the environment. Possible target compounds containing only one chlorine atom could be further s-triazine herbicides, like simazine or terbuthylazine, or the chloroacetanilide herbicides acetochlor, propachlor and alachlor. Recent studies[32, 69] and especially the results presented in Chapter 2 and 4 showed that chlorine isotope values of s-triazines and chloroacetanilides can be measured via gas chromatography and mass spectrometry methods. Furthermore,

Chapter 2 and Table 5-1 illustrated that substance-specific chlorine working standards of these compounds can be generated via certain strategies or are already available. Since biodegradation pathways of these herbicides can involve a cleavage of the C-Cl bond[140-143], chlorine isotope fractionation could serve as sensitive indicator for detecting and identifying natural transformation processes at contaminated field sites. Another possible target compound could be the chlorine-containing pharmaceutical product diclofenac. A previous study[144] already analyzed carbon and nitrogen isotope effects of diclofenac to distinguish reductive and oxidative transformation pathways and to track the commercial sources of different products. Due to a relatively narrow range of carbon and nitrogen isotope values, a clear distinction of some products was not possible which limits the use of CSIA for source identification. By developing an analytical method for chlorine isotope analysis of diclofenac and by generating substance-specific working standards as depicted in Table 5-1, additional information from chlorine isotope analysis could improve source identification and pathway differentiation of this pharmaceutical product.

This thesis highlighted the possibilities of compound-specific isotope analysis in illuminating underlying transformation processes of chlorohydrocarbons. The constant optimization and advancement of methods and instruments together with the ongoing development of new calibration standards in chlorine isotope analysis will increase the power of this approach even further in the future (Chapter 2). Especially dual element isotope analysis has the potential to bridge the gap between *in vitro* and *in vivo* by identifying reaction mechanisms in model systems and recognizing and differentiating them in bacteria and at contaminated sites (Chapter 3). Furthermore, for less chlorinated micropollutants chlorine isotope fractionation can sensitively indicate degradation if a chlorine is involved in the rate-determining step of the reaction (Chapter 4). Therefore, CSIA is a promising tool for analyzing transformation processes of chlorohydrocarbons and understanding the chemical mechanisms behind chlorohydrocarbon degradation which is very important since this knowledge is crucial for the development of successful bioremediation strategies.

6

Appendix

6.1 Supporting Information of Chapter 2
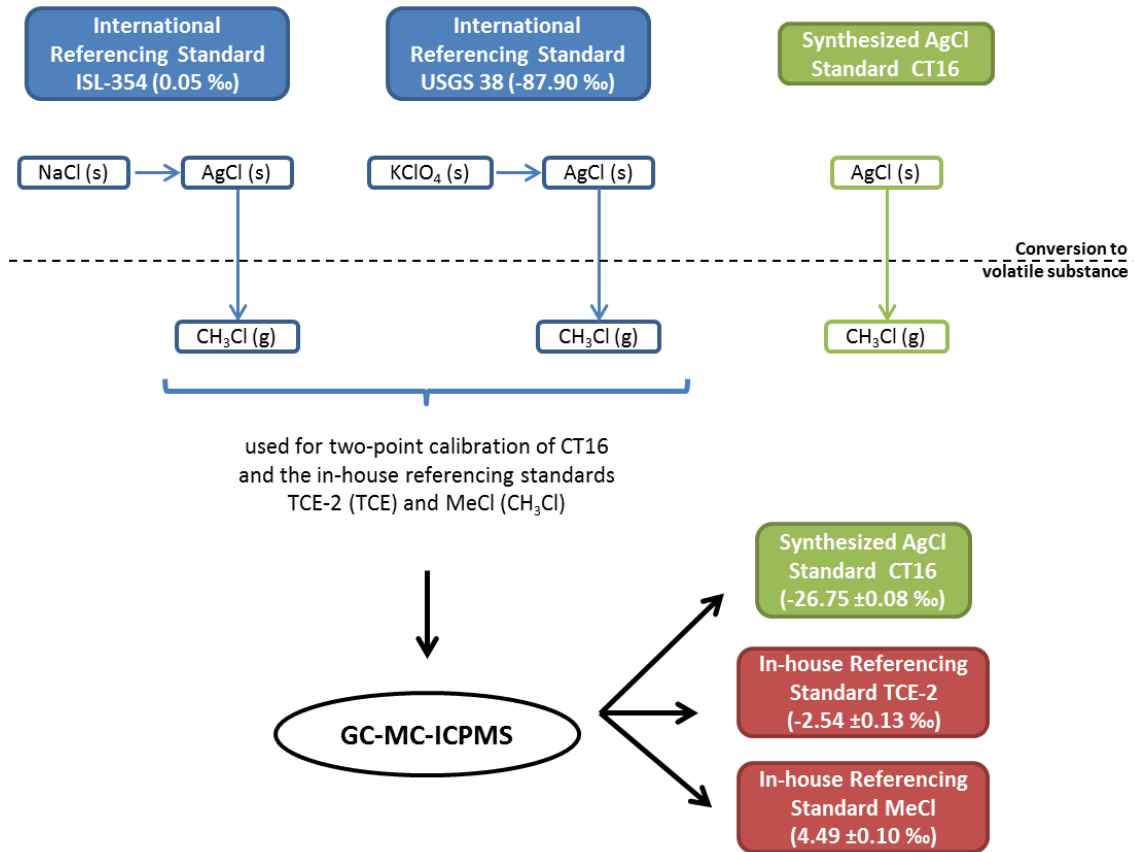
Scheme 6A-S1. Illustrating the workflow of the isotopic characterization of CT16, TCE-2 and MeCl via GC-MC-ICPMS.
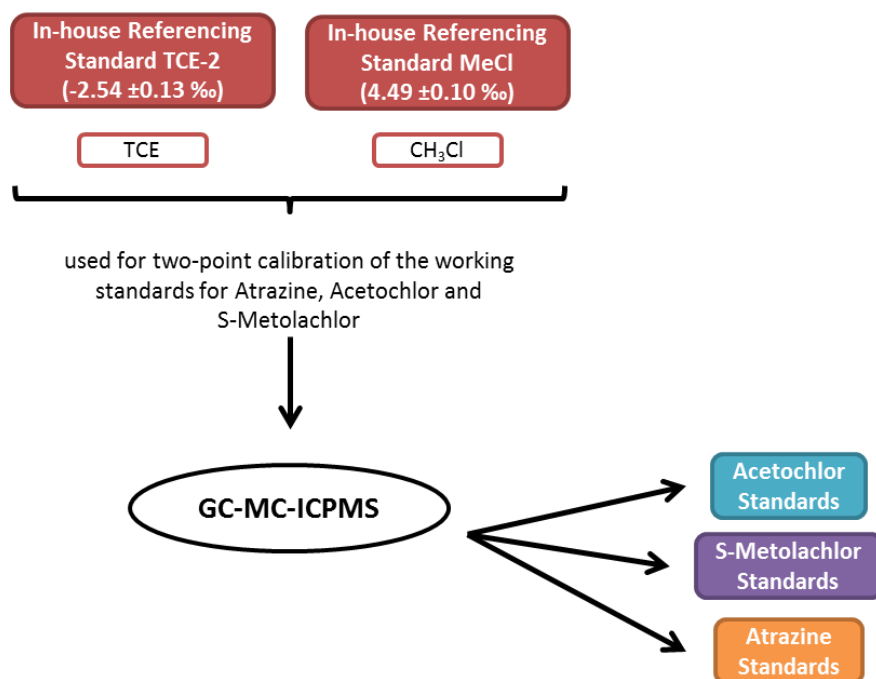
Scheme 6A-S2. Illustrating the workflow of the isotopic characterization of atrazine, acetochlor and S-metolachlor working standards via GC-MC-ICPMS.
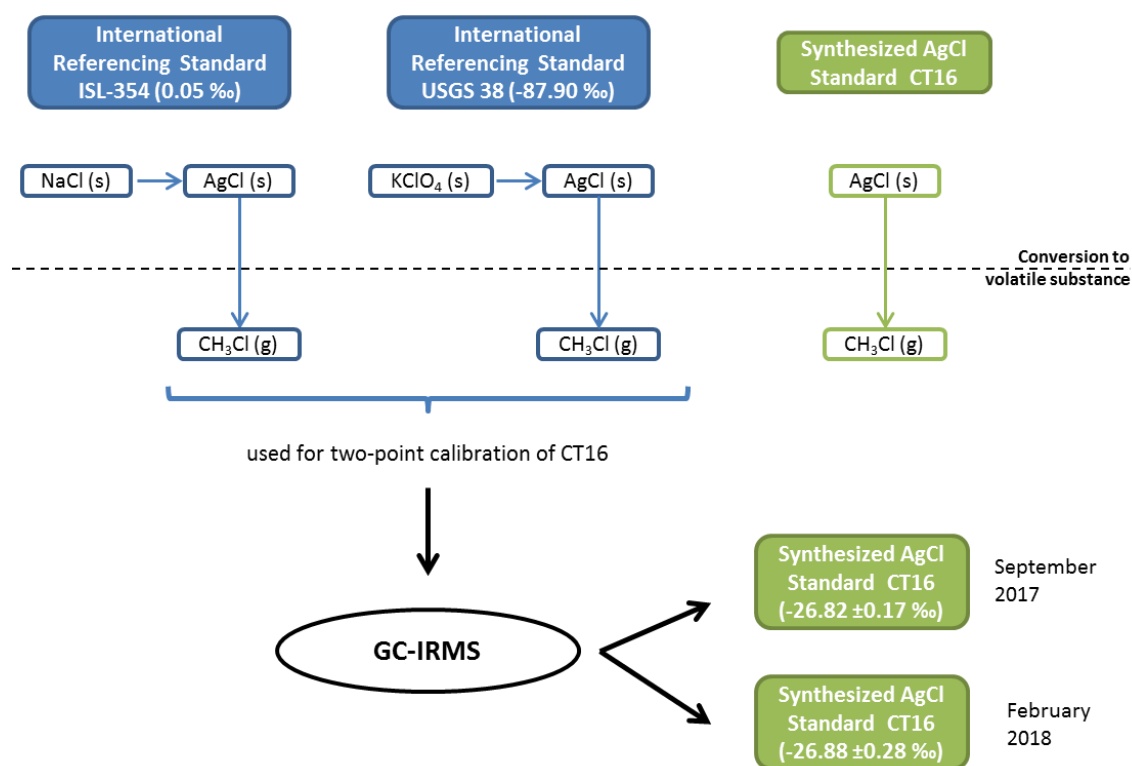
Scheme 6A-S3. Illustrating the workflow of the isotopic characterization of CT16 via GC-IRMS.

Table 6A-S1. List of purchased semi-volatile substances, which were calibrated against the in-house referencing standards TCE-2 and MeCl to be used as working standards in the future.

Working Standard	Substance	Supplier	$\delta^{37}Cl \pm SD^*$ [‰]
ATR #4	Atrazine	Oskar Tropitzsch	-0.89 ± 0.24
ATR #11	Atrazine	Riedel-de Haën	3.59 ± 0.37
ATR_A	Atrazine	Oskar Tropitzsch	-0.89 ± 0.05
ACETO_A	Acetochlor	Chemos	-0.12 ± 0.16
METO_A	S-Metolachlor	Oskar Tropitzsch	-0.01 ± 0.12
METO_B	S-Metolachlor	Chemos	-2.75 ± 0.09

*SD = standard deviation

6.2 Supporting Information of Chapter 3

6.2.1 Material and Methods

Concentration measurements of *cis*-DCE and TCE. The concentrations of the substrates *cis*-DCE and TCE and the dechlorination products *cis*-DCE and VC were measured by gas chromatography coupled to a flame ionization detector (GC-FID, Varian CP-3800, Hewlett Packard 5980 Series II, Varian CP-3400). Samples were injected by a CombiPal autosampler (CTC Analytics). To achieve optimal separation, appropriate columns (e.g.: GS-Q fused silica capillary column (30 m $\times$ 0.53 mm)) were used together with suitable GC temperature programs (e.g., start at 100 °C (1 min), increase to 225 °C at 50 °C/min and hold for 2.5 min). Injector and detector temperatures were between 200 °C and 250 °C. For TCE reductive dechlorination experiments changes in TCE, *cis*-DCE and partly VC concentrations over time are depicted in Figure 6B-S1.
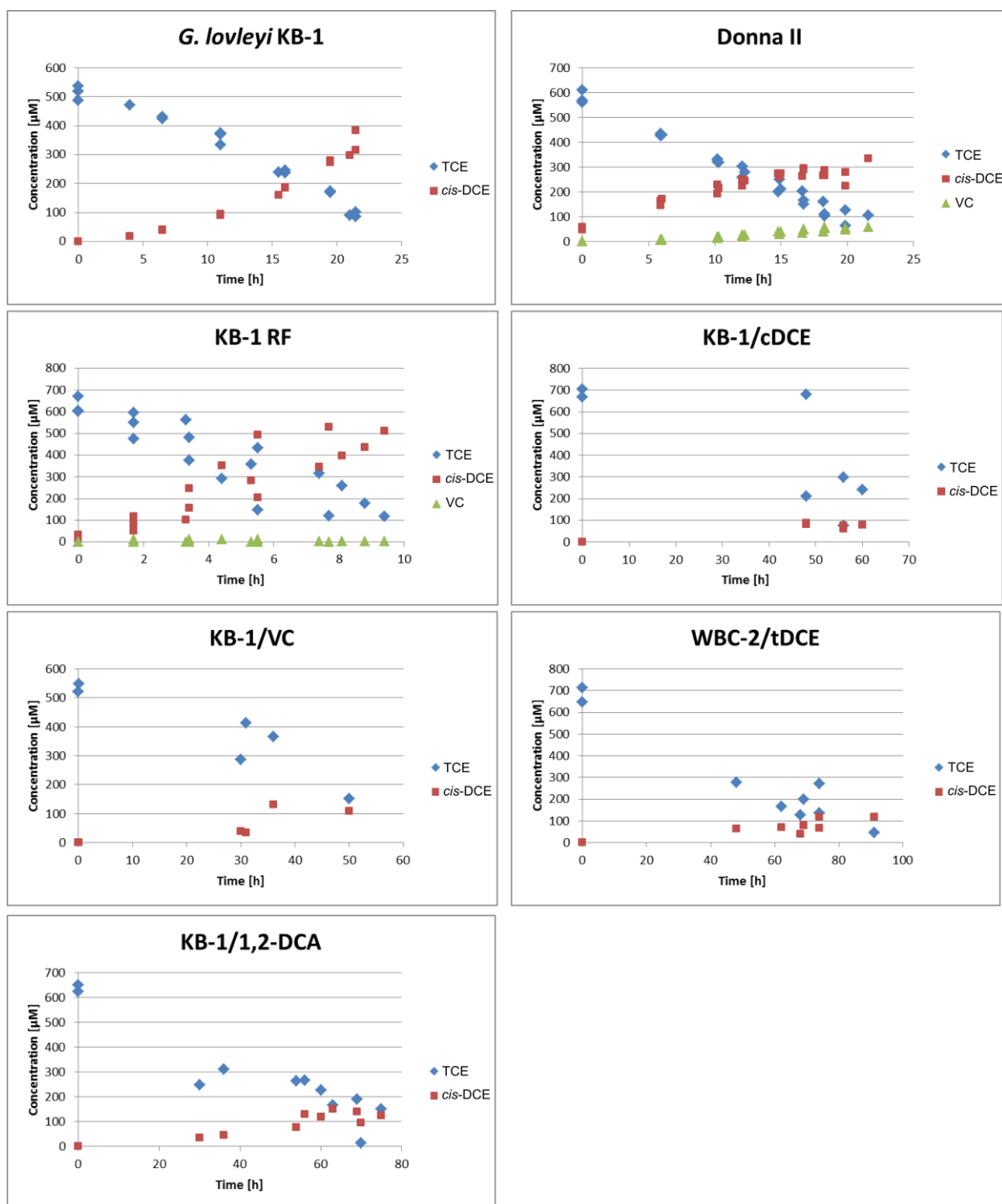
Figure 6B-S1. Concentration measurements during TCE reductive dechlorination experiments.

Stable carbon isotope analysis of *cis*-DCE and TCE. *cis*-DCE samples were transferred into a 40 mL purge & trap vial with a PTFE coated septum. For preconcentration the samples were taken up by a purge & trap system (Teledyne Tekmar, Velocity XTP Purge & Trap). TCE samples were thawed at room temperature and transferred into 10 mL headspace

vials. Carbon isotope analysis was performed on a gas chromatograph (Thermo Scientific, Trace GC Ultra) coupled to an isotope ratio mass spectrometer (Thermo Scientific, Finnegan MAT 253 IRMS) via a GC/C III combustion interface at 940 °C. To achieve optimal separation a Vocol column (Supelco, 30 m × 0.25 mm, 1.5 µm film thickness) was used. For *cis*-DCE the injection into the GC was performed automatically by the purge & trap system at a split ratio of 1:10. TCE samples from the headspace (1 mL) were injected by a Concept autosampler (PAS Technology) at a split ratio of 6:1. Suitable GC temperature programs were used (e.g.: start at 60 °C (4 min), increase to 80 °C at 25 °C/min and hold for 1 min, increased to 200 °C at 30 °C/min and hold for 1 min). The analytical uncertainty 2σ of carbon isotope analysis was ± 0.5 ‰.

Stable chlorine isotope analysis of *cis*-DCE and TCE. Samples were thawed and transferred into a 10 mL headspace vial which were closed and crimped with PTFE coated septa. The method for chlorine isotope analysis was adapted from Shouakar-Stash et al.[22]. Measurements were performed on the same GC-IRMS system as described above with the exception that the GC/C combustion interface was bypassed with a transfer line so that *cis*-DCE and TCE were directly transferred from the GC to the IRMS in a He carrier stream. There, the compounds were ionized and fragmented for isotope ratio analysis at the masses m/z 96/98 (*cis*-DCE) and m/z 95/97 (TCE), respectively. To achieve optimal separation a Vocol column (Supelco, 30 m × 0.25 mm, 1.5 µm film thickness) was used. Samples from the headspace (1 mL) were injected into the GC at a split ratio of 1:10. A typical GC oven temperature program was run (e.g.: start at 65 °C (2 min), increase to 92 °C at 10 °C/min and increase to 175 °C at 60 °C/min). *cis*-DCE and TCE reference gas pulses were injected via a dual inlet system at the beginning and end of each measurement as described in Bernstein et al.[23]. External two-point calibrations were performed with characterized standards of *cis*-DCE ("cisF" ($\delta^{37}Cl$ = -1.52 ‰) and "IS63" ($\delta^{37}Cl$ = +0.07 ‰)) and TCE ("Eil-1" ($\delta^{37}Cl$ = -2.7 ‰) and "Eil-2" ($\delta^{37}Cl$ = +3.05 ‰) (Department of Earth Sciences, University of Waterloo)) and used to convert measurements to $\delta^{37}Cl$ values relative to standard mean ocean chloride (SMOC)[98]. Multiple measurements of these standards were performed before, during and at the end of each sequence, in order to calibrate the obtained values of the samples. The analytical uncertainty 2σ of chlorine isotope analysis was ± 0.2 ‰.

qPCR analysis of KB-1/1,2-DCA, KB-1/VC, KB-1/cDCE and WBC-2/tDCE. The following Tables 6B-S1 - S3 contain detailed information regarding the qPCR analysis.

Table 6B-S1. Primer sets, sequences and annealing temperatures for qPCR analyses.

Target	Primer	5' → 3' Sequence	Annealing Temp. [°C]	Reference
vcrA	VcrA 670F	GCCCTCCAGATGCTCCCTTTAC	60	Molenda et al. 2016[76]
	VcrA 440R	TGCCCTTCCTCACCACTACCAG		
tceA	TceA_500F	TAATATATGCCGCCACGAATGG	64	Fung et al. 2007[92]
	TceA_795R	ATCGTATACCAAGGCCCGAGG		
bvcA	Rdh6_318F	ATTTAGCGTGGGCAAAACAG	60	Waller et al. 2005[145]
	Rdh6_555R	CCTTCCCACCTTGGGTATTT		
tdrA	TdrA1404F	GCCTCTCGCCCCCACTAAACC	62.5	Molenda et al. 2016[76]
	TdrA1516R	GCCATCCTTCATAACCACTCACGCA		
Dehalococcoides	Dhc 1F	GATGAACGCTAGCGGCG	60	Grostern & Edwards 2009[146]
	Dhc 264R	CCTCTCAGACCAGCTACCGATCGAA		
Dehalogenimonas	Dhg273F	TAGCTCCCGGTCGCCCG	59	Manchester et al. 2012[147]
	Dhg537R	CCTCACCAGGGTTTGACATGTTAGAAG		
Total Archaea	Arch 787F	ATTAGATACCCGBGTAGTCC	60	Yu et al. 2005[148]
	Arch 1059R	GCCATGCACCWCCTCT		
Total Bacteria	Bac 1055F	ATGGCTGTCGTCAGCT	55	Dionisi et al. 2003[149]
	Bac 1392R	ACGGGCGGTGTGTAC		

Table 6B-S2. Quality details for qPCR analyses of *rdhA* genes, *Dehalococcoides* 16S rRNA and *Dehalogenimonas* 16S rRNA gene copies.

Reaction	Highest Std. (copies/µL)	Lowest Std. (copies/µL)	Highest Blank (copies/µL)	Efficiency (%)	R^2	Detection Limit (copies/mL)
vcrA	4.00E+07	4.00E+02	4.00E+03	93.4	0.981	2.50E+05
bvcA	1.07E+06	1.07E+00	1.07E+00	92.5	0.997	6.69E+01
tceA	3.86E+07	3.86E+04	3.86E+02	95.9	0.998	2.41E+06
tdrA	4.66E+07	4.66E+01	4.66E+02	87	0.996	2.91E+04
Dehalococcoides	6.90E+07	6.90E+02	6.90E+02	81.7	0.996	4.31E+04
Dehalogenimonas	4.59E+07	4.59E+02	4.59E+03	96.1	0.997	2.87E+05
General Archaea	1.08E+07	1.08E+03	1.08E+03	81.6	0.997	6.75E+04
General Bacteria	4.59E+07	4.59E+02	4.59E+02	88.9	0.996	2.87E+04

Table 6B-S3. qPCR analyses of *rdhA* genes, *Dehalococcoides* 16S rRNA and *Dehalogenimonas* 16S rRNA gene copies in *Dehalococcoides*-containing mixed cultures KB-1/1,2-DCA, KB-1/VC, KB-1/cDCE, and WBC-2/tDCE following TCE dehalogenation experiments.

	KB-1/1,2-DCA	KB-1/VC	KB-1/cDCE	WBC-2/tDCE
vcrA (copies/mL)	1.20E+08	5.60E+07	8.30E+07	1.30E+08
	5.30E+07	5.00E+07	9.60E+07	5.40E+07
bvcA (copies/mL)	6.00E+03	-	6.00E+03	2.20E+04
	5.50E+03	-	5.50E+03	1.20E+03
tceA (copies/mL)	1.10E+08	-	2.90E+07	8.70E+06
	5.70E+07	-	1.50E+07	5.80E+06
tdrA (copies/mL)	1.10E+05	1.90E+05	1.90E+05	6.90E+07
	1.60E+05	2.60E+05	2.60E+05	5.10E+07
Dehalococcoides (copies/mL)	7.40E+07	3.70E+07	4.30E+07	5.60E+07
		2.60E+07	3.70E+07	3.90E+07
Dehalogenimonas (copies/mL)	-	-	-	1.40E+07
	-	-	-	1.30E+07
General Bacteria (copies/mL)	1.40E+08	8.60E+07	1.50E+08	9.90E+07
	7.70E+07	7.50E+07	9.50E+07	3.60E+07
General Archea (copies/mL)	2.70E+06	1.40E+06	7.90E+06	2.30E+06
	2.50E+06	2.70E+06	2.90E+06	2.30E+06

* Samples shaded in grey were below the detection limit.
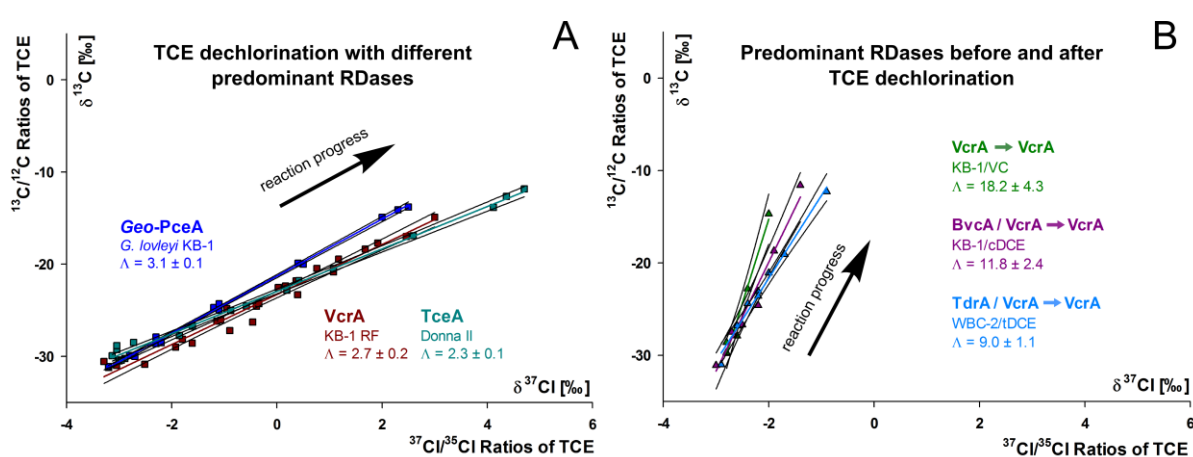
6.2.2 Results

Figure 6B-S2. Carbon and chlorine isotope effects in TCE dechlorination by (A) *G. lovleyi* KB-1 (blue), KB-1 RF (brown) and Donna II (cyan) and (B) KB-1/VC (green), KB-1/cDCE (purple) and WBC-2/tDCE (light blue) with special regards to predominant RDases. (95 % confidence intervals are given as values and as black lines next to the regression slopes).

Table 6B-S4. Data of previous studies used for Figure 3-5.

	System	ε$_C$ [‰]	95% CI	Λ	95% CI	Study
TCE	*Desulfitobacterium hafniense* Y51	-9.1	0.6	3.4	0.2	Cretnik et al. 2013[98]
	Geobacter lovleyi strain SZ	-12.2	0.5	3.4	0.2	
	Enrichment culture (*Desulfitobacterium aromaticivorans*)	-8.8	0.2	2.5		Wiegert et al. 2013[59]
	Desulfitobacterium hafniense Y51	-8.8	0.2	3.4	0.2	Buchner et al. 2015[102]
	Desulfitobacterium hafniense Y51	-9.0	0.2	2.8	0.3	
	Desulfitobacterium hafniense Y51	-9.0	0.2	3.5	0.2	
	Desulfitobacterium hafniense Y51	-8.6	0.0	3.2	0.2	
	Dehalococcoides culture (two species)	-16.4	0.4	4.5		Kuder et al. 2013[103]
	Aquifer microcosms	-12.2	1.0	3.4	0.1	Dogan-Subasi et al. 2017[104]
	RDase from *Sulfurospirillum multivorans* (norpseudo-B12)	-20.0	0.5	5.3	0.3	Renpenning et al. 2014[61]
	RDase from *Sulfurospirillum multivorans* (nor-B12)	-20.2	1.1	5.0	0.8	
	norpseudo-B12 (purified cofactor)	-18.5	2.8	4.5	0.8	
	nor-B12 (purified cofactor)	-15.1	2.7	3.7	0.3	
	dicyanocobinamid (purified cofactor)	-16.5	0.7	4.2	0.6	
	cyano-vitamin B12 (purified cofactor)	-15.0	2.0	4.4	0.7	
	Cyanocobalamin (purified cofactor)	-16.1	0.9	3.9	0.2	Cretnik et al. 2013[98]
	Cobaloxime (model system)	-21.3	0.5	6.1	0.5	
	Vitamin B12 pH 5.0 (model system)	-16.3	0.9	12.8	1.4	Heckel et al. 2018[17]
	Vitamin B12 pH 5.5 (model system)	-15.8	0.9	9.1	0.5	
	Vitamin B12 pH 6.5 (model system)	-16.3	1.1	5.2	0.2	
	Vitamin B12 pH 11 (model system)	-17.5	1.0	3.3	0.1	
	Geobacter lovleyi strain KB-1	-10.3	0.8	3.1	0.1	this study
	KB-1 RF	-9.6	0.5	2.7	0.2	
	Donna II	-13.5	0.6	2.3	0.1	
	KB-1/cDCE	-8.3	3.4	11.8	2.4	
	KB-1/VC	-10.6	9.3	18.2	4.3	
	WBC-2/tDCE	-7.0	1.9	9.0	1.1	
	KB-1/1,2-DCA	-5.4	1.5	4.5	0.8	
cDCE	KB-1 (containing *Dehalococcoides*)	-18.5	1.8	11.6	0.9	Abe et al. 2009[62]
	Aquifer microcosms	-18.0	4.0	4.5	3.4	Dogan-Subasi et al. 2017[104]
	Vitamin B12 pH 6.5 (model system)	-28.4	1.1	18.2	2.2	Heckel et al. 2018[17]
	D. mccartyi 195	-23.2	4.1	10.0	0.4	this study
	D. mccartyi BTF08	-31.1	6.3	17.8	1.0	
PCE	*Desulfitobacterium* sp. strain Viet1	-19.0	0.9	3.8	0.2	Cretnik et al. 2014[58]
	Vitamin B12 pH 6.5 (model system)	-16.7	1.0	3.9	0.3	Heckel et al. 2018[17]
	Vitamin B12 pH 9.0 (model system)	-17.0	1.2	4.2	0.3	
	Vitamin B12 pH 11 (model system)	-16.6	2.7	3.9	0.4	
	Enrichment culture (*Desulfitobacterium aromaticivorans*)	-5.6	0.7	2.8	0.8	Wiegert et al. 2013[59]
	Sulfurospirillum (PceA-TCE)	-3.6	0.2	2.7	0.3	Badin et al. 2014[60]
	Sulfurospirillum (PceA-DCE)	-0.7	0.1	0.7	0.2	
	RDase from *Sulfurospirillum multivorans* (norpseudo-B12)	-1.4	0.1	2.2	0.7	Renpenning et al. 2014[61]
	RDase from *Sulfurospirillum multivorans* (nor-B12)	-1.3	0.1	2.8	0.5	
	norpseudo-B12 (purified cofactor)	-25.3	0.8	6.9	0.7	
	nor-B12 (purified cofactor)	-23.7	1.2	5.0	0.8	
	cyano-B12 (purified cofactor)	-22.4	0.8	4.6	0.2	
	dicyanocobinamid (purified cofactor)	-25.2	0.5	7.0	0.8	

6.3 Supporting Information of Chapter 4

6.3.1 Gradient Programs for HPLC Analysis

A. aurescens **TC1: Separation of atrazine and 2-hydroxyatrazine.** The compounds were separated by using a gradient elution at a flow rate of 1.0 mL/min. The initial conditions (20 % acetonitrile, 80 % buffer of 2 mM K_3PO_4, pH 7.0) were immediately followed by a linear gradient to 65 % acetonitrile within 9 min. These conditions were maintained isocratic for 2 min. A subsequent gradient led back to the initial conditions of 20 % acetonitrile within 1 min, which was maintained for 5 min.

Rhodococcus **sp. NI86/21: Separation of atrazine, desethylatrazine and desisopropylatrazine.** The compounds were separated by using a gradient elution at a flow rate of 0.8 mL/min. The initial conditions (5 % acetonitrile, 95 % buffer of 2 mM K_3PO_4, pH 7.0) were maintained isocratic for 2 min. Afterwards, a linear gradient led to 55 % acetonitrile within 12 min followed by another linear gradient which led to 75 % acetonitrile within 2 min. These conditions were maintained isocratic for 2 min. A subsequent gradient led back to the initial conditions of 5 % acetonitrile within 2 min, which was maintained for 5 min.

6.3.2 Chlorine Isotope Analysis via GC-qMS according to Ponsin et al. – Method Optimization

For method optimization standards in the range of 1 - 200 mg/L were measured ten times each at three different dwell times (30/60/100 ms) for defining the linearity range and the uncertainty of the method. Furthermore, a long-term stability test over 50 days was conducted.
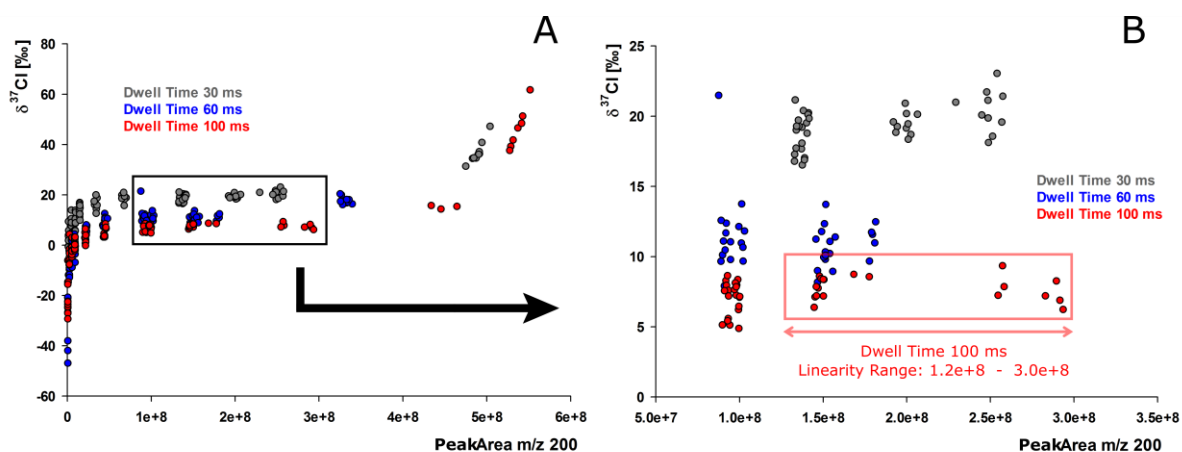
Figure 6C-S1. Analysis of different dwell times (30 ms grey, 60 ms blue, 100 ms red) and concentrations (corresponding to different peak areas) in order to define the optimal dwell time and the linearity range of analysis.

Table 6C-S1. Ten-fold standard injection at dwell time 100 ms at different concentrations and resulting standard deviations. Grey shaded lines are located inside the linearity range.

Concentration	Standard Deviation
1 mg/L	7.2 ‰
5 mg/L	4.4 ‰
7 mg/L	5.8 ‰
10 mg/L	6.8 ‰
20 mg/L	2.0 ‰
30 mg/L	2.0 ‰
40 mg/L	1.4 ‰
50 mg/L	1.1 ‰
75 mg/L	0.7 ‰
100 mg/L	1.0 ‰
200 mg/L	16.7 ‰

Figure 6C-S2. Analysis of the atrazine standard Atr #4 over a period of 50 days. Red dots represent the mean of a ten-fold measurement while error bars illustrate the standard deviations. The mean over all measurements is given as value and as red line, while the standard deviation is given as value and as black line.
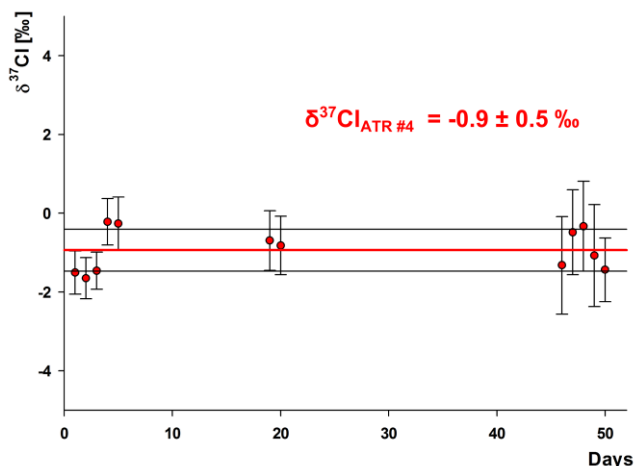
As illustrated in Figure 6C-S1, a dwell time of 100 ms was chosen as method parameter for analysis and the linearity range for analysis was defined as the peak area (m/z 200) of $1.2 - 3.0 \times 10^8$. Inside the linearity range the precision of the method is associated with a maximal uncertainty of ± 1.1 ‰ (see Table 6C-S1). The final concentration of standards and samples for analysis should be approx. 75 mg/L which corresponds to a peak area (m/z 200) of approx. 1.7×10^8. The long-term stability test (see Figure 6C-S2) resulted in chlorine values of standard injections (Atr #4, 75 mg/L, dwell time 100 ms) which showed no significant differences over the tested period of 50 days.

6.3.3 Comparison of the GC-qMS Methods for Chlorine Analysis of This Study and Ponsin et al.

Both, the GC-qMS method optimized here and that shown by Ponsin et al.[69], can be used to measure chlorine isotope values of atrazine. The main difference between the two methods is the amount of atrazine injected on the analytical column (and the corresponding optimum concentration): this study: 150 ng on column (75 mg/L), Ponsin et al.[69]: 10 ng on column (5 mg/L). For 5 mg/L (corresponding to 10 ng on column in our method), we observed a strong dependency between peak area (concentration) and chlorine isotope values. Additionally, very large variations leading to large standard deviations (> 4 ‰) were observed (see Table 6C-S1). However, 5 mg/L was outside of our defined linearity range.

The linearity range was defined at higher concentrations, between 50 and 100 mg/L (see Table 6C-S1), and thus samples were only measured within this range. Ponsin et al.[69] measured their samples at lower concentrations, but due to their requirement that standards and samples had to have the same concentration (20 % tolerance), chlorine isotope values could be corrected, leading to accurate results. An advantage of the method of Ponsin et al.[69] is that lower concentrations can be measured. However, regarding the precision our method seems to be more optimized. We observed a maximal standard deviation of ± 1.1 ‰ (for an atrazine concentration of 50 mg/L) while Ponsin et al.[69] reported a standard error of ± 1 ‰ (n = 10) corresponding to a standard deviation of approx. ± 3.2 ‰, for the atrazine concentration range between 10 and 30 mg/L.

Table 6C-S2. Comparison of the method parameters of this study and the study of Ponsin et al.[69].

	Ponsin et al.[69]	This study
Injectionvolume/-temperature	1 µL / 250 °C	2 µL / 220 °C
Analytical Column	DB-17 MS	DB-5 MS
GC Temperature Program	60 °C (1 min), 30 °C/min to 190 °C (3 min), 3 °C/min to 210 °C (3 min)	65 °C (1 min), 20 °C/min to 180 °C (10 min), 15 °C/min to 230 °C (8 min)
Column Flow	1.2 mL/min	1.4 mL/min
Split Flow	splitless	1 min splitless, then split mode (split ratio 1:10)
Temperature MS Quad/MS Source	150 °C / 230 °C	150 °C / 230 °C
Dwell Time	30 ms	100 ms
Concentration Optimum → Amount on Analytical Column	10 ppm → 10 ng	75 ppm → 150 ng
Amount Dependency	Measurement of standards with similar concentration as samples, 20 % tolerance between sample and standard concentration	Defining linearity range, where no amount dependency is observed (peak area between 1.2×10^8 and 3.0×10^8)

6.3.4 Consideration of Interfering Fragments

The constructive-critical comments of a reviewer pointed out that H-transfer reactions can occur from one fragment to the other in the ions source during GC-qMS analysis. It was questioned whether this could bias chlorine isotope measurements. Specifically, (I) ions that *do not* contain ^{37}Cl may contribute to m/z 202; (II) ions may turn up as m/z 200 even though they *do* contain ^{37}Cl.

Case (I). In combination with the substitutions of ^{13}C and ^{15}N, H-transfer can lead to the formation of fragments with m/z 202 ($[^1H_{12}{}^{12}C_6{}^{13}C^{14}N_5{}^{35}Cl]^+$, $[^1H_{12}{}^{12}C_7{}^{14}N_4{}^{15}N^{35}Cl]^+$) which may add up to the "correct" peak of ($[^1H_{11}{}^{12}C_7{}^{14}N_5{}^{37}Cl]^+$ and, therefore, interfere with chlorine CSIA. The probability of occurrence of these fragments was calculated by using the ratio of the peaks of m/z 200 ($[^1H_{11}{}^{12}C_7{}^{14}N_5{}^{35}Cl]^+$) and m/z 201 ($[^1H_{11}{}^{12}C_6{}^{13}C^{14}N_5{}^{35}Cl]^+$, $[^1H_{11}{}^{12}C_7{}^{14}N_4{}^{15}N^{35}Cl]^+$, $[^1H_{12}{}^{12}C_7{}^{14}N_5{}^{35}Cl]^+$) in the atrazine mass spectrum (see Figure 6C-S3).
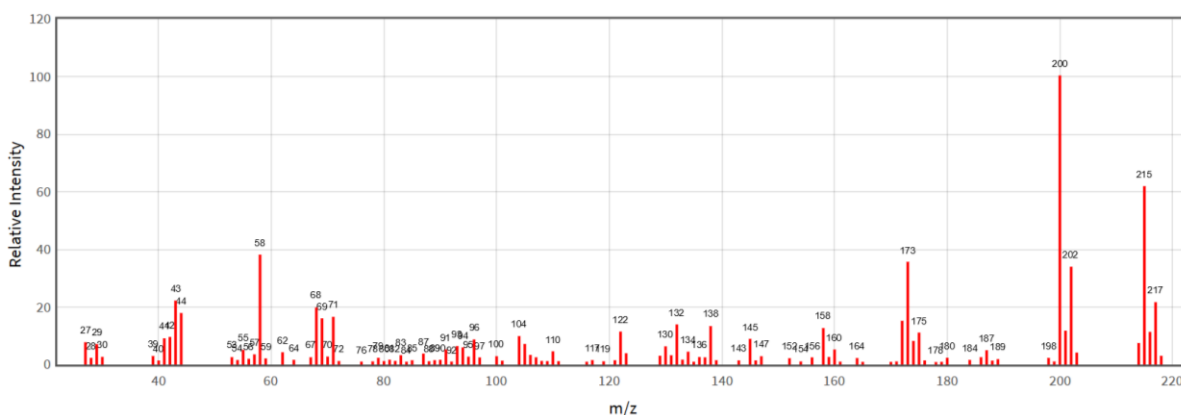
Figure 6C-S3. Mass spectrum of atrazine (taken from NIST 2020[150]).

By using the relative intensities shown in Figure 6C-S3, it can be observed that the probability for a fragment with m/z 201 (that is, the mass of a fragment that has received a hydrogen atom) is approx. 11.8 %. However, ions at this mass may also represent "true" ^{13}C and ^{15}N isotopologues of mass m/z 201. Taking into account the natural abundance of ^{13}C and ^{15}N, as well as the number of C and N atoms in the molecule, it becomes clear that, indeed, most of this abundance is attributable to "true" ^{13}C and ^{15}N isotopologues

$[^1H_{11}{}^{12}C_6{}^{13}C^{14}N_5{}^{35}Cl]^+$ = 7.7 %, $[^1H_{11}{}^{12}C_7{}^{14}N_4{}^{15}N^{35}Cl]^+$ = 1.8 %, and only a minor fraction is attributable to artefacts from hydrogen transfer: $[^1H_{12}{}^{12}C_7{}^{14}N_5{}^{35}Cl]^+$ = 2.3 % (see Table 6C-S3).

Table 6C-S3. Probability of occurrence of fragments with m/z 201.

Fragment with m/z 201	Probability of occurrence*
$[^1H_{11}{}^{12}C_6{}^{13}C^{14}N_5{}^{35}Cl]^+$	~ 7.7 %
$[^1H_{11}{}^{12}C_7{}^{14}N_4{}^{15}N^{35}Cl]^+$	~ 1.8 %
$[^1H_{12}{}^{12}C_7{}^{14}N_5{}^{35}Cl]^+$	11.8 % - 7.7 % - 1.8 % ≈ 2.3 %

* Based on natural abundance for each stable isotope considered (^{13}C: 0.011056, ^{15}N: 0.00366)[33]

Also for the mass m/z 202 one can, hence, assume that the probability of a hydrogen transfer from mass 201 is 2.3 %. Hence, this probability still needs to be multiplied with the probability that a ^{13}C and ^{15}N is present in the molecule. This gives the probability of occurrence of the interfering fragments with m/z 202: $[^1H_{12}{}^{12}C_6{}^{13}C^{14}N_5{}^{35}Cl]^+$ = (7.7 % × 2.3 %) = 1.8 ‰, and $[^1H_{12}{}^{12}C_7{}^{14}N_4{}^{15}N^{35}Cl]^+$ = (1.8 % × 2.3 %) = 0.4 ‰. Hence, 1.8 ‰ of all ions of m/z 202 are $[^1H_{12}{}^{12}C_6{}^{13}C^{14}N_5{}^{35}Cl]^+$ instead of true ^{37}Cl isotopologues, and 0.4 ‰ of all ions of m/z 202 are $[^1H_{12}{}^{12}C_7{}^{14}N_4{}^{15}N^{35}Cl]^+$ instead of true ^{37}Cl isotopologues.

These numbers already show that the effect is very small. However, much of this effect can actually be corrected by the identical treatment of standard and sample. The exception is if the standard has a different $\delta^{13}C$ compared to the sample. To estimate the artifact introduced by this difference, one can assume that $\delta^{13}C$ of atrazine would vary by about 20 ‰ when biodegradation occurs. Hence, the artifact of protonated ^{13}C isotopologues *that cannot be corrected by the identical treatment of standard and sample* would be $\Delta[^1H_{12}{}^{12}C_6{}^{13}C^{14}N_5{}^{35}Cl]^+$ = 20 ‰ × 1.8 ‰ = 0.036 ‰. In a next step we therefore need to calculate how much such a variability in Δ[m/z 202] would influence the $\delta^{37}Cl$ measurement.

The natural abundance ratio of $^{37}Cl/^{35}Cl$ and, therefore, of the peaks m/z 202 and m/z 200, is about 0.33 (see Figure 6C-S3). Hence, a shift of $\Delta\delta^{37}Cl$ = 1 ‰ would correspond to a change in the relative peak abundance of m/z 202 to 200 of about 0.33 × 1 ‰ = 0.33 ‰. In comparison, the contribution of the variability introduced by the "artefact" peak

$\Delta[^1H_{12}{}^{12}C_6{}^{13}C^{14}N_5{}^{35}Cl]^+$ to the variability in $\Delta[m/z\ 202]$ (0.036 ‰) is a factor of ten smaller. This artefact, therefore, is expected to affect the measured $\delta^{37}Cl$ values by 0.1 ‰ at most. Therefore, within the precision of our methods, the influence of H-abstraction during chlorine CSIA is negligible.

Case (2). In a similar way, H-atoms can also be cleaved off during GC-qMS analysis. Therefore, a molecular isotopologue of atrazine with m/z 202 ($[^1H_{11}{}^{12}C_7{}^{14}N_5{}^{37}Cl]^+$) could transform to m/z 200 ($[^1H_9{}^{12}C_7{}^{14}N_5{}^{37}Cl]^+$) which could interfere with chlorine CSIA. Since the transformation rate of m/z 202 to m/z 200 corresponds to the transformation rate of m/z 200 to m/z 198, this can be easily investigated by analyzing the peak of m/z 198 in the mass spectrum of atrazine (see Figure 6C-S3). Since the relative abundance of the peak of mass m/z 198 is very low ($< 2\%$), it can be concluded that the loss of H-atoms is negligible and thus it does not interfere with chlorine CSIA.

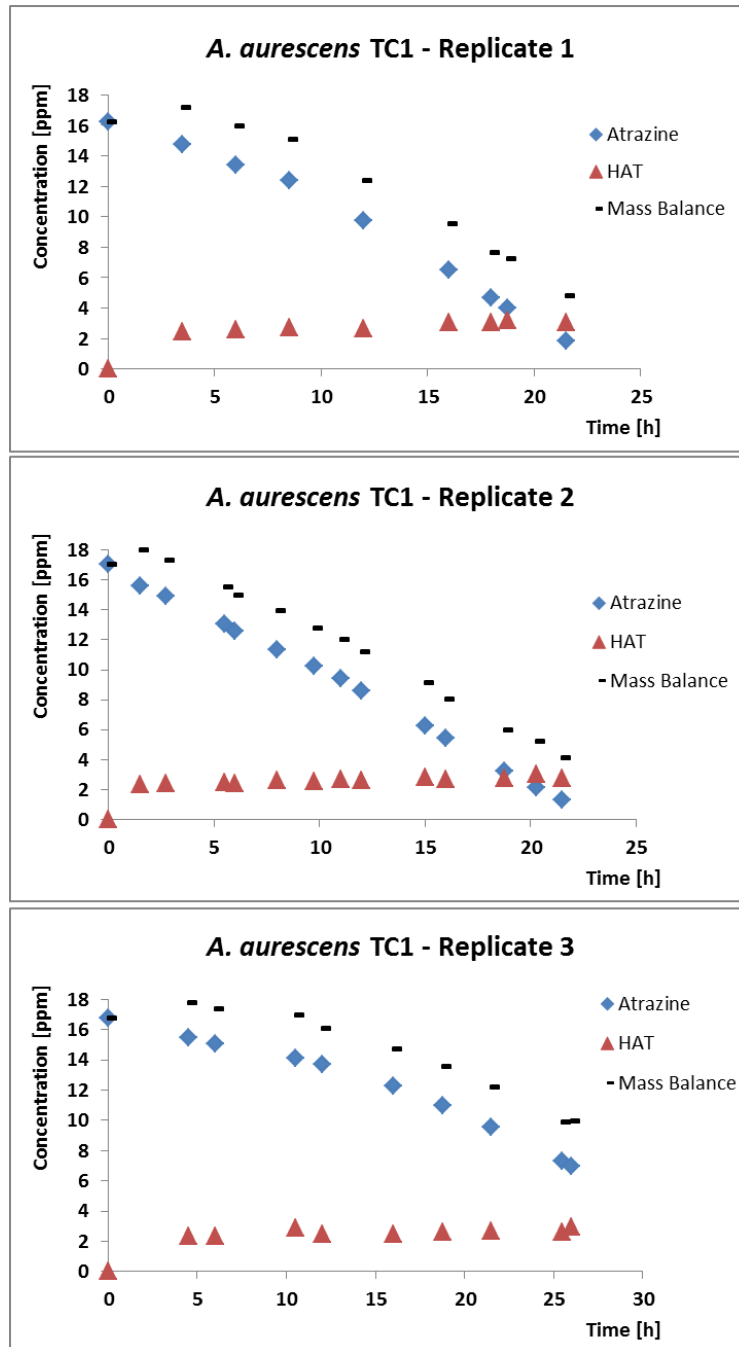### 6.3.5 Concentration Analysis of Atrazine and its Metabolites

Figure 6C-S3. Degradation of atrazine to 2-hydroxyatrazine (HAT) with *A. aurescens* TC1. The mass balance is not closed due to further degradation of HAT[39].
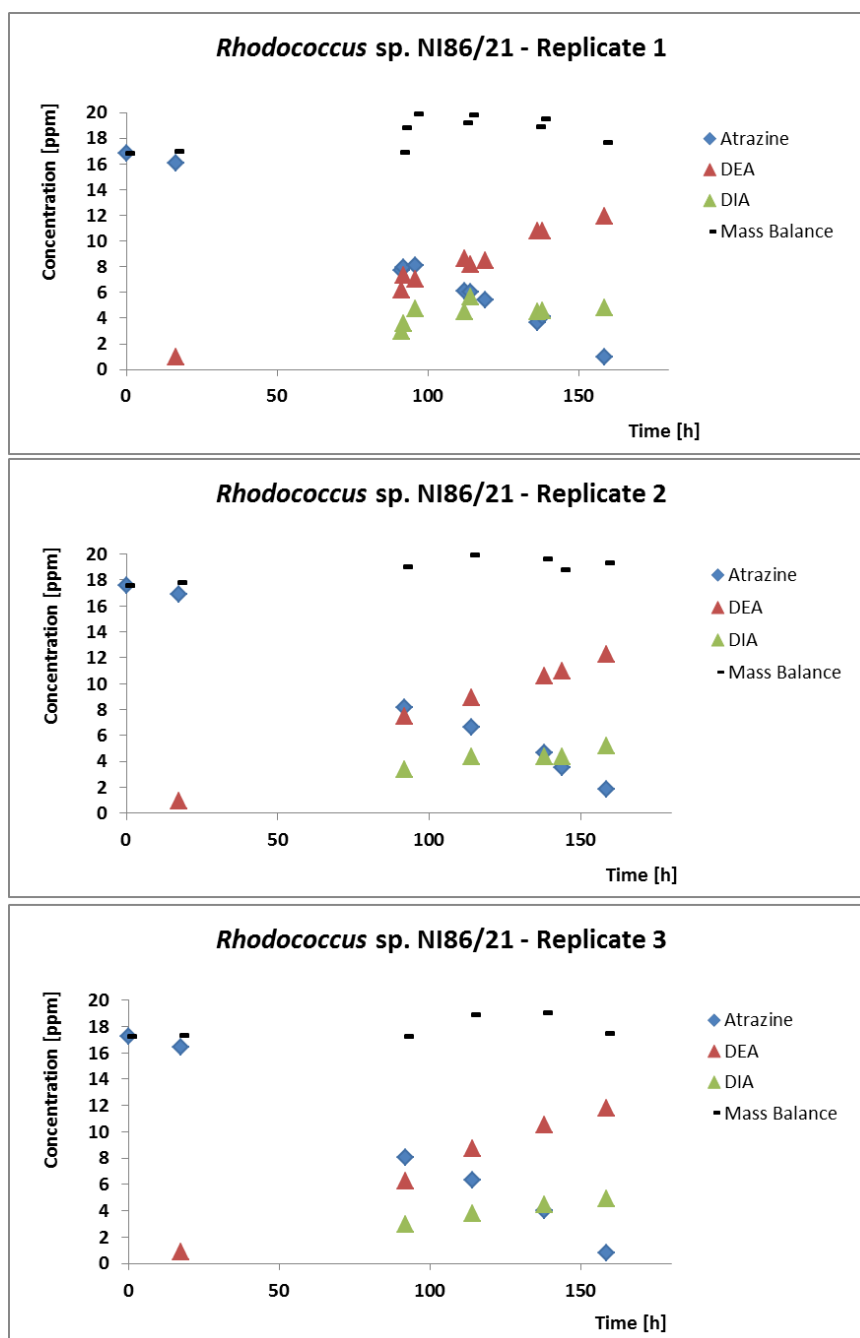
Figure 6C-S4. Degradation of atrazine to desethylatrazine (DEA) and desisopropylatrazine (DIA) with *Rhodococcus* sp. NI86/21.
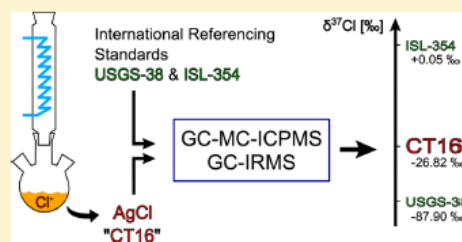
6.4 Published Manuscripts

Toward Improved Accuracy in Chlorine Isotope Analysis: Synthesis Routes for In-House Standards and Characterization via Complementary Mass Spectrometry Methods

Christina Lihl,[†] Julian Renpenning,[‡] Steffen Kümmel,[‡] Faina Gelman,[§] Heide K. V. Schürner,[†] Martina Daubmeier,[†] Benjamin Heckel,[∥] Aileen Melsbach,[†] Anat Bernstein,[⊥] Orfan Shouakar-Stash,[@] Matthias Gehre,[‡] and Martin Elsner[*,†,∥]

[†]Institute of Groundwater Ecology, Helmholtz Zentrum München, Ingolstädter Landstraße 1, 85764 Neuherberg, Germany

[‡]Department of Isotope Biogeochemistry, Helmholtz Centre for Environmental Research − UFZ, Permoserstraße 15, 04318 Leipzig, Germany

[§]Geological Survey of Israel, 32 Yeshayahu Leibowitz Street, 9692100 Jerusalem, Israel

[∥]Chair of Analytical Chemistry and Water Chemistry, Technical University of Munich, Marchioninistraße 17, 81377 München, Germany

[⊥]Zuckerberg Institute for Water Research, Department of Environmental Hydrology and Microbiology, Ben-Gurion University of the Negev, 84990 Sede Boqer, Israel

[@]Department of Earth Sciences, University of Waterloo, 200 University Avenue, Waterloo, Ontario, Canada N2L 3G1

S Supporting Information

ABSTRACT: Increasing applications of compound-specific chlorine isotope analysis (CSIA) emphasize the need for chlorine isotope standards that bracket a wider range of isotope values in order to ensure accurate results. With one exception (USGS38), however, all international chlorine isotope reference materials (chloride and perchlorate salts) fall within the narrow range of one per mille. Furthermore, compound-specific working standards are required for chlorine CSIA but are not available for most organic substances. We took advantage of isotope effects in chemical dehalogenation reactions to generate (i) silver chloride (CT16) depleted in $^{37}Cl/^{35}Cl$ and (ii) compound-specific standards of the herbicides acetochlor and S-metolachlor (Aceto2, Metola2) enriched in $^{37}Cl/^{35}Cl$. Calibration against the international reference standards USGS38 (-87.90 ‰) and ISL-354 ($+0.05$ ‰) by complementary methods (gas chromatography-isotope ratio mass spectrometry, GC-IRMS, versus gas chromatography-multicollector inductively coupled plasma mass spectrometry, GC-MC-ICPMS) gave a consensus value of $\delta^{37}Cl_{CT16} = -26.82 \pm 0.18$ ‰. Preliminary GC-MC-ICPMS characterization of commercial Aceto1 and Metola1 versus Aceto2 and Metola2 resulted in tentative values of $\delta^{37}Cl_{Aceto1} = 0.29 \pm 0.29$ ‰, $\delta^{37}Cl_{Aceto2} = 18.54 \pm 0.20$ ‰, $\delta^{37}Cl_{Metola1} = -4.28 \pm 0.17$ ‰ and $\delta^{37}Cl_{Metola2} = 5.12 \pm 0.27$ ‰. The possibility to generate chlorine isotope in-house standards with pronounced shifts in isotope values offers a much-needed basis for accurate chlorine CSIA.

Isotopes, atomic nuclei that are identical in their chemical properties but show differences in their atomic mass, may be present in varying proportions. Stable isotope ratios are typically expressed in the δ-notation relative to a common international reference material (see eq 1). This has the advantage that values, when measured in different laboratories against the same reference material, are comparable on an absolute scale.[1,2]

$$\delta^h E = [(^h E/^l E)_{Sample} - (^h E/^l E)_{Reference}]/(^h E/^l E)_{Reference} \quad (1)$$

$\delta^h E$ refers to the isotope value of an element E and $(^h E/^l E)$ to the absolute ratio of the respective heavy (h) and light (l) isotopes. Positive delta values imply an enrichment, and negative delta values indicate a depletion of heavy relative to

light isotopes when compared to the international reference standard.[3,4] Isotope ratios are used in a wide field of applications. In archeology, stable isotope ratios inform about prehistoric lifestyle and diet;[5] in food sciences, they serve to test the quality and the origin of foods.[6] In forensic science, isotope analysis can help trace the production site of drugs,[7] and in competitive sports it can reveal doping violations.[8] Isotope analysis is equally important in the field of environmental sciences where environmental contaminants threaten the quality of groundwater resources. By analyzing

isotope ratios of single compounds, compound-specific isotope analysis (CSIA) is able to allocate a contaminant to a certain source.[9] In addition, CSIA can help to detect and quantify isotope fractionation to trace degradation processes of environmental contaminants. Since bonds of molecules with heavy versus light isotopes are transformed at different rates, isotope ratios change during degradation. Hence, isotope analysis has the potential to identify degradation of contaminants even if no metabolites can be detected. As isotope effects are reaction-specific, isotope ratio analysis of the parent compound may in addition deliver information about chemical transformation pathways, even without metabolite analysis.[2,4,10−12]

Chlorine isotope analysis ($^{37}Cl/^{35}Cl$) has increased in importance with its role in deciphering central geochemical and biological processes. Since chloride is one of the most abundant anions in geological fluids, its isotopes were measured early on to obtain information about geological processes and about the origin of chlorine found in brines and basalts.[13,14] Furthermore, chlorine isotope analysis of perchlorate has been used to identify the source of environmental contamination.[15] "Offline" methods such as the Holt method[16] were for a long time the only way to accomplish such chlorine stable isotope analysis. They rely on a chemical conversion of a compound in sealed glass or metal tubes and complex vacuum lines followed by isotope ratio mass spectrometry (IRMS). Hence, to enable isotope analysis of single compounds, target substances have to be purified beforehand. Afterward they must be converted into a suitable analyte containing only one chlorine atom such as methyl chloride in the case of the Holt method[16] or CsCl for thermal ionization mass spectrometry.[17] This approach, however, is rather time, labor, and cost intensive, requires a large sample amount,[16,18] and is therefore prohibitive for compound-specific isotope analysis (CSIA) of organic compounds in trace concentrations. In turn, such chlorine CSIA has recently been made possible by advancing and optimizing instrumentation for online chlorine isotope analysis. Chromatographic separation of a sample is combined with subsequent isotope ratio analysis by a dedicated IRMS.[19] First instrumental solutions for chlorine CSIA were realized by transferring the separated chlorinated compounds in a helium carrier gas stream directly to an IRMS with dedicated cup configuration[9] or into a quadrupole mass spectrometer (qMS).[20−22] In a most recent development, chlorine isotope analysis via a GC-MC-ICPMS (gas chromatography-multi-collector inductively coupled plasma mass spectrometer) has even been realized by converting organic compounds into Cl^+ ions in an inductively coupled plasma and, therefore, offering for the first time an opportunity of universal online chlorine CSIA at very low analyte concentrations (2−3 nmol of Cl).[23,24]

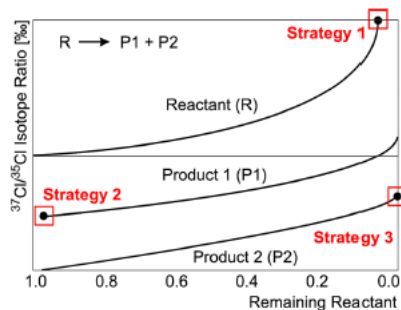Chlorine CSIA has played a key role in elucidating chlorinated ethene transformation mechanisms in lab studies[25−30] and is at the verge of becoming a method of choice to study the environmental fate of chlorinated hydrocarbons at contaminated sites. Even chlorinated compounds with more complex structures like herbicides are getting within reach. At this point, however, an issue is becoming increasingly important that is crucial for chlorine CSIA on unconverted target compounds and is particularly warranted for comparison of analyses by different instrumental approaches: the need for chlorine isotope reference materials and compound-specific in-house isotope working standards.

As expressed by eq 1, isotope reference standards, ideally two standards which bracket the isotope values of the samples, are crucial for true isotope measurements.[1,22,31,32] International reference materials are highly valuable, rather expensive, and sometimes even available only in limited amounts. Therefore, laboratories are advised to prepare their own in-house reference standards. These standards should be calibrated against the international reference standards.[33] In the case of chlorine, two international reference materials are available, ISL-354 (NaCl, $\delta^{37}Cl$ = +0.05 ± 0.03 ‰) and NIST SRM 975a (NaCl, $\delta^{37}Cl$ = +0.01 ‰).[34−36] Additionally, Böhlke et al.[36] were able to synthesize and characterize the oxygen and chlorine isotope reference materials USGS37 (KClO$_4$, $\delta^{37}Cl$ = +0.90 ± 0.04 ‰), USGS38 (KClO$_4$, $\delta^{37}Cl$ = −87.90 ± 0.24 ‰), and USGS39 (KClO$_4$, $\delta^{37}Cl$ = +0.05 ‰) on the international scale for ClO_4^- isotopic analysis. Unfortunately, most of these standards show very similar chlorine isotope values. Only one perchlorate standard, USGS38, shows a large isotopic shift, which has solved the long-standing problem that working standards for daily chlorine isotope analysis could be characterized against only one international reference standard. The availability of the standard USGS38 with its pronounced negative $\delta^{37}Cl$-value enables for the first time a two-point calibration of other chlorine standards. Since such international reference materials are very valuable, the next logical step is the preparation of in-house standards with a pronounced isotopic shift that can be routinely used for calibration on the delta scale. For example, this approach is well-entrenched for hydrogen and oxygen isotope analysis of water, where laboratories typically possess their own in-house standards that have been calibrated against the international water standards SLAP (standard light antarctic precipitation) and VSMOW (Vienna standard mean ocean water).[33]

A second challenge lies in the upcoming opportunity of chlorine CSIA which requires sets of compound-specific working standards that bracket a suitable range of isotope values. For chlorine CSIA, these working standards have to be substance-specific since there is no combustion to an analyte gas. In accordance with the IT-Principal (principal of identical treatment of referencing material and sample), the process of measurement can include isotope fractionating steps. Therefore, for each substance, the trueness of analysis has to be validated by using chemically identical standards with a known isotope value, which are subject to the same reaction conditions as the sample.[21,37,38] Hence, our second objective was to create such compound-specific working standards.

Even though it is well established that isotopologues can be separated by physical properties like diffusivity or vapor pressure, the corresponding processes require an extensive number of repetitions. To this end, dedicated instrumentation is needed that is beyond the scope of typical isotope laboratories. Alternatively, because most chemical reactions are accompanied by larger isotopic fractionation than physical processes, chemical reactions can be used as a tool to synthesize standards with a more negative or a more positive isotope value than the starting material. To harvest the isotope fractionation of such a chemical reaction, three strategies may be pursued (see Scheme 1). Strategy 1: a substrate may be converted to a large degree, the reaction may be stopped, and the remaining substrate may be purified from the reaction mixture. Strategy 2: a product may be continuously recovered in the presence of a large pool of substrate. Strategy 3: if two products are formed simultaneously, a reaction may be brought

Scheme 1. Possible Strategies to Generate a Standard with a Shifted Chlorine Isotope Ratio Compared to the Starting Material

Scheme 2. (A) Synthesis Route to the Silver Chloride Reference Standard CT16 via Reductive Elimination of Cl⁻ and Subsequent Precipitation with AgNO₃, and (B) Expected Fractionation and the Corresponding Strategy to Recover Chloride with Pronounced Changes in Chlorine Isotope Values

to completion, and the products may be separated to take advantage of the differences in isotope effects to the parallel products.

The first objective of this study was to identify a synthesis route to easily generate and to characterize a chloride salt as chlorine isotope in-house standard. To this end, strategy 3 of Scheme 1 was pursued to synthesize a chloride in-house standard with a negative isotope value. Subsequently, this standard was characterized against the international chlorine reference standards USGS38 and ISL-354.
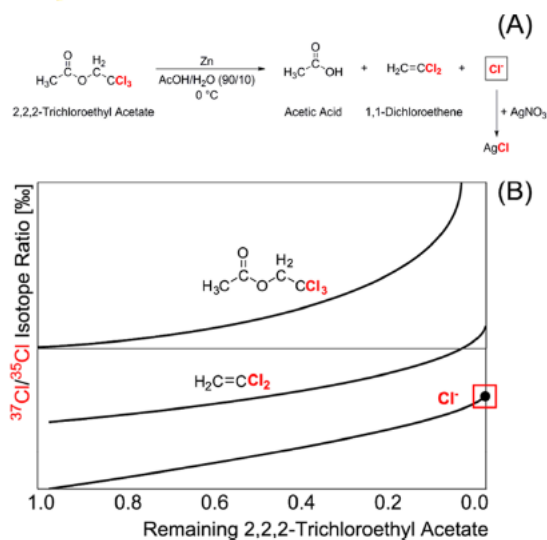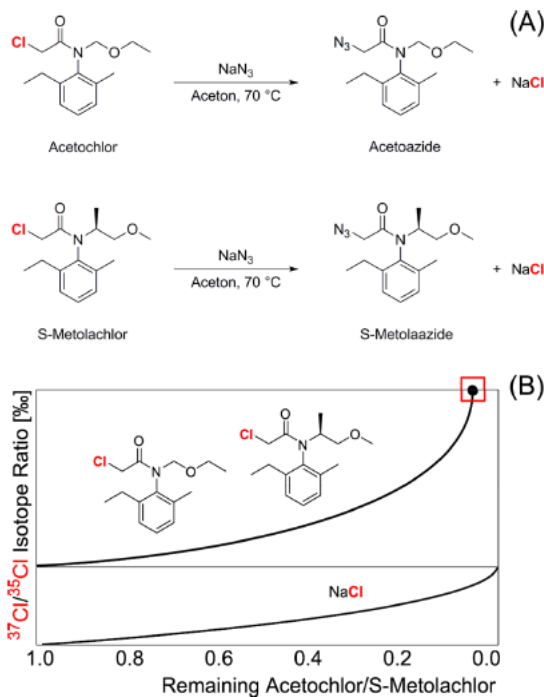
The second objective of this study was to show that chemical reactions and their corresponding isotope fractionation can be used according to strategy 1 to generate in-house working standards for chlorine CSIA of specific organic compounds. Since isotope fractionation of micropollutants such as pesticides is receiving increasing attention,[39] the herbicides S-metolachlor and acetochlor were chosen. These compounds are among the most commonly used herbicides for the protection of plants against weeds in U.S. agriculture.[40] In the environment, they can have toxic effects on living organisms.[41] Thus, studying the environmental fate and the transformation pathways of these herbicides by chlorine CSIA is of particular interest.

■ EXPERIMENTAL SECTION

Synthesis of the Chlorine Isotope In-House Standard CT16. Following the protocol of Somsák et al.,[42] 2,2,2-trichloroethyl acetate (14 mL) was used as a starting material. As depicted in Scheme 2A, the trichloroethyl group was removed by zinc in 90% aqueous acetic acid (140 mL) via a reductive elimination process under reflux conditions at 0 °C. After 24 h, a silver nitrate solution (350 mL, 17 g/L) was added to precipitate the formed chloride as silver chloride. After filtering, the pure silver chloride (2.61 g) was dried at 40 °C overnight in the dark. Silver chloride decomposes upon exposure to light but remains perfectly stable when stored in a desiccator in the dark (brown glass bottles wrapped with aluminum foil). Even through its use may, therefore, be limited as a reference material, it represents an ideal in-house standard because it may be directly converted to methyl chloride, which is the common measurement gas in chlorine isotope analysis.

Synthesis of the Chlorine Isotope Working Standards Aceto2 for Acetochlor and Metola2 for S-Metolachlor. Acetochlor and S-metolachlor were purchased in their pure forms (Chemos). As such, they could be used as primary

working standards Aceto1 and Metola1, representing one anchor point of the two-point calibration. To generate working standards with an isotopic shift for a second anchor point, 18 g of the purchased acetochlor and S-metolachlor, respectively, and NaN₃ (21.6 g/20.7 g) were dissolved in acetone (500 mL) according to the protocol of Weigl and Wünsch.[43] Like that illustrated in Scheme 3A, the solution was heated up to 70 °C under reflux. During the reaction, chloride was substituted by an azide group. The progress of the reaction was monitored via HPLC analysis. The reactions were stopped when 32.2% of the initial acetochlor (approximately after 40 h) and 29.4% of the initial S-metolachlor (approximately after 94 h) were left. By flushing the solution with N₂, the solvent was evaporated at room temperature. The residue was twice dissolved in diethyl ether (200 mL), and the ether phase was washed three times with H₂O (300 mL) and dried over Na₂SO₄. After filtering and evaporating with a rotary evaporator, the unconverted respective chloroacetanilide was purified and recovered from the rest of the reaction mixture via silica column chromatography. The eluent was n-hexane/ethyl acetate (6/1) for acetochlor, (R_f = 0.36) and n-hexane/ethyl acetate (4/1) for S-metolachlor (R_f = 0.447), respectively. In a last step, the eluent was removed by rotary evaporation. 1.43 g of Acetochlor (reddish oil) and 2.53 g S-Metolachlor (yellowish oil) were obtained.

Monitoring of the Reaction Progress of Acetochlor and S-Metolachlor via HPLC. For HPLC analysis, 1 mL of reaction solution was sampled and the solvent was evaporated by flushing the sample with N₂. The residue was dissolved in 1 mL acetonitrile and analyzed on a Shimadzu UHPLC-20A system. To this end, samples were diluted (1:200) with Milli-Q/acetonitrile (80/20). A C18 column [Purospher STAR, RP-18 end-capped (5 μm), LiChroCART 125−2, Merck] was used together with acetonitrile and a KH₂PO₄ buffer (0.1 mM)

Scheme 3. (A) Synthesis of Chlorine Isotope Working Standards of Acetochlor Aceto2 and S-Metolachlor Metola2, and (B) Expected Fractionation and Resultant Strategy to Recover Unreacted Acetochlor/S-Metolachlor with Pronounced Changes in Chlorine Isotope Values

as eluents. A volume of 5 μL was injected, and the oven temperature was set to 40 °C. Separation was accomplished by gradient elution at a flow rate of 0.3 mL/min starting with 40% acetonitrile and 60% buffer. For separation of acetochlor and acetoazide, a linear gradient to 70% acetonitrile within 33 min was used, whereas S-metolachlor and S-metolaazide were separated in a linear gradient to 60% acetonitrile within 22 min. The respective final conditions were maintained isocratic for 4 and 3 min, respectively, before a subsequent gradient led back to the initial conditions of 40% acetonitrile within 1 and 0.5 min, respectively. Subsequent equilibration was for 5 min (acetochlor) and 7.5 min (S-metolachlor). Compound detection took place by UV absorbance at a wavelength of 216 nm for acetochlor and at 214 nm for S-metolachlor. Quantification was performed by the software "Lab Solutions".

Conversion of the International Reference Standard ISL-354 (NaCl) to Silver Chloride. The conversion of ISL-354 (NaCl (56 mg) dissolved in 50 mL Milli-Q) was accomplished by precipitation with 30 mL of silver nitrate solution (20.3 mg/mL). The precipitated silver chloride was washed twice with methanol and once with acetone. Afterward it was dried at room temperature in the dark.

Conversion of the International Reference Standard USGS38 (KClO$_4$) to Silver Chloride. Following the protocol of Böhlke et al.,[36] KClO$_4$ (2.5 mg) was filled into quartz glass ampules which were then evacuated and sealed with an oxygen torch. After heating the ampules to 720 °C for 20 min in a preheated oven, they were cracked and the Cl$^-$ that was

formed from decomposed ClO$_4^-$ was dissolved in 2 mL warm Milli-Q water. Silver chloride was precipitated by adding 0.1 mL of silver nitrate solution (83.3 mg/mL). The silver chloride was then washed twice with methanol and once with acetone and dried at room temperature in the dark.

Conversion of Silver Chloride to Methyl Chloride. A method for the conversion of silver chloride to methyl chloride was modified from Holt et al.[16] Silver chloride (300 μg) was weighted into 10 mL headspace vials and flushed for 20 s with N$_2$ gas. Methyl iodide (150 μL) which was filled into 1.5 mL quartz glass inserts was added. Afterward, the vials were closed and tightly crimped with PTFE coated septa (Carl Roth) and put into the oven at 80 °C for 48 h.

Chlorine Isotope Analysis via GC-IRMS (Munich). The method for chlorine isotope analysis was adapted from Shouakar-Stash et al.[44] Measurements were performed on a gas chromatograph (Thermo Scientific, Trace GC Ultra) coupled to an isotope ratio mass spectrometer (Thermo Scientific, Finnegan MAT 253 IRMS) equipped with a direct transfer line so that the MeCl samples were directly transferred from the GC to the IRMS in a He carrier stream. There, the compounds were ionized and fragmented for isotope ratio analysis at the masses m/z of 50/52. To achieve optimal separation, a Vocol column (Supelco, 30 m $\times$ 0.25 mm, 1.5 μm film thickness) was used. Samples from the headspace (250 μL) were injected into the GC at a split ratio of 1:50. The GC oven temperature program started at 40 °C (1 min), increased to 100 °C at 30 °C/min, and was held for 2 min. MeCl reference gas pulses were injected via a dual inlet system at the beginning and at the end of each measurement as described in Bernstein et al.[22] Two-point calibrations were performed with the international reference standards ISL-354 (δ^{37}Cl = +0.05 ‰)[34] and USGS38 (δ^{37}Cl = −87.90 ‰)[36] to convert measurements to δ^{37}Cl values relative to standard mean ocean chloride (SMOC).

Chlorine Isotope Analysis via GC-MC-ICPMS (Leipzig). Measurements were performed according to the protocols described in Horst et al.[24] and Renpenning et al.[23] Samples were separated using a gas chromatograph (Thermo Scientific, Trace 1310) equipped with a Zebron ZB-1 column (Phenomenex Inc., 60 m $\times$ 0.32 mm, 1 μm film thickness). A heated transfer line coupled the GC to a multicollector inductively coupled plasma mass spectrometer (MC-ICPMS, Thermo Fisher Scientific, Neptune). For analysis of methyl chloride, 80 μL of gaseous sample were manually injected into a split/splitless injector at a temperature of 280 °C. For achieving chromatographic separation of methyl chloride and methyl iodide, the GC started at 30 °C (8 min) followed by a gradient of 10 °C/min to 100 °C. The transfer line was kept at 160 °C. A constant column flow of 2 mL/min with a split ratio of 1:10 was applied. For the analysis of acetochlor and S-metolachlor, the pure substances were diluted in acetone to a final concentration of 2 ppm. Three microliters of liquid sample were manually injected into the same injector kept at a temperature of 250 °C. The GC started at a temperature of 100 °C, and after 3 min, it increased to 240 °C at 20 °C/min, followed by an increase to 300 °C at 5 °C/min where the temperature was held for 5 min. The transfer line had a temperature of 280 °C. A constant column flow of 2 mL/min with a split ratio of 1:10 was applied. In-house referencing standards "TCE-2" (−2.54 ± 0.13 ‰) and "MeCl" (4.49 ± 0.10 ‰) were calibrated against methyl chloride from ISL-354 and USGS38 and subsequently used for preliminary character-

Figure 1. Characterization of the synthesized silver chloride reference standard CT16 against the international reference standards ISL-354 ($\delta^{37}Cl$ = +0.05 ‰) and USGS38 ($\delta^{37}Cl$ = −87.90 ‰). (A, B) CT16 measured via GC-IRMS in Munich at two different time points in (A) September 2017 and (B) February 2018, and (C) CT16 measured via GC-MC-ICPMS in Leipzig in February 2018. (The mean is given as a value and as a red line, while standard deviations are given as values and as black lines).

ization of acetochlor and S-metolachlor. In addition, further compounds (acetochlor, S-metolachlor, and atrazine) were purchased and calibrated in the same way. For results see Table S1.

■ RESULTS AND DISCUSSION

Synthesis Route to a Chlorine Isotope In-House Standard on the International Scale. Reductive dehalogenation of 2,2,2-trichloroethyl acetate by zinc powder produced 1,1-dichloroethene (not analyzed) and chloride, which could be precipitated and isolated as AgCl. The pure silver chloride in-house reference standard was given the name "CT16". For chlorine isotope analysis, it was subsequently converted to methyl chloride in order to facilitate isotopic characterization by GC-MC-ICPMS and GC-IRMS against international reference standards treated in the same way.

Figure 1 shows that the synthesized CT16 in-house chlorine isotope reference standard was adequately bracketed by the international reference standards ISL-354 and USGS38. A first characterization of CT16 via GC-IRMS in September 2017

APPENDIX

resulted in a value of $\delta^{37}Cl_{CT16} = -26.82 \pm 0.17$ ‰ (see Figure 1A). These measurements were repeated in February 2018, yielding a value of $\delta^{37}Cl_{CT16} = -26.88 \pm 0.28$ ‰ that was identical to the first one within the analytical uncertainty (see Figure 1B). In a third approach, CT16 was characterized via GC-MC-ICPMS giving even more precise values ($\delta^{37}Cl_{CT16} = -26.75 \pm 0.08$ ‰) which were in accordance with the GC-IRMS results (see Figure 1C). Consequently, the mean value over all measurements, $\delta^{37}Cl_{CT16} = -26.82 \pm 0.18$ ‰ ($n = 16$), is considered as a "true" consensus value for this in-house standard. As intended, this value shows a relatively large shift when compared to most international chlorine isotope reference standards which center on an isotope value of 0 ‰.[34−36]

This strong negative value can be explained by the isotope effect of the reaction. During the reductive elimination depicted in Scheme 2A, chlorine isotope fractionation is expected to take place according to Scheme 2B. Bonds containing heavy isotopes are slightly more stable than bonds containing light isotopes so that bonds with light isotopes break faster.[2,25] Consequently, ^{35}Cl is preferentially cleaved off from 2,2,2-trichloroethyl acetate meaning that the produced chloride in solution is expected to contain less ^{37}Cl per ^{35}Cl. This leads to isotope values that are strongly negative compared to the formed 1,1-dichloroethene, compared to the original substrate, and also compared to most available reference materials to date.

Identifying this synthesis route provides every laboratory the opportunity to create materials with negative chlorine isotope values. This represents a significant advance for future characterization of chlorine isotope standards: in-house working standards can be calibrated against two different reference standards, against one reference standard with an isotope value close to 0 ‰ and against a negative reference standard like CT16. By covering a wider range of isotope values, also results for the characterization of secondary in-house chlorine working standards will become more accurate which will consequently propagate into the precision and trueness of daily chlorine isotope measurements of samples. With regard to interlaboratory comparability, characterization against two reference standards leads to very accurate results relative to the international SMOC scale which will improve the quality and the international comparability of the obtained chlorine isotope values.[1,22,31]

Candidate Compounds for Compound-Specific Chlorine Isotope Working Standards. Reactions of acetochlor and S-metolachlor with sodium azide were stopped when ~70% of the substrates were converted to sodium chloride and acetoazide and metolaazide, respectively. The remaining substrates were named "Aceto2" and "Metola2". Together with the original substances, which were named "Aceto1" and "Metola1", the isolated Aceto2 and Metola2 were measured via GC-MC-ICPMS.

Figure 2 shows that the synthesized working standards Aceto2 and Metola2 exhibit significantly more positive chlorine isotope values than the initial substances Aceto1 and Metola1. For acetochlor, the initial substance Aceto1 was characterized to have an isotope value of $\delta^{37}Cl_{Aceto1} = 0.29 \pm 0.29$ ‰ tentatively determined by GC-MC-ICPMS. The synthesized working standard Aceto2 shows an isotope value of $\delta^{37}Cl_{Aceto2} = 18.54 \pm 0.20$ ‰ corresponding to an isotopic shift of ~18 ‰ (see Figure 2A). Measurements of S-metolachlor resulted in an isotopic shift of ~9 ‰. By the
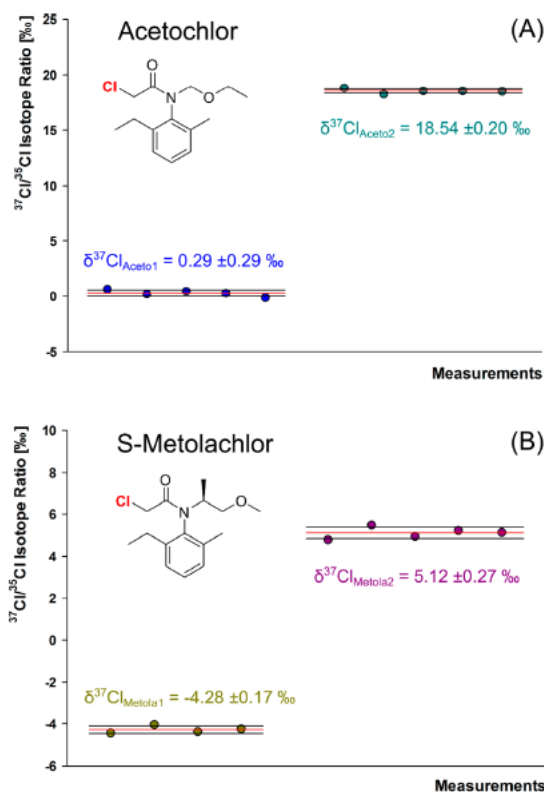
Figure 2. Characterization of (A) the acetochlor working standards Aceto1 and Aceto2 and (B) the S-metolachlor working standards Metola1 and Metola2. (The mean is given as a value and as a red line, while standard deviations are given as values and as black lines).

same GC-MC-ICPMS analysis, Metola1, the initial substance, was attributed a chlorine isotope value of $\delta^{37}Cl_{Metola1} = -4.28 \pm 0.17$ ‰ and the synthesized working standard, Metola2, a value of $\delta^{37}Cl_{Metola2} = 5.12 \pm 0.27$ ‰ (see Figure 2B).

The change in chlorine isotope values for each of the two substances happened due to the isotope effect of the underlying second order nucleophilic chemical substitution reaction (S_N2, Scheme 3A). As illustrated in Scheme 3B, owing to the leaving group isotope effect associated with chloride substitution, the remaining substrate got enriched in heavy relative to light chlorine isotopes leading to a more positive chlorine isotope value compared to the value of the original substrate before the start of the reaction.

These results illustrate that organic chemistry can be used to generate substance-specific working standards with pronounced shifts in chlorine isotope values. Thus, working standards for other chlorinated complex organic compounds may also be generated in the future so that stable chlorine isotope analysis of these compounds will help to further illuminate sources and transformation (pathways).

■ CONCLUSION

Specific synthesis routes were identified to generate five standards, the in-house anchor CT16 and the working standards Aceto1/Aceto2 and Metola1/Metola2, for stable

chlorine isotope analysis. In particular, the synthesis route to silver chloride (CT16) provides an opportunity to generate much-needed in-house standards for chlorine isotope analysis. The possibility to use two standards which differ in their chlorine isotope value will optimize future characterization results of secondary chlorine working standards. More accurate in-house working standards will in turn optimize the precision and trueness of daily chlorine isotope measurements. In addition, the synthesis of the working standards for acetochlor (Aceto1 and Aceto2) and S-metolachlor (Metola1 and Metola2) showed that organic synthesis can generate substance-specific isotope working standards also of more complex chlorinated organic compounds. These working standards become even more important as GC-qMS methods for stable chlorine isotope analysis of acetochlor and S-metolachlor were recently developed by Ponsin et al.[45] However, two of the working standards show a chlorine isotope value larger than 0 ‰ ($\delta^{37}\text{Cl}_{\text{Aceto2}}$ = 18.54 ± 0.20 ‰ and $\delta^{37}\text{Cl}_{\text{Metola2}}$ = 5.12 ± 0.27 ‰). Therefore, future work has to strive for synthesis routes to generate AgCl in-house standards with a more positive chlorine isotope value that would optimize the characterization process of secondary in-house working standards even further. The ongoing development of new calibration standards together with the advancement of stable chlorine isotope analysis now offers a suite of accurate methods for chlorine isotope analysis (offline DI-IRMS, online GC-MS and GC-IRMS, offline and online MC-ICPMS). By using these synergistic effects, the development of stable isotope analysis of chlorine can be further accelerated which will open up new perspectives to study environmental contaminants and to characterize commercial products in the future.

■ ASSOCIATED CONTENT

⑤ Supporting Information

The Supporting Information is available free of charge on the ACS Publications website at DOI: 10.1021/acs.anal-chem.9b02463.

Three schemes illustrating the workflow of isotopic characterization, and one table showing additional preliminary results of chlorine working standards for other semivolatile chlorinated compounds (PDF)

■ AUTHOR INFORMATION

Corresponding Author
*E-mail: m.elsner@tum.de. Tel: +49 89/2180-78231.

ORCID ⓞ
Faina Gelman: 0000-0002-2332-4193
Anat Bernstein: 0000-0001-9758-3254
Matthias Gehre: 0000-0001-7177-0422
Martin Elsner: 0000-0003-4746-9052

Author Contributions
The manuscript was written through contributions of all authors. All authors have given approval to the final version of the manuscript.

Notes
The authors declare no competing financial interest.

■ REFERENCES

(1) Coplen, T. B.; Böhlke, J. K.; De Bievre, P.; Ding, T.; Holden, N. E.; Hopple, J. A.; Krouse, H. R.; Lamberty, A.; Peiser, H. S.; Revesz, K.; Rieder, S. E.; Rosman, K. J. R.; Roth, E.; Taylor, P. D. P.; Vocke, R. D.; Xiao, Y. K. Pure Appl. Chem. 2002, 74 (10), 1987−2017.
(2) Elsner, M. J. Environ. Monit. 2010, 12 (11), 2005−2031.
(3) Coplen, T. B. Rapid Commun. Mass Spectrom. 2011, 25 (17), 2538−2560.
(4) Hunkeler, D.; Meckenstock, R. U.; Sherwood Lollar, B.; Schmidt, T.; Wilson, J.; Schmidt, T.; Wilson, J. A Guide for Assessing Biodegradation and Source Identification of Organic Ground Water Contaminants using Compound Specific Isotope Analysis (CSIA); PA 600/R-08/148; US EPA: Oklahoma, USA, 2008; www.epa.gov/ada.
(5) Hakenbeck, S.; McManus, E.; Geisler, H.; Grupe, G.; O'Connell, T. Am. J. Phys. Anthropol. 2010, 143 (2), 235−249.
(6) Rossmann, A. Food Rev. Int. 2001, 17 (3), 347−381.
(7) Desage, M.; Guilluy, R.; Brazier, J. L.; Chaudron, H.; Girard, J.; Cherpin, H.; Jumeau, J. Anal. Chim. Acta 1991, 247 (2), 249−254.
(8) Cawley, A. T.; Flenker, U. J. Mass Spectrom. 2008, 43 (7), 854−864.
(9) Schmidt, T. C.; Zwank, L.; Elsner, M.; Berg, M.; Meckenstock, R. U.; Haderlein, S. B. Anal. Bioanal. Chem. 2004, 378 (2), 283−300.
(10) Hofstetter, T. B.; Berg, M. TrAC, Trends Anal. Chem. 2011, 30 (4), 618−627.
(11) Aelion, C. M.; Hohener, P.; Hunkeler, D.; Aravena, R. Environmental Isotopes in Bioremediation and Biodegradation; CRC Press, 2009.
(12) Fenner, K.; Canonica, S.; Wackett, L. P.; Elsner, M. Science 2013, 341 (6147), 752−758.
(13) Magenheim, A. J.; Spivack, A. J.; Michael, P. J.; Gieskes, J. M. Earth Planet. Sci. Lett. 1995, 131 (3−4), 427−432.
(14) Bonifacie, M.; Jendrzejewski, N.; Agrinier, P.; Humler, E.; Coleman, M.; Javoy, M. Science 2008, 319 (5869), 1518−1520.
(15) Böhlke, J. K.; Sturchio, N. C.; Gu, B.; Horita, J.; Brown, G. M.; Jackson, W. A.; Batista, J.; Hatzinger, P. B. Anal. Chem. 2005, 77 (23), 7838−7842.
(16) Holt, B. D.; Sturchio, N. C.; Abrajano, T. A.; Heraty, L. J. Anal. Chem. 1997, 69 (14), 2727−2733.
(17) Xiao, Y.-K.; Zhang, C.-G. Int. J. Mass Spectrom. Ion Processes 1992, 116 (3), 183−192.
(18) de Groot, P. A. Carbon: Organic materials. In Handbook of Stable Isotope Analytical Techniques; de Groot, P. A., Ed.; Elsevier: Amsterdam, 2009; Vol. 2, pp 229−269.
(19) Shouakar-Stash, O.; Drimmie, R. J.; Frape, S. K. Rapid Commun. Mass Spectrom. 2005, 19 (2), 121−127.
(20) Sakaguchi-Soder, K.; Jager, J.; Grund, H.; Matthaus, F.; Schuth, C. Rapid Commun. Mass Spectrom. 2007, 21 (18), 3077−3084.
(21) Aeppli, C.; Holmstrand, H.; Andersson, P.; Gustafsson, O. Anal. Chem. 2010, 82 (1), 420−426.
(22) Bernstein, A.; Shouakar-Stash, O.; Ebert, K.; Laskov, C.; Hunkeler, D.; Jeannottat, S.; Sakaguchi-Soder, K.; Laaks, J.; Jochmann, M. A.; Cretnik, S.; Jager, J.; Haderlein, S. B.; Schmidt, T. C.; Aravena, R.; Elsner, M. Anal. Chem. 2011, 83 (20), 7624−7634.
(23) Renpenning, J.; Horst, A.; Schmidt, M.; Gehre, M. J. Anal. At. Spectrom. 2018, 33 (2), 314−321.
(24) Horst, A.; Renpenning, J.; Richnow, H.-H.; Gehre, M. Anal. Chem. 2017, 89 (17), 9131−9138.
(25) Cretnik, S.; Bernstein, A.; Shouakar-Stash, O.; Löffler, F.; Elsner, M. Molecules 2014, 19 (5), 6450−6473.
(26) Wiegert, C.; Mandalakis, M.; Knowles, T.; Polymenakou, P. N.; Aeppli, C.; Macháčková, J.; Holmstrand, H.; Evershed, R. P.; Pancost,

R. D.; Gustafsson, Ö. *Environ. Sci. Technol.* **2013**, *47* (12), 6449–6456.

(27) Badin, A.; Buttet, G.; Maillard, J.; Holliger, C.; Hunkeler, D. *Environ. Sci. Technol.* **2014**, *48* (16), 9179–9186.

(28) Renpenning, J.; Keller, S.; Cretnik, S.; Shouakar-Stash, O.; Elsner, M.; Schubert, T.; Nijenhuis, I. *Environ. Sci. Technol.* **2014**, *48* (20), 11837–11845.

(29) Abe, Y.; Aravena, R.; Zopfi, J.; Shouakar-Stash, O.; Cox, E.; Roberts, J. D.; Hunkeler, D. *Environ. Sci. Technol.* **2009**, *43* (1), 101–107.

(30) Heckel, B.; McNeill, K.; Elsner, M. *ACS Catal.* **2018**, *8* (4), 3054–3066.

(31) Paul, D.; Skrzypek, G.; Forizs, I. *Rapid Commun. Mass Spectrom.* **2007**, *21* (18), 3006–3014.

(32) Heckel, B.; Rodríguez-Fernández, D.; Torrentó, C.; Meyer, A.; Palau, J.; Domènech, C.; Rosell, M.; Soler, A.; Hunkeler, D.; Elsner, M. *Anal. Chem.* **2017**, *89* (6), 3411–3420.

(33) Hut, G. Consultants' group meeting on stable isotope reference samples for geochemical and hydrological investigations, International Atomic Energy Agency, Vienna, Austria, 1987.

(34) Xiao, Y.; Yinming, Z.; Qingzhong, W.; Haizhen, W.; Weiguo, L.; Eastoe, C. *Chem. Geol.* **2002**, *182* (2–4), 655–661.

(35) Gröning, M. International stable isotope reference materials. In *Handbook of Stable Isotope Analytical Techniques*; Elsevier, 2004; Vol. I, pp 874–906.

(36) Böhlke, J.; Mroczkowski, S. J.; Sturchio, N. C.; Heraty, L. J.; Richman, K. W.; Sullivan, D. B.; Griffith, K. N.; Gu, B.; Hatzinger, P. B. *Rapid Commun. Mass Spectrom.* **2017**, *31*, 85.

(37) Elsner, M.; Jochmann, M. A.; Hofstetter, T. B.; Hunkeler, D.; Bernstein, A.; Schmidt, T. C.; Schimmelmann, A. *Anal. Bioanal. Chem.* **2012**, *403* (9), 2471–2491.

(38) Werner, R. A.; Brand, W. A. *Rapid Commun. Mass Spectrom.* **2001**, *15*, 501–519.

(39) Elsner, M.; Imfeld, G. *Curr. Opin. Biotechnol.* **2016**, *41*, 60–72.

(40) Pesticides Industry Sales and Usage: 2008–2012 Market Estimates. US Environmental Protection Agency, Washington, DC, 2017.

(41) Dearfield, K. L.; McCarroll, N. E.; Protzel, A.; Stack, H. F.; Jackson, M. A.; Waters, M. D. *Mutat. Res., Genet. Toxicol. Environ. Mutagen.* **1999**, *443* (1), 183–221.

(42) Somsák, L.; Czifrák, K.; Veres, E. *Tetrahedron Lett.* **2004**, *45* (49), 9095–9097.

(43) Weigl, M.; Wünsch, B. *Tetrahedron* **2002**, *58* (6), 1173–1183.

(44) Shouakar-Stash, O.; Drimmie, R. J.; Zhang, M.; Frape, S. K. *Appl. Geochem.* **2006**, *21* (5), 766–781.

(45) Ponsin, V.; Torrentó, C.; Lihl, C.; Elsner, M.; Hunkeler, D. *Compound-specific chlorine isotope analysis of the herbicides atrazine, acetochlor and metolachlor*, in preparation.

Mechanistic Dichotomy in Bacterial Trichloroethene Dechlorination Revealed by Carbon and Chlorine Isotope Effects

Christina Lihl,[†] Lisa M. Douglas,[‡] Steffi Franke,[§] Alfredo Pérez-de-Mora,[†] Armin H. Meyer,[†] Martina Daubmeier,[†] Elizabeth A. Edwards,[‖] Ivonne Nijenhuis,[§] Barbara Sherwood Lollar,[‡] and Martin Elsner*,[†,⊥]

[†]Institute of Groundwater Ecology, Helmholtz Zentrum München, Ingolstädter Landstrasse 1, 85764 Neuherberg, Germany

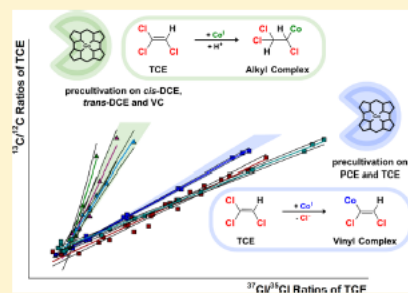[‡]Department of Earth Sciences, University of Toronto, Toronto, Ontario M5S 3B5, Canada

[§]Department for Isotope Biogeochemistry, Helmholtz-Centre for Environmental Research, UFZ, Permoserstrasse 15, 04318 Leipzig, Germany

[‖]Department of Chemical Engineering and Applied Chemistry, University of Toronto, Toronto, Ontario M5S 3E5, Canada

[⊥]Chair of Analytical Chemistry and Water Chemistry, Technical University of Munich, Marchioninistrasse 17, 81377 Munich, Germany

S *Supporting Information*

ABSTRACT: Tetrachloroethene (PCE) and trichloroethene (TCE) are significant groundwater contaminants. Microbial reductive dehalogenation at contaminated sites can produce nontoxic ethene but often stops at toxic *cis*-1,2-dichloroethene (*cis*-DCE) or vinyl chloride (VC). The magnitude of carbon relative to chlorine isotope effects (as expressed by $\Lambda_{C/Cl}$, the slope of $\delta^{13}C$ versus $\delta^{37}Cl$ regressions) was recently recognized to reveal different reduction mechanisms with vitamin B_{12} as a model reactant for reductive dehalogenase activity. Large $\Lambda_{C/Cl}$ values for *cis*-DCE reflected cob(I)alamin addition followed by protonation, whereas smaller $\Lambda_{C/Cl}$ values for PCE evidenced cob(I)alamin addition followed by Cl^- elimination. This study addressed dehalogenation in actual microorganisms and observed identical large $\Lambda_{C/Cl}$ values for *cis*-DCE ($\Lambda_{C/Cl}$ = 10.0 to 17.8) that contrasted with identical smaller $\Lambda_{C/Cl}$ for TCE and PCE ($\Lambda_{C/Cl}$ = 2.3 to 3.8). For TCE, the trend of small $\Lambda_{C/Cl}$ could even be reversed when mixed cultures were precultivated on VC or DCEs and subsequently confronted with TCE ($\Lambda_{C/Cl}$ = 9.0 to 18.2). This observation provides explicit evidence that substrate adaptation must have selected for reductive dehalogenases with different mechanistic motifs. The patterns of $\Lambda_{C/Cl}$ are consistent with practically all studies published to date, while the difference in reaction mechanisms offers a potential answer to the long-standing question of why bioremediation frequently stalls at *cis*-DCE.

INTRODUCTION

Chlorinated ethenes such as tetrachloroethene (PCE) and trichloroethene (TCE) are among the most frequent groundwater pollutants at contaminated sites worldwide.[1] Under anoxic conditions, they may be reductively dechlorinated by microorganisms in a process known as organohalide respiration. Chloroethenes act as electron acceptors so that their C−Cl bonds are reduced to C−H bonds (sequential hydrogenolysis), leading to nontoxic ethene as final product (see Figure 1).[2] While this reaction stoichiometry is straightforward, the exact nature of the underlying biochemical reaction mechanism has been elusive.

Transformation frequently stalls at the stage of *cis*-1,2-dichloroethene (*cis*-DCE) or vinyl chloride (VC), constituting one of the long-standing barriers to successful bioremediation of these ubiquitous priority pollutants. Only specialized degrader strains, bacteria belonging to the class Dehalococcoidia (e.g., certain *Dehalococcoides mccartyi* and *Dehalogenimonas*
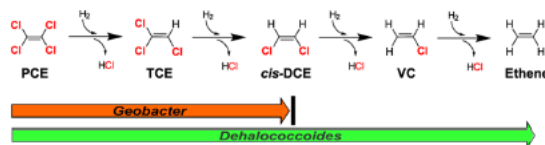

Figure 1. Reductive dechlorination of PCE to ethene with different end-points for two bacterial cultures.

strains), were found to be capable of complete dechlorination to harmless ethene.[3−10] In contrast, other microorganisms, such as *Geobacter lovleyi*, cannot dechlorinate beyond *cis*-DCE[4]

4245

(see Figure 1). Pinpointing the underlying mechanistic reasons, however, has remained an elusive goal. Even though the catalytic site of all known reductive dehalogenases (RDases) contains cobalamin as an essential Co(I)-containing corrinoid cofactor, these enzymes occur in a great structural variety.[2,4,11−13] Very few dehalogenase protein structures have been solved yet,[11,12] and no reductive dehalogenase has been uniquely characterized for its underlying biochemical transformation mechanism (i.e., bond cleavage and formation). Consequently, critical research gaps in the chemistry of reductive dechlorination exist. Is the mechanism the same for all substrates? Does the mechanism correlate with a given substrate? Or do mechanisms vary with the observed variety of reductive dehalogenases and organisms?

With reduced vitamin B_{12} as a chemical model system, we recently achieved a breakthrough in understanding reaction mechanisms in vitro.[14] Our evidence suggests that cob(I)-alamin acts as a supernucleophile and adds to the double bond in chlorinated ethenes so that a carbanion complex is formed. If the free electron pair of this complex faces two vicinal Cl substituents (as in the reaction of PCE), one of them will be in the anti- position, leading to fast elimination of Cl^- and producing a cobalamin chlorovinyl complex as short-lived intermediate (Scheme 1). In contrast, if there is only one

Scheme 1. Reaction Mechanisms for the Reductive Dehalogenation of Chlorinated Ethenes via Addition Protonation or Addition Elimination (Adapted from Heckel et al.[14])

vicinal Cl substituent (as in the reaction of cis-DCE), the molecular conformation is unfavorable for subsequent elimination so the carbanion is protonated instead. This results in a slower reaction pathway involving an intermediate chloroalkyl complex (Scheme 1). If there can be either one or two vicinal Cl substituents (as in the reaction of TCE), the addition−protonation pathway is favored at low pH, whereas the addition−elimination pathway is favored at high pH (Scheme 1). In contrast, the number and position of geminal Cl substituents does not seem to have an effect on the reaction mechanism.

Both TCE dechlorination pathways eventually produce cis-DCE as the respective hydrogenolysis product (Scheme 1) so that the different mechanisms are difficult to distinguish from product analysis alone. Additional experimental evidence is, therefore, warranted to determine whether the mechanistic dichotomy identified with vitamin B_{12} is also at work in reductive dehalogenases or in dehalogenating organisms.

Compound-specific stable isotope effect analysis offers precisely such a complementary line of evidence. Gas chromatography (GC) coupled to isotope ratio mass spectrometry (IRMS) measures carbon $(^{13}C/^{12}C)$[15,16] and chlorine $(^{37}Cl/^{35}Cl)$ isotope ratios at natural isotopic abundance.[17−19] Measured isotope ratios are expressed in the δ-notation; for example, for carbon:

$$\delta^{13}C = [(^{13}C/^{12}C)_{sample} - (^{13}C/^{12}C)_{reference}]$$
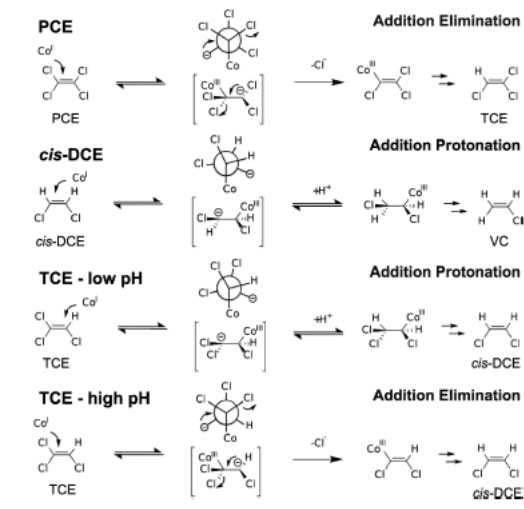$$/(^{13}C/^{12}C)_{reference} \qquad (1)$$

where $(^{13}C/^{12}C)_{reference}$ is the isotope ratio of an international reference material to ensure comparability between laboratories.[20,21] An analogous equation applies to chlorine. When correlating these isotope values of two elements relative to each other the regression slope:

$$\Lambda_{C/Cl} = (\delta^{13}C - \delta^{13}C_0)/(\delta^{37}Cl - \delta^{37}Cl_0) \approx \varepsilon_C/\varepsilon_{Cl} \qquad (2)$$

reflects the magnitude of the underlying compound-specific isotope effects during a reaction.[22] Here, δ-values express the isotope ratios of carbon and chlorine at a given time and at the beginning of the reaction ($\delta^{13}C_0$ and $\delta^{37}Cl_0$), respectively. Carbon and chlorine enrichment factors (ε_C and ε_{Cl}, respectively) reflect compound-specific isotope effects[22] that express by how much molecules with heavy isotopes react slower than molecules with light isotopes.[20,23] A value of $\varepsilon = -10$ ‰, for example, corresponds to a compound-specific isotope effect of $^{12}k/^{13}k = 1.01$ (for the experimental evaluation of ε, see eq 3 below). Our vitamin B_{12} study demonstrated that the slope $\Lambda_{C/Cl}$ can provide a sensitive indicator of the underlying reaction mechanisms in reductive chlorinated ethene dehalogenation with vitamin B_{12}.[14] Values of $\Lambda_{C/Cl}$ were much larger in the addition−protonation mechanism, reflecting the fact that no C−Cl bond was cleaved in the initial step so that chlorine isotope effects were small. In contrast, values of $\Lambda_{C/Cl}$ were smaller in the addition−elimination mechanism, reflecting the larger chlorine isotope effect associated with C−Cl bond cleavage.

The objective of this study was to analyze carbon and chlorine isotope effects during reductive dehalogenation of chloroethenes with different bacterial cultures. The resulting $\Lambda_{C/Cl}$ values were compared with the $\Lambda_{C/Cl}$ values of two mechanistic trends recently observed in a vitamin B_{12} model system. To this end, we investigated in particular whether the isotope fractionation trends in microbial dechlorination of cis-DCE and PCE correlate with trends of the addition−protonation and the addition−elimination mechanisms observed with vitamin B_{12}, respectively. For TCE dechlorination both mechanisms were observed in the vitamin B_{12} study depending on pH. To test whether evidence of both mechanisms may be observed for TCE in living bacteria as well, microbial dechlorination of TCE was studied in seven different experiments, either varying in precultivation substrate or in the type of predominant RDases inside the bacteria. Finally, the isotopic data of the dechlorination experiments of

Table 1. Summary of Precultivation Conditions, RDases, and Compound-Specific Isotope Enrichment Factors of Carbon and Chlorine

Substrate for Dehalogenation and Isotope Analysis	Culture	Dechlorinators	Precultivation Substrate (Electron Acceptor)	Most Abundant Functional rdhA Genes[a]		Slope, $\Lambda_{C/Cl}$[b]	ε_{Cl} (‰)[b]	ε_{C} (‰)[b]	Duration
				before	after				
cis-DCE	D. mccartyi 195	D. mccartyi 195 (pure culture)	cis-DCE (hydrogen)	tceA[32]	tceA[32]	10.0 ± 0.4	−2.3 ± 0.4	−23.2 ± 4.1	no lag period, cis-DCE dehalogenation completed after 1 month
cis-DCE	D. mccartyi BTF08	D. mccartyi BTF08 (enrichment culture)	cis-DCE (hydrogen)	tceA[7]	tceA[7]	17.8 ± 1.0	−1.7 ± 0.4	−31.1 ± 6.3	no lag period, cis-DCE dehalogenation completed after 1 month
TCE	G. lovleyi KB-1	G. lovleyi KB-1 (pure culture)	PCE (acetate)	Geo-pceA[33]	Geo-pceA[33]	3.1 ± 0.1	−3.3 ± 0.3	−10.3 ± 0.8	no lag period, TCE dehalogenation completed within 1 day
TCE	KB-1 RF	multiple D. mccartyi strains (enrichment culture; no Geobacter)	TCE (methanol)	vcrA[33]	vcrA[33]	2.7 ± 0.2	−3.3 ± 0.3	−9.6 ± 0.5	no lag period, TCE dehalogenation completed within 1 day
TCE	Donna II	D. mccartyi 195 (mixed culture; only one strain of D. mccartyi)	TCE (butyrate)	tceA[34]	tceA[34]	2.3 ± 0.1	−5.7 ± 0.4	−13.5 ± 0.6	no lag period, TCE dehalogenation completed within 1 day
TCE	KB-1/1,2-DCA	multiple D. mccartyi strains (enrichment cultures)	1,2-DCA (methanol)	tceA[35]	tceA, vcrA	4.5 ± 0.8	−1.2 ± 0.3	−5.4 ± 1.5	long lag period (30−40 days), TCE dehalogenation completed after 70−100 days
TCE	KB-1/VC	multiple D. mccartyi strains (enrichment cultures)	VC (methanol)	vcrA[33]	vcrA	18.2 ± 4.3	−0.5 ± 0.6	−10.6 ± 9.3	long lag period (30−40 days), TCE dehalogenation completed after 70−100 days
TCE	KB-1/cDCE	multiple D. mccartyi strains (enrichment cultures)	cis-DCE (methanol)	bvcA, vcrA[33]	vcrA (tceA)	11.8 ± 2.4	−0.7 ± 0.2	−8.3 ± 3.4	long lag period (30−40 days), TCE dehalogenation completed after 70−100 days
TCE	WBC-2/tDCE	Dehalogenimonas sp., D. mccartyi (enrichment cultures)	trans-DCE (lactate/ethanol)	tdrA (Dhgm), vcrA (Dhc)[9]	vcrA (tceA, tdrA)	9.0 ± 1.1	−0.7 ± 0.3	−7.0 ± 1.9	long lag period (30−40 days), TCE dehalogenation completed after 70−100 days

[a]The abundance of specific rdhA genes known to be present in the cultures was used as a way to track which of the multiple strains grew in the mixed culture; rdhA genes in brackets were only detected in minor abundance; the KB-1 enrichments were selected because each harbored a different dominant expressed RDase initially. [b]±95% confidence intervals.

4247

106

this study were compared with the literature data of available C/Cl isotope studies to test whether the picture of a mechanistic dichotomy is consistent with published evidence to date.

■ MATERIALS AND METHODS

***cis*-DCE and TCE Dechlorinating Cultures.** Dehalogenation experiments with *cis*-DCE were carried out using *Dehalococcoides mccartyi* strain 195[6] and the highly enriched *Dehalococcoides mccartyi* strain BTF08 culture.[8,24] Dehalogenation experiments with TCE were conducted with a single pure culture (*Geobacter lovleyi* strain KB-1) and 6 mixed cultures (KB-1/1,2-DCA, KB-1/VC, KB-1/cDCE, WBC-2/tDCE, KB-1 RF, and Donna II) (see Table 1 for further details). *G. lovleyi* strain KB-1, KB-1/1,2-DCA, KB-1/VC, KB-1/cDCE, and KB-1 RF were derived from KB-1, a commercially available enrichment culture, which is specialized in the dehalogenation of chlorinated ethenes. It contains *G. lovleyi* strain KB-1 and a minimum of three strains of *Dehalococcoides* as well as nondechlorinating bacteria such as acetogens and methanogens.[25−29] Prior to the experiment, the cultures were enriched on different maintenance substrates for many years (see Table 1).

Biotic Dechlorination of *cis*-DCE under Anoxic Conditions with *D. mccartyi* Strain 195 and Strain BTF08. *D. mccartyi* strain 195 was cultivated as described in Cichocka et al.[30] and Maymo-Gatell et al.[6] with addition of butyrate pellets. *D. mccartyi* strain BTF08 was cultivated following the protocol of Cichocka et al.[8] and Schmidt et al.[31] For each strain, a set of 23 serum bottles (50 mL) was filled with 25 mL of anoxic medium and flushed with N_2 and CO_2 (70/30%). After closing the bottles by crimping with Teflon-lined gray butyl rubber stoppers, they were sterilized for 40 min at 120 °C. Next, they were spiked with *cis*-DCE (500 μM) as electron acceptor and equilibrated overnight. On the next day, the bottles were inoculated with a culture grown on *cis*-DCE (2.5% v/v for strain 195, 5% v/v for strain BTF08). For each set, three non-inoculated bottles with substrate served as the negative control. The bottles were complemented with hydrogen as electron donor (0.5 bar overpressure). All cultures were incubated in the dark without shaking at 20 °C (BTF08) or 30 °C (195). Progress of substrate dehalogenation was monitored by concentration measurements with gas chromatography paired with flame ionization detection (GC-FID). At different levels of dechlorination, bottles were sacrificed for analysis by stopping the dechlorination reaction with 1 mL of acidic sodium sulfate solution (280 g/L, pH ≈1) following the protocol of Cichocka et al.[30] Samples were stored at 4 °C in the dark for later carbon and chlorine isotope analysis *via* gas chromatography-isotope ratio mass spectrometry (GC-IRMS).

Biotic Dehalogenation of TCE under Anoxic Conditions with *G. lovleyi* Strain KB-1, KB-1/1,2-DCA, KB-1/VC, KB-1/cDCE, and WBC-2/tDCE. A total of 200 mL of defined mineral medium[36] and 55 μL of resazurin (0.4%) were filled in glass bottles (250 mL). Subsequently they were capped with Mininert valves (Supelco) and purged for 40 min with a N_2/CO_2 gas mixture (80/20%). Each bottle of *G. lovleyi* strain KB-1 was complemented with 50 μL of acetate (1 M) and 9 μL of TCE, whereas each bottle of KB-1/VC, KB-1/cDCE, and KB-1/1,2-DCA was complemented with 20 μL of methanol and 9 μL of TCE, and each bottle of WBC-2/tDCE was complemented with 22 μL of lactate solution (75 g/L), 44 μL of ethanol, and 9 μL of TCE. All substances and solutions

for complementation were taken from anoxic stocks. Afterwards, all bottles were continuously agitated on an orbital shaker at 60 rpm at room temperature for 24 h for equilibration. Biotic dehalogenation started by inoculating each bottle with 20 mL of active culture. To eliminate the carryover of volatile organic compounds, the active cultures had been purged for 1 h with a N_2/CO_2 gas mixture (80/20%). The bottles were prepared in triplicates for each culture. Furthermore, for each culture, non-inoculated bottles with substrate served as negative control and were monitored alongside the experimental bottles. A total of 5 min after inoculation, the first samples were taken. The next samples were taken in intervals throughout the dehalogenation process. At each sampling point, 7 mL of liquid were removed from all the bottles. The sample of 7 mL was then divided into 1 mL aliquots that were distributed into 7 glass vials (1.5 mL each) and closed with PTFE-lined screw-top caps. All samples were fixed with 50 μL NaOH (1 M) to stop biological activity. One of the seven vials was used for instant concentration analysis that was performed on a GC-FID. The other six vials were frozen upside down for later isotope analysis of carbon and chlorine performed via GC-IRMS.[37,38] Preparation of the cultures (except the purging with N_2/CO_2) and taking of the samples was conducted in a glovebox containing an anoxic atmosphere (80% N_2, 20% H_2).

Biotic Dehalogenation of TCE under Anoxic Conditions with KB-1 RF and Donna II. The whole experiment was conducted in a glovebox containing an anoxic atmosphere (80% N_2, 10% H_2, 10% CO_2). Glass bottles (260 mL) were filled with 200 mL (KB-1 RF) or 210 mL (Donna II) of defined mineral medium[36] and inoculated with 20 mL (KB-1 RF) or 10 mL (Donna II) of active culture. Beforehand, the cultures were purged with a N_2/CO_2 gas mixture for 30 min to eliminate carryover of volatile organic compounds. Triplicate experimental bottles were capped with Mininert valves (Supelco) and complemented by adding 20 μL of methanol (KB-1 RF), 8.75 μL of butyrate (Donna II), and 9 μL of TCE. Furthermore, for each culture non-inoculated bottles with substrate and killed control bottles (sterilized before TCE addition) served as negative control and were monitored alongside the experimental bottles. All replicates were continuously shaken at 350 rpm at room temperature (24 °C). At each time point, headspace samples were removed first for concentration measurements via GC-FID and then for carbon isotope analysis via GC-IRMS. Subsequently 4 mL liquid samples were removed and split into 1 mL aliquots. Liquid samples were acidified to a pH of <2 with 50 μL of 1 M H_2SO_4 and closed with PTFE-lined screw-top caps and then frozen upside down in 1.5 mL glass vials for later chlorine isotope measurements via GC-IRMS.[37,38] Sample volumes removed were compensated with identical volumes of glovebox atmosphere to maintain a constant pressure within the bottle. Septa inside the stopper of the Mininert valves were replaced after every second piercing to minimize leakage.

Concentration Measurements and Carbon and Chlorine Isotope Analysis. Concentration measurements via GC-FID and compound-specific isotope analysis of carbon and chlorine via GC-IRMS were performed according to defined protocols (see the Supporting Information).

Evaluation of Carbon and Chlorine Isotope Fractionation. Carbon and chlorine enrichment factors (ε_C and ε_{Cl}) of *cis*-DCE and TCE dechlorination were calculated according to the Rayleigh equation (eq 3) using Sigma-Plot. The

Rayleigh equation describes the gradual enrichment of the residual substrate fraction f with molecules containing heavy isotopes;[20,22] for example, for carbon:

$$\ln[(\delta^{13}C + 1)/(\delta^{13}C_0 + 1)] = \varepsilon_C \cdot \ln f \qquad (3)$$

The isotope ratios of carbon refer to certain time points, with one of them at the beginning of an experiment $(\delta^{13}C_0)$. By plotting values of $\delta^{13}C$ versus $\delta^{37}Cl$ (see eq 2), dual element isotope plots were obtained. These processes are also illustrated in Figure 2. 95% confidence intervals (CI) show the uncertainties of the calculated slopes $\Lambda_{C/Cl}$ $(\Delta\delta^{13}C/\Delta\delta^{37}Cl)$. In chemical reactions, isotope effects occur predominantly at the reacting position. Therefore, in many cases, a position-specific apparent kinetic isotope effect (AKIE) may be estimated under the assumption that there are no isotope effects at the other positions according to:

$$AKIE_{position\text{-}specific} = 1/(n \cdot \varepsilon_{reacting\,position} + 1) \qquad (4)$$

where n is the number of atoms in intramolecular competition.[22] However, for chlorinated ethene reduction our mechanistic picture (Scheme 1) suggests that the situation is more complex because isotope effects occur in different steps of the reaction sequence, and they may occur at different positions of the molecule.[14,39] In addition, from IRMS measurements alone, intramolecular isotope effects are difficult to resolve. Thus, in this study, we decided not to estimate position-specific isotope effects but instead to report compound-specific isotope effects in the form of ε values.

qPCR Analysis of KB-1/1,2-DCA, KB-1/VC, KB-1/cDCE, and WBC-2/tDCE. Quantitative polymerase chain reaction (qPCR) analyses were conducted after the completion of the TCE experiment. An 8.5 mL sample of each culture was collected and, subsequently, 1.5 mL of 50% glycerol were added. The samples were stored at −80 °C after freezing in liquid nitrogen. For qPCR analysis, 8 mL of each thawed sample were filtered through a sterile 0.22 μM Sterivex filter (Millipore) using an Air Cadet vacuum/pressure pump 400−1902 (Barnant Company). After filtration, the Sterivex filters were immediately frozen at −80 °C. The filters were removed from the filter casing, sliced into small pieces with a sterile surgical blade, and then transferred to a bead-beating tube. For DNA extraction, the PowerSoil DNA isolation kit (Mo Bio Laboratories Inc.) was used. The DNA was extracted by following the manufacturer's protocol for maximum yields except that DNA was eluted in 50 μL of sterile UltraPure distilled water (Invitrogen) rather than in the eluent provided with the kit. Using a spectrophotometer (NanoDrop ND-1000; NanoDrop Technologies) the DNA concentration and quality were assessed. Afterwards, the DNA samples were 10 times diluted with sterile UltraPure distilled water. All subsequent steps were performed in a PCR cabinet (ESCO Technologies). qPCR reactions were run in triplicates in which each run was calibrated by constructing a standard curve using known plasmid DNA concentrations containing the gene insert of interest. The standard curve was run with 8 concentrations ranging from 10 to 108 gene copies per microliter. qPCR reaction solutions (20 μL) were prepared in sterile UltraPure distilled water containing 10 μL of EvaGreen Supermix, 0.5 μL of each primer (forward and reverse, each from 10 μM stock solutions), and 2 μL of diluted template (DNA extract or standard plasmids). The qPCR reactions were conducted using a CFX96 real-time PCR detection system with a C1000
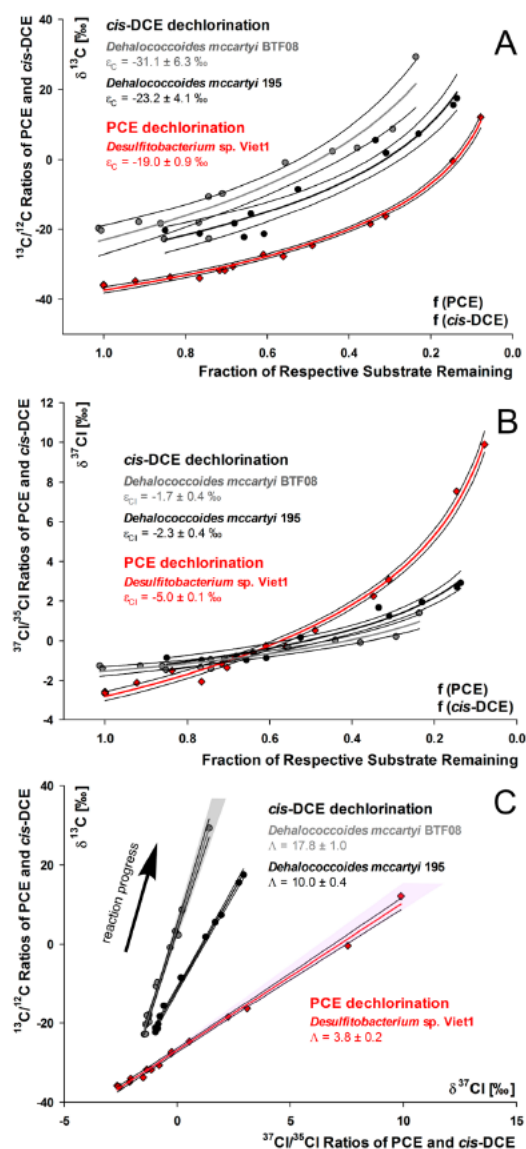
Figure 2. Carbon and chlorine isotope effects in reductive dehalogenation of *cis*-DCE by *D. mccartyi* BTF08 (gray) and *D. mccartyi* 195 (black) and PCE by *Desulfitobacterium* sp. Viet1 (red) (data from Cretnik et al.[39]), resulting in a dual element isotope plot. (The 95% confidence intervals are given as values and as black lines next to the regression slopes). (A) Carbon isotope fractionation and corresponding carbon enrichment factors ε_C. (B) Chlorine isotope fractionation and corresponding chlorine enrichment factors ε_{Cl}. (Both ε values were evaluated according to eq 3). (C) Resulting dual element isotope plots ($\delta^{13}C$ versus $\delta^{37}Cl$) indicate the occurrence of different underlying transformation mechanisms corresponding to mechanisms observed with *cis*-DCE (shaded in gray) and PCE (shaded in pink) by model reactions with vitamin B$_{12}$.[14]

Thermo Cycler using SsoFast EvaGreen supermix (Bio-Rad Laboratories). The thermocycling program started with the

initial denaturation at 95 °C for 2 min, followed by 40 cycles of denaturation at 98 °C for 5 s, annealing for 10 s (see Table S1 for annealing temperatures), and a plate read. A final melting curve analysis was conducted at the end of the program. The following genes were targeted by qPCR using the defined primer sets (see Table S1): the phylogenetic 16S rRNA genes of *Dehalococcoides* and *Dehalogenimonas*; the functional genes *vcrA*, *tceA*, *bvcA*, and *tdrA*; as well as the 16S rRNA genes of total bacteria and total archaea.

RESULTS AND DISCUSSION

Starkly Contrasting Carbon and Chlorine Isotope Effects in Microbial Dechlorination of *cis*-DCE and PCE. To take advantage of compound-specific isotope effects and evaluate whether the mechanistic dichotomy observed *in vitro* can also be identified in pure strains of living organisms, we began with a comparison between PCE and *cis*-DCE. Carbon and chlorine isotope values of *cis*-DCE were measured in dehalogenation experiments with the strictly anaerobic organism *D. mccartyi* strain 195[6] and the highly enriched *D. mccartyi* strain BTF08 culture.[8,24] Results were compared with our previous data on reductive dechlorination of PCE by *Desulfitobacterium* sp. strain Viet1.[39] Figure 2 shows the changes in carbon and chlorine isotope ratios with decreasing fraction of respective substrate and the corresponding enrichment factors. Combining the isotope ratios of panel A (carbon) and B (chlorine) leads to a dual element isotope plot as illustrated in panel C.

The dual element isotope trends with bacteria reproduced the trends obtained with vitamin B_{12} and were reflected on the level of compound-specific carbon and chlorine isotope effects, illustrated by ε_C and ε_{Cl}. The dechlorination of *cis*-DCE was associated with large carbon and small chlorine isotope effects ($D. mccartyi$ 195: $\varepsilon_C = -23.2 \pm 4.1$ ‰, $\varepsilon_{Cl} = -2.3 \pm 0.4$ ‰; $D. mccartyi$ BTF08: $\varepsilon_C = -31.1 \pm 6.3$ ‰, $\varepsilon_{Cl} = -1.7 \pm 0.4$ ‰), resulting in large dual element isotope slopes $\Lambda_{195} = 10.0 \pm 0.4$ and $\Lambda_{BTF08} = 17.8 \pm 1.0$. In contrast, dechlorination of PCE was associated with pronounced isotope effects in both elements ($\varepsilon_C = -19.0 \pm 0.9$ ‰, $\varepsilon_{Cl} = -5.0 \pm 0.1$ ‰), giving rise to a smaller dual element isotope slope $\Lambda_{Desulfitobacterium} = 3.8 \pm 0.2$. This large chlorine isotope effect is even more striking when one considers that it is averaged over four chlorine atoms in PCE (of which only one is cleaved off), while in *cis*-DCE, the average is taken over only two chlorine atoms. Hence, kinetic isotope effects of PCE and *cis*-DCE at the reacting position (after correcting for the dilution by nonreacting chlorine atoms) would show even greater differences.[40] The same would be true for dual element isotope slopes $\Lambda_{C/Cl}$. Our results therefore provide key lines of evidence, suggesting that *cis*-DCE and PCE must be dechlorinated via different mechanisms, and that they exemplify the pattern observed for addition–protonation versus addition–elimination pathways (Scheme 1 and Figure 2).[14]

Dual Element Isotope Trends in TCE Dechlorination by Pure Cultures: Indication of an Addition–Elimination Mechanism. In an *in vitro* study using vitamin B_{12} as model system, TCE was recently observed to be dechlorinated via two different reaction mechanisms depending on pH (see Figure 3A and Scheme 1). To probe which mechanism would be observed for TCE *in vivo* with bacterial pure cultures, a *Geobacter* subculture (*Geobacter lovleyi* KB-1) of the mixed consortium KB-1 that had been cultivated to purity was investigated and compared with previously observed trends for
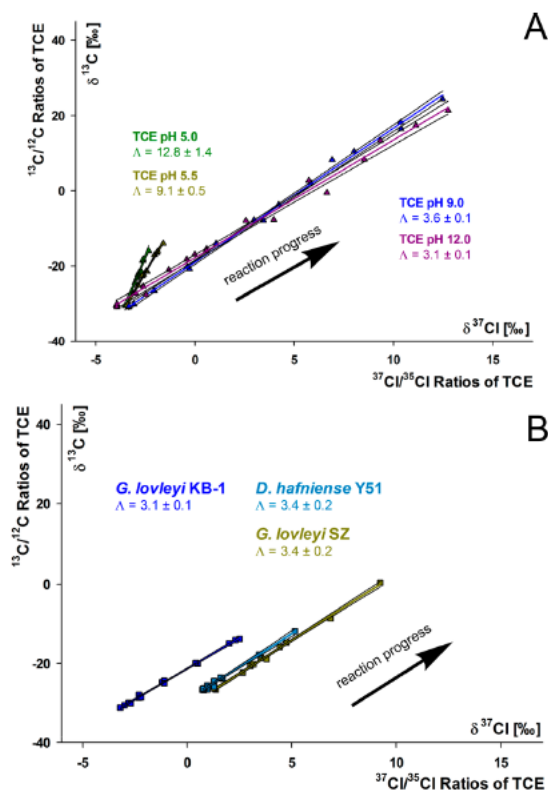

Figure 3. Carbon and chlorine isotope effects in TCE reductive dehalogenation (A) by vitamin B_{12} at different pH values and (B) with pure cultures resulted in similar dual element isotope plots. (The 95% confidence intervals are given as values and as black lines next to the regression slopes). (A) TCE reductive dehalogenation at low (green/yellow) and high (purple/blue) pH values (adapted from Heckel et al.[14]). (B) TCE reductive dehalogenation with the pure culture *G. lovleyi* KB-1 (dark blue, this work) and the pure cultures *G. lovleyi* SZ (yellow) and *D. hafniense* Y51 (blue) (adapted from Cretnik et al.[38]).

Geobacter lovleyi SZ and *Desulfitobacterium hafniense* Y51[38] (Figure 3B). The dual element isotope slopes of the pure cultures correspond to the dual element isotope slopes of the vitamin B_{12} study at high pH values, indicating that *in vivo* TCE is dechlorinated via the addition–elimination pathway.

Precultivation of Bacteria on Less Chlorinated Ethenes and TCE Dual Element Isotope Trends: Indication of an Addition–Protonation Mechanism. To investigate whether a different reaction mechanism can nonetheless be observed for TCE when using precultivation conditions to select for organisms with a different substrate preference, we conducted another set of experiments. Mixed cultures, Donna II and KB-1 RF, were precultivated on PCE or TCE for years (see Table 1), meaning that they were already adapted to TCE (substrate or daughter product of PCE dechlorination). However, we maintained another set of cultures on less chlorinated precultivation substrates: three subcultures of the dechlorinating consortium KB-1 RF that were maintained on *cis*-DCE (KB-1/cDCE), VC (KB-1/VC), and 1,2-DCA (KB-1/1,2-DCA) for at least 2 years and a fourth

mixed culture that was enriched on *trans*-DCE (WBC-2/tDCE) for many years. As expected, cultures precultivated on TCE and PCE started to dechlorinate TCE immediately and the dechlorination was completed within 1 day (see Table 1). In contrast, the set of cultures enriched and precultivated on less chlorinated ethenes showed a lag period of 30−40 days before they started to dechlorinate TCE, and dechlorination took 70−100 days for completion.

Figure 4 shows that precultivation affected the carbon and chlorine isotope effects. A clear divide appears between two
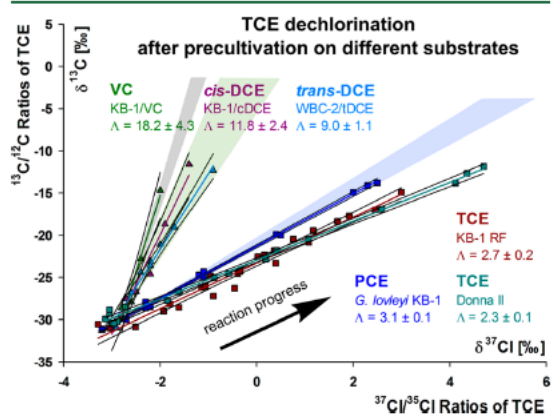

Figure 4. Dual element isotope trends indicate a mechanistic divide between TCE dechlorination by cultures precultivated on PCE (*G. lovleyi* KB-1, dark blue) and TCE (KB-1 RF, brown and Donna II, cyan) versus cultures precultivated on VC (KB-1/VC, light green), *cis*-DCE (KB-1/cDCE, purple), and *trans*-DCE (WBC-2/tDCE, light blue). Shaded areas show the corresponding trends observed with *cis*-DCE (gray) and TCE (green, low pH/blue, high pH) in the vitamin B_{12} model.[14] (The 95% confidence intervals are given as values and as black lines next to the regression slopes).

dual element isotope trends depending on precultivation conditions. Cultures precultivated on less chlorinated ethenes such as VC (KB-1/VC), *cis*-DCE (KB-1/cDCE), and *trans*-DCE (WBC-2/tDCE) showed large carbon isotope effects in combination with small chlorine isotope effects corresponding to $\Lambda_{C/Cl}$ values between 9.0 and 18.2 ($\Lambda_{KB-1/VC}$ = 18.2 ± 4.3, $\Lambda_{KB-1/cDCE}$ = 11.8 ± 2.4, and $\Lambda_{WBC-2/tDCE}$ = 9.0 ± 1.1). In contrast the cultures *G. lovleyi* strain KB-1, KB-1 RF, and Donna II, precultivated on TCE or PCE, showed significantly smaller $\Lambda_{C/Cl}$ values of 2.3 to 3.1 ($\Lambda_{Donna\ II}$ = 2.3 ± 0.1, $\Lambda_{KB-1\ RF}$ = 2.7 ± 0.2, $\Lambda_{G.\ lovleyi\ KB-1}$ = 3.1 ± 0.1), indicative of larger chlorine isotope effects. These results are similar to the dual element isotope slopes $\Lambda_{C/Cl}$ observed for an addition−elimination mechanism with vitamin B_{12}. In contrast, cultures precultivated on less chlorinated substrates [*cis*-DCE (KB-1/cDCE), VC (KB-1/VC), and *trans*-DCE (WBC-2/tDCE)] resulted in $\Lambda_{C/Cl}$ values of TCE dechlorination that correspond to an addition−protonation pathway with vitamin B_{12}.

Our observations suggest that in the bacterial cells a similar mechanistic dichotomy of cob(I)alamin addition−elimination versus cob(I)alamin addition−protonation took place as in the model reaction with vitamin B_{12} at different pH (Scheme 1). In experiments with bacterial cells, however, both the medium and the inside of the cells were buffered so that catalysis of the different pathways must be effectuated by functional groups inside the enzymes' catalytic sites rather than by a different pH

in bulk solution. We therefore hypothesize that the enzyme architecture of RDases is tailored to different specific reaction mechanisms, possibly due to the presence/absence of amino acids with specific protonation functionalities.

Mechanism-Specific Dual Element Isotope Trends of TCE: Lack of Correlation with RDase Predominance. Given that we observed evidence of different reaction mechanisms in bacterial reductive dehalogenation of TCE, we further explored whether this mechanistic dichotomy could be correlated with the predominance of specific reductive dehalogenases. Therefore, three different bacterial cultures, which had been adapted to TCE and for which the predominance of different RDases can be inferred (see Table 1), were compared. *G. lovleyi* strain KB-1 has been shown to harbor only one RDase, *Geo*-PceA.[33] For the mixed-culture KB-1 RF, the RDase VcrA is considered to be responsible for dechlorination.[33] In the mixed culture Donna II, *D. mccartyi* strain 195 is the organism responsible for dechlorination, and the RDase TceA was identified as the most prominent dechlorinating enzyme.[34]

The key outcome of this approach was that the dual element isotope plot of these three cultures shows similar regression slopes ($\Lambda_{Donna\ II}$ = 2.3 ± 0.1, $\Lambda_{KB-1\ RF}$ = 2.7 ± 0.2, and $\Lambda_{G.\ lovleyi\ KB-1}$ = 3.1 ± 0.1, see Table 1 and Figure S2) for all three experiments, indicating that TCE was dechlorinated via a similar chemical mechanism, irrespective of the type of RDase (*Geo*-PceA versus VcrA versus TceA). The three slopes agree with those at high pH in the vitamin B_{12} study,[14] suggesting that in all three cases, a sequence of addition−elimination was the predominant reaction pathway.

Subsequently, quantitative polymerase chain reaction (qPCR) analysis was applied to detect changes in the reductive dehalogenase gene (*rdhA*) composition when cultures that had been precultivated on less chlorinated ethenes were adapting to TCE reductive dechlorination (see Table 1). qPCR analysis indicated a significant shift in the culture KB-1/cDCE after changing the electron acceptor from *cis*-DCE to TCE. Typically, KB-1/cDCE is dominated by the RDase BvcA when precultivated on *cis*-DCE.[33] After the TCE dechlorination experiment, however, the *rdhA* gene *bvcA* was no longer detected in the qPCR analysis. Instead, the *rdhA* gene *vcrA* was most abundant, indicating that TCE dechlorination was likely performed by a *vcrA*-containing strain of *Dehalococcoides*. For the WBC-2/tDCE culture, only minor changes in the RDase composition were observed. Here the *vcrA* and *tdrA* genes were predominant before[9] and after the experiment. WBC-2/tDCE contains *Dehalogenimonas* sp., which expresses TdrA for the dechlorination of *trans*-DCE to VC.[9] Additionally, after the TCE dechlorination experiment, a small number of *tceA* genes were detected by qPCR. In case of KB-1/VC, no changes in the *rdhA* gene composition were discernible. Before[33] and after the TCE dechlorination experiment with KB-1/VC, *vcrA* was the most-abundant RDase gene analyzed. The information obtained from the qPCR data therefore suggests that the maintenance on one specific precultivation substrate has a significant influence on the microbial community and the prevalence of RDase genes.[35] Nevertheless, isotope effects of all cultures still gave evidence of the same addition−protonation mechanism (see Table 1 and Figure S2), suggesting that the reaction mechanism was conserved in precultivated cultures, even though shifts in the dominantly expressed RDase were observed.

Finally, a comparison of Figure 4 and the qPCR data on predominant RDases (see Table 1 and Figure S2) suggests that there can be different mechanisms at work ($\Lambda_{\text{KB-1 RF}}$ = 2.7 ± 0.2 versus $\Lambda_{\text{KB-1/VC}}$ = 18.2 ± 4.3) even though the same nominal RDase gene (*vcrA*) was predominant. One possibility is that the VrcA dehalogenase complex in organisms adapted to less chlorinated substrates is different from those enriched on TCE. Kublik et al.[41] showed that in *Dehalococcoides*, the reductive dehalogenase is part of a complex containing a variety of proteins. Potentially, these other electron transport proteins may affect the enzyme and its isotope fractionation. In addition, the role of corrinoid prosthetic groups, which can affect dechlorination,[13,42] has to be further investigated because it was unclear what types of corrinoids were produced in the mixed cultures. Another possibility is that the RDase catalyzing the dechlorination in the non-TCE-adapted cultures is not VcrA, even though the strains contained that gene. Quantitative polymerase chain reaction can only reveal that the *vcrA* gene became more abundant after switching the electron acceptor, but qPCR cannot provide direct information about whether the RDase was actually expressed. For example, Heavner et al.[43] described that in all *Dehalococcoides* spp., particularly in KB-1, a specific RDase (DET 1545 homologue) shows elevated expression upon stress.

The observation that the predominance of nominal RDases did not correlate with isotope effect trends therefore highlights the need for a complementary approach to classify degradation in natural and engineered systems: a classification based not only on the metagenomic detection of RDase genes but also on dual element (C, Cl) isotope fractionation as indicator of underlying (bio)chemical transformation mechanisms. For the transformation of TCE with different pure corrinoid cofactors, dual element isotope slopes between 3.7 and 4.5 were recently observed,[44] which we may now interpret as indicative of an addition–elimination mechanism.

Previously Observed Stable Isotope Fractionation: Consistency with the Mechanistic Dichotomy Observed in This Study. Figure 5 shows our data in the context of previously reported dual element isotope trends $\Lambda_{\text{C/Cl}}$ in reductive dehalogenation by bacteria,[38,39,45–50] in enzyme extracts,[44] and by pure cofactors[38,44] or model systems.[14,38] To account for the potential effect of masking, these values of $\Lambda_{\text{C/Cl}}$ are plotted against the corresponding carbon isotope enrichment factors ε_C. Pronounced negative ε_C values indicate that intrinsic isotope effects are strongly expressed meaning that the influence of masking is small. Vice versa, only slightly negative ε_c values (corresponding to data points Figure 5, region shaded in green) indicate that intrinsic isotope effects were strongly masked meaning that observable $\Lambda_{\text{C/Cl}}$ values did not necessarily reflect the intrinsic biochemical reaction. Data points located in this putative masking-dominated domain are derived from microbial degradation of PCE ($\Lambda_{\text{C/Cl}}$ values of 0.7 to 2.8 and slightly negative ε_C values of −0.7 ‰ to −5.6 ‰),[44,45,50] as well as from the TCE dechlorinating culture KB-1/1,2-DCA (ε_C = −5.4 ± 1.5 ‰ and $\Lambda_{\text{KB-1/1,2-DCA}}$ = 4.5 ± 0.8) of this study. These smaller dual element isotope slopes potentially do not reflect the chemical bond conversion but rather a preceding step (e.g., mass transfer into the cell, substrate-enzyme binding, etc.)[44] and are, therefore, not discussed further here.

Pronounced negative ε_C, together with moderate $\Lambda_{\text{C/Cl}}$ values (Figure 5, region shaded in yellow) are indicative of the addition–elimination mechanism[14] brought forward in this
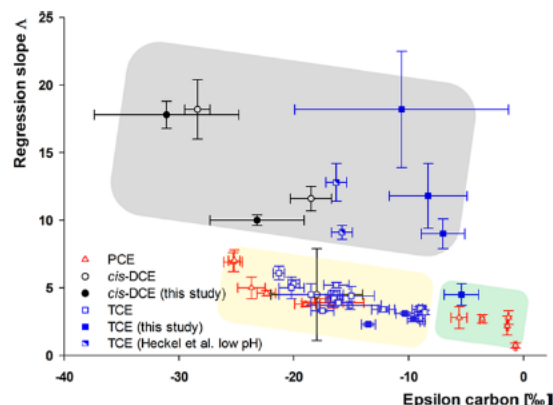

Figure 5. Carbon isotope fractionation factors ε_C and dual element isotope regression slopes $\Lambda_{\text{C/Cl}}$ in reductive chlorinated ethene dehalogenation by bacteria,[38,39,45–50] in enzyme extracts,[44] by pure cofactors[38,44] or model systems[14,38] observed in this study (filled symbols), and reported from previous studies (empty and half-filled symbols). Reductive dechlorination of PCE is depicted by red triangles, of TCE by blue squares and of *cis*-DCE by black circles. (Error bars show 95% confidence intervals of respective values). Shaded areas illustrate regions which indicate that intrinsic isotope effects are masked (green) or that they follow an addition–elimination mechanism (yellow) or an addition–protonation mechanism (gray).

study. Indeed, the microbial data in this domain[38,39,45–48] originate almost exclusively from the dechlorination of PCE and TCE, including this study's data with cultures adapted to TCE ($\Lambda_{\text{Donna II}}$ = 2.3 ± 0.1, $\Lambda_{\text{KB-1 RF}}$ = 2.7 ± 0.2, and $\Lambda_{G.\ lovleyi\ \text{KB-1}}$ = 3.1 ± 0.1). Similar trends were observed in transformation of TCE with enzymatic extracts[44] and purified cofactors[38,44] in which all values fell in a rather narrow experimental range ($\Lambda_{\text{C/Cl}}$ = 3.7–5.3), indicating that the predominance of an addition–elimination mechanism can be traced down to the enzyme level.[14] An exception is a former *cis*-DCE degradation study ($\Lambda_{\text{C/Cl}}$ = 4.5). The nature of this degradation with field sediment rather than bacterial cultures was, however, little constrained, so general conclusions are difficult.[48]

In contrast, data points corresponding to pronounced negative ε_C, together with large $\Lambda_{\text{C/Cl}}$ values (Figure 5, region shaded in gray) are indicative of the addition–protonation mechanism.[14] Indeed, all data are derived from either *cis*-DCE dechlorination (this and previous[48,49] studies) or from TCE reductive dechlorination at low pH in the vitamin B_{12} model system[14] or by cultures precultivated on less chlorinated ethenes (this study). Taken together, the regions of Figure 5 confirm that also all dual element isotope trends reported so far are consistent with the mechanistic dichotomy observed in this study.

Environmental Significance. Available dual element isotope data reveal a surprising dichotomy in reductive dechlorination chemistry of microbial communities. These results suggest that for dehalogenation of chlorinated ethenes catalyzed by RDases two different reductive dechlorination mechanisms exist, which are mimicked by the addition–elimination versus addition–protonation pathways identified in a recent vitamin B_{12} study.[14] The evidence that reductive dehalogenases may be optimized to catalyze fundamentally

different mechanisms, despite an identical net reaction (hydrogenolysis), offers an explanation why some RDases can be specialized in the dechlorination of PCE and TCE but cannot dechlorinate cis-DCE or VC. These results, therefore, hold promise to potentially resolve a fundamental challenge to our understanding of reductive dechlorination that has been a long-standing barrier to successful bioremediation in the field: why dechlorination of chlorinated ethenes often stops at cis-DCE or VC. A new RDase classification system based on catalyzed mechanisms may, therefore, represent a transformative advance to the field in the future. Finally, this study highlights the potential of dual element compound-specific stable isotope analysis as an enabling technology with which to overcome these long-standing dilemmas of organic (bio)chemistry: to bridge the gap between in vitro and in vivo, to probe for reaction mechanisms in organisms, and to directly observe a change of the involved RDases by detecting underlying dechlorination mechanisms at contaminated sites.

■ ASSOCIATED CONTENT

⑤ Supporting Information

The Supporting Information is available free of charge on the ACS Publications website at DOI: 10.1021/acs.est.8b06643.

Concentration measurements via GC-FID; figures depicting concentration vs time for TCE reductive dehalogenation, dual element isotope plots for TCE dechlorination, and stable isotope analysis of carbon and chlorine via GC-IRMS; tables with detailed information regarding qPCR and previous studies used for Figure 5 (PDF)

■ AUTHOR INFORMATION

Corresponding Author
*E-mail: m.elsner@tum.de.

ORCID ⑩
Elizabeth A. Edwards: 0000-0002-8071-338X
Ivonne Nijenhuis: 0000-0001-9737-9501
Martin Elsner: 0000-0003-4746-9052

Notes
The authors declare no competing financial interest.

■ ACKNOWLEDGMENTS

■ REFERENCES

(1) Bradley, P. M. Microbial degradation of chloroethenes in groundwater systems. Hydrogeol. J. 2000, 8 (1), 104−111.

(2) Hug, L. A.; Maphosa, F.; Leys, D.; Löffler, F. E.; Smidt, H.; Edwards, E. A.; Adrian, L. Overview of organohalide-respiring bacteria and a proposal for a classification system for reductive dehalogenases. Philos. Trans. R. Soc., B 2013, 368, 1616.

(3) Taş, N.; van Eekert, M. H. A.; De Vos, W. M.; Smidt, H. The little bacteria that can-diversity, genomics and ecophysiology of 'Dehalococcoides' spp. in contaminated environments. Microb. Biotechnol. 2010, 3 (4), 389−402.

(4) Smidt, H.; de Vos, W. M. Anaerobic microbial dehalogenation. Annu. Rev. Microbiol. 2004, 58, 43−73.

(5) Maymó-Gatell, X.; Anguish, T.; Zinder, S. H. Reductive dechlorination of chlorinated ethenes and 1, 2-dichloroethane by "Dehalococcoides ethenogenes" 195. Appl. Environ. Microbiol. 1999, 65 (7), 3108−3113.

(6) Maymo-Gatell, X.; Chien, Y.-T.; Gossett, J. M.; Zinder, S. H. Isolation of a Bacterium That Reductively Dechlorinates Tetrachloroethene to Ethene. Science 1997, 276 (5318), 1568−1571.

(7) Pöritz, M.; Goris, T.; Wubet, T.; Tarkka, M. T.; Buscot, F.; Nijenhuis, I.; Lechner, U.; Adrian, L. Genome sequences of two dehalogenation specialists-Dehalococcoides mccartyi strains BTF08 and DCMB5 enriched from the highly polluted Bitterfeld region; Blackwell Publishing Ltd.: Oxford, UK, 2013.

(8) Cichocka, D.; Nikolausz, M.; Haest, P. J.; Nijenhuis, I. Tetrachloroethene conversion to ethene by a Dehalococcoides-containing enrichment culture from Bitterfeld. FEMS Microbiol. Ecol. 2010, 72 (2), 297−310.

(9) Molenda, O.; Quaile, A. T.; Edwards, E. A. Dehalogenimonas sp. strain WBC-2 genome and identification of its trans-dichloroethene reductive dehalogenase, TdrA. Appl. Environ. Microbiol. 2016, 82 (1), 40−50.

(10) Yang, Y.; Higgins, S. A.; Yan, J.; Şimşir, B.; Chourey, K.; Iyer, R.; Hettich, R. L.; Baldwin, B.; Ogles, D. M.; Löffler, F. E. Grape pomace compost harbors organohalide-respiring Dehalogenimonas species with novel reductive dehalogenase genes. ISME J. 2017, 11 (12), 2767−2780.

(11) Payne, K. A. P.; Quezada, C. P.; Fisher, K.; Dunstan, M. S.; Collins, F. A.; Sjuts, H.; Levy, C.; Hay, S.; Rigby, S. E. J.; Leys, D. Reductive dehalogenase structure suggests a mechanism for B12-dependent dehalogenation. Nature 2015, 517 (7535), 513−516.

(12) Bommer, M.; Kunze, C.; Fesseler, J.; Schubert, T.; Diekert, G.; Dobbek, H. Structural basis for organohalide respiration. Science 2014, 346 (6208), 455−458.

(13) Yan, J.; Simsir, B.; Farmer, A. T.; Bi, M.; Yang, Y.; Campagna, S. R.; Loffler, F. E. The corrinoid cofactor of reductive dehalogenases affects dechlorination rates and extents in organohalide-respiring Dehalococcoides mccartyi. ISME J. 2016, 10, 1092−1101.

(14) Heckel, B.; McNeill, K.; Elsner, M. Chlorinated Ethene Reactivity with Vitamin B₁₂ Is Governed by Cobalamin Chloroethylcarbanions as Crossroads of Competing Pathways. ACS Catal. 2018, 8 (4), 3054−3066.

(15) Matthews, D. E.; Hayes, J. M. Isotope-Ratio-Monitoring Gas Chromatography-Mass Spectrometry. Anal. Chem. 1978, 50 (11), 1465−1473.

(16) Sessions, A. L. Isotope-ratio detection for gas chromatography. J. Sep. Sci. 2006, 29, 1946−1961.

(17) Shouakar-Stash, O.; Drimmie, R. J.; Frape, S. K. Determination of inorganic chlorine stable isotopes by continuous flow isotope ratio mass spectrometry. Rapid Commun. Mass Spectrom. 2005, 19 (2), 121−127.

(18) Bernstein, A.; Shouakar-Stash, O.; Ebert, K.; Laskov, C.; Hunkeler, D.; Jeannottat, S.; Sakaguchi-Soder, K.; Laaks, J.; Jochmann, M. A.; Cretnik, S.; Jager, J.; Haderlein, S. B.; Schmidt, T. C.; Aravena, R.; Elsner, M. Compound-Specific Chlorine Isotope Analysis: A Comparison of Gas Chromatography/Isotope Ratio Mass Spectrometry and Gas Chromatography/Quadrupole Mass Spectrometry Methods in an Interlaboratory Study. Anal. Chem. 2011, 83 (20), 7624−7634.

(19) Shouakar-Stash, O.; Drimmie, R. J.; Zhang, M.; Frape, S. K. Compound-specific chlorine isotope ratios of TCE, PCE and DCE isomers by direct injection using CF-IRMS. Appl. Geochem. 2006, 21 (5), 766−781.

(20) Hunkeler, D.; Meckenstock, R. U.; Sherwood, Lollar B.; Schmidt, T.; Wilson, J.; Schmidt, T.; Wilson, J. A Guide for Assessing Biodegradation and Source Identification of Organic Ground Water

Contaminants using Compound Specific Isotope Analysis (CSIA); US EPA: Oklahoma City, OK, 2008.

(21) Coplen, T. B. Guidelines and recommended terms for expression of stable-isotope-ratio and gas-ratio measurement results. *Rapid Commun. Mass Spectrom.* **2011**, 25 (17), 2538−2560.

(22) Elsner, M. Stable isotope fractionation to investigate natural transformation mechanisms of organic contaminants: principles, prospects and limitations. *J. Environ. Monit.* **2010**, 12 (11), 2005−2031.

(23) Bigeleisen, J. Chemistry of Isotopes: Isotope chemistry has opened new areas of chemical physics, geochemistry, and molecular biology. *Science* **1965**, 147, 463−471.

(24) Kaufhold, T.; Schmidt, M.; Cichocka, D.; Nikolausz, M.; Nijenhuis, I. Dehalogenation of diverse halogenated substrates by a highly enriched Dehalococcoides-containing culture derived from the contaminated mega-site in Bitterfeld. *FEMS Microbiol. Ecol.* **2013**, 83 (1), 176−188.

(25) Duhamel, M.; Wehr, S. D.; Yu, L.; Rizvi, H.; Seepersad, D.; Dworatzek, S.; Cox, E. E.; Edwards, E. A. Comparison of anaerobic dechlorinating enrichment cultures maintained on tetrachloroethene, trichloroethene, cis-dichloroethene and vinyl chloride. *Water Res.* **2002**, 36 (17), 4193−4202.

(26) Duhamel, M.; Mo, K.; Edwards, E. A. Characterization of a highly enriched Dehalococcoides-containing culture that grows on vinyl chloride and trichloroethene. *Appl. Environ. Microbiol.* **2004**, 70 (9), 5538−5545.

(27) Duhamel, M.; Edwards, E. A. Microbial composition of chlorinated ethene-degrading cultures dominated by Dehalococcoides. *FEMS Microbiol. Ecol.* **2006**, 58 (3), 538−549.

(28) Duhamel, M.; Edwards, E. A. Growth and Yields of Dechlorinators, Acetogens, and Methanogens during Reductive Dechlorination of Chlorinated Ethenes and Dihaloelimination of 1,2-Dichloroethane. *Environ. Sci. Technol.* **2007**, 41 (7), 2303−2310.

(29) Hug, L. A. A Metagenome-based Examination of Dechlorinating Enrichment Cultures: Dehalococcoides and the Role of the Non-dechlorinating Microorganisms. Ph.D. Thesis, University of Toronto, Toronto, Ontario, Canada, 2012.

(30) Cichocka, D.; Imfeld, G.; Richnow, H.-H.; Nijenhuis, I. Variability in microbial carbon isotope fractionation of tetra- and trichloroethene upon reductive dechlorination. *Chemosphere* **2008**, 71 (4), 639−648.

(31) Schmidt, M.; Lege, S.; Nijenhuis, I. Comparison of 1,2-dichloroethane, dichloroethene and vinyl chloride carbon stable isotope fractionation during dechlorination by two Dehalococcoides strains. *Water Res.* **2014**, 52 (0), 146−154.

(32) Magnuson, J. K.; Romine, M. F.; Burris, D. R.; Kingsley, M. T. Trichloroethene reductive dehalogenase from Dehalococcoides ethenogenes: Sequence of tceA and substrate range characterization. *Appl. Environ. Microbiol.* **2000**, 66 (12), 5141−5147.

(33) Liang, X.; Molenda, O.; Tang, S.; Edwards, E. A. Identity and Substrate Specificity of Reductive Dehalogenases Expressed in Dehalococcoides-Containing Enrichment Cultures Maintained on Different Chlorinated Ethenes. *Appl. Environ. Microbiol.* **2015**, 81 (14), 4626−4633.

(34) Fung, J. M.; Morris, R. M.; Adrian, L.; Zinder, S. H. Expression of reductive dehalogenase genes in Dehalococcoides ethenogenes strain 195 growing on tetrachloroethene, trichloroethene, or 2, 3-dichlorophenol. *Appl. Environ. Microbiol.* **2007**, 73 (14), 4439−4445.

(35) Pérez-de-Mora, A.; Lacourt, A.; McMaster, M. L.; Liang, X.; Dworatzek, S. M.; Edwards, E. A. Chlorinated Electron Acceptor Abundance Drives Selection of Dehalococcoides mccartyi (D. mccartyi) Strains in Dechlorinating Enrichment Cultures and Groundwater Environments. *Front. Microbiol.* **2018**, 9 (812), 1 DOI: 10.3389/fmicb.2018.00812.

(36) Edwards, E. A.; Grbić-Galić, D. Complete mineralization of benzene by aquifer microorganisms under strictly anaerobic conditions. *Appl. Environ. Microbiol.* **1992**, 58 (8), 2663−2666.

(37) Elsner, M.; Couloume, G. L.; SherwoodLollar, B. Freezing To Preserve Groundwater Samples and Improve Headspace Quantifica-tion Limits of Water-Soluble Organic Contaminants for Carbon Isotope Analysis. *Anal. Chem.* **2006**, 78 (21), 7528−7534.

(38) Cretnik, S.; Thoreson, K. A.; Bernstein, A.; Ebert, K.; Buchner, D.; Laskov, C.; Haderlein, S.; Shouakar-Stash, O.; Kliegman, S.; McNeill, K.; Elsner, M. Reductive Dechlorination of TCE by Chemical Model Systems in Comparison to Dehalogenating Bacteria: Insights from Dual Element Isotope Analysis (13C/12C, 37Cl/35Cl). *Environ. Sci. Technol.* **2013**, 47 (13), 6855−6863.

(39) Cretnik, S.; Bernstein, A.; Shouakar-Stash, O.; Löffler, F.; Elsner, M. Chlorine Isotope Effects from Isotope Ratio Mass Spectrometry Suggest Intramolecular C-Cl Bond Competition in Trichloroethene (TCE) Reductive Dehalogenation. *Molecules* **2014**, 19 (5), 6450−6473.

(40) Elsner, M.; Zwank, L.; Hunkeler, D.; Schwarzenbach, R. P. A new concept linking observable stable isotope fractionation to transformation pathways of organic pollutants. *Environ. Sci. Technol.* **2005**, 39 (18), 6896−6916.

(41) Kublik, A.; Deobald, D.; Hartwig, S.; Schiffmann, C. L.; Andrades, A.; von Bergen, M.; Sawers, R. G.; Adrian, L. Identification of a multi-protein reductive dehalogenase complex in D ehalococcoides mccartyi strain CBDB 1 suggests a protein-dependent respiratory electron transport chain obviating quinone involvement. *Environ. Microbiol.* **2016**, 18 (9), 3044−3056.

(42) Men, Y.; Seth, E. C.; Yi, S.; Crofts, T. S.; Allen, R. H.; Taga, M. E.; Alvarez-Cohen, L. Identification of specific corrinoids reveals corrinoid modification in dechlorinating microbial communities. *Environ. Microbiol.* **2015**, 17 (12), 4873−4884.

(43) Heavner, G. L.; Mansfeldt, C. B.; Debs, G. E.; Hellerstedt, S. T.; Rowe, A. R.; Richardson, R. E. Biomarkers' Responses to Reductive Dechlorination Rates and Oxygen Stress in Bioaugmentation Culture KB-1TM. *Microorganisms* **2018**, 6 (1), 13.

(44) Renpenning, J.; Keller, S.; Cretnik, S.; Shouakar-Stash, O.; Elsner, M.; Schubert, T.; Nijenhuis, I. Combined C and Cl Isotope Effects Indicate Differences between Corrinoids and Enzyme (Sulfurospirillum multivorans PceA) in Reductive Dehalogenation of Tetrachloroethene, But Not Trichloroethene. *Environ. Sci. Technol.* **2014**, 48 (20), 11837−11845.

(45) Wiegert, C.; Mandalakis, M.; Knowles, T.; Polymenakou, P. N.; Aeppli, C.; Macháčková, J.; Holmstrand, H.; Evershed, R. P.; Pancost, R. D.; Gustafsson, Ö. Carbon and Chlorine Isotope Fractionation During Microbial Degradation of Tetra- and Trichloroethene. *Environ. Sci. Technol.* **2013**, 47 (12), 6449−6456.

(46) Buchner, D.; Behrens, S.; Laskov, C.; Haderlein, S. B. Resiliency of Stable Isotope Fractionation (δ13C and δ37Cl) of Trichloroethene to Bacterial Growth Physiology and Expression of Key Enzymes. *Environ. Sci. Technol.* **2015**, 49, 13230−13237.

(47) Kuder, T.; van Breukelen, B. M.; Vanderford, M.; Philp, P. 3D-CSIA: Carbon, Chlorine, and Hydrogen Isotope Fractionation in Transformation of TCE to Ethene by a Dehalococcoides Culture. *Environ. Sci. Technol.* **2013**, 47 (17), 9668−9677.

(48) Doğan-Subaşi, E.; Elsner, M.; Qiu, S.; Cretnik, S.; Atashgahi, S.; Shouakar-Stash, O.; Boon, N.; Dejonghe, W.; Bastiaens, L. Contrasting dual (C, Cl) isotope fractionation offers potential to distinguish reductive chloroethene transformation from breakdown by permanganate. *Sci. Total Environ.* **2017**, 596−597, 169−177.

(49) Abe, Y.; Aravena, R.; Zopfi, J.; Shouakar-Stash, O.; Cox, E.; Roberts, J. D.; Hunkeler, D. Carbon and Chlorine Isotope Fractionation during Aerobic Oxidation and Reductive Dechlorination of Vinyl Chloride and cis-1,2-Dichloroethene. *Environ. Sci. Technol.* **2009**, 43 (1), 101−107.

(50) Badin, A.; Buttet, G.; Maillard, J.; Holliger, C.; Hunkeler, D. Multiple Dual C-Cl Isotope Patterns Associated with Reductive Dechlorination of Tetrachloroethene. *Environ. Sci. Technol.* **2014**, 48 (16), 9179−9186.

PAPER

Check for updates

Compound-specific chlorine isotope fractionation in biodegradation of atrazine†

Christina Lihl,[ab] Benjamin Heckel,[ab] Anna Grzybkowska,[c] Agnieszka Dybala-Defratyka, [c] Violaine Ponsin, [de] Clara Torrentó, [df] Daniel Hunkeler[d] and Martin Elsner [*ab]

Atrazine is a frequently detected groundwater contaminant. It can be microbially degraded by oxidative dealkylation or by hydrolytic dechlorination. Compound-specific isotope analysis is a powerful tool to assess its transformation. In previous work, carbon and nitrogen isotope effects were found to reflect these different transformation pathways. However, chlorine isotope fractionation could be a particularly sensitive indicator of natural transformation since chlorine isotope effects are fully represented in the molecular average while carbon and nitrogen isotope effects are diluted by non-reacting atoms. Therefore, this study explored chlorine isotope effects during atrazine hydrolysis with *Arthrobacter aurescens* TC1 and oxidative dealkylation with *Rhodococcus* sp. NI86/21. Dual element isotope slopes of chlorine *vs.* carbon isotope fractionation ($\Lambda_{Cl/C}^{Arthro} = 1.7 \pm 0.9$ *vs.* $\Lambda_{Cl/C}^{Rhodo} = 0.6 \pm 0.1$) and chlorine *vs.* nitrogen isotope fractionation ($\Lambda_{Cl/N}^{Arthro} = -1.2 \pm 0.7$ *vs.* $\Lambda_{Cl/N}^{Rhodo} = 0.4 \pm 0.2$) provided reliable indicators of different pathways. Observed chlorine isotope effects in oxidative dealkylation ($\varepsilon_{Cl} = -4.3 \pm 1.8\%$) were surprisingly large, whereas in hydrolysis ($\varepsilon_{Cl} = -1.4 \pm 0.6\%$) they were small, indicating that C–Cl bond cleavage was not the rate-determining step. This demonstrates the importance of constraining expected isotope effects of new elements before using the approach in the field. Overall, the triple element isotope information brought forward here enables a more reliable identification of atrazine sources and degradation pathways.

Environmental significance

Atrazine is an important chlorinated micropollutant. Although degradable *via* different pathways (dealkylation and hydrolytic dechlorination), it is often recalcitrant and persists in groundwater. To assess and understand its degradation pathways, compound-specific carbon and nitrogen isotope analysis has been advanced, but information from chlorine isotope fractionation has been missing until today. This study explores the added benefit of chlorine isotope fractionation as an indicator of natural atrazine transformation. Together with carbon and nitrogen isotope analysis, this enables a multi-element approach which can improve source identification and differentiation of microbial transformation pathways in the environment.

[a]Institute of Groundwater Ecology, Helmholtz Zentrum München, Ingolstädter Landstraße 1, 85764 Neuherberg, Germany. E-mail: m.elsner@tum.de; Tel: +49-89-2180-78231

[b]Chair of Analytical Chemistry and Water Chemistry, Technical University of Munich, Marchioninistraße 17, 81377 Munich, Germany

[c]Institute of Applied Radiation Chemistry, Faculty of Chemistry, Lodz University of Technology, Zeromskiego 116, 90-924 Lodz, Poland

[d]Centre of Hydrogeology and Geothermics (CHYN), University of Neuchâtel, 2000 Neuchâtel, Switzerland

[e]Département des sciences de la Terre et de l'atmosphère, Université du Québec à Montréal, 201 Avenue du Président Kennedy, Montréal, QC, Canada

[f]Grup MAiMA, Departament de Mineralogia, Petrologia i Geologia Aplicada, Facultat de Ciències de la Terra, Universitat de Barcelona (UB), C/Martí i Franquès s/n, 08028, Barcelona, Spain

† Electronic supplementary information (ESI) available: Information concerning the HPLC temperature programs, two figures and one table illustrating the GC-qMS method optimization for chlorine analysis, one table illustrating the method comparison of the GC-qMS for chlorine analysis, one figure and one table considering H-abstraction during chlorine CSIA, two figures illustrating the results of HPLC concentration analysis. See DOI: 10.1039/c9em00503j

Introduction

The herbicide atrazine has been used in agriculture to inhibit growth of broadleaf and grassy weeds.[1] In the U.S. atrazine was the second most commonly used herbicide in 2012 and is still in use today.[2] In the European Union atrazine was banned in 2004,[3] but together with its metabolites it is still frequently detected at high concentrations in groundwater.[4,5] The massive and widespread use has led to a wide-ranging presence of atrazine in the environment, which can have harmful effects on living organisms and humans.[6] Therefore, the environmental fate of atrazine is of significant concern and much attention has been directed at detecting and enhancing its natural biodegradation. However, assessing microbial degradation of atrazine in the environment is challenging with conventional methods like concentration analysis. Sorption and remobilization of the

parent compound and its metabolites, as well as further transformation of the metabolites inevitably lead to fluctuations in concentrations,[7–10] which make it difficult to assess the net extent of atrazine degradation in the field.

In recent years, compound-specific isotope analysis (CSIA) has been proposed as an alternative approach to detect and quantify the degradation of atrazine.[11–13]

In contrast to, and complementary to traditional methods, CSIA informs about transformation without the need to detect metabolites. The reason is that during (bio)chemical transformations molecules with heavy isotopes are typically enriched in the remaining substrate since their bonds are more stable and, therefore, usually react slower than molecules containing light isotopes (normal kinetic isotope effect). The ratios of heavy to light isotopes (*e.g.* $^{13}C/^{12}C$ for carbon) in the remaining substrate, therefore, change during transformation. Observing such changes can be used as direct (and concentration-independent) indicator of degradation.[14,15]

Isotope values are reported in the δ-notation relative to an international reference material, *e.g.* for carbon:[14,15]

$$\delta^{13}C = [(^{13}C/^{12}C)_{sample} - (^{13}C/^{12}C)_{reference}]/(^{13}C/^{12}C)_{reference} \quad (1)$$

The magnitude of the degradation-induced isotope fractionation depends on different factors, which can make isotope ratios of specific elements particularly attractive to observe degradation-induced isotope fractionation. To this end, first, an element needs to be directly involved in the (bio)chemical reaction. For example, a carbon isotope effect would be quite generally expected in organic molecules, whereas a chlorine isotope effect would be primarily expected if a C–Cl bond is cleaved. Second, isotope fractionation depends on the underlying kinetic isotope effect (see above), but also on the extent to which this effect is represented in the molecular average isotope fractionation described by the enrichment factor ε (see below). Atrazine, for example, contains only one chlorine atom but eight carbon and five nitrogen atoms. Hence, chlorine isotope effects at the reacting position are fully represented in the molecular average, whereas position-specific carbon and nitrogen isotope effects are diluted by non-reacting atoms.[14,15]

Most of the publications studying the chemical mechanisms of abiotic and microbial atrazine degradation have focused on the analysis of carbon ($^{13}C/^{12}C$) and nitrogen ($^{15}N/^{14}N$) isotope fractionation. Thereby, ε-values in the range of -5.4% to -1.8% for carbon and -1.9% to 3.3% for nitrogen were observed.[9,10,16,17] Chlorine isotope effects for microbial atrazine degradation were so far not reported due to analytical challenges:[18] until recently,[19,20] suitable methods were not available for chlorine isotope analysis of atrazine. However, from the magnitude of chlorine isotope effects observed for dechlorination of trichloroethenes (-5.7% to -3.3%, where intrinsic isotope effects are diluted by a factor of three[21]) very large chlorine enrichment factors ε_{Cl} (-8% to -10% or even larger) could potentially occur for a C–Cl bond cleavage in atrazine. For example, enzymatic hydrolysis of the structural homologue ametryn (atrazine structure with a –SCH$_3$ instead of a –Cl group) yielded a sulfur isotope enrichment factor ε_S of $-14.7 \pm 1.0\%$.[17]

If the cleavage of carbon–chlorine bonds is involved in the rate-determining step of a (bio)transformation, chlorine isotope effects could, therefore, enable a particularly sensitive detection of natural transformation processes by compound-specific (*i.e.*, molecular average) isotope analysis.

The measurement of chlorine isotope fractionation is attractive for yet another reason – multiple element isotope analysis bears potential for a better distinction of sources and transformation pathways. From isotope analysis of one element alone, it is difficult to distinguish sources of a particular compound, or competing transformation pathways that may lead to metabolites of different toxicity.[15] For example, two different microbial transformation pathways can lead to the degradation of atrazine in the environment. Hydrolysis forms the nontoxic dehalogenated product 2-hydroxyatrazine (HAT) whereas oxidative dealkylation degrades atrazine to the still herbicidal products desethyl- (DEA) or desisopropyl-atrazine (DIA).[22,23] Prominent examples for microorganisms catalyzing these pathways are *Arthrobacter aurescens* TC1 and *Rhodococcus* sp. NI86/21 (see Fig. 1). *A. aurescens* TC1 was directly isolated from an atrazine-contaminated soil.[24] By expressing the enzyme TrzN, it is capable of performing hydrolysis of atrazine.[24,25] *Rhodococcus* sp. NI86/21 uses a cytochrome P450 system for catalyzing oxidative dealkylation of atrazine.[26]

For these two pathways, carbon isotope fractionation was very similar, but significant differences were observed in nitrogen isotope effects.[9,10,16,17] Plotting the changes of isotope ratios of these two elements relative to each other results in the regression slope Λ for carbon and nitrogen[27,28]

$$\Lambda_{C/N} = \Delta\delta^{15}N/\Delta\delta^{13}C \approx \varepsilon_N/\varepsilon_C \quad (2)$$

Hence, dual element (C, N) isotope trends for oxidative dealkylation of atrazine with *Rhodococcus* sp. NI86/21 ($\Lambda_{C/N}^{Rhodo} = 0.4 \pm 0.1$)[16] were significantly different compared to hydrolysis with *A. aurescens* TC1 ($\Lambda_{C/N}^{Arthro} = -0.6 \pm 0.1$)[9] offering an opportunity to distinguish atrazine degradation pathways in the field. However, in environmental assessments it is advantageous to have isotopic information of as many elements as possible in order to distinguish degradation pathways and sources at the same time.[29–31] Therefore, information from a third element, chlorine, would be highly valuable. Also on the mechanistic end, information gained from a change in the chlorine isotope value could lead to a more reliable differentiation of transformation pathways and contribute to a better mechanistic understanding of the underlying chemical reaction.[31] Along these lines, triple element (3D) isotope analysis was already accomplished for chlorinated alkanes[31,32] and alkenes.[33,34]

Until now, however, compound-specific chlorine isotope analysis has not been accessible so that chlorine isotope ratio changes for hydrolysis of atrazine have only been analyzed in abiotic systems or *via* computational calculations.[35,36] For oxidative dealkylation, chlorine isotope effects have, so far, not been studied. Recently a GC-qMS method for chlorine isotope analysis of atrazine has been brought forward[20] which offers the opportunity to enable deeper mechanistic insights into its

Arthrobacter aurescens TC1 (TrzN): Hydrolysis

Atrazine   Meisenheimer Complex   2-Hydroxyatrazine

Rhodococcus sp. NI86/21 (Cytochrome P450): Oxidative Dealkylation

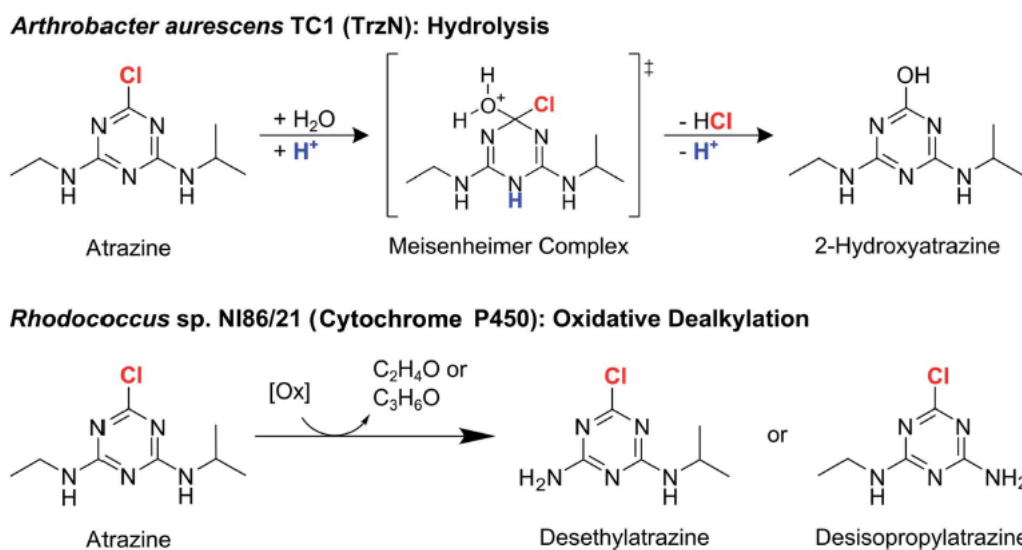Atrazine   Desethylatrazine   or   Desisopropylatrazine

Fig. 1 Microbial degradation of atrazine by *Arthrobacter aurescens* TC1 and *Rhodococcus* sp. NI86/21 (adapted from Meyer *et al.*[9] and Meyer & Elsner[10]).

transformation processes. Therefore, our objective was to analyze carbon, nitrogen and chlorine isotope effects associated with the biodegradation of atrazine *via* hydrolysis with *A. aurescens* TC1 and *via* oxidative dealkylation with *Rhodococcus* sp. NI86/21. In addition, we computationally predicted the chlorine isotope effect associated with hydrolysis and oxidative dealkylation for comparison. Further, we evaluated whether the additional information from chlorine isotope fractionation is a particularly sensitive indicator for transformation processes and whether it can confirm previously proposed mechanisms of different pathways. With this study, we bring forward information about degradation-induced chlorine isotope fractionation of atrazine as a basis to apply triple element (3D) isotope analysis in environmental assessments.

Material & methods

Bacterial strains and cultivation

A. aurescens strain TC1 was grown in mineral salt medium supplemented with approx. 20 mg L^{-1} of atrazine according to the protocol of Meyer *et al.*[9] Likewise, *Rhodococcus* sp. strain NI86/21 was cultivated in autoclaved nutrient broth (8 g L^{-1}, Difco™) with approx. 20 mg L^{-1} of atrazine according to the protocol of Meyer *et al.*[16] In the late-exponential growth phase the strains were harvested *via* centrifugation (4000 rpm, 15 min). For the start of the degradation experiments, cell pellets of each strain were transferred to 400 mL fresh media and atrazine was added to achieve a starting concentration of 20 mg L^{-1}. All experiments were performed in triplicate at 21 °C on a shaker at 150 rpm. Control experiments, which were performed without the bacterial strains, did not show any degradation of atrazine.

Concentration measurements *via* HPLC

The process of atrazine degradation was monitored by concentration measurements. For analysis, 1 mL samples were taken and filtered through a 0.22 μm filter. Atrazine and its degradation products were directly analyzed using a Shimadzu UHPLC-20A system, which was equipped with an ODS column 30 (Ultracarb 5 μM, 150 × 4.6 mm, Phenomenex). After sample injection (10 μL) an adequate gradient program (see ESI†) was used for compound separation. The oven temperature was set to 45 °C and the compounds were detected by their UV absorbance at 222 nm. Quantitation was performed by the software "Lab Solutions" based on internal calibration curves.

Preparation of samples for isotope analysis

According to the protocol of Meyer *et al.*[9] between 10 and 260 mL of sample were taken for isotope analysis of atrazine at every sampling event. After centrifugation (15 min, 4000 rpm) the supernatant was collected in a new vial. Subsequently, samples were extracted by adding dichloromethane (5–130 mL) and shaking the vial for at least 20 min. The sample extracts were dried at room temperature under the fume hood. Afterwards, the dried extracts were dissolved in ethyl acetate to a final atrazine concentration of approx. 200 mg L^{-1}.

Isotope analysis of carbon and nitrogen

The protocol for isotope analysis of carbon and nitrogen was adapted from the studies of Meyer *et al.*[9,16] A TRACE GC Ultra gas chromatograph hyphenated with a GC-III combustion interface and coupled to a Finnigan MAT253 isotope ratio mass spectrometer (GC-C-IRMS, all Thermo Fisher Scientific) was used. Each sample was analyzed in triplicate. Sample injection

794 | *Environ. Sci.: Processes Impacts*, 2020, **22**, 792–801

This journal is © The Royal Society of Chemistry 2020

116

(2–3 μL) was performed by a Combi-PAL autosampler (CTC analysis). The injector had a constant temperature of 220 °C, was equipped with an "A" type packed liner for large volume injections (GL Sciences) and was operated for 1 min in splitless and then in split mode (split ratio 1 : 10) with a flow rate of 1.4 mL min^{-1}. For peak separation, the GC oven was equipped with a DB-5 MS column (30 m × 0.25 mm, 1 μm film thickness, Agilent). The temperature program of the oven started at 65 °C (held for 1 min), ramped at 20 °C min^{-1} to 180 °C (held for 10 min) and ramped again at 15 °C min^{-1} to 230 °C (held for 8 min). In the combustion interface, a GC Isolink II reactor (Thermo Fisher Scientific) was installed, which was operated at a temperature of 1000 °C. After combustion of the analytes to CO_2 and subsequent reduction of any nitrogen oxides, the compounds were analyzed as CO_2 for carbon and N_2 for nitrogen isotope measurements. Three pulses of CO_2 or N_2, respectively, were introduced at the beginning and at the end of each run as monitoring gas. Beforehand, these monitoring gases were calibrated against RM8563 (CO_2) and NSVEC (N_2), which were supplied by the International Atomic Energy Agency (IAEA). The analytical uncertainty 2σ was ±0.5‰ for carbon isotope values and ±1.0‰ for nitrogen isotope values.

Isotope analysis of chlorine

For chlorine isotope analysis of atrazine, a 7890A gas chromatograph coupled to a 5975C quadrupole mass spectrometer (GC-qMS, both Agilent) was used. Sample injection (2 μL) was performed by a Pal Combi-xt autosampler (CTC analysis). For the injector and the GC oven, the same parameters as for carbon and nitrogen isotope analysis were used with the exception that a different liner type, a "FocusLiner" (SGE), was used. The ion source had a constant temperature of 230 °C and the quadrupole of 150 °C. Prior to sample analysis, the method of Ponsin et al.[20] was tested and optimized for our instrument (see details in ESI†). Chlorine isotope ratios were evaluated by monitoring the mass-to-charge ratio m/z of 202/200. Standards and samples were measured ten times each and uncertainties were reported as standard deviation. Results were only evaluated if the peak areas of samples were inside a defined linearity range (peak area of 1.2×10^8 to 3.0×10^8 for m/z 200). Inside the linearity range, the determined precision of the method is associated with a maximal deviation of ±1.1‰. For analysis, the samples were diluted with ethyl acetate to a final concentration of approx. 75 mg L^{-1} and measured with a dwell time of 100 ms. Correction of the chlorine isotope values relative to Standard Mean Ocean Chloride (SMOC) was performed by an external two-point calibration with characterized standards of atrazine (Atr #4 $\delta^{37}Cl = -0.89$‰ and Atr #11 $\delta^{37}Cl = +3.59$‰).[37] To this end, the standards were measured at the beginning, in between and at the end of each sequence.

Evaluation of stable isotope fractionation

Determination of isotope enrichment factors ε was achieved by the Rayleigh equation, which describes the gradual enrichment of the residual substrate fraction f with molecules containing heavy isotopes, as expressed by isotope values according to eqn (1).[15,38] For example, for chlorine:

$$\ln[(\delta^{37}Cl + 1)/(\delta^{37}Cl_0 + 1)] = \varepsilon_{Cl} \ln f \tag{3}$$

Here $\delta^{37}Cl_0$ refers to the chlorine isotope value at the starting point ($t = 0$) of an experiment. Regression slopes Λ of dual element isotope plots were obtained by plotting isotope ratios of two different elements against each other, e.g. carbon vs. nitrogen (see eqn (2)). The uncertainties of the calculated ε-values and Λ-values are reported as 95% confidence intervals (CI). Furthermore, (apparent) kinetic isotope values, (A)KIE$_{Cl}$, that express the ratio of reaction rates ^{35}k and ^{37}k of heavy and light isotopologues, respectively,

$$KIE_{Cl} = {}^{35}k/{}^{37}k \tag{4}$$

were calculated according to Elsner et al.[15] by converting ε_{Cl}-values into (A)KIE$_{Cl}$ and taking into account that atrazine contains only one chlorine atom ($n = 1$):

$$(A)KIE_{Cl} = 1/(n \times \varepsilon_{Cl} + 1) \tag{5}$$

Prediction of chlorine kinetic isotope effects during oxidative dealkylation and hydrolysis of atrazine

In the computational part of the study, we considered hydrogen atom transfer and hydride transfer taking place at the α-position of the ethyl side chain of the atrazine molecule in the oxidative dealkylation reaction promoted by permanganate and the hydronium ion, respectively. Furthermore, we considered hydrolysis under acidic/enzymatic, neutral and alkaline conditions. All molecular structures and analytical vibrational frequencies for involved reactant complexes and transition states were taken from a previous study.[16] Chlorine kinetic isotope effects on dealkylation were calculated using the complete Bigeleisen equation[39] implemented in the ISOEFF program[40] at 300 K. Additional isotope effects predictions for hydrolysis under acidic as well as neutral conditions were performed following the previous computational protocol.[36] The tunneling contributions to the overall kinetic isotope effect were omitted.

Results & discussion

Observation of normal chlorine isotope effects in biotic hydrolysis and oxidative dealkylation

Atrazine degradation by A. aurescens TC1 resulted in the metabolite 2-hydroxyatrazine, whereas the metabolites DEA and DIA were observed for Rhodococcus sp. NI86/21 (see Fig. S4 and S5 in the ESI†). Detection of these expected degradation products (Fig. 1) demonstrates that hydrolysis and oxidative dealkylation were the underlying biochemical reactions during atrazine degradation, respectively. In both biodegradation experiments – biotic hydrolysis with A. aurescens TC1 and oxidative dealkylation with Rhodococcus sp. NI86/21 – normal chlorine isotope fractionation was observed (see Fig. 2A). In the three replicates of hydrolytic degradation by A. aurescens TC1

90%, 90% and 60% transformation of atrazine was reached after approx. 26 h, respectively (see ESI, Fig. S4†). Evaluation of δ^{37}Cl values during biotic hydrolysis according to eqn (3) resulted in a small normal isotope effect of $\varepsilon_{Cl} = -1.4 \pm 0.6\%$. In oxidative dealkylation with *Rhodococcus* sp. NI86/21 approx. 90% degradation was reached after approx. 186 h in all three replicates (see ESI, Fig. S5†). Evaluation of changes in chlorine

isotope ratios resulted in a surprisingly large normal isotope effect of $\varepsilon_{Cl} = -4.3 \pm 1.8\%$ considering that the C–Cl bond is not broken during the reaction (see Fig. 1). In a next step, carbon and nitrogen isotope effects were therefore analyzed to confirm whether the same reactions mechanisms are at work as observed in previous studies.[9,16]

Observed carbon and nitrogen isotope fractionation is consistent with previous studies

Carbon and nitrogen isotope fractionation for atrazine degradation by *A. aurescens* TC1 and *Rhodococcus* sp. NI86/21 was consistent with previous studies: both experiments showed significant changes in isotope ratios (see Fig. 2B and C). For hydrolysis with *A. aurescens* TC1, an inverse nitrogen isotope effect ($\varepsilon_N = 2.3 \pm 0.3\%$) and a normal carbon isotope effect ($\varepsilon_C = -3.7 \pm 0.4\%$) were observed, which were slightly smaller compared to the results of a former publication of Meyer *et al.* ($\varepsilon_N = 3.3 \pm 0.4\%$, $\varepsilon_C = -5.4 \pm 0.6\%$),[9] but gave the same dual element isotope plot ($\Lambda_{C/N}^{Arthro} = -0.6 \pm 0.1$) confirming that the same mechanism was at work (see Fig. 3A).

Oxidative dealkylation of atrazine with *Rhodococcus* sp. NI86/21 resulted in a normal nitrogen isotope effect of $\varepsilon_N = -2.0 \pm 0.3\%$ and a normal carbon isotope effect of $\varepsilon_C = -2.9 \pm 0.7\%$. These ε-values are similar to those published by Meyer & Elsner[10] ($\varepsilon_N = -1.5 \pm 0.3\%$, $\varepsilon_C = -4.0 \pm 0.2\%$) and Meyer *et al.*[16] ($\varepsilon_N = -1.4 \pm 0.3\%$, $\varepsilon_C = -3.8 \pm 0.2\%$). The slightly more pronounced nitrogen isotope fractionation in this study can probably be attributed to the fact that oxidation was primarily observed at the C–H bond adjacent to the nitrogen atom (α-position of the ethyl or isopropyl group, see closed mass balance in Fig. S5 in the ESI†).[16] In the study of Meyer *et al.*[16] 48% of the oxidation was observed at the β-position of the ethyl or isopropyl group resulting in a smaller nitrogen isotope fractionation effect. The obtained regression slope of $\Lambda_{C/N}^{Rhodo} = 0.7 \pm 0.1$ in this study is slightly larger than the previously reported regression slopes ($\Lambda_{C/N}^{Rhodo} = 0.4 \pm 0.1$)[10,16] which may again be explained by the small difference in average nitrogen isotope effects. Also here, however, the similar dual element isotope trend confirms that in this study atrazine was transformed by the same mechanism as in Meyer *et al.*[16] leading to the observed oxidative dealkylation products by *Rhodococcus* sp. NI86/21.

Multi-element isotope approach

Results of chlorine isotope analysis were combined with data for carbon and nitrogen isotope measurements in dual element isotope plots (see Fig. 3B and C). For hydrolysis with *A. aurescens* TC1 regression slopes of $\Lambda_{Cl/C}^{Arthro} = 1.7 \pm 0.9$ and $\Lambda_{Cl/N}^{Arthro} = -1.2 \pm 0.7$ were obtained. Oxidative dealkylation by *Rhodococcus* sp. NI86/21 resulted in regression slopes of $\Lambda_{Cl/C}^{Rhodo} = 0.6 \pm 0.1$ and $\Lambda_{Cl/N}^{Rhodo} = 0.4 \pm 0.2$. Since the dual element isotope plots of chlorine and carbon and of chlorine and nitrogen provide significantly different regression slopes for the respective elements, they can provide an additional line of evidence to differentiate the two degradation mechanisms of atrazine from each other.
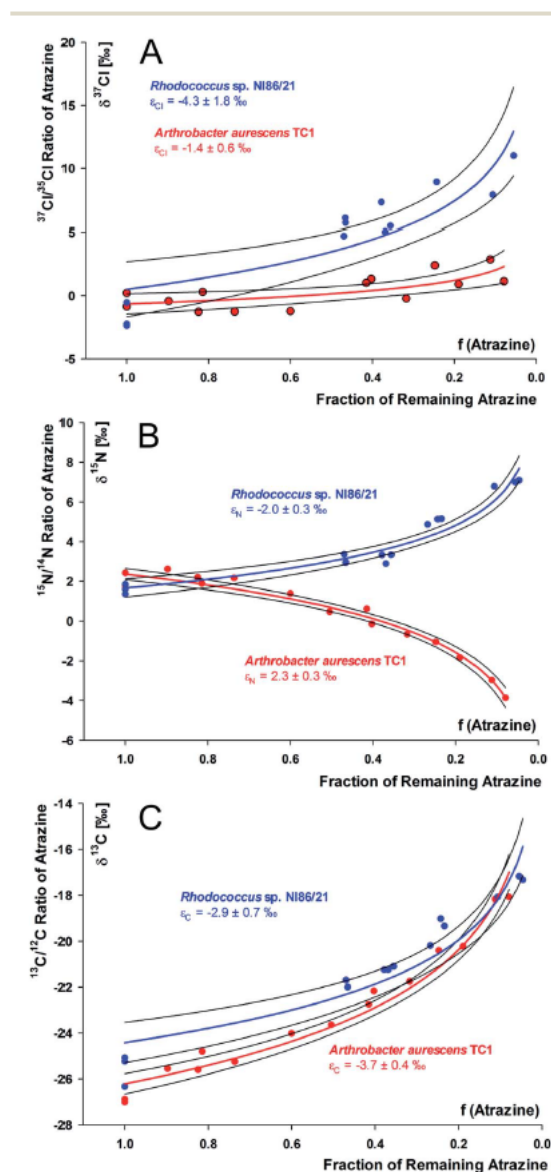

Fig. 2 Isotope fractionation of (A) chlorine, (B) nitrogen and (C) carbon during microbial degradation of atrazine by *A. aurescens* TC1 (red) and *Rhodococcus* sp. NI86/21 (blue) and corresponding enrichment factors ε evaluated according to eqn (3) (the 95% confidence intervals are given as values and as black lines).

796 | *Environ. Sci.: Processes Impacts*, 2020, **22**, 792–801
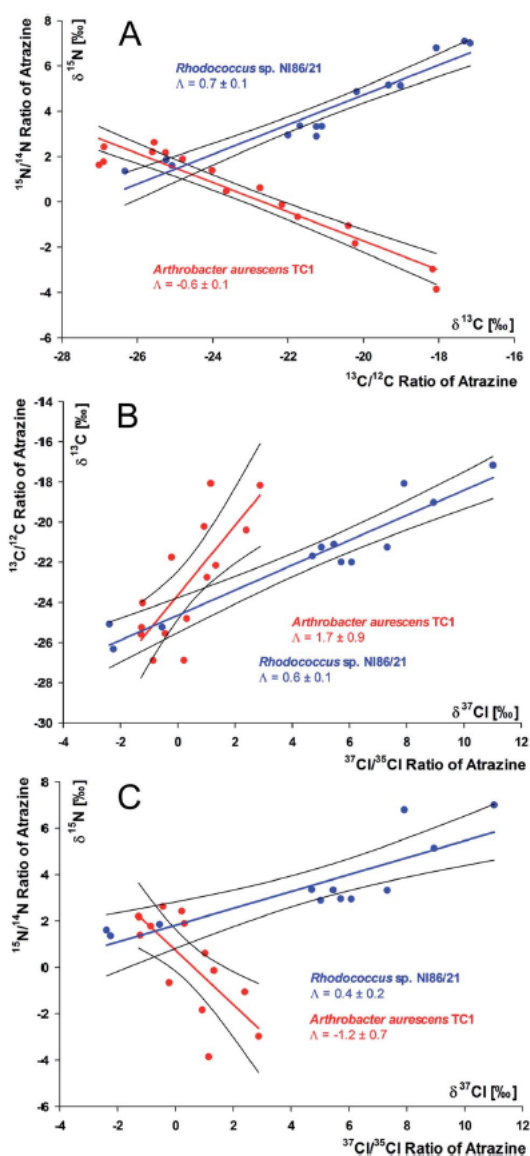
This journal is © The Royal Society of Chemistry 2020

Fig. 3 Isotope effects in microbial degradation of atrazine by *A. aurescens* TC1 (red) and *Rhodococcus* sp. NI86/21 (blue) resulting in dual element isotope plots (the 95% confidence intervals are given as values and as black lines next to the regression slopes). (A) Regression slopes of nitrogen and carbon isotope values ($\Lambda_{C/N}$). (B) Regression slopes of chlorine and carbon isotope values ($\Lambda_{Cl/C}$). (C) Regression slopes of chlorine and nitrogen isotope values ($\Lambda_{Cl/N}$).

Surprising mechanistic evidence from chlorine isotope effects

For degradation with *A. aurescens* TC1, rather small chlorine isotope fractionation was observed ($\varepsilon_{Cl} = -1.4 \pm 0.6\%_{00}$) despite the fact that the chlorine is cleaved off during hydrolysis (see Fig. 1). For oxidative dealkylation with *Rhodococcus* sp. NI86/21,

the chlorine is not cleaved off (see Fig. 1), therefore, no or just a small chlorine isotope effect was expected. However, here more pronounced chlorine isotope fractionation was observed ($\varepsilon_{Cl} = -4.3 \pm 1.8\%_{00}$).

The corresponding apparent kinetic isotope effects (AKIE$_{Cl}$, see Table 1) were compared to the AKIE$_{Cl}$ values of other studies focusing on the same degradation mechanisms. In addition, the AKIE$_{Cl}$ values were compared to the theoretical maximum Streitwieser limit associated with the cleavage of a C–Cl bond (KIE$_{Cl} = 1.02$)[41–43] and to the predictions of computational calculations (Table 2).

For microbial hydrolysis of atrazine an experimental AKIE$_{Cl}^{Arthro}$ value of 1.0014 ± 0.0006 was calculated (see Table 1). Dybala-Defratyka *et al.*[35] reported a more pronounced AKIE$_{Cl}^{alk.hydrol.}$ value of 1.0069 ± 0.0005 (see Table 1). However, that study[35] was conducted in an abiotic alkaline solution at 21 °C so that another hydrolysis pathway was involved. Newer data reported a much smaller value of AKIE$_{Cl}^{alk.hydrol.} = 1.0009 \pm 0.0006$[36] for the same alkaline hydrolysis at 50 °C. Later on it was confirmed that abiotic alkaline hydrolysis performed earlier at 21 °C resembles rather neutral than alkaline conditions.[36] Table 2 illustrates the different computed mechanisms that lie at the heart of the computational predictions. It shows the different mechanistic routes between the alkaline (substitution of Cl without protonation of the atrazine ring) and the acidic/enzymatic pathway characterized in Meyer *et al.*[9] (substitution of Cl with protonation of the atrazine ring) including different possible transition states. Chlorine KIEs are, among other factors,[45] determined by the percent extension of the C–Cl bond in the transition state. As this is directly related to the structure of the transition state, it can be linked to the C–Cl bond orders (Table 2), which decrease in the studied hydrolysis reactions when the C–Cl bond is more ruptured as compared to its length in the reactants, resulting in increased chlorine KIEs. Previously performed computations[36] and computations of this study mimicking alkaline, acidic, and neutral conditions indicated that the largest AKIE$_{Cl}$ should be expected under neutral conditions (except for transition state 2 of acidic/enzymatic hydrolysis). Under neutral conditions the C–Cl bond is elongated leading to a transition state geometry which differs substantially from hydrolysis reactions promoted either by alkaline or acidic conditions (see Table 2). However, hydrolysis at neutral pH is too slow to be of relevance. Computational calculations taking into account the transition state structures at a molecular level predicted AKIE$_{Cl}$ values ranging from 0.9996 to 1.0014 for alkaline, acidic and enzymatic hydrolysis (see Tables 1 and 2).[36,44] Hence, on the mechanistic level, the computational studies predict that the formation of a Meisenheimer complex rather than the subsequent C–Cl bond cleavage is the rate-determining step during the nucleophilic aromatic substitution reaction catalyzed by TrzN.[36,44] In both abiotic pathways the C–Cl bond at the transition state of the rate-determining step is almost intact giving rise to very small AKIE$_{Cl}$ (the computed bond orders for both alkaline and acidic hydrolysis are the same and equal to 1.03, see also Table 2). In this study, we therefore observed a similarly small AKIE$_{Cl}^{Arthro}$ value for enzymatic hydrolysis in *A. aurescens* TC1

This journal is © The Royal Society of Chemistry 2020
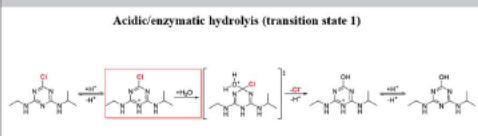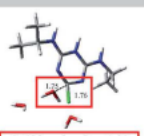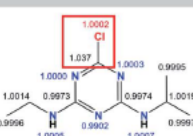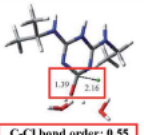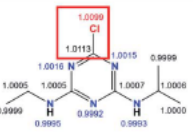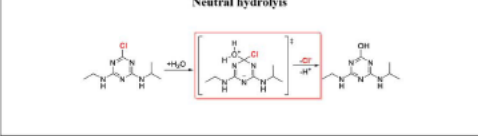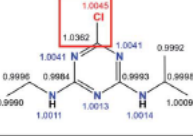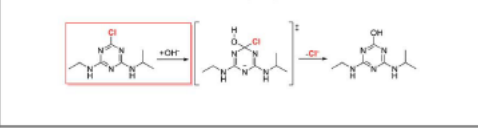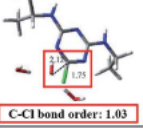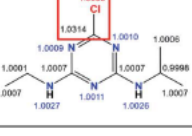
Environ. Sci.: Processes Impacts, 2020, **22**, 792–801 | **797**
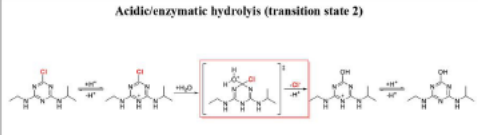
Table 1 AKIE$_{Cl}$ values associated with atrazine degradation

Mechanism	AKIE$_{Cl}$	Study
Experimental data		
Abiotic alkaline hydrolysis (21 °C)	1.0069 ± 0.0005	Dybala-Defratyka et al.[35]
Abiotic alkaline hydrolysis (50 °C),	1.0009 ± 0.0006	Grzybkowska et al.[36]
Microbial hydrolysis (A. aurescens TC1)	1.0014 ± 0.0006^{a}	This study
Microbial dealkylation (Rhodococcus sp. NI86/21)	1.0043 ± 0.0018^{a}	This study
Computational data		
Abiotic acidic/enzymatic hydrolysis (transition state 1)	Range of 1.0002 to 1.0011	Grzybkowska et al.[36]
Abiotic acidic/enzymatic hydrolysis (transition state 2)	1.0099	This study
Abiotic neutral hydrolysis	1.0045	This study
Abiotic alkaline hydrolysis	Range of 1.0003 to 1.0014	Grzybkowska et al.[36]
Enzymatic hydrolysis	Range of 0.9996 to 1.0003	Szatkowski et al.[44]
Abiotic dealkylation (hydrogen atom transfer by MnO_4^{-})	0.9999	This study
Abiotic dealkylation (hydride transfer by H_3O^{+})	0.9997	This study

^{a} Calculated according to eqn (5).

which resembles acid-catalyzed hydrolysis rather than alkaline hydrolysis.[9] Hence, the picture emerges that different hydrolytic pathways give rise to experimental AKIE$_{Cl}$ values much lower than the Streitwieser limit of 1.02 [41–43] indicating that the chlorine isotope effect is masked in all cases and that the C–Cl bond cleavage is not the rate-determining step. Interestingly, this is in contrast to ametryn hydrolysis where strong sulphur isotope effects were observed in enzymatic hydrolysis by TrzN.[17] Further experimental work, including degradation experiments with other strains, hydrolysis and crude enzyme experiments, will be required to further substantiate the picture on chlorine isotope effects observed in this study. For the moment, since

Table 2 Mechanisms and transition states of acidic/enzymatic, neutral and alkaline hydrolysis and corresponding calculated and measured isotope effects

^{a} Taken from Grzybkowska et al.[36] ^{b} Calculated according to eqn (5) with $n = 5$ for N and $n = 8$ for C. ^{c} Taken from Meyer et al.[9]

798 | Environ. Sci: Processes Impacts, 2020, **22**, 792–801

This journal is © The Royal Society of Chemistry 2020

120

chlorine isotope effects were found to be masked, we must conclude, however, that information from chlorine isotope analysis alone would not be enough to differentiate the different reaction mechanisms. This illustrates the importance of analyzing more than one element for mechanistic differentiation.

For oxidative dealkylation, so far, no chlorine isotope effects were reported. Regarding the reaction mechanism, Meyer et al.[16] concluded that oxidative dealkylation of atrazine with Rhodococcus sp. NI86/21 is initiated by hydrogen atom transfer based on the observed product distribution and the carbon and nitrogen isotope effects. Hydrogen atom transfer leads directly to a homolytic cleavage of the C–H bond adjacent to the nitrogen atom (α-position of the ethyl or isopropyl group) producing a relative unstable 1,1-aminoalcohol which is then further transformed to DEA or DIA.[16] In parallel, two additional products could be detected which were formed by oxidation of the C–H bond in the β-position of the ethyl or isopropyl group. For this mechanistic pathway, chlorine isotope effects would be expected to be rather small since the chlorine is not involved in the reaction steps. The closed mass balance of the concentration analysis (see Fig. S5 in the ESI†) of this study and the results of product distribution of Meyer et al.[16] also indicate that there is no C–Cl bond cleavage taking place since corresponding hydrolysis products were not detected. Furthermore, our computations for hydrogen atom transfer at a catalytic center mimicking cytochrome P450 predicted no chlorine isotope effect ($\mathrm{AKIE}_{Cl}^{\mathrm{hydro.atom\ trans.}} = 0.9999$, see Table 1). Hydride transfer promoted by the hydronium ion also resulted in no chlorine isotope effect ($\mathrm{AKIE}_{Cl}^{\mathrm{hydride\ trans.}} = 0.9997$, see Table 1). At previously located transition state structures for these two reactions[16] the carbon–chlorine bond remains intact and no stretching of this bond is involved in the reaction coordinate (hydrogen transfer) mode. The observed more pronounced $\mathrm{AKIE}_{Cl}^{\mathrm{Rhodo}}$ value of 1.0043 ± 0.0018 in this study (see Table 1) could, therefore, be indicative of isotope effects caused by enzymatic interactions. Meyer et al.[16] proposed that for oxidative dealkylation no selectivity itself is observed, however, the preferred oxidation of the α-position over the β-position could be explained by steric factors of the catalyzing enzyme which could have an influence on the transformation pathway. Thus, the sensitive chlorine isotope effect, which is observed even though the C–Cl bond is not cleaved during degradation, can be interpreted as an indicator that non-covalent interactions between the cytochrome P450 complex and the chlorine cause significant chlorine isotope fractionation.[46]

Conclusion

Since atrazine is frequently detected in groundwater systems, major efforts should be put into understanding its environmental fate. We provide an approach to 3D-isotope (C, N, Cl) analysis of atrazine and explored isotope fractionation in different transformation pathways. Together, this provides the basis to more confidently assess sources and degradation of atrazine in the environment. Specifically, we demonstrated that pronounced changes in chlorine isotope values are not an indicator of microbial hydrolysis (as one might have expected without knowledge of our experimental data), but – surprisingly – rather of oxidative dealkylation. Therefore, although trends are different than expected, they can nonetheless be used for a more confident identification of different sources and transformation pathways in field samples. Regarding the sensitivity of chlorine isotope effects, our study demonstrates the importance of performing controlled laboratory experiments before applying the approach in the field. Specifically, in other cases chlorine isotope fractionation can be much more pronounced than observed for atrazine in this study. Large chlorine isotope effects were observed in proof-of-principle experiments by Ponsin et al.[20] studying hydrolytic dechlorination of S-metolachlor, an herbicide containing also only one chlorine atom. Here preliminary data suggest a large chlorine isotope effect of $\varepsilon_{Cl} = -9.7 \pm 2.9\%$ for abiotic alkaline hydrolysis. Therefore, in the case of other substances, chlorine isotope effects can be even more sensitive indicators of degradation provided that the C–Cl bond cleavage occurs in the rate-determining step of a reaction. Further, gaining deeper insights into these chemical processes is the basis for understanding the biotic catalysis of organic micropollutant degradation. This, in turn, is essential for identifying and developing optimized strategies for micropollutant removal in order to make successful bioremediation possible.

Conflicts of interest

There are no conflicts to declare.

Acknowledgements

References

1 H. Gysin and E. Knusli, Chemistry and herbicidal properties of triazine derivatives, Adv. Pest Control Res., 1960, 3, 289–353.
2 EPA, Pesticides Industry Sales and Usage, 2008–2012 Market Estimates, US Environmental Protection Agency, Washington (DC), 2017.
3 European Commission, Commission Decision of 10 March 2004 Concerning the Non-Inclusion of Atrazine in Annex I to Council Directive 91/414/EEC and the Withdrawal of Authorisations for Plant Protection Products Containing this Active Substance, Official Journal of the European Union, 2004, 78, 53–55.

4 R. Loos, G. Locoro, S. Comero, S. Contini, D. Schwesig, F. Werres, P. Balsaa, O. Gans, S. Weiss, L. Blaha, M. Bolchi and B. M. Gawlik, Pan-European survey on the occurrence of selected polar organic persistent pollutants in ground water, *Water Res.*, 2010, 44, 4115–4126.

5 D. Vonberg, J. Vanderborght, N. Cremer, T. Pütz, M. Herbst and H. Vereecken, 20 years of long-term atrazine monitoring in a shallow aquifer in western Germany, *Water Res.*, 2014, 50, 294–306.

6 S. Singh, V. Kumar, A. Chauhan, S. Datta, A. B. Wani, N. Singh and J. Singh, Toxicity, degradation and analysis of the herbicide atrazine, *Environ. Chem. Lett.*, 2018, 16, 211–237.

7 S. Kern, H. P. Singer, J. Hollender, R. P. Schwarzenbach and K. Fenner, Assessing exposure to transformation products of soil-applied organic contaminants in surface water: comparison of model predictions and field data, *Environ. Sci. Technol.*, 2011, 45, 2833–2841.

8 C. Moreau-Kervevan and C. Mouvet, Adsorption and desorption of atrazine, deethylatrazine, and hydroxyatrazine by soil components, *J. Environ. Qual.*, 1998, 27, 46–53.

9 A. H. Meyer, H. Penning and M. Elsner, C and N isotope fractionation suggests similar mechanisms of microbial atrazine transformation despite involvement of different enzymes (AtzA and TrzN), *Environ. Sci. Technol.*, 2009, 43, 8079–8085.

10 A. H. Meyer and M. Elsner, $^{13}C/^{12}C$ and $^{15}N/^{14}N$ Isotope Analysis To Characterize Degradation of Atrazine: Evidence from Parent and Daughter Compound Values, *Environ. Sci. Technol.*, 2013, 47, 6884–6891.

11 A. H. Meyer, H. Penning, H. Lowag and M. Elsner, Precise and accurate compound specific carbon and nitrogen isotope analysis of atrazine: critical role of combustion oven conditions, *Environ. Sci. Technol.*, 2008, 42, 7757–7763.

12 S. Reinnicke, D. Juchelka, S. Steinbeiss, A. H. Meyer, A. Hilkert and M. Elsner, Gas chromatography-isotope ratio mass spectrometry (GC-IRMS) of recalcitrant target compounds: performance of different combustion reactors and strategies for standardization, *Rapid Commun. Mass Spectrom.*, 2012, 26, 1053–1060.

13 K. Schreglmann, M. Hoeche, S. Steinbeiss, S. Reinnicke and M. Elsner, Carbon and nitrogen isotope analysis of atrazine and desethylatrazine at sub-microgram per liter concentrations in groundwater, *Anal. Bioanal. Chem.*, 2013, 405, 2857–2867.

14 T. C. Schmidt, L. Zwank, M. Elsner, M. Berg, R. U. Meckenstock and S. B. Haderlein, Compound-specific stable isotope analysis of organic contaminants in natural environments: a critical review of the state of the art, prospects, and future challenges, *Anal. Bioanal. Chem.*, 2004, 378, 283–300.

15 M. Elsner, Stable isotope fractionation to investigate natural transformation mechanisms of organic contaminants: principles, prospects and limitations, *J. Environ. Monit.*, 2010, 12, 2005–2031.

16 A. H. Meyer, A. Dybala-Defratyka, P. J. Alaimo, I. Geronimo, A. D. Sanchez, C. J. Cramer and M. Elsner, Cytochrome P450-catalyzed dealkylation of atrazine by *Rhodococcus* sp. strain NI86/21 involves hydrogen atom transfer rather than single electron transfer, *Dalton Trans.*, 2014, 43, 12111–12432.

17 H. K. V. Schürner, J. L. Seffernick, A. Grzybkowska, A. Dybala-Defratyka, L. P. Wackett and M. Elsner, Characteristic Isotope Fractionation Patterns in s-Triazine Degradation Have Their Origin in Multiple Protonation Options in the s-Triazine Hydrolase TrzN, *Environ. Sci. Technol.*, 2015, 49, 3490–3498.

18 T. B. Hofstetter and M. Berg, Assessing transformation processes of organic contaminants by compound-specific stable isotope analysis, *TrAC, Trends Anal. Chem.*, 2011, 30, 618–627.

19 J. Renpenning, A. Horst, M. Schmidt and M. Gehre, Online isotope analysis of $^{37}Cl/^{35}Cl$ universally applied for semi-volatile organic compounds using GC-MC-ICPMS, *J. Anal. At. Spectrom.*, 2018, 33, 314–321.

20 V. Ponsin, C. Torrentó, C. Lihl, M. Elsner and D. Hunkeler, Compound-specific chlorine isotope analysis of the herbicides atrazine, acetochlor and metolachlor, *Anal. Chem.*, 2019, 91, 14290–14298.

21 C. Lihl, L. M. Douglas, S. Franke, A. Pérez-de-Mora, A. H. Meyer, M. Daubmeier, E. A. Edwards, I. Nijenhuis, B. Sherwood Lollar and M. Elsner, Mechanistic Dichotomy in Bacterial Trichloroethene Dechlorination Revealed by Carbon and Chlorine Isotope Effects, *Environ. Sci. Technol.*, 2019, 53, 4245–4254.

22 L. E. Erickson, Degradation of atrazine and related s-triazines, *Crit. Rev. Environ. Control*, 1989, 19, 1–14.

23 H. M. LeBaron, J. E. McFarland and O. C. Burnside, *The triazine herbicides*, Elsevier, Oxford, 1st edn, 2008.

24 L. C. Strong, C. Rosendahl, G. Johnson, M. J. Sadowsky and L. P. Wackett, *Arthrobacter aurescens* TC1 metabolizes diverse s-triazine ring compounds, *Appl. Environ. Microbiol.*, 2002, 68, 5973–5980.

25 K. Sajjaphan, N. Shapir, L. P. Wackett, M. Palmer, B. Blackmon, J. Tomkins and M. J. Sadowsky, *Arthrobacter aurescens* TC1 Atrazine Catabolism Genes *trzN, atzB*, and *atzC* Are Linked on a 160-Kilobase Region and Are Functional in *Escherichia coli, Appl. Environ. Microbiol.*, 2004, 70, 4402–4407.

26 I. Nagy, F. Compernolle, K. Ghys, J. Vanderleyden and R. De Mot, A single cytochrome P-450 system is involved in degradation of the herbicides EPTC (S-ethyldipropylthiocarbamate) and atrazine by Rhodococcus sp. strain NI86/21, *Appl. Environ. Microbiol.*, 1995, 61, 2056–2060.

27 M. Elsner, L. Zwank, D. Hunkeler and R. P. Schwarzenbach, A new concept linking observable stable isotope fractionation to transformation pathways of organic pollutants, *Environ. Sci. Technol.*, 2005, 39, 6896–6916.

28 L. Zwank, M. Berg, M. Elsner, T. C. Schmidt, R. P. Schwarzenbach and S. B. Haderlein, New evaluation scheme for two-dimensional isotope analysis to decipher biodegradation processes: application to groundwater

800 | *Environ. Sci.: Processes Impacts*, 2020, **22**, 792–801

This journal is © The Royal Society of Chemistry 2020

contamination by MTBE, *Environ. Sci. Technol.*, 2005, 39, 1018–1029.

29 S. Reinnicke, A. Simonsen, S. R. Sørensen, J. Aamand and M. Elsner, C and N Isotope Fractionation during Biodegradation of the Pesticide Metabolite 2,6-Dichlorobenzamide (BAM): Potential for Environmental Assessments, *Environ. Sci. Technol.*, 2012, 46, 1447–1454.

30 T. Gilevska, M. Gehre and H. H. Richnow, Multidimensional isotope analysis of carbon, hydrogen and oxygen as tool for identification of the origin of ibuprofen, *J. Pharm. Biomed. Anal.*, 2015, 115, 410–417.

31 J. Palau, O. Shouakar-Stash, S. Hatijah Mortan, R. Yu, M. Rosell, E. Marco-Urrea, D. L. Freedman, R. Aravena, A. Soler and D. Hunkeler, Hydrogen Isotope Fractionation during the Biodegradation of 1,2-Dichloroethane: Potential for Pathway Identification Using a Multi-element (C, Cl, and H) Isotope Approach, *Environ. Sci. Technol.*, 2017, 51, 10526–10535.

32 S. Franke, C. Lihl, J. Renpenning, M. Elsner and I. Nijenhuis, Triple-element compound-specific stable isotope analysis of 1,2-dichloroethane for characterization of the underlying dehalogenation reaction in two dehalococcoides mccartyi strains, *FEMS Microbiol. Ecol.*, 2017, 93, fix137.

33 T. Kuder, B. M. van Breukelen, M. Vanderford and P. Philp, 3D-CSIA: Carbon, Chlorine, and Hydrogen Isotope Fractionation in Transformation of TCE to Ethene by a Dehalococcoides Culture, *Environ. Sci. Technol.*, 2013, 47, 9668–9677.

34 B. Heckel, K. McNeill and M. Elsner, Chlorinated Ethene Reactivity with Vitamin B12 is Governed by Cobalamin Chloroethylcarbanions as Crossroads of Competing Pathways, *ACS Catal.*, 2018, 8, 3054–3066.

35 A. Dybala-Defratyka, L. Szatkowski, R. Kaminski, M. Wujec, A. Siwek and P. Paneth, Kinetic isotope effects on dehalogenations at an aromatic carbon, *Environ. Sci. Technol.*, 2008, 42, 7744–7750.

36 A. Grzybkowska, R. Kaminski and A. Dybala-Defratyka, Theoretical predictions of isotope effects *versus* their experimental values for an example of uncatalyzed hydrolysis of atrazine, *Phys. Chem. Chem. Phys.*, 2014, 16, 15164–15172.

37 C. Lihl, J. Renpenning, S. Kümmel, F. Gelman, H. K. V. Schürner, M. Daubmeier, B. Heckel, A. Melsbach, A. Bernstein, O. Shouakar-Stash, M. Gehre and M. Elsner, Toward Improved Accuracy in Chlorine Isotope Analysis: Synthesis Routes for In-House Standards and Characterization *via* Complementary Mass Spectrometry Methods, *Anal. Chem.*, 2019, 91, 12290–12297.

38 D. Hunkeler, R. U. Meckenstock, B. Sherwood Lollar, T. Schmidt, J. Wilson, T. Schmidt and J. Wilson, *A Guide for Assessing Biodegradation and Source Identification of Organic Ground Water Contaminants using Compound Specific Isotope Analysis (CSIA), O. o. R. a. Development Report PA 600/R-08/148/December 2008*, US EPA, Oklahoma, USA, 2008, http://www.epa.gov/ada.

39 J. Bigeleisen, The relative reaction velocities of isotopic molecules, *J. Chem. Phys.*, 1949, 17, 675–679.

40 V. Anisimov and P. Paneth, ISOEFF98. A program for studies of isotope effects using Hessian modifications, *J. Math. Chem.*, 1999, 26, 75–86.

41 A. Streitwieser Jr, R. Jagow, R. Fahey and S. Suzuki, Kinetic isotope effects in the acetolyses of deuterated cyclopentyl tosylates1, 2, *J. Am. Chem. Soc.*, 1958, 80, 2326–2332.

42 K. Świderek and P. Paneth, Extending limits of chlorine kinetic isotope effects, *J. Org. Chem.*, 2012, 77, 5120–5124.

43 L. Szatkowski and A. Dybala-Defratyka, A computational study on enzymatically driven oxidative coupling of chlorophenols: an indirect dehalogenation reaction, *Chemosphere*, 2013, 91, 258–264.

44 L. Szatkowski, R. N. Manna, A. Grzybkowska, R. Kamiński, A. Dybala-Defratyka and P. Paneth, in *Methods in enzymology*, Elsevier, 2017, vol. 596, pp. 179–215.

45 A. Dybala-Defratyka, M. Rostkowski, O. Matsson, K. C. Westaway and P. Paneth, A New Interpretation of Chlorine Leaving Group Kinetic Isotope Effects; A Theoretical Approach, *J. Org. Chem.*, 2004, 69, 4900–4905.

46 A. Siwek, R. Omi, K. Hirotsu, K. Jitsumori, N. Esaki, T. Kurihara and P. Paneth, Binding modes of DL-2-haloacid dehalogenase revealed by crystallography, modeling and isotope effects studies, *Arch. Biochem. Biophys.*, 2013, 540, 26–32.

123

Abbreviations

%	per centum (Latin) – percent; parts per hundred
‰	pro mille (Latin) – per mille; parts per thousand
°C	degree Celsius, 0 °C = 273.15 K
µg	microgram; $1 µg = 1 \times 10^{-6}$ g
µL	micoliter; $1\ µL = 1 \times 10^{-6}$ L
µm	micrometer, $1\ mm = 1 \times 10^{-6}$ m
µmol	micromole; $1\ µmol = 1 \times 10^{-6}$ mol
Aceto1	chlorine in-house standard, acetochlor, $\delta^{37}Cl_{Aceto1} = 0.29 \pm 0.29$ ‰
Aceto2	chlorine in-house standard, acetochlor, $\delta^{37}Cl_{Aceto2} = 18.54 \pm 0.20$ ‰
AKIE	Apparent Kinetic Isotope Effect
approx.	approximately
Atr #4	chlorine in-house standard, atrazine, $\delta^{37}Cl_{Atr\ \#4} = -0.89 \pm 0.24$ ‰
Atr #11	chlorine in-house standard, atrazine, $\delta^{37}Cl_{Atr\ \#11} = 3.59 \pm 0.37$ ‰
CI	confidence interval
cis-DCE	*cis*-1,2- dichloroethene
cisF	chlorine in-house standard, *cis*-DCE, $\delta^{37}Cl = -1.52$ ‰
cm	centimeter; 1×10^{-2} m
CSIA	Compound-specific Stable Isotope Analysis
CT16	chlorine in-house standard, AgCl, $\delta^{37}Cl_{CT16} = -26.82 \pm 0.18$ ‰
DEA	desethylatrazine
DIA	desisopropylatrazine
DI	Dual Inlet
Dr. rer. nat.	doctor rerum naturalium (Latin) – Doctor of Natural Science
Dr.	Doktor (German) – Doctor, equivalent to PhD
e.g.	exempli gratia (Latin) – for example

Eil-1	chlorine in-house standard, TCE, $\delta^{37}Cl$ = -2.7 ‰
Eil-2	chlorine in-house standard, TCE, $\delta^{37}Cl$ = +3.05 ‰
et al.	et alii (Latin) – and others
FID	Flame Ionization Detection
g	gram; 1 g = 1 × 10^{-3} kg
GC	Gas Chromatography
h	hour; 1 h = 60 min
HAT	2-hydroxyatrazine
HPLC	High Performance Liquid Chromatography
IAEA	International Atomic Energy Agency
i.e	*id est* (Latin) – that is; in other words
IRMS	Isotope Ratio Mass Spectrometry
IS63	chlorine in-house standard, *cis*-DCE, $\delta^{37}Cl$ = +0.07 ‰
ISL-354	international reference material, NaCl, $\delta^{37}Cl_{ISL-354}$ = +0.05 ± 0.03 ‰
K	Kelvin
kg	kilogram
KIE	Kinetic Isotope Effect
L	Liter
M	molar; 1 M = 1 mol·L^{-1}
MC-ICPMS	Multicollector – Inductively Coupled Plasma Mass Spectrometry
MeCl	chlorine in-house standards, methyl chloride, $\delta^{37}Cl_{MeCl}$ = 4.49 ± 0.10 ‰
Metola1	chlorine in-house standard, S-metolachlor, $\delta^{37}Cl_{Metola1}$ = −4.28 ± 0.17 ‰
Metola2	chlorine in-house standard, S-metolachlor, $\delta^{37}Cl_{Metola2}$ = 5.12 ± 0.27 ‰
mg	milligram; 1 mg = 1 × 10^{-6} kg
Milli-Q	ultrapure water
min	minute; 1 min = 60 s
mL	milliliter; 1 mL = 1 × 10^{-3} L
mm	millimeter, 1 mm = 1 × 10^{-3} m

mM	millimolar; 1 mM = 1×10^{-3} M
mmol	millimol; 1 mmol = 1×10^{-3} mol
mol	mole
ms	millisecond; 1 ms = 1×10^{-3} s
MS	Mass Spectrometry
m/z	ratio of molecular (or atomic) mass to the charge number of the ion
NIST SRM 975a	international reference material, NaCl, $\delta^{37}Cl_{NIST}$ = 0.01 ‰
nm	nanometer, 1nm = 1×10^{-9} m
nmol	nanomole, 1 nmol = 1×10^{-9} M
PCE	tetrachloroethene
pH	potential Hydrogenii (Latin) – decimal logarithm of the reciprocal of the hydrogen activity in water
ppm	parts per million; 1 ppm = 1×10^{-6}
qMS	Quadrupole Mass Spectrometry
qPCR	Quantitative Polymerase Chain Reaction
RDase	reductive dehalogenase
R_f	retardation factor
rpm	rounds per minute
rRNA	Ribosomal Ribonucleic Acid
s	second
SLAP	Standard Light Antarctic Precipitation
SMOC	Standard Mean Ocean Chloride
TCE	trichloroethene
TCE-2	chlorine in-house standard, trichloroethene $\delta^{37}Cl_{TCE-2}$ = -2.54 ± 0.13 ‰
trans-DCE	*trans*-1,2-dichloroethene
USGS37	international reference material, KClO$_4$, $\delta^{37}Cl_{USGS37}$ = 0.90 ± 0.04 ‰
USGS38	international reference material, KClO$_4$, $\delta^{37}Cl_{USGS38}$ = -87.9 ± 0.24 ‰
USGS39	international reference material, KClO$_4$, $\delta^{37}Cl_{USGS39}$ = 0.05 ‰

UV	ultra violet
VC	vinyl chloride
vs.	versus (Latin) – compared to; against
VSMOW	Vienna Standard Mean Ocean Water
v/v	volume/volume
z.B.	zum Beispiel (German) – for example

References

(1) Oki, T.; Kanae, S. Global hydrological cycles and world water resources. *Science* **2006,** *313*, (5790), 1068-1072.

(2) Schwarzenbach, R. P.; Egli, T.; Hofstetter, T. B.; von Gunten, U.; Wehrli, B. Global Water Pollution and Human Health. *Annual Review of Environment and Resources* **2010,** *35*, (1), 109-136.

(3) Bradley, P. M. Microbial degradation of chloroethenes in groundwater systems. *Hydrogeol. J.* **2000,** *8*, (1), 104-111.

(4) Hvězdová, M.; Kosubová, P.; Košíková, M.; Scherr, K. E.; Šimek, Z.; Brodský, L.; Šudoma, M.; Škulcová, L.; Sáňka, M.; Svobodová, M. Currently and recently used pesticides in Central European arable soils. *Sci. Total Environ.* **2018,** *613*, 361-370.

(5) Hug, L. A.; Maphosa, F.; Leys, D.; Löffler, F. E.; Smidt, H.; Edwards, E. A.; Adrian, L. Overview of organohalide-respiring bacteria and a proposal for a classification system for reductive dehalogenases. *Philos. Trans. R. Soc. London, Ser. B* **2013,** *368*, (1616), DOI: 10.1098/rstb.2012.0322.

(6) Gysin, H.; Knusli, E. Chemistry and herbicidal properties of triazine derivatives. *Adv. in Pest Control Res.* **1960,** *3*, 289-353.

(7) EPA. Pesticides Industry Sales and Usage: 2008–2012 Market Estimates. *US Environmental Protection Agency, Washington (DC)* **2017**.

(8) LFU. *Pflanzenschutzmittel-Metaboliten Vorkommen und Bewertung: Fachtagung des Bayerischen Landesamtes für Umwelt* 2008.

(9) European Commission. Commission decision of 10 March 2004 concerning the non-inclusion of atrazine in Annex I to Council Directive 91/414/EEC and the withdrawal of authorisations for plant protection products containing this active substance. *Official Journal of the European Union* **2004,** *78*, 53-55.

(10) Vonberg, D.; Vanderborght, J.; Cremer, N.; Pütz, T.; Herbst, M.; Vereecken, H. 20 years of long-term atrazine monitoring in a shallow aquifer in western Germany. *Water Res.* **2014,** *50*, 294-306.

(11) Singh, S.; Kumar, V.; Chauhan, A.; Datta, S.; Wani, A. B.; Singh, N.; Singh, J. Toxicity, degradation and analysis of the herbicide atrazine. *Environ. Chem. Lett.* **2018,** *16*, (1), 211-237.

(12) Schmidt, T. C.; Zwank, L.; Elsner, M.; Berg, M.; Meckenstock, R. U.; Haderlein, S. B. Compound-specific stable isotope analysis of organic contaminants in natural environments: a critical review of the state of the art, prospects, and future challenges. *Anal. Bioanal. Chem.* **2004,** *378*, (2), 283-300.

(13) Elsner, M. Stable isotope fractionation to investigate natural transformation mechanisms of organic contaminants: principles, prospects and limitations. *J. Environ. Monit.* **2010,** *12*, (11), 2005-2031.

(14) Hunkeler, D.; Chollet, N.; Pittet, X.; Aravena, R.; Cherry, J. A.; Parker, B. L. Effect of source variability and transport processes on carbon isotope ratios of TCE and PCE in two sandy aquifers. *Journal of Contaminant Hydrology* **2004,** *74*, (1-4), 265-282.

(15) Meckenstock, R. U.; Morasch, B.; Griebler, C.; Richnow, H. H. Stable isotope fractionation analysis as a tool to monitor biodegradation in contaminated acquifers. *J. Contam. Hydrol.* **2004,** *75*, (3-4), 215-255.

(16) Hofstetter, T. B.; Schwarzenbach, R. P.; Bernasconi, S. M. Assessing Transformation Processes of Organic Compounds Using Stable Isotope Fractionation. *Environ. Sci. Technol.* **2008,** *42*, (21), 7737-7743.

(17) Heckel, B.; McNeill, K.; Elsner, M. Chlorinated Ethene Reactivity with Vitamin B12 Is Governed by Cobalamin Chloroethylcarbanions as Crossroads of Competing Pathways. *ACS Catal.* **2018,** *8*, (4), 3054-3066.

(18) Hoefs, J. *Stable Isotope Geochemistry*. Springer-Verlag: Berlin, 1997.

(19) Elsner, M.; Zwank, L.; Hunkeler, D.; Schwarzenbach, R. P. A new concept linking observable stable isotope fractionation to transformation pathways of organic pollutants. *Environ. Sci. Technol.* **2005,** *39*, (18), 6896-6916.

(20) Elsner, M.; Jochmann, M. A.; Hofstetter, T. B.; Hunkeler, D.; Bernstein, A.; Schmidt, T. C.; Schimmelmann, A. Current challenges in compound-specific stable isotope analysis of environmental organic contaminants. *Anal. Bioanal. Chem.* **2012,** *403*, (9), 2471-2491.

(21) Brand, W. A. High precision isotope ratio monitoring techniques in mass spectrometry. *J. Mass Spectrom.* **1996,** *31*, (3), 225-235.

(22) Shouakar-Stash, O.; Drimmie, R. J.; Zhang, M.; Frape, S. K. Compound-specific chlorine isotope ratios of TCE, PCE and DCE isomers by direct injection using CF-IRMS. *Appl. Geochem.* **2006,** *21*, (5), 766-781.

(23) Bernstein, A.; Shouakar-Stash, O.; Ebert, K.; Laskov, C.; Hunkeler, D.; Jeannottat, S.; Sakaguchi-Soder, K.; Laaks, J.; Jochmann, M. A.; Cretnik, S.; Jager, J.; Haderlein, S. B.; Schmidt, T. C.; Aravena, R.; Elsner, M. Compound-Specific Chlorine Isotope Analysis: A Comparison of Gas Chromatography/Isotope Ratio Mass Spectrometry and Gas Chromatography/Quadrupole Mass Spectrometry Methods in an Interlaboratory Study. *Anal. Chem.* **2011,** *83*, (20), 7624-7634.

(24) Zwank, L.; Berg, M.; Elsner, M.; Schmidt, T. C.; Schwarzenbach, R. P.; Haderlein, S. B. New evaluation scheme for two-dimensional isotope analysis to decipher biodegradation processes: application to groundwater contamination by MTBE. *Environ. Sci. Technol.* **2005,** *39*, (4), 1018-1029.

(25) Northrop, D. B. On the meaning of K-m and V/K in enzyme kinetics. *J. Chem. Educ.* **1998,** *75*, (9), 1153-1157.

(26) Renpenning, J.; Rapp, I.; Nijenhuis, I. Substrate hydrophobicity and cell composition influence the extent of rate limitation and masking of isotope fractionation during microbial reductive dehalogenation of chlorinated ethenes. *Environ. Sci. Technol.* **2015,** *49*, (7), 4293-4301.

(27) Palau, J.; Shouakar-Stash, O.; Hatijah Mortan, S.; Yu, R.; Rosell, M.; Marco-Urrea, E.; Freedman, D. L.; Aravena, R.; Soler, A.; Hunkeler, D. Hydrogen Isotope Fractionation during the Biodegradation of 1,2-Dichloroethane: Potential for Pathway Identification Using a Multi-element (C, Cl, and H) Isotope Approach. *Environ. Sci. Technol.* **2017,** *51*, (18), 10526-10535.

(28) Franke, S.; Lihl, C.; Renpenning, J.; Elsner, M.; Nijenhuis, I. Triple-element compound-specific stable isotope analysis of 1,2-dichloroethane for characterization of the underlying dehalogenation reaction in two Dehalococcoides mccartyi strains. *FEMS Microbiol. Ecol.* **2017,** *93*, (12), fix137.

(29) Sakaguchi-Soder, K.; Jager, J.; Grund, H.; Matthaus, F.; Schuth, C. Monitoring and evaluation of dechlorination processes using compound-specific chlorine isotope analysis. *Rapid Commun. Mass Spectrom.* **2007,** *21*, (18), 3077-3084.

(30) Aeppli, C.; Holmstrand, H.; Andersson, P.; Gustafsson, O. Direct compound-specific stable chlorine isotope analysis of organic compounds with quadrupole GC/MS using standard isotope bracketing. *Anal. Chem.* **2010,** *82*, (1), 420-426.

(31) Horst, A.; Renpenning, J.; Richnow, H.-H.; Gehre, M. Compound Specific Stable Chlorine Isotopic Analysis of Volatile Aliphatic Compounds Using Gas Chromatography Hyphenated with

Multiple Collector Inductively Coupled Plasma Mass Spectrometry. *Anal. Chem.* **2017,** *89*, (17), 9131-9138.

(32) Renpenning, J.; Horst, A.; Schmidt, M.; Gehre, M. Online isotope analysis of 37Cl/35Cl universally applied for semi-volatile organic compounds using GC-MC-ICPMS. *J. Anal. At. Spectrom.* **2018,** *33*, (2), 314-321.

(33) Coplen, T. B.; Böhlke, J. K.; De Bievre, P.; Ding, T.; Holden, N. E.; Hopple, J. A.; Krouse, H. R.; Lamberty, A.; Peiser, H. S.; Revesz, K.; Rieder, S. E.; Rosman, K. J. R.; Roth, E.; Taylor, P. D. P.; Vocke, R. D.; Xiao, Y. K. Isotope-abundance variations of selected elements - (IUPAC Technical Report). *Pure Appl. Chem.* **2002,** *74*, (10), 1987-2017.

(34) Hut, G. Consultants' group meeting on stable isotope reference samples for geochemical and hydrological investigations. **1987**.

(35) Werner, R. A.; Brand, W. A. Referencing strategies and techniques in stable isotope ratio analysis. *Rapid Commun. Mass Spectrom.* **2001,** *15*, 501-519.

(36) Xiao, Y.; Yinming, Z.; Qingzhong, W.; Haizhen, W.; Weiguo, L.; Eastoe, C. A secondary isotopic reference material of chlorine from selected seawater. *Chem. Geol.* **2002,** *182*, (2-4), 655-661.

(37) Böhlke, J.; Mroczkowski, S. J.; Sturchio, N. C.; Heraty, L. J.; Richman, K. W.; Sullivan, D. B.; Griffith, K. N.; Gu, B.; Hatzinger, P. B. Stable isotope analyses of oxygen (18O: 17O: 16O) and chlorine (37Cl: 35Cl) in perchlorate: Reference materials, calibrations, and interferences. *Rapid Commun. Mass Spectrom.* **2017,** *31*, (1), 85-110.

(38) Elsner, M.; Imfeld, G. Compound-specific isotope analysis (CSIA) of micropollutants in the environment — current developments and future challenges. *Curr. Opin. Biotechnol.* **2016,** *41*, 60-72.

(39) Meyer, A. H.; Penning, H.; Elsner, M. C and N isotope fractionation suggests similar mechanisms of microbial atrazine transformation despite involvement of different Enzymes (AtzA and TrzN). *Environ. Sci. Technol.* **2009,** *43*, (21), 8079-8085.

(40) Meyer, A. H.; Elsner, M. 13C/12C and 15N/14N Isotope Analysis To Characterize Degradation of Atrazine: Evidence from Parent and Daughter Compound Values. *Environ. Sci. Technol.* **2013,** *47*, (13), 6884-6891.

(41) Meyer, A. H.; Dybala-Defratyka, A.; Alaimo, P. J.; Geronimo, I.; Sanchez, A. D.; Cramer, C. J.; Elsner, M. Cytochrome P450-catalyzed dealklyation of atrazine by *Rhodococcus* sp. strain NI86/21 involves hydogen atom transfer rather than single electorn transfer. *Dalton Trans.* **2014,** *43*, (32), 12111-12432.

(42) Coplen, T. B. Guidelines and recommended terms for expression of stable-isotope-ratio and gas-ratio measurement results. *Rapid Commun. Mass Spectrom.* **2011,** *25*, (17), 2538-2560.

(43) Hunkeler, D.; Meckenstock, R. U.; Sherwood Lollar, B.; Schmidt, T.; Wilson, J.; Schmidt, T.; Wilson, J. *A Guide for Assessing Biodegradation and Source Identification of Organic Ground Water Contaminants using Compound Specific Isotope Analysis (CSIA)*; PA 600/R-08/148 | December 2008 | www.epa.gov/ada; US EPA: Oklahoma, USA, 2008.

(44) Hakenbeck, S.; McManus, E.; Geisler, H.; Grupe, G.; O'Connell, T. Diet and mobility in Early Medieval Bavaria: a study of carbon and nitrogen stable isotopes. *Am. J. Phys. Anthropol.* **2010,** *143*, (2), 235-249.

(45) Rossmann, A. Determination of stable isotope ratios in food analysis. *Food Rev. Int.* **2001,** *17*, (3), 347-381.

(46) Desage, M.; Guilluy, R.; Brazier, J. L.; Chaudron, H.; Girard, J.; Cherpin, H.; Jumeau, J. Gas chromatography with mass spectrometry or isotope-ratio mass spectrometry in studying the geographical origin of heroin. *Anal. Chim. Acta* **1991,** *247*, (2), 249-254.

(47) Cawley, A. T.; Flenker, U. The application of carbon isotope ratio mass spectrometry to doping control. *J. Mass Spectrom.* **2008,** *43*, (7), 854-864.

(48) Hofstetter, T. B.; Berg, M. Assessing transformation processes of organic contaminants by compound-specific stable isotope analysis. *TrAC, Trends Anal. Chem.* **2011,** *30*, (4), 618-627.

(49) Aelion, C. M.; Hohener, P.; Hunkeler, D.; Aravena, R. *Environmental Isotopes in Bioremediation and Biodegradation*. CRC Press: 2009.

(50) Fenner, K.; Canonica, S.; Wackett, L. P.; Elsner, M. Evaluating Pesticide Degradation in the Environment: Blind Spots and Emerging Opportunities. *Science* **2013,** *341*, (6147), 752-758.

(51) Magenheim, A. J.; Spivack, A. J.; Michael, P. J.; Gieskes, J. M. Chlorine stable isotope composition of the oceanic crust: Implications for Earth's distribution of chlorine. *Earth Planet. Sci. Lett.* **1995,** *131*, (3-4), 427-432.

(52) Bonifacie, M.; Jendrzejewski, N.; Agrinier, P.; Humler, E.; Coleman, M.; Javoy, M. The chlorine isotope composition of Earth's mantle. *Science* **2008,** *319*, (5869), 1518-1520.

(53) Böhlke, J. K.; Sturchio, N. C.; Gu, B.; Horita, J.; Brown, G. M.; Jackson, W. A.; Batista, J.; Hatzinger, P. B. Perchlorate isotope forensics. *Anal. Chem.* **2005,** *77*, (23), 7838-7842.

(54) Holt, B. D.; Sturchio, N. C.; Abrajano, T. A.; Heraty, L. J. Conversion of chlorinated volatile organic compounds to carbon dioxide and methyl chloride for isotopic analysis of carbon and chlorine. *Anal. Chem.* **1997,** *69*, (14), 2727-2733.

(55) Xiao, Y.-K.; Zhang, C.-G. High precision isotopic measurement of chlorine by thermal ionization mass spectrometry of the Cs2Cl+ ion. *Int. J. Mass Spectrom. Ion Processes* **1992,** *116*, (3), 183-192.

(56) de Groot, P. A. Carbon: Organic materials. . In *Handbook of Stable Isotope Analytical Techniques, Vol. 2* de Groot, P. A., Ed. Elsevier: Amsterdam, 2009; pp 229-269.

(57) Shouakar-Stash, O.; Drimmie, R. J.; Frape, S. K. Determination of inorganic chlorine stable isotopes by continuous flow isotope ratio mass spectrometry. *Rapid Commun. Mass Spectrom.* **2005,** *19*, (2), 121-127.

(58) Cretnik, S.; Bernstein, A.; Shouakar-Stash, O.; Löffler, F.; Elsner, M. Chlorine Isotope Effects from Isotope Ratio Mass Spectrometry Suggest Intramolecular C-Cl Bond Competition in Trichloroethene (TCE) Reductive Dehalogenation. *Molecules* **2014,** *19*, (5), 6450-6473.

(59) Wiegert, C.; Mandalakis, M.; Knowles, T.; Polymenakou, P. N.; Aeppli, C.; Macháčková, J.; Holmstrand, H.; Evershed, R. P.; Pancost, R. D.; Gustafsson, Ö. Carbon and Chlorine Isotope Fractionation During Microbial Degradation of Tetra- and Trichloroethene. *Environ. Sci. Technol.* **2013,** *47*, (12), 6449-6456.

(60) Badin, A.; Buttet, G.; Maillard, J.; Holliger, C.; Hunkeler, D. Multiple Dual C–Cl Isotope Patterns Associated with Reductive Dechlorination of Tetrachloroethene. *Environ. Sci. Technol.* **2014,** *48*, (16), 9179-9186.

(61) Renpenning, J.; Keller, S.; Cretnik, S.; Shouakar-Stash, O.; Elsner, M.; Schubert, T.; Nijenhuis, I. Combined C and Cl Isotope Effects Indicate Differences between Corrinoids and Enzyme (Sulfurospirillum multivorans PceA) in Reductive Dehalogenation of Tetrachloroethene, But Not Trichloroethene. *Environ. Sci. Technol.* **2014,** *48*, (20), 11837–11845.

(62) Abe, Y.; Aravena, R.; Zopfi, J.; Shouakar-Stash, O.; Cox, E.; Roberts, J. D.; Hunkeler, D. Carbon and Chlorine Isotope Fractionation during Aerobic Oxidation and Reductive Dechlorination of Vinyl Chloride and cis-1,2-Dichloroethene. *Environ. Sci. Technol.* **2009,** *43*, (1), 101-107.

(63) Debajyoti, P.; Grzegorz, S.; István, F. Normalization of measured stable isotopic compositions to isotope reference scales – a review. *Rapid Commun. Mass Spectrom.* **2007,** *21*, (18), 3006-3014.

(64) Heckel, B.; Rodríguez-Fernández, D.; Torrentó, C.; Meyer, A.; Palau, J.; Domènech, C.; Rosell, M.; Soler, A.; Hunkeler, D.; Elsner, M. Compound-Specific Chlorine Isotope Analysis of Tetrachloromethane and Trichloromethane by Gas Chromatography-Isotope Ratio Mass Spectrometry vs Gas Chromatography-Quadrupole Mass Spectrometry: Method Development and Evaluation of Precision and Trueness. *Anal. Chem.* **2017,** *89*, (6), 3411-3420.

(65) Gröning, M. International stable isotope reference materials. In *Handbook of Stable Isotope Analytical Techniques: Volume I*, Elsevier: 2004; pp 874-906.

(66) Dearfield, K. L.; McCarroll, N. E.; Protzel, A.; Stack, H. F.; Jackson, M. A.; Waters, M. D. A survey of EPA/OPP and open literature on selected pesticide chemicals: II. Mutagenicity and carcinogenicity of selected chloroacetanilides and related compounds. *Mutat. Res., Genet. Toxicol. Environ. Mutagen.* **1999,** *443*, (1), 183-221.

(67) Somsák, L.; Czifrák, K.; Veres, E. Selective removal of 2, 2, 2-trichloroethyl-and 2, 2, 2-trichloroethoxycarbonyl protecting groups with Zn–N-methylimidazole in the presence of reducible and acid-sensitive functionalities. *Tetrahedron Lett.* **2004,** *45*, (49), 9095-9097.

(68) Weigl, M.; Wünsch, B. Synthesis of chiral non-racemic 3-(dioxopiperazin-2-yl)propionic acid derivatives. *Tetrahedron* **2002,** *58*, (6), 1173-1183.

(69) Ponsin, V.; Torrentó, C.; Lihl, C.; Elsner, M.; Hunkeler, D. Compound-specific chlorine isotope analysis of the herbicides atrazine, acetochlor and metolachlor. *Anal. Chem.* **2019,** *91*, (22), 14290-14298.

(70) Taş, N.; Eekert, V.; Miriam, H.; De Vos, W. M.; Smidt, H. The little bacteria that can – diversity, genomics and ecophysiology of 'Dehalococcoides' spp. in contaminated environments. *Microb. Biotechnol.* **2010,** *3*, (4), 389-402.

(71) Smidt, H.; de Vos, W. M. Anaerobic microbial dehalogenation. *Annu. Rev. Microbiol.* **2004,** *58*, 43-73.

(72) Maymó-Gatell, X.; Anguish, T.; Zinder, S. H. Reductive dechlorination of chlorinated ethenes and 1, 2-dichloroethane by "Dehalococcoides ethenogenes" 195. *Appl. Environ. Microbiol.* **1999,** *65*, (7), 3108-3113.

(73) Maymo-Gatell, X.; Chien, Y.-T.; Gossett, J. M.; Zinder, S. H. Isolation of a Bacterium That Reductively Dechlorinates Tetrachloroethene to Ethene. *Science* **1997,** *276*, (5318), 1568-1571.

(74) Pöritz, M.; Goris, T.; Wubet, T.; Tarkka, M. T.; Buscot, F.; Nijenhuis, I.; Lechner, U.; Adrian, L. Genome sequences of two dehalogenation specialists–Dehalococcoides mccartyi strains BTF08 and DCMB5 enriched from the highly polluted Bitterfeld region. In Blackwell Publishing Ltd Oxford, UK: 2013.

(75) Cichocka, D.; Nikolausz, M.; Haest, P. J.; Nijenhuis, I. Tetrachloroethene conversion to ethene by a Dehalococcoides-containing enrichment culture from Bitterfeld. *FEMS Microbiol. Ecol.* **2010,** *72*, (2), 297-310.

(76) Molenda, O.; Quaile, A. T.; Edwards, E. A. Dehalogenimonas sp. strain WBC-2 genome and identification of its trans-dichloroethene reductive dehalogenase, TdrA. *Appl. Environ. Microbiol.* **2016,** *82*, (1), 40-50.

(77) Yang, Y.; Higgins, S. A.; Yan, J.; Şimşir, B.; Chourey, K.; Iyer, R.; Hettich, R. L.; Baldwin, B.; Ogles, D. M.; Löffler, F. E. Grape pomace compost harbors organohalide-respiring Dehalogenimonas species with novel reductive dehalogenase genes. *ISME J.* **2017,** *11*, (12), 2767-2780.

(78) Payne, K. A. P.; Quezada, C. P.; Fisher, K.; Dunstan, M. S.; Collins, F. A.; Sjuts, H.; Levy, C.; Hay, S.; Rigby, S. E. J.; Leys, D. Reductive dehalogenase structure suggests a mechanism for B12-dependent dehalogenation. *Nature* **2015,** *517*, (7535), 513-516.

(79) Bommer, M.; Kunze, C.; Fesseler, J.; Schubert, T.; Diekert, G.; Dobbek, H. Structural basis for organohalide respiration. *Science* **2014,** *346*, (6208), 455-458.

(80) Yan, J.; Simsir, B.; Farmer, A. T.; Bi, M.; Yang, Y.; Campagna, S. R.; Loffler, F. E. The corrinoid cofactor of reductive dehalogenases affects dechlorination rates and extents in organohalide-respiring Dehalococcoides mccartyi. *ISME J.* **2016,** *10*, 1092-1101.

(81) Matthews, D. E.; Hayes, J. M. Isotope-Ratio-Monitoring Gas Chromatography-Mass Spectrometry. *Anal. Chem.* **1978,** *50*, (11), 1465-1473.

(82) Sessions, A. L. Isotope-ratio detection for gas chromatography. *J. Sep. Sci.* **2006,** *29*, 1946-1961.

(83) Bigeleisen, J. Chemistry of Isotopes: Isotope chemistry has opened new areas of chemical physics, geochemistry, and molecular biology. *Science* **1965,** *29*, 463-471.

(84) Kaufhold, T.; Schmidt, M.; Cichocka, D.; Nikolausz, M.; Nijenhuis, I. Dehalogenation of diverse halogenated substrates by a highly enriched Dehalococcoides-containing culture derived from the contaminated mega-site in Bitterfeld. *FEMS Microbiol. Ecol.* **2012,** *83*, (1), 176-188.

(85) Duhamel, M.; Wehr, S. D.; Yu, L.; Rizvi, H.; Seepersad, D.; Dworatzek, S.; Cox, E. E.; Edwards, E. A. Comparison of anaerobic dechlorinating enrichment cultures maintained on tetrachloroethene, trichloroethene, cis-dichloroethene and vinyl chloride. *Water Res.* **2002,** *36*, (17), 4193-4202.

(86) Duhamel, M.; Mo, K.; Edwards, E. A. Characterization of a highly enriched Dehalococcoides-containing culture that grows on vinyl chloride and trichloroethene. *Appl. Environ. Microbiol.* **2004,** *70*, (9), 5538-5545.

(87) Duhamel, M.; Edwards, E. A. Microbial composition of chlorinated ethene-degrading cultures dominated by Dehalococcoides. *FEMS Microbiol. Ecol.* **2006,** *58*, (3), 538-549.

(88) Duhamel, M.; Edwards, E. A. Growth and Yields of Dechlorinators, Acetogens, and Methanogens during Reductive Dechlorination of Chlorinated Ethenes and Dihaloelimination of 1,2-Dichloroethane. *Environ. Sci. Technol.* **2007,** *41*, (7), 2303-2310.

(89) Hug, L. A. A Metagenome-based Examination of Dechlorinating Enrichment Cultures: Dehalococcoides and the Role of the Non-dechlorinating Microorganisms. Ph.D. Thesis, University of Toronto, Toronto, Ontario, Canada, 2012.

(90) Magnuson, J. K.; Romine, M. F.; Burris, D. R.; Kingsley, M. T. Trichloroethene reductive dehalogenase from Dehalococcoides ethenogenes: Sequence of tceA and substrate range characterization. *Appl. Environ. Microbiol.* **2000,** *66*, (12), 5141-5147.

(91) Liang, X.; Molenda, O.; Tang, S.; Edwards, E. A. Identity and Substrate Specificity of Reductive Dehalogenases Expressed in Dehalococcoides-Containing Enrichment Cultures Maintained on Different Chlorinated Ethenes. *Appl. Environ. Microbiol.* **2015,** *81*, (14), 4626-4633.

(92) Fung, J. M.; Morris, R. M.; Adrian, L.; Zinder, S. H. Expression of reductive dehalogenase genes in Dehalococcoides ethenogenes strain 195 growing on tetrachloroethene, trichloroethene, or 2, 3-dichlorophenol. *Appl. Environ. Microbiol.* **2007,** *73*, (14), 4439-4445.

(93) Pérez-de-Mora, A.; Lacourt, A.; McMaster, M. L.; Liang, X.; Dworatzek, S. M.; Edwards, E. A. Chlorinated Electron Acceptor Abundance Drives Selection of Dehalococcoides mccartyi (D. mccartyi) Strains in Dechlorinating Enrichment Cultures and Groundwater Environments. *Front. Microbiol.* **2018,** *9*, (812), DOI: 10.3389/fmicb.2018.00812.

(94) Cichocka, D.; Imfeld, G.; Richnow, H.-H.; Nijenhuis, I. Variability in microbial carbon isotope fractionation of tetra- and trichloroethene upon reductive dechlorination. *Chemosphere* **2008,** *71*, (4), 639-648.

(95) Schmidt, M.; Lege, S.; Nijenhuis, I. Comparison of 1,2-dichloroethane, dichloroethene and vinyl chloride carbon stable isotope fractionation during dechlorination by two Dehalococcoides strains. *Water Res.* **2014,** *52*, (0), 146-154.

(96) Edwards, E. A.; Grbić-Galić, D. Complete mineralization of benzene by aquifer microorganisms under strictly anaerobic conditions. *Appl. Environ. Microbiol.* **1992,** *58*, (8), 2663-2666.

(97) Elsner, M.; Couloume, G. L.; SherwoodLollar, B. Freezing To Preserve Groundwater Samples and Improve Headspace Quantification Limits of Water-Soluble Organic Contaminants for Carbon Isotope Analysis. *Anal. Chem.* **2006,** *78*, (21), 7528-7534.

(98) Cretnik, S.; Thoreson, K. A.; Bernstein, A.; Ebert, K.; Buchner, D.; Laskov, C.; Haderlein, S.; Shouakar-Stash, O.; Kliegman, S.; McNeill, K.; Elsner, M. Reductive Dechlorination of TCE by

Chemical Model Systems in Comparison to Dehalogenating Bacteria: Insights from Dual Element Isotope Analysis (13C/12C, 37Cl/35Cl). *Environ. Sci. Technol.* **2013,** *47*, (13), 6855-6863.

(99) Kublik, A.; Deobald, D.; Hartwig, S.; Schiffmann, C. L.; Andrades, A.; von Bergen, M.; Sawers, R. G.; Adrian, L. Identification of a multi-protein reductive dehalogenase complex in D ehalococcoides mccartyi strain CBDB 1 suggests a protein-dependent respiratory electron transport chain obviating quinone involvement. *Environ. Microbiol.* **2016,** *18*, (9), 3044-3056.

(100) Men, Y.; Seth, E. C.; Yi, S.; Crofts, T. S.; Allen, R. H.; Taga, M. E.; Alvarez-Cohen, L. Identification of specific corrinoids reveals corrinoid modification in dechlorinating microbial communities. *Environ. Microbiol.* **2015,** *17*, (12), 4873-4884.

(101) Heavner, G. L.; Mansfeldt, C. B.; Debs, G. E.; Hellerstedt, S. T.; Rowe, A. R.; Richardson, R. E. Biomarkers' Responses to Reductive Dechlorination Rates and Oxygen Stress in Bioaugmentation Culture KB-1TM. *Microorganisms* **2018,** *6*, (1), DOI: 10.3390/microorganisms6010013.

(102) Buchner, D.; Behrens, S.; Laskov, C.; Haderlein, S. B. Resiliency of Stable Isotope Fractionation (δ13C and δ37Cl) of Trichloroethene to Bacterial Growth Physiology and Expression of Key Enzymes. *Environ. Sci. Technol.* **2015,** *49*, 13230−13237.

(103) Kuder, T.; van Breukelen, B. M.; Vanderford, M.; Philp, P. 3D-CSIA: Carbon, Chlorine, and Hydrogen Isotope Fractionation in Transformation of TCE to Ethene by a Dehalococcoides Culture. *Environ. Sci. Technol.* **2013,** *47*, (17), 9668-9677.

(104) Doğan-Subaşı, E.; Elsner, M.; Qiu, S.; Cretnik, S.; Atashgahi, S.; Shouakar-Stash, O.; Boon, N.; Dejonghe, W.; Bastiaens, L. Contrasting dual (C, Cl) isotope fractionation offers potential to distinguish reductive chloroethene transformation from breakdown by permanganate. *Sci. Total Environ.* **2017,** *596–597*, 169-177.

(105) Loos, R.; Locoro, G.; Comero, S.; Contini, S.; Schwesig, D.; Werres, F.; Balsaa, P.; Gans, O.; Weiss, S.; Blaha, L.; Bolchi, M.; Gawlik, B. M. Pan-European survey on the occurrence of selected polar organic persistent pollutants in ground water. *Water Res.* **2010,** *44*, (14), 4115-4126.

(106) Kern, S.; Singer, H. P.; Hollender, J.; Schwarzenbach, R. P.; Fenner, K. Assessing exposure to transformation products of soil-applied organic contaminants in surface water: comparison of model predictions and field data. *Environ. Sci. Technol.* **2011,** *45*, (7), 2833-2841.

(107) Moreau-Kervevan, C.; Mouvet, C. Adsorption and desorption of atrazine, deethylatrazine, and hydroxyatrazine by soil components. *J. Environ. Qual.* **1998,** *27*, 46-53.

(108) Meyer, A. H.; Penning, H.; Lowag, H.; Elsner, M. Precise and accurate compound specific carbon and nitrogen isotope analysis of atrazine: critical role of combustion oven conditions. *Environ. Sci. Technol.* **2008,** *42*, (21), 7757-7763.

(109) Reinnicke, S.; Juchelka, D.; Steinbeiss, S.; Meyer, A. H.; Hilkert, A.; Elsner, M. Gas chromatography-isotope ratio mass spectrometry (GC-IRMS) of recalcitrant target compounds: performance of different combustion reactors and strategies for standardization. *Rapid. Commun. Mass. Sp.* **2012,** *26*, (9), 1053-1060.

(110) Schreglmann, K.; Hoeche, M.; Steinbeiss, S.; Reinnicke, S.; Elsner, M. Carbon and nitrogen isotope analysis of atrazine and desethylatrazine at sub-microgram per liter concentrations in groundwater. *Anal. Bioanal. Chem.* **2013,** *405*, (9), 2857-2867.

(111) Schürner, H. K. V.; Seffernick, J. L.; Grzybkowska, A.; Dybala-Defratyka, A.; Wackett, L. P.; Elsner, M. Characteristic Isotope Fractionation Patterns in s-Triazine Degradation Have Their Origin in Multiple Protonation Options in the s-Triazine Hydrolase TrzN. *Environ. Sci. Technol.* **2015,** *49*, (6), 3490-3498.

(112) Lihl, C.; Douglas, L. M.; Franke, S.; Pérez-de-Mora, A.; Meyer, A. H.; Daubmeier, M.; Edwards, E. A.; Nijenhuis, I.; Sherwood Lollar, B.; Elsner, M. Mechanistic Dichotomy in Bacterial Trichloroethene Dechlorination Revealed by Carbon and Chlorine Isotope Effects. *Environ. Sci. Technol.* **2019,** *53*, (8), 4245-4254.

(113) Erickson, L. E. Degradation of atrazine and related s-triazines. *Crit. Rev. Env. Con.* **1989,** *19*, 1-14.

(114) LeBaron, H. M.; McFarland, J. E.; Burnside, O. C. *The triazine herbicides*. 1 ed.; Elsevier: Oxford, 2008; p 600.

(115) Strong, L. C.; Rosendahl, C.; Johnson, G.; Sadowsky, M. J.; Wackett, L. P. *Arthrobacter aurescens* TC1 metabolizes diverse s-triazine ring compounds. *Appl. Environ. Microbiol.* **2002,** *68*, (12), 5973-5980.

(116) Sajjaphan, K.; Shapir, N.; Wackett, L. P.; Palmer, M.; Blackmon, B.; Tomkins, J.; Sadowsky, M. J. *Arthrobacter aurescens* TC1 Atrazine Catabolism Genes *trzN*, *atzB*, and *atzC* Are Linked on a 160-Kilobase Region and Are Functional in *Escherichia coli*. *Appl. Environ. Microbiol.* **2004,** *70*, (7), 4402-4407.

(117) Nagy, I.; Compernolle, F.; Ghys, K.; Vanderleyden, J.; De Mot, R. A single cytochrome P-450 system is involved in degradation of the herbicides EPTC (S-ethyl dipropylthiocarbamate) and atrazine by Rhodococcus sp. strain NI86/21. *Appl. Environ. Microbiol.* **1995,** *61*, (5), 2056-2060.

(118) Reinnicke, S.; Simonsen, A.; Sørensen, S. R.; Aamand, J.; Elsner, M. C and N Isotope Fractionation during Biodegradation of the Pesticide Metabolite 2,6-Dichlorobenzamide (BAM): Potential for Environmental Assessments. *Environ. Sci. Technol.* **2012,** *46*, (3), 1447-1454.

(119) Gilevska, T.; Gehre, M.; Richnow, H. H. Multidimensional isotope analysis of carbon, hydrogen and oxygen as tool for identification of the origin of ibuprofen. *J. Pharm. Biomed. Anal.* **2015,** *115*, 410-417.

(120) Dybala-Defratyka, A.; Szatkowski, L.; Kaminski, R.; Wujec, M.; Siwek, A.; Paneth, P. Kinetic isotope effects on dehalogenations at an aromatic carbon. *Environ. Sci. Technol.* **2008,** *42*, (21), 7744-7750.

(121) Grzybkowska, A.; Kaminski, R.; Dybala-Defratyka, A. Theoretical predictions of isotope effects versus their experimental values for an example of uncatalyzed hydrolysis of atrazine. *Phys. Chem. Chem. Phys.* **2014,** *16*, 15164-15172.

(122) Lihl, C.; Renpenning, J.; Kümmel, S.; Gelman, F.; Schürner, H. K. V.; Daubmeier, M.; Heckel, B.; Melsbach, A.; Bernstein, A.; Shouakar-Stash, O.; Gehre, M.; Elsner, M. Toward Improved Accuracy in Chlorine Isotope Analysis: Synthesis Routes for In-House Standards and Characterization via Complementary Mass Spectrometry Methods. *Anal. Chem.* **2019,** *91*, (19), 12290-12297.

(123) Bigeleisen, J. The relative reaction velocities of isotopic molecules. *J. Chem. Phys.* **1949,** *17*, 675-679.

(124) Anisimov, V.; Paneth, P. ISOEFF98. A program for studies of isotope effects using Hessian modifications. *J. Math. Chem.* **1999,** *26*, (75-86).

(125) Streitwieser Jr, A.; Jagow, R.; Fahey, R.; Suzuki, S. Kinetic isotope effects in the acetolyses of deuterated cyclopentyl tosylates1, 2. *J. Am. Chem. Soc.* **1958,** *80*, (9), 2326-2332.

(126) Świderek, K.; Paneth, P. Extending limits of chlorine kinetic isotope effects. *J. Org. Chem.* **2012,** *77*, (11), 5120-5124.

(127) Szatkowski, L.; Dybala-Defratyka, A. A computational study on enzymatically driven oxidative coupling of chlorophenols: An indirect dehalogenation reaction. *Chemosphere* **2013,** *91*, (3), 258-264.

(128) Szatkowski, L.; Manna, R. N.; Grzybkowska, A.; Kamiński, R.; Dybala-Defratyka, A.; Paneth, P. Measurement and prediction of chlorine kinetic isotope effects in enzymatic systems. In *Methods in enzymology*, Elsevier: 2017; Vol. 596, pp 179-215.

(129) Dybala-Defratyka, A.; Rostkowski, M.; Matsson, O.; Westaway, K. C.; Paneth, P. A New Interpretation of Chlorine Leaving Group Kinetic Isotope Effects; A Theoretical Approach. *J. Org. Chem.* **2004,** *69*, (15), 4900-4905.

(130) Siwek, A.; Omi, R.; Hirotsu, K.; Jitsumori, K.; Esaki, N.; Kurihara, T.; Paneth, P. Binding modes of DL-2-haloacid dehalogenase revealed by crystallography, modeling and isotope effects studies. *Arch. Biochem. Biophys.* **2013,** *540*, (1–2), 26-32.

(131) Burrows, H. D.; Santaballa, J.; Steenken, S. Reaction pathways and mechanisms of photodegradation of pesticides. *J. Photochem. Photobiol., B* **2002,** *67*, (2), 71-108.

(132) De Corte, S.; Sabbe, T.; Hennebel, T.; Vanhaecke, L.; De Gusseme, B.; Verstraete, W.; Boon, N. Doping of biogenic Pd catalysts with Au enables dechlorination of diclofenac at environmental conditions. *Water Res.* **2012,** *46*, (8), 2718-2726.

(133) Keen, O. S.; Thurman, E. M.; Ferrer, I.; Dotson, A. D.; Linden, K. G. Dimer formation during UV photolysis of diclofenac. *Chemosphere* **2013,** *93*, (9), 1948-1956.

(134) Sykes, P. *Reaktionsmechanismen der organischen Chemie*. Verlag Chemie: Weinheim, 1972.

(135) Gafni, A.; Lihl, C.; Gelman, F.; Elsner, M.; Bernstein, A. δ13C and δ37Cl Isotope Fractionation To Characterize Aerobic vs Anaerobic Degradation of Trichloroethylene. *Environ. Sci. Technol. Lett.* **2018,** *5*, (4), 202-208.

(136) Gafni, A.; Gelman, F.; Ronen, Z.; Bernstein, A. Variable carbon and chlorine isotope fractionation in TCE co-metabolic oxidation. *Chemosphere* **2019**, 125130.

(137) Elsner, M.; Hofstetter Thomas, B. Current Perspectives on the Mechanisms of Chlorohydrocarbon Degradation in Subsurface Environments: Insight from Kinetics, Product Formation, Probe Molecules, and Isotope Fractionation. In *Aquatic Redox Chemistry*, American Chemical Society: 2011; Vol. 1071, pp 407-439.

(138) Audí-Miró, C.; Cretnik, S.; Torrentó, C.; Rosell, M.; Shouakar-Stash, O.; Otero, N.; Palau, J.; Elsner, M.; Soler, A. C, Cl and H compound-specific isotope analysis to assess natural versus Fe (0) barrier-induced degradation of chlorinated ethenes at a contaminated site. *J. Hazard. Mater.* **2015,** *299*, 747-754.

(139) Audí-Miró, C.; Cretnik, S.; Otero, N.; Palau, J.; Shouakar-Stash, O.; Soler, A.; Elsner, M. Cl and C isotope analysis to assess the effectiveness of chlorinated ethene degradation by zero-valent iron: Evidence from dual element and product isotope values. *Appl. Geochem.* **2013,** *32*, (0), 175-183.

(140) Stamper, D. M.; Tuovinen, O. H. Biodegradation of the acetanilide herbicides alachlor, metolachlor, and propachlor. *Crit. Rev. Microbiol.* **1998,** *24*, (1), 1-22.

(141) Gunasekara, A. S.; Troiano, J.; Goh, K. S.; Tjeerdema, R. S. Chemistry and fate of simazine. In *Reviews of environmental contamination and toxicology*, Springer: 2007; pp 1-23.

(142) Xu, J.; Yang, M.; Dai, J.; Cao, H.; Pan, C.; Qiu, X.; Xu, M. Degradation of acetochlor by four microbial communities. *Bioresour. Technol.* **2008,** *99*, (16), 7797-7802.

(143) Jurina, T.; Terzić, S.; Ahel, M.; Stipičević, S.; Kontrec, D.; Kurtanjek, Ž.; Udiković-Kolić, N. Catabolism of terbuthylazine by mixed bacterial culture originating from s-triazine-contaminated soil. *Appl. Microbiol. Biotechnol.* **2014,** *98*, (16), 7223-7232.

(144) Maier, M. P.; De Corte, S.; Nitsche, S.; Spaett, T.; Boon, N.; Elsner, M. C & N Isotope Analysis of Diclofenac to Distinguish Oxidative and Reductive Transformation and to Track Commercial Products. *Environ. Sci. Technol.* **2014,** *48*, (4), 2312-2320.

(145) Waller, A. S.; Krajmalnik-Brown, R.; Löffler, F. E.; Edwards, E. A. Multiple reductive-dehalogenase-homologous genes are simultaneously transcribed during dechlorination by Dehalococcoides-containing cultures. *Appl. Environ. Microbiol.* **2005,** *71*, (12), 8257-8264.

(146) Grostern, A.; Edwards, E. A. Characterization of a Dehalobacter coculture that dechlorinates 1, 2-dichloroethane to ethene and identification of the putative reductive dehalogenase gene. *Appl. Environ. Microbiol.* **2009,** *75*, (9), 2684-2693.

(147) Manchester, M. J.; Hug, L. A.; Zarek, M.; Zila, A.; Edwards, E. A. Discovery of a trans-dichloroethene-respiring Dehalogenimonas species in the 1, 1, 2, 2-tetrachloroethane-dechlorinating WBC-2 consortium. *Appl. Environ. Microbiol.* **2012,** *78*, (15), 5280-5287.

(148) Yu, Y.; Lee, C.; Kim, J.; Hwang, S. Group-specific primer and probe sets to detect methanogenic communities using quantitative real-time polymerase chain reaction. *Biotechnol. Bioeng.* **2005,** *89*, (6), 670-679.

(149) Dionisi, H. M.; Harms, G.; Layton, A. C.; Gregory, I. R.; Parker, J.; Hawkins, S. A.; Robinson, K. G.; Sayler, G. S. Power analysis for real-time PCR quantification of genes in activated sludge and analysis of the variability introduced by DNA extraction. *Appl. Environ. Microbiol.* **2003,** *69*, (11), 6597-6604.

(150) NIST. NIST Chemistry WebBook. www.webbook.nist.gov/chemistry/ (15.01.2020),